Charles University in Prague
1st Faculty of Medicine

Doctoral studies in Biomedicine
Biochemistry and Pathobiochemistry

Academy of Sciences of the Czech Republic
Institute of Physiology, v.v.i.

M.Sc. Tomáš Jeleník

Analysis of the involvement of α2-AMPK in the beneficial effects of n–3 polyunsaturated fatty acids on obesity-associated metabolic derangements

Ph. D. Thesis

Supervisor: Martin Rossmeisl, MD, Ph.D.

Prague 2010

Prohlášení:

Prohlašuji, že jsem závěrečnou práci zpracoval samostatně a že jsem uvedl všechny použité informační zdroje. Současně dávám svolení k tomu, aby tato závěrečná práce byla archivována v Ústavu vědeckých informací 1. lékařské fakulty Univerzity Karlovy v Praze a zde užívána ke studijním účelům. Za předpokladu, že každý, kdo tuto práci použije pro svou přednáškovou nebo publikační aktivitu, se zavazuje, že bude tento zdroj informací řádně citovat. Souhlasím se zpřístupněním elektronické verze mé práce v Digitálním repozitáři Univerzity Karlovy v Praze (http://repozitar.cuni.cz). Práce je zpřístupněna pouze v rámci Univerzity Karlovy v Praze.

Souhlasím – Nesouhlasím

V Praze dne Ing. Tomáš Jeleník

Acknowledgements

I would like to express my thanks to my supervisor Martin Rossmeisl and to Jan Kopecký, the head of the department, for the scientific and financial support through my PhD studies and to all collaborators who contributed to this work.

LIST OF ABBREVIATIONS

ADP	adenosine diphosphate
ACC	acetyl CoA carboxylase
AICAR	5-aminoimidazole-4-carboxyamide ribonucleoside
AMP	adenosine monophosphate
AMPK	AMP-activated protein kinase
AOX-1	acyl-CoA oxidase-1
ATP	adenosine-5'-triphosphate
CaMKKβ	Ca^{2+}/calmodulin-dependent protein kinase β
CD68	cluster of differentiation 68
CLS	crown-like structures
CPT-1α	carnitine palmitoyltransferase-1α
cHF	corn oil based high-fat diet
cHF+F	corn oil based high-fat diet supplemented with fish oil
cHF+F+TZD	cHF+F diet supplemented with thiazolidinedione
cHF+TZD	cHF diet supplemented with thiazolidinedione
ChREBP	carbohydrate responsive element-binding protein
DAG	diacylglycerol
DHA	docosahexaenoic acid (22:6 n–3)
EDL	extensor digitorum longus
EPA	eicosapentaenoic acid (20:3 n–5)
FAS	fatty acid synthase
FDPS	farnesyl diphosphate synthase
G6Pase	glucose-6-phosphatase
GPAT	glycerol-3-phosphate acyltransferase
GLUT-4	glucose transporter-4
HMG-CoA	3-hydroxy-3-methylglutaryl-CoA
IL-6	interleukin-6
IRS-2	insulin receptor substrate-2
LC-PUFA	long-chain polyunsaturated fatty acids
MCP-1	monocyte chemoattractant protein-1
MUFA	monounsaturated fatty acids
NEFA	non-esterified fatty acids
PDK-4	pyruvate dehydrogenase kinase-4
PEPCK	phosphoenolpyruvate carboxykinase
PGC-1α	peroxisome proliferator-activated receptor-γ coactivator-1α
PKCε	protein kinase C-ε
PPAR	peroxisome proliferator-activated receptor
PPIB	peptidylpropyl isomerase β
RBP-4	retinol binding protein 4
RQ	respiratory quotient
SCD1	stearoyl-coenzyme A desaturase-1
SPOT-14	thyroid hormone responsive SPOT 14
SREBP-1c	sterol regulatory element binding protein-1c
TNFα	tumor necrosis factor α
TZD	thiazolidinedione

VLDL	very low-density lipoprotein
WAT	white adipose tissue
WT	wild type
KO	knock-out (genetic model)

CONTENTS

1 INTRODUCTION

1.1 Mechanisms linking obesity to insulin resistance

Obesity has reached epidemic proportions globally and is a major contributor to the global burden of chronic disease and disability. It results from positive energy balance, when energy intake exceeds energy expenditure (e.g. overfeeding with energy dense food of poor nutritional value, lack of physical activity). Excess energy in the form of triacylglycerols is stored in adipose tissue and, at some point, also in other metabolically active organs of the body.

Obesity is a major risk factor for insulin resistance. Together with genetic predispositions, it can lead into a loss of metabolic fuel homeostasis and outbreak of type 2 diabetes. There is an evidence that rather than total body fat content, intra-abdominal, or visceral, obesity is highly correlated with insulin resistance and the features of metabolic syndrome (1).

Main role of insulin is to stimulate glucose uptake by peripheral tissues and suppress glucose production in the liver and lipolysis in the adipose tissue. Insulin resistance is characterized by an inadequate response of insulin target tissues such as muscle, liver and adipose tissue to perform their physiological functions. To maintain glucose and lipid homeostasis, body can, at least partially, compensate for decreased efficiency of insulin by increased insulin secretion. However, insufficient metabolic action of insulin leads to metabolic complications such as hyperglycemia and/or dyslipidemia, which further promote insulin resistance and cause serious tissue damage by subsequent mechanisms (see below). The state of long-term overloading of metabolic pathways can remain unchanged for a relatively long time before the appearance of type 2 diabetes characterized by β-cells exhaustion and failure (2).

Among the main mechanisms responsible for the development of insulin resistance in different organs could be overloading with toxic metabolites, induction of inflammation, disruption of secretory functions and activation of anti-stress mechanisms.

1.1.1 Central role of adipose tissue

Adipose tissue has a regulatory role in the development of obesity-associated insulin resistance. It has two main physiological functions. Firstly, it plays an important role in the storage and release of lipids, thus managing the energy reserve of the body according to the needs of the organism. Secondly, adipose tissue is an endocrine organ that synthesizes and secretes a large group of hormones and cytokines, called adipokines, as well as “active” lipid metabolites, known as lipokines (3). They act both at the local (autocrine/paracrine) and systemic (endocrine) level, and mediate communication networks between all major organs involved in the regulation of body homeostasis. Metabolic overload of adipose tissue (but also lipodystrophy - the absence of fat stores) can result in dysregulation of its normal functions, which can negatively impact other organs in the body (see
Figure 1.1-1).

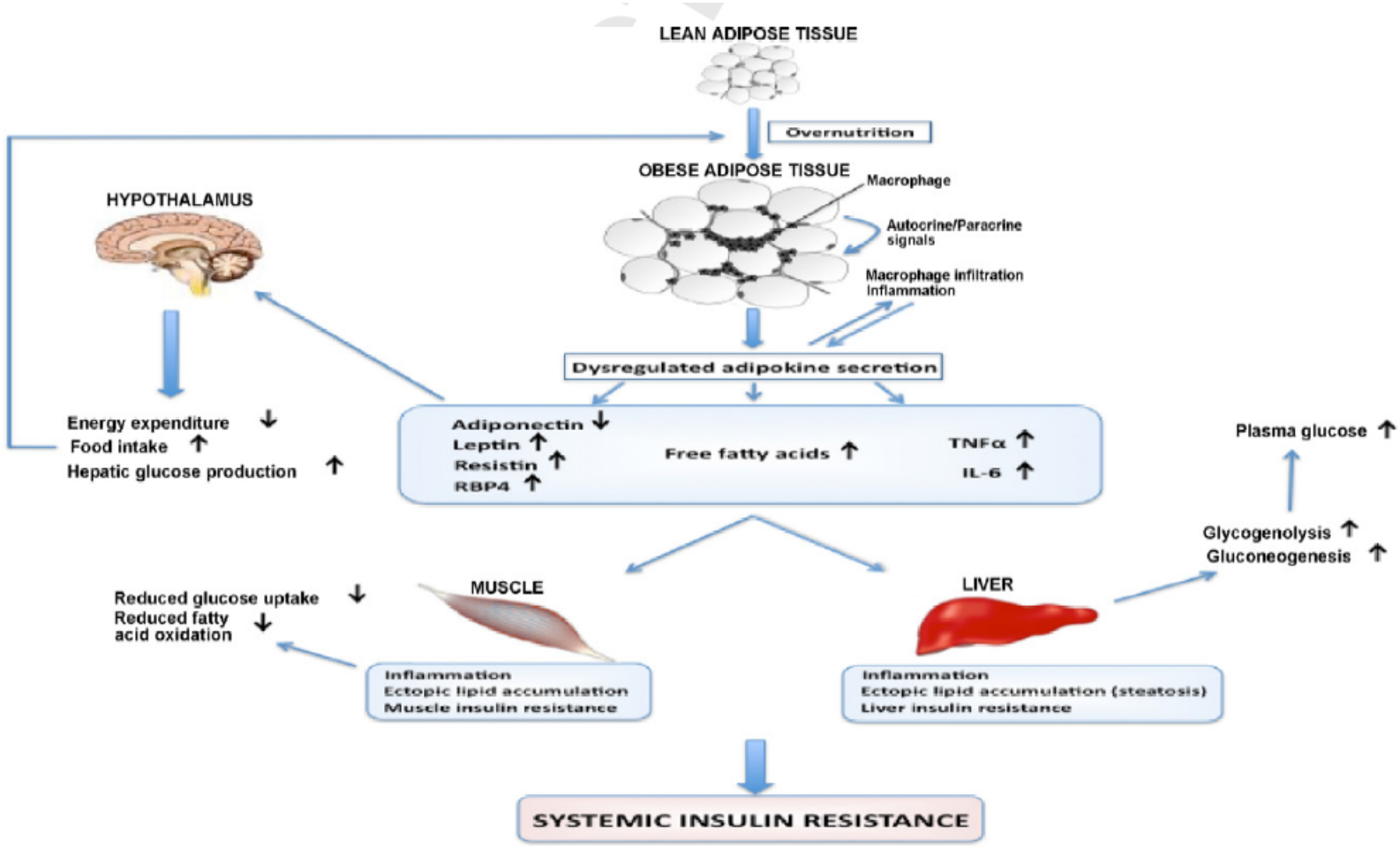

Figure 1.1-1 Mechanisms linking obesity to systemic insulin resistance. Adapted from (4).

Positive energy balance causes adipose tissue to become hypertrophic and subsequently hyperplastic, both conditions resulting in obesity. Adipocytes can store excess energy up to the state of fullness and cannot expand beyond a "critical size" (5). Excess lipids are then ectopically stored in the liver, muscle or heart and provoke insulin resistance of these tissues (6). Moreover, hypertrophied adipocytes are characterised by a hyperlipolytic state that is resistant to the antilipolytic effect of insulin (7). Elevated levels of non-esterified fatty acids (NEFA) are observed in obesity and type 2 diabetes, and are associated with the insulin resistance (8). Increased flux of NEFA may impair liver metabolism, leading to increased hepatic glucose production (hyperglycemia) and stimulation of very low-density lipoprotein triacylglycerol (VLDL-triacylglycerol) secretion (hyperlipidemia).

The profile of adipokines secreted from adipose tissue also varies depending on the degree of obesity and the size of adipocytes (9). Among the many known adipokines produced by adipose tissue, adipocytes secrete leptin, adiponectin, resistin and retinol binding protein-4 (RBP-4). Leptin, firstly revealed as an adipocyte-derived signaling molecule, was found to have a profound role in the regulation of whole-body metabolism by stimulating energy expenditure, inhibiting food intake and restoring euglycemia (10). Circulating levels of serum leptin and total body fat mass are positively correlated (11), however, in most cases of obesity leptin resistance limits its biological efficacy (12). Unlike leptin, adiponectin secretion is decreased in obese individuals. Adiponectin is an insulin-sensitizing molecule, abundant in the circulation (13). The structure of adiponectin, its multimeric forms as well as target receptors are well explored. It has been shown, that decreased expression of adiponectin correlated with insulin resistance in mouse models of altered insulin sensitivity (14). On the other hand, adiponectin reversed obesity-induced insulin resistance and improved dyslipidemia and hyperglycemia by increasing fatty acid oxidation, energy expenditure and reducing hepatic glucose production (15). These beneficial effects of adiponectin were mediated through the phosphorylation and activation of AMPK in the liver and skeletal muscle. Adipose tissue AMPK was also stimulated by adiponectin in primary rat adipocytes, which resulted in increased glucose uptake in these cells (16). Adiponectin also exhibits anti-inflammatory properties (17) by inhibiting phagocytic activity of macrophages. The

mRNA levels of resistin and RBP-4 are increased during obesity and negatively affect insulin sensitivity.

It has been demonstrated that the larger is the adipocyte, the more fragile it becomes when submitted to a common physical stress (18). Therefore, adipocyte size is an important determinant of cell death. Subsequently, macrophages infiltrate adipose tissue to remove dead adipocytes and this process results in a low-grade inflammation. The secretion profile of adipose tissue-derived adipokines changes; there is a shift towards pro-inflammatory adipokines and cytokines such as tumor necrosis factor α (TNF α) and interleukin-6 (IL6) (9), which have been shown to impair insulin sensitivity (19).

1.1.2 Hepatic insulin resistance

The sensitivity of liver to insulin is important to maintain glucose and lipid homeostasis. Glucose is absorbed from the intestine and taken up by hepatocytes. Glucose can enter various pathways to be converted into glycogen, fatty acids or triacylglycerols. Insulin stimulates all of these pathways. On the other hand, hepatic gluconeogenesis is suppressed by insulin. The overall content of liver triacylglycerols is the result of their production and secretion from the liver. Fatty acids in the liver are taken up from the circulation or synthesized *de novo*. The source of blood-derived fatty acids is either from the diet in the form of chylomicrons or from the lipolysis of triacylglycerol stores in adipose tissue. Liver fatty acids are esterified into triacylglycerols and secreted in the form of VLDL-triacylglycerols. Impairments of these pathways may result in a development of liver steatosis as illustrated in the Figure 1.1-2 (20).

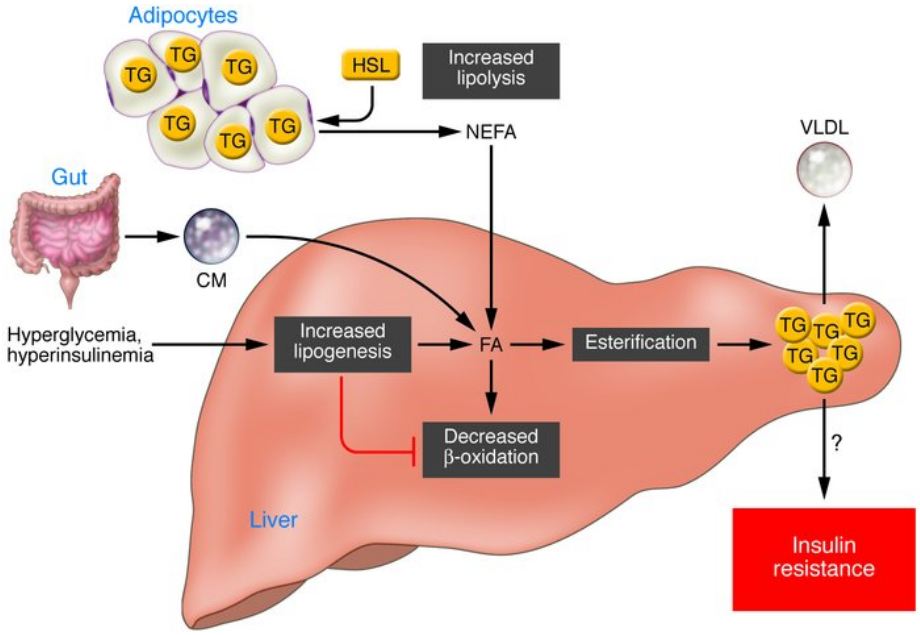

Figure 1.1-2 Metabolic defects leading to the development of hepatic steatosis. Adapted from (20)

It has been shown, that liver steatosis is associated with insulin resistance (21), and lowering liver triacylglycerol pools correlates with improved insulin sensitivity in several rodent models as well as in humans [(22); (23)]. However, whether the impaired insulin sensitivity is a consequence of hepatic steatosis or vice versa remains still unresolved (24). Furthermore, dissociations of hepatic steatosis and insulin resistance have been found (25). For instance, increased flux of fatty acids into neutral triacylglycerols protects liver from the cytotoxic effects of fatty acid side products (26). There are several lines of evidence, that diacylglycerol accumulation affects the development of insulin resistance. Mitochondrial glycerol-3-phosphate acyltransferase (GPAT) is the rate-limiting enzyme of diacylglycerol formation. GPAT-knockout mice showed reduced levels of diacylglycerols and were protected against high-fat/high-sucrose diet-induced insulin resistance (27). Furthermore, it has been shown that excess diacylglycerols cause insulin resistance by activating protein kinase C-ε (PKCε). PKCε is a serine-threonine kinase and its activation interferes with insulin ability to phosphorylate IRS-2 on tyrosine residues, thus inhibiting insulin signaling (28) (see Figure 1.1-3). Moreover, inhibition of PKCε prevents hepatic insulin resistance in fatty liver disease (28).

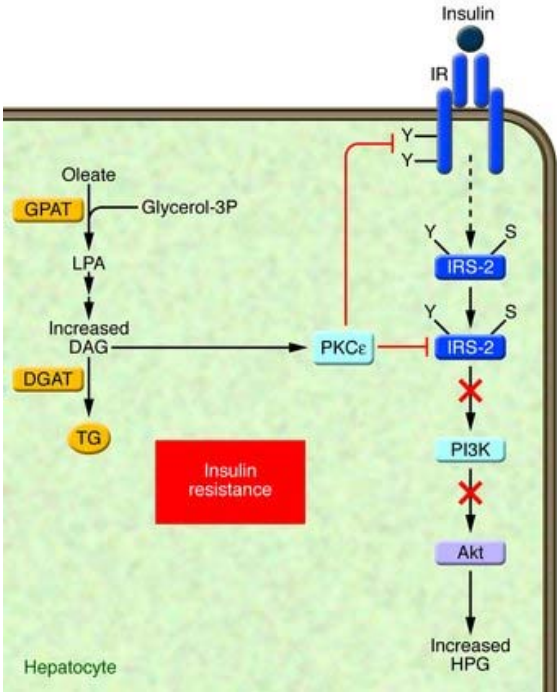

Figure 1.1-3 Mechanism by which diacylglycerols affect insulin sensitivity in the liver. Adapted from ((20))

1.1.3 Skeletal muscle insulin resistance

Fatty acids and glucose are metabolized in the skeletal muscle, depending on the metabolic state of the tissue. Oversupply of fatty acids, for example from increased lipolysis of triacylglycerol stores in insulin-resistant adipocytes, can lead to accumulation of various lipid metabolites, which was shown to negatively correlate with insulin sensitivity. Ceramide and diacylglycerol levels seem to be the most important players (29). Insulin-resistant muscle is metabolically inflexible, i.e. the ability to switch from lipid to carbohydrate metabolism is low (30). Glucose uptake and glycogen synthesis of insulin-resistant muscle is decreased and this can be observed in obese and diabetic patients (31).

1.2 Role of AMPK in regulating whole body metabolism

Obesity-related insulin resistance and type 2 diabetes are characterised by defective energy metabolism. Preservation of intracellular ATP concentrations within an appropriate range is needed to sustain unimpaired metabolism. Adenosine

monophosphate-activated protein kinase (AMPK) is considered to be in the centre of the mechanisms that regulate metabolism on the cellular and whole-body level. Activation of AMPK by various stimuli leads to induction and inhibition of energy-producing and energy-consuming metabolic pathways, respectively. It can be achieved acutely by modifying the activity of various enzymes or by a long-term impact on gene mRNA expression levels. Although it appears that AMPK malfunction is not responsible for the induction of type 2 diabetes, activation of this enzyme could beneficially contribute to the treatment of this disease.

1.2.1 AMPK structure and tissue distribution

AMPK is a heterotrimeric protein comprising one catalytic α subunit and two regulatory subunits (β and γ) (32). Homologues of AMPK have been identified in all eukaryotic species with known genome sequences and their structure has been highly conserved throughout the evolution. In mammals, two isoforms for α (α1, α2) and β (β1, β2) and three for γ-subunit (γ1, γ2, γ3) are known, while all 12 isoform combinations are possible. AMPK acts as a fuel sensor in most tissues and organs, including liver, skeletal muscle, heart, hypothalamus and adipose tissue. In the liver, α1- and α2-AMPK subunits account each for about 50 % of total AMPK activity and expression of β1 and γ1 regulatory subunits predominates (33). In adipose tissue, the α1 catalytic subunit is the predominant isoform expressed and accounts for the major part of AMPK activity (34). On the other hand, muscle cells mainly express AMPK complexes containing the α2 catalytic subunit (35).

1.2.2 Upstream targets of AMPK

AMPK can be activated both allosterically by AMP binding on the γ subunit and by reversible phosphorylation on Thr-172. Two upstream kinases have been identified to activate AMPK: LKB1 kinase and Ca^{2+}/calmodulin-dependent protein kinase β (CaMKKβ). LKB1 kinase mediates mainly AMP-dependent phosphorylation of AMPK and its crucial role is in the regulation of the glucose and lipid metabolism (36). CaMKKβ is involved in AMP-independent activation of AMPK in response to increased Ca^{2+} concentrations during contraction in skeletal muscle [(37); (38)]. Simultaneous allosteric activation and phosphorylation of AMPK causes >1000-fold increase in its

activity, thus allowing high sensitivity to small changes in energy status of the cells (39). Finally, adiponectin is known to activate AMPK (15) and both, LKB1 and CaMKK are involved in the mechanism of AMPK activation by adiponectin (40).

1.2.3 Downstream targets of AMPK

A number of downstream targets and processes that are regulated by AMPK have been described. Generally, activation of AMPK downregulates biosynthetic pathways such as fatty acid and cholesterol synthesis and switches on catabolic pathways that generate ATP, such as fatty acid oxidation, glucose uptake and glycolysis. Mechanisms, by which AMPK mediates its action, are based on the change of enzymes activity by phosphorylation and/or the regulation of gene expression. Nuclear localization of α2-AMPK complexes after AMPK activation could be involved in the direct regulation of gene expression (41). Furthermore, AMPK regulates gene expression of various transcription factors and can also affect the stability of mRNA (42).

In the liver, activation of AMPK by the AMP analogue AICAR (5-aminoimidazole-4-carboxyamide ribonucleoside) or by anti-diabetic drug metformin led to the inhibition of glycolytic and lipogenic gene expression. For example, mRNA levels of sterol regulatory element binding protein-1c (SREBP-1c) (43) and carbohydrate responsive element-binding protein (ChREBP) (44) were decreased. These transcription factors play a key role in the regulation of lipogenic and glycolytic genes by insulin and glucose (reviewed in (20)). Malonyl-CoA is both the precursor of fatty acids biosynthesis and an inhibitor of mitochondrial fatty acid oxidation via the allosteric inhibition of the fatty acid transporter carnitin palmitoyltransferase-1 (CPT-1). Acetyl CoA carboxylase (ACC) is a rate-controlling enzyme of malonyl-CoA synthesis, while activated AMPK has been shown to inactivate ACC by phosphorylation, which led to the decrease of malonyl-CoA levels and subsequent effects on fatty acid synthesis and oxidation described above (45). The AMPK-dependent decrease in cholesterol biosynthesis is mediated by the phosphorylation and inhibition of 3-hydroxy-3-methylglutaryl-CoA (HMG-CoA) reductase. Also mitochondrial biogenesis and function can be influenced by AMPK. Resveratrol, naturally occurring antioxidant which protects against diet-induced insulin resistance, increased mitochondrial number together with

AMPK activation (46). Furthermore, liver α1α2-AMPK knockout mice had decreased expression of key mitochondrial constituents (47). Also glucose metabolism is affected by AMPK in the liver. AICAR infusion led to the inhibition of hepatic glucose production in normal and insulin-resistant obese rats (48). AICAR treatment in rodents has hypoglycemic effects but along with the liver, muscle AMPK participates in this effect by increasing glucose uptake into muscle cells (see below). The down-regulation of gluconeogenic gene expression like phosphoenolpyruvate carboxykinase (PEPCK) and glucose-6-phosphatase (G6Pase) accompanied decreased hepatic glucose production (44). However, in other study, while mRNA levels of these enzymes remained unchanged, the enzymatic activities were affected (49).

AMPK plays an important role also in adipose tissue. It has been suggested, that AMPK activation could inhibit preadipocyte differentiation (50), but there is only a little evidence to support this idea. Similarly as in the liver, lipogenesis and lipid oxidation were shown to be regulated by AMPK through the change in malonyl-CoA content in the adipose tissue (51). The study by Sullivan (51) also showed that AMPK activation by AICAR inhibited β-adrenergic-induced lipolysis. This was later confirmed by others using different AMPK activators. The mechanism accounting for the inhibition of lipolysis by AMPK is via the phosphorylation and consequent inactivation of hormone-sensitive lipase, the regulatory enzyme of lipolysis in adipose tissue (52). The role of recently identified complementary lipase, the adipose triacylglycerol lipase, in the regulation of lipolysis by AMPK remains to be determined. Finally, inactivating AMPK in adipocytes abolished adiponectin-stimulated glucose uptake (16). Thus, AMPK could have the role in mediating insulin-independent glucose transport in adipocytes.

In the skeletal muscle, AMPK activity promotes glucose metabolism by stimulating glucose uptake via glucose transporters (GLUT4) and glycogen storage [(53); (54)]. On the other hand, AMPK is inhibited by glycogen and can be able to sense the status of cellular energy reserves in the form of glycogen (55). AMPK favors a shift from glucose to lipid metabolism under the conditions of increased demand of energy production during exercise or fasting. This is mediated through the regulation of malonyl-CoA (56). Metabolic flexibility, i.e. the switch between carbohydrate utilization in insulin-stimulated post-prandial state and lipid utilization in the fasting state is

impaired in obese and insulin-resistant diabetic patients (57). AICAR has been shown to normalize states of impaired metabolic flexibility in obese rats (48).

Various treatments, which led to the activation of AMPK and the subsequent change of metabolic processes, were associated with beneficial effects on metabolic parameters in the models of insulin resistance and dyslipidemia. For example, AICAR lowered plasma glucose levels, improved insulin sensitivity, adiposity and plasma triacylglycerol levels in obese and insulin resistant rat model (48). Furthermore, over-expression of AMPK in the liver led to the similar effects in the obese mice (44). Finally, AICAR infusion in type 2 diabetic patients decreased hepatic glucose production and plasma glucose levels (58). Thus, targeting AMPK by therapeutic treatments could be useful in the prevention or reversal of metabolic disorders such as obesity, insulin resistance and metabolic syndrome.

1.3 Long-chain polyunsaturated fatty acids of n-3 family

1.3.1 Nomenclature

Long-chain polyunsaturated fatty acids of the n-3 series (n-3 LC-PUFA), for example eicosapentaenoic (EPA) and docosahexaenoic (DHA) acids, are important essential fatty acids (Table 1.3-1). Humans or rodents can not synthesize n–3 LC-PUFA *de novo*. Therefore, the supplementation of these substances from the diet is needed. Dietary n–3 α–linolenic acid (ALA) can be elongated and desaturated to form EPA and DHA, however this reaction is quite inefficient and increased amounts of ALA decelerate the formation of DHA (59). Hence, increased dietary uptake of EPA and DHA is preferred. Main pathways of n–3 LC-PUFA utilization in the body are: 1) incorporation into plasma phospholipids; 2) precursors for the formation of eicosanoid and docosanoid signaling molecules; and 3) regulation of gene transcription by acting as ligands of transcription factors.

Table 1.3-1 Nomenclature of selected n–3 LC-PUFA

Trivial name	Abbreviation	Systematic name	Carboxyl reference
α–Linoleic acid	ALA	(Z,Z,Z)-9,12,15-octadecatrienoic acid	C 18:3 (Δ9,12,15)
Eicosapentaenoic acid	EPA	(5Z,8Z,11Z,14Z,17Z)-icosa-5,8,11,14,17-pentaenoic acid	C 20:5 (Δ5,8,11,14,17)
Docosahexaenoic acid	DHA	(4Z,7Z,10Z,13Z,16Z,19Z)-docosa-4,7,10,13,16,19-hexaenoic acid	C 22:6 (Δ4,8,12,15,19)

1.3.2 Biological effects and mechanisms

Naturally occurring n–3 LC-PUFA are obtained mainly from oils of marine fish. Their health benefits were firstly recognized over 30 years ago when epidemiological data indicated that Greenland Eskimos, despite their consumption of a diet with nearly twice the cholesterol content of their Danish counterpart, had a decreased incidence of myocardial infarction together with nearly 10 times higher ratio of n-3/n-6 PUFA in the diet (60). n-3 LC-PUFA act as hypolipidemics, suppressors of VLDL-triacylglycerol production (61), while they also reduce cardiac events and decrease progression of atherosclerosis (62). Therefore, n–3 LC-PUFA are now regarded as healthy constituents of diets for diabetic patients [(63); (64)]. Several studies in obese humans even demonstrated reduction of adiposity after n–3 LC-PUFA supplementation [(65); (66)]. However, in diabetic patients n–3 LC-PUFA appear to have little effect on glycaemic control [(65); (67); (68)]. In rodents fed a high-fat diet, n–3 LC-PUFA efficiently prevented development of obesity [(69); (70); (71)], as well as impaired glucose tolerance [(72); (73)]. Low–grade inflammation of white adipose tissue could be also prevented (74).

Hypolipidaemic and anti-obesity effects of n–3 LC-PUFA probably depend on the in situ suppression of lipogenesis and increase of fatty acid oxidation in several tissues [(71); (75); (76)]. This metabolic switch might reduce accumulation of toxic fatty acid-derivatives, while protecting insulin sensitivity in the liver and muscle [(72); (73)]. n-3 LC-PUFA have been shown to decrease the levels of main glycolytic and lipogenic transcription factors including SREBP-1c (77) , ChREBP (24) as well as other genes that

are regulated by these transcription factors (ACC, fatty acid synthase (FAS), stearoyl-coenzyme A desaturase-1 (SCD1)). In addition, n-3 LC-PUFA diminish malonyl-CoA concentration in the liver (78), which acutely regulates the rates of fatty acid synthesis and oxidation. The effects of n–3 LC-PUFA are furthermore largely mediated by peroxisome proliferator-activated receptors PPAR–α and PPAR–β/δ (79), i.e. transcription factors involved in the regulation of lipid and glucose metabolism. However, PPAR–γ, liver X receptor α and hepatic nuclear factor-4 are also involved [(73); (75); (80)]. It has been show by our group that substitution of only 15 % of dietary lipids in high-fat diet (mainly corn oil) by EPA/DHA concentrate prevented fat accumulation in abdominal fat depots in mice ((70;71)). In cell culture experiments, DHA inhibited differentiation of preadipocytes and even induced their apoptosis (81). n-3 LC-PUFA from fish oil are capable of inducing adiponectin (82), while influencing the secretion of other adipokines [(83); (19)]. The beneficial effects of n-3 LC-PUFA on the prevention of diet-induced insulin resistance were associated with increased glucose uptake and GLUT4 mRNA and protein levels in adipocytes (84).

Besides acting directly as regulatory ligands, n–3 LC-PUFA act also through their active metabolites, eicosanoids, and other lipid molecules (85). Adipocytes produce series-2 eicosanoids from arachidonic acid, and higher availability of n–3 LC-PUFA can shift their production in favor of series-3 and -5 of eicosanoids. This could be crucial for the prevention of white adipose tissue inflammation, because eicosanoids of the series-3 and -5 are distinguished by the lower pro-inflamatory properties that series-2 eicosanoids. Production of a particular prostaglandin of the 2-series, PGD2, which is a known PPAR–γ ligand promoting adipocyte differentiation, is reduced after n–3 LC-PUFA administration (86), supporting the idea that n–3 LC-PUFA are able to decrease accumulation of fat stores.

Another mechanism of n-3 LC-PUFA action is mediated by the change in the biological membranes properties. n-3 LC-PUFA incorporate into biological membranes, thus increasing their unsaturation index and fluidity. In this way, the mobility of membrane-associated proteins, enzymes, and hormones can be affected.

1.4 Involvement of AMPK in the mechanisms of n-3 LC-PUFA action

As described above, n-3 LC-PUFA ingestion has beneficial effects on the lipid and glucose metabolism, in particular on the suppression of hepatic lipogenesis and gluconeogenesis, induction of fatty acid oxidation, and glucose uptake. All of these events have been shown to be affected by AMPK activation. Furthermore, it has been demonstrated that feeding rodents with n-3 LC PUFA enhanced AMPK activity in the liver (87), intestine (88), and adipose tissue [(89); (90)]. Therefore, it can be suggested, that n-3 LC-PUFA could mediate their effects, at least on the metabolic events mentioned above, by modulating the AMPK activity. Possible mechanisms of AMPK activation by n-3 LC-PUFA could involve: 1) changes in energy status of the cells, reflected by the change in AMP/ATP ratio; 2) modulation of upstream kinases or phostphatase activity; 3) induction of adiponectin secretion from adipose tissue or 4) other indirect mechanism. However, the precise mechanism of AMPK activation by n-3 LC-PUFA is not known.

2 SPECIFIC AIMS OF WORK

The main objective of this thesis was to analyze mechanisms involved in the beneficial effect of n-3 LC-PUFA on the development of obesity and associated impairments of insulin sensitivity and other metabolic disturbances.

The specific aims of this thesis were:

1. to study the involvement of α2-AMPK in the beneficial effects of n-3 LC-PUFA by using knock-out mice with a targeted deletion of α2 catalytic subunit of AMPK (study 1),

2. to investigate the efficacy of n-3 LC-PUFA chemical derivatives to prevent and reverse the impairment of lipid and glucose metabolism by high-fat feeding (study 2),

3. to evaluate possible additive improvements of insulin sensitivity induced by the combination treatments of n-3 LC-PUFA and anti-diabetic drug rosiglitazone in the model of high-fat diet-induced obesity in mice (study 3).

3 METHODS

3.1 Animals and diets

We used the following mouse strains in our studies:

1. male and female whole-body α2-AMPK knock-out mice (α2-AMPK KO) and WT littermate controls (WT), originally generated on a hybrid C57BL/6 and 129/Sv genetic background (91) and subsequently backcrossed to C57BL/6J mice for 9 generations;
2. male C57BL/6N mice (Charles River Laboratories, Sulzfeld, Germany);
3. male C57BL/6J mice (The Jackson Laboratory, Bar Harbor, ME, USA).

Mice were bred in the animal facility of the Department of Adipose Tissue Biology, Institute of Physiology, Academy of the Sciences of the Czech Republic, v.v.i. At 4 weeks of age, mice were weaned onto a standard laboratory chow (Chow; lipid content ~3.4 % wt/wt; extruded R/MH diet; Ssniff Spezialdiäten, Soest, Germany) and maintained at 22 °C on a 12h light–dark cycle (light on from 06:00 a.m.) with a free access to food and water until the initiation of the experiment. Table 3.1-1 briefly summarizes the names and lipid composition of the experimental diets used in the studies described in this thesis.

Table 3.1-1 High-fat diets used in the experiments

Name	Lipid composition
cHF	lipids ~35% wt/wt (~60 energy %), mostly corn oil
Substances 1-4	based on cHF; 1,5 % of dietary lipids replaced by various DHA derivatives termed Substance 1-4
DHA	based on cHF; 15 % of dietary lipids replaced by DHA (~99%; ethyl ester; Pronova BioPharma AS, Lysaker, Norway)
cHF+F	based on cHF; 15 % of dietary lipids replaced by n-3 LC-PUFA concentrate (46% DHA, 14% EPA); (EPAX 1050TG of the EPAX AS, Lysaker, Norway)
cHF+TZD	based on cHF; supplemented with rosiglitazone (10 mg/kg diet) (Avandia, GlaxoSmithKline)
cHF+F+TZD	based on cHF; 15 % of dietary lipids replaced by n-3 LC-PUFA and supplemented with rosiglitazone (10 mg/kg diet)

All high-fat diets contained 210 mg α-tocopherol/kg diet. Protein content was ~20.5 % wt/wt, carbohydrate content was ~35 % wt/wt and energy density 22.8 kJ/g.

3.2 Experimental design

3.2.1 Study 1

Two separate experiments were performed. In both experiments, 4-month-old WT and α2-AMPK KO mice of both genders were randomly assigned (n = 13-15) to either chow, cHF or cHF+F diet (Table 3.1-1). Macronutrient and fatty acid compositions of all the diets have been described before (92). During dietary treatments, which lasted for 9 weeks, fresh rations of food were distributed every 2 days. Food consumption and body weights were recorded once a week.

Mice from the first experiment were sacrificed by cervical dislocation under diethyl ether anesthesia in a random-fed state (between 8:00 am and 10:00 am) and EDTA-plasma and tissues (liver; gastrocnemius, quadriceps and EDL muscles; epididymal and subcutaneous dorsolumbar white adipose tissue (WAT)) were sampled for various analyses (see below). One week before killing of male mice (i.e. at 8th week of dietary treatments), plasma samples were collected either from mice in fasted state (15 hours, from 8.00 am to 11:00 pm) or in 're-fed' state (fasting for 11 hours from 8.00 am to 7:00 pm, then on the respective diet for 3 hours).

Female mice from the second experiment were randomly divided into 2 subgroups. First group was used to measure *in vivo* VLDL-triacylglycerol synthesis, while the second one was used to assess *in vivo* glycemic control using intraperitoneal glucose tolerance test. Male mice underwent hyperinsulinemic-euglycemic clamp to determine *in vivo* insulin sensitivity in these mice.

3.2.2 Study 2

At 3 months of age, male mice of either C57BL/6N or C57BL/6J genetic background were randomly assigned to a cHF diet, while some mice were maintained on STD diet. Two experimental approaches were used:

1) In the "*prevention study"*, various DHA-derivatives (93) were admixed to the cHF diet (Substances-1 to -4) and administered to the 3-month-old C57BL/6N mice for a period of 4 months. The DHA-derivatives were tested in three separate experiments A, B, and C

(Experiment A: Substance-1; Experiment B: Substance-2 and -3; Experiment C: Substance-4).

2) In the "*reversal study"*, obesity and impaired glucose tolerance were induced in C57BL/6J mice by feeding cHF diet for a period of 4 months prior to the subsequent 2-month-long administration of Substance-2 admixed to the cHF diet. To analyze potential contribution of a lower food intake in the beneficial effect of Substance-2 on glucose homeostasis (as observed in the "*prevention study"*), food intake in a subgroup of cHF-fed mice was reduced by 12% compared with mice fed cHF diet *ad libitum* during the final 2 months of the "*reversal study"*. A separate experiment was also performed to evaluate the effect of cHF+F, as well as of pure DHA (~99%; ethyl ester; 15 % of cHF lipids replaced, Pronova BioPharma AS) in *ad libitum* fed mice.

cHF-fed mice always served as controls. Mice were killed by cervical dislocation under diethylether anesthesia between 9–11 a.m., subcutaneous dorsolumbar and epididymal WAT, interscapular brown adipose tissue (BAT), liver, and skeletal muscle (*musculus quadriceps femoris*) were dissected and snap-freezed in liquid nitrogen. Truncal blood was collected into the EDTA-containing tubes and plasma was isolated by centrifugation.

3.2.3 Study 3

The study was performed in oder to characterize the effects of n-3 LC-PUFA, rosiglitazone, and their combination, on developing obesity and impaired glucose tolerance in mice fed a high-fat diet. At 3 month of age, male C57BL/6N mice were randomly assigned to a cHF diet or to the treatments by cHF+F, cHF+TZD and cHF+F+TZD. Some mice were maintained on the chow diet. Various analyses were performed after 5 to 20 weeks after initiation of the treatment (92). Mice were killed under anaesthesia (9.00–11.00 a.m.) by cervical dislocation in *ad libitum* fed state, unless stated otherwise.

All experiments were conducted under the guidelines for the use and care of laboratory animals of the Institute of Physiology and followed the 'Principles of laboratory animal care' (NIH publication no. 85-23, revised 1985).

3.3 Plasma metabolites, hormones and enzymes

Blood glucose was measured from the tail bleeds using calibrated glucometers OneTouchUltra (Life Scan, Milpitas, CA, USA). Other metabolites were determined in EDTA-plasma obtained from centrifuged blood as supernatant (7000g, 10 min, 4°C). Non-esterified fatty acids (NEFA), triacylglycerols and cholesterol were detected by using commercial kits (NEFA C, Wako Chemicals, Neuss, Germany; Triacylglycerols Liquid, PLIVA-Lachema Diagnostika, Brno, CZ and Cholesterol Liquid, PLIVA-Lachema Diagnostika, Brno, CZ; respectively). Plasma insulin levels were determined by the Sensitive Rat Insulin RIA Kit (LINCO Research, St Charles, MO). Distribution of adiponectin multimeric complexes was assessed using western blotting (94).

3.4 Tissue glycerolipid content

Liver and muscle glycerolipid content was estimated in ethanolic KOH tissue solubilisates. Tissue fragments (~50 mg) were digested in 0.15 ml of 3 M alcoholic KOH (70°C, 2 hours) and the resulting homogenates were diluted 10-fold with H_2O. Liberated glycerol was assayed in supernatants (3 μl) by Triacylglycerols Liquid (Pliva-Lachema Diagnostika, Brno, Czech Republic). Tissue glycerolipid concentration was calculated relative to a triacylglycerol standard (1.65 mmol/l; Lyonorm Calibrator, Pliva-Lachema Diagnostika, Brno, Czech Republic).

3.5 Fatty acid composition of lipid fractions

The samples were pulverized in an aluminum mortar precooled in liquid nitrogen. The powder was transferred to a tube containing ice-cold methanol and 0.01% butylated hydroxytoluene (Sigma) as an antioxidant. Internal standards (1,2-diheptadecanoin, triheptadecanoin and 1,2-diheptadecanoyl-sn-glycero-3-phosphatidylcholine, Larodan Fine Chemicals, Sweden) were then added to the samples and lipids were extracted by the method of Folch. The fractions of total phospholipids, triacylglycerols and diacylglycerols were separated by thin-layer chromatography (95). Lipid class standards were spotted on the outside lanes of the chromatography plate to enable localization of the sample lipid classes. The gel bands corresponding to the standards were scrapped off the plates, transferred into fresh tubes and then transmethylated in 14% methanolic boron trifluoride (Sigma) at 100°C

for either 10 or 30 minutes (phospholipids and triacylglycerols). The content of resulting fatty acid methyl esters was determined by means of gas-liquid chromatography (96).

3.6 Tissue ceramide content

The content of ceramides was determined as described previously (97) with the exception that N-palmitoyl-D-*erythro*-sphingosine was used as an internal standard.

3.7 RNA extraction and real-time quantitative analysis

Total RNA was isolated from liver samples (stored in RNA*later* Solution; Ambion, Austin, TX) by homogenization and using TRIzol Reagent (Invitrogen, Carlsbad, CA). A quantity of 0.5 µg of total RNA was reverse transcribed to DNA and gene expression was analyzed by real-time PCR, using the LightCycler Instrument (Roche Diagnostics, Mannheim, Germany) and qPCR kit (DyNAmoCapillary SYBRGreen, Finzymes, Espoo, Finland). Oligonucleotide primers, described in Table 3.7-1, were designed using Lasergene software (DNAStar, Madison, WI). Levels of transcripts were standardised using the gene encoding peptidylpropyl isomerase B (*Ppib,* also called cyclophilin B). Gene expression data were expressed as a percentage of the cHF-fed controls.

Table 3.7-1 List of oligonucleotide primers used in the study

Gene	Primer (forward/reverse)
AOX-1	GCTGGGCTGAAGGCTTTTACTACC/CACCTGCTGCGGCTGGATAC
CD68	CACTTCGGGCCATGTTTCTCTTG/AGGGGCTGGTAGGTTGATTGTCGT
ChREB	TGCCACTGCCAGAGACAACAACC/ACGGGCACGGGGGATTTCA
CPT-1α	GCAGCTCGCACATTACAAGGACAT/AGCCCCCGCCACAGGACACATAGT
FAS	GGCTGCCTCCGTGGACCTTATC/GTCTAGCCCTCCCGTACACTCACTCGT
FDPS	ATGCCATCAACGACGCTCTGCT/TGGCCCTGGGGTGCTGTCA
GLUT-4	ACCGGCTGGGCTGATGTGTCT/GCCGACTCGAAGATGCTGGTTGAATAG
MCP-1	GTTAACGCCCCACTCAC/GGTTCCGATCCAGGTTT
PDK-4	GGCTTGCCAATTTCTCGTCTCTA/TTCGCCAGGTTCTTCGGTTCC
PGC-1α	CCCAAAGGATGCGCTCTCGTT/TGCGGTGTCTGTAGTGGCTTGATT
PPAR-α	TGCGCAGCTCGTACAGGTCATCAA/CCCCCATTTCGGTAGCAGGTAGTCTTA
PPIB	GGGAGATGGCACAGGAGGAAAGAG/ACCCAGCCAGGCCCGTAGTG
SCD-1	ACTGGGGCTGCTAATCTCTGGGTGTA/GGCTTTATCTCTGGGGTGGGTTTGTTA
SPOT 14	GCTGCTGCCAAGGGAGGAATG/CCGGGTCAGGTGGGTAAGGATG
SREBP-1c	TACCCGTCCGTGTCCCCCTTTTC/TGCGCTTCTCACCACGGCTCTG

AOX-1, acyl-CoA oxidase-1; CD68, cluster of differentiation 68; CPT-1α, carnitine palmitoyltransferase-1α; FDPS, farnesyl diphosphate synthase; GLUT-4, glucose transporter-4; MCP-1, monocyte chemoattractant protein-1; PDK-4, pyruvate dehydrogenase kinase-4; PGC-1α, peroxisome proliferator-activated receptor-γ coactivator-1α; PPAR-α, peroxisome proliferator-activated receptor-α; PPIB, peptidylpropyl isomerase β; SCD-1, stearoyl-coenzyme A desaturase-1; SPOT 14, thyroid hormone responsive SPOT 14; SREBP-1c, sterol regulatory element binding protein-1c; ChREBP, carbohydrate responsive element-binding protein; FAS, fatty acid synthase.

3.8 Activity of α1 and α2 AMPK isoforms

Livers of female mice from the second experiment (Study 1) were collected by freeze-clamp technique. AMPK was immunoprecipitated from tissue extracts prepared by homogenization in buffer A and the activity was assayed using a peptide substrate (98).

3.9 Determination of liver ATP, ADP and AMP

Flash-frozen liver samples were extracted by homogenization in liquid nitrogen and 6% (w/v) perchloric acid (500 μl of solution/100 mg of tissue). Supernatants (10 min, 10000 *g*, 4 °C) were neutralized with 0.4 M triethanolamine/1.8 M KOH and pH was adjusted to 6-7. ATP, ADP and AMP were determined using the HPLC procedure (99). Separation and quantification was performed using a Hewlett-Packard HP 1100 system with a diode array detector. Calibration was performed using the appropriate standards.

3.10 Light microscopy and immunohistochemical analysis

Samples of epididymal WAT and liver were fixed in 4% formaldehyde, embedded in paraffin and cut into 5 μm-sections. The liver sections were stained by hematoxylin-eosine, while the sections of epididymal fat were processed to detect a macrophage marker, MAC-2/galectin-3, by the use of specific antibodies (100). Digital images were captured using Olympus AX70 light microscope and a DP 70 camera (Olympus, Tokyo, Japan). Adipocyte morphometry was performed using a Lucia IMAGE version 4.81 (Laboratory Imaging, Prague, Czech Republic).

3.11 Intraperitoneal glucose tolerance test

An intraperitoneal glucose tolerance test was performed to evaluate glucose tolerance, i.e. how quickly the exogenous bolus of glucose is cleared from the blood circulation. Mice fasted overnight (15-16 h) were loaded intraperitoneally with a water solution of D-glucose (1g/kg body weight). Blood glucose was measured from tail bleeds at baseline and at 15, 30, 60, 120 and 180 min after the glucose bolus injection. Glucose tolerance was calculated from the glycemic curves as the area under the curve (AUC). AUC is inversely proportional to the glucose tolerance.

3.12 Hyperinsulinemic-euglycemic clamp technique

Hyperinsulinemic-euglycemic clamp technique is a gold-standard method to measure insulin sensitivity *in vivo* in the well-defined conditions and it can quantify the individual glucose fluxes in the body, i.e. glucose turnover in the peripheral tissues, hepatic glucose production, glycolysis and glycogen synthesis.

3.12.1 Surgery

To perform hyperinsulinemic-euglycemic clamp, catheter is inserted into a femoral vein. Five days before the experiment, mice were anaesthetized with a mixture of Ketamin (10%, Narkamon, Spofa, CR) and Xylazine (2%, Xylazin, Riemser, SRN) dissolved in saline. Mice were injected with a dose of 1 µl of anaesthesia per 1 g of body weight. 5-10 min after the injection, animal was attached to the surface lying on its back. By using a microscope, 10 cm-long nylon catheter (Medical grade nylon tubing, internal ∅=0.3048 mm, external ∅=0.635 mm, Ulrich Swiss, Switzerland), filled with saline, was placed into the left femoral vein using the following procedure: 1) cutting the skin line stretching between the left lower leg and right upper leg (101), 2) careful cleaning of the vein, 3) inserting the proximal, distal and medial ligatures onto the vein and finally 4) cutting the vein with special scissors (Vannas titanium scissors; WPI, USA), making a small transversal cut. Catheter was affixed to the surrounding tissue using the surgical glue (Histoacryl®; B. Braun Medical, CR). The opposite ending of the catheter was lead under the skin and externalized behind the neck.

3.12.2 Hyperinsulinemic-euglycemic clamp procedure

Mice were allowed to recover for 5-7 days after the surgery. The experiment was conducted in conscious mice fasted for 6 h (from 8:00 a.m. to 2:00 p.m.). At the beginning of the experiment, basal blood glucose was measured using calibrated glucometer (see Chapter 3.3) and 5 µl of blood was sampled. The test was initiated by the constant infusion of insulin (4.79 mU · kg^{-1} · min^{-1}; Actrapid, NovoNordisk) and D-[3-^{3}H]glucose (15.9 kBq · kg^{-1} . min^{-1}) in the buffer consisting of 0.02% BSA, 0.02M

HCl and 0.9% NaCl (CMA Microdialysis pump, Sweden). The blood glucose level was measured in 10-min intervals. When glycemia began to fall, the variable infusion of glucose (33 % w/v) was initiated (Figure 3.12-1). The rate of glucose infusion was periodically adjusted to maintain euglycemia (blood glucose concentration ~ 5.5 mmol/l) during first two hours of the test. The blood aliquots (5 μl) for the biochemical analysis were sampled in 10-minute intervals during the last hour of the clamp.

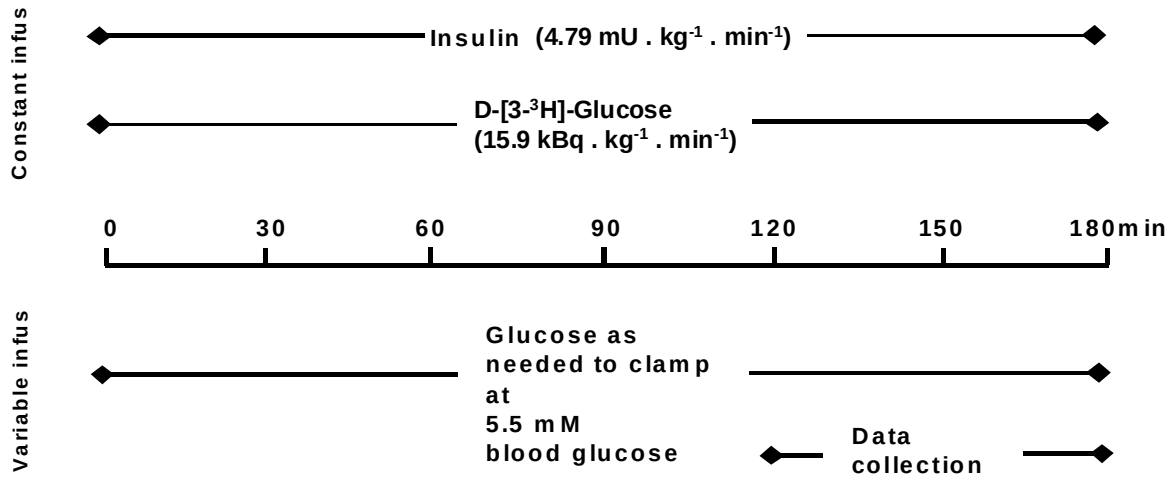

Figure 3.12-1 The scheme of hyperinsulinemic-euglycemic clamp test

At the end of the 3-hour-infusion period, mice were sacrificed by cervical dislocation under diethyl ether anesthesia and EDTA-plasma and tissues (liver and quadriceps muscle) were collected for biochemical analysis.

3.12.3 Analysis of blood and tissue samples

To assess D-[3-^{3}H]glucose, ^3H_2O and total glucose concentrations, blood samples were firstly de-proteinized by precipitation with a $ZnSO_4/Ba(OH)_2$, followed by centrifugation (10 min, 5000 *g*,4°C). The first aliquot of the supernatant was evaporated to dryness to determine the radioactivity corresponding to D-[3-^{3}H]glucose. The second aliquot was used for the determination of the radioactivity of both D-[3-^{3}H]glucose and ^3H_2O. Plasma ^3H_2O radioactivity was then calculated as the difference between radioactivity in the second and the first sample. In the third aliquot of the supernatant,

total glucose concentration was assessed by the glucose oxidase method (Glukosa God 1500, PLIVA-Lachema, Czech Republic).

To assess the content of D-[3-^{3}H]glucose in the liver and quadriceps or gastrocnemius skeletal muscle, the glycogen was firstly isolated from the individual tissues. Tissues were digested in the 1M KOH by incubating at 80°C for 45 min. The supernatant (10 min, 10000 *g*, 22°C) was precipitated in 96% ethanol over-night (-20°C). The pellet of precipitate (30 min, 1680 *g*, 4°C) was washed with 70% ethanol, air-dried and dissolved in the 4M H_2SO_4 at 100°C for 15 min. After the neutralization with 4M NaOH, the supernatant (2 min, 10000 *g,* 22°C) was de-proteinized by precipitation with a $ZnSO_4$/$Ba(OH)_2$, followed by centrifugation (10 min, 5000 *g*,4°C). One aliquot of the glycogen extract was used to measure the content of D-[3-^{3}H]glucose, the second one to evaluate the total glycogen content using de-proteinized glucose standards.

3.12.4 Calculations

The whole-body insulin sensitivity assessed by hyperinsulinemic-euglycemic clamp is characterized by the rate of exogenous glucose infusion needed to maintain steady euglycemia in the organism during the test. The glucose infusion rate (GIR; μmol.kg^{-1}.min^{-1}) can be easily calculated from the rate of the glucose infusion read on the infusion pump (gir; μmol.min^{-1}), glucose concentration in the infusion solution (c; μM) and body weight of the animal (m; kg):

$$GIR = \frac{gir \times c}{m} \quad \left[\mu mol \cdot kg^{-1} \cdot \min^{-1}\right]$$

The rate of whole-body glucose turnover (GTR; μmol.kg^{-1}.min^{-1}) was determined as the ratio of D-[3-^{3}H]glucose infusion rate (R_a^*, dpm . min-^{1}) to the specific activity (Sa_g) of plasma glucose (dpm/μmol) and body weight (m; kg):

$$GTO = \frac{R_a^*}{SA_g \cdot m} \quad [\mu mol \cdot kg^{-1} \cdot \min^{-1}]$$

$$SA_g = \frac{c([3\text{–}^3H]Gluc)}{c(Gluc)} \quad [dpm \cdot \mu mol^{-1}]$$

Glucose turnover rate is the sum of the infused exogenous glucose and the glucose produced endogenously in the liver (Figure 3.12-2).

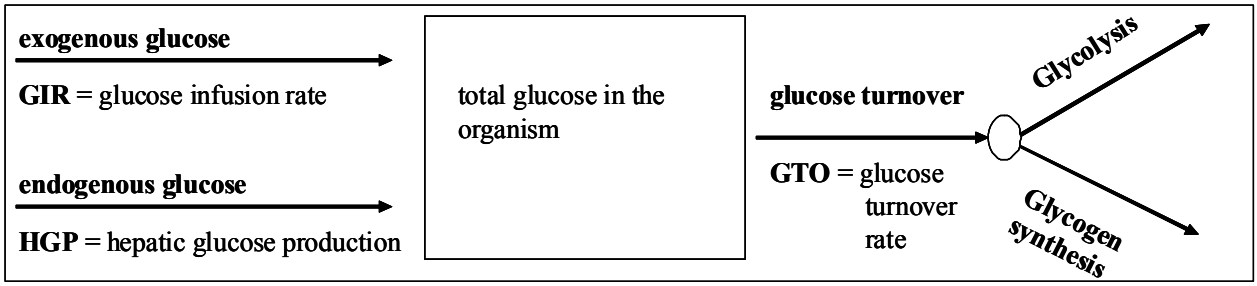

Figure 3.12-2 The simplistic model of glucose fluxes within the organism

Thus, the rate of the hepatic glucose production (HGP, μmol.kg^{-1}.min^{-1}) can be easily calculated by subtracting the glucose infusion rate from the glucose turnover rate:

$$HGP = GTO - GIR \quad [\mu mol \cdot kg^{-1} \cdot \min^{-1}]$$

Assuming that tritium on the C-3 position of glucose is lost to water during glycolysis, it can be assumed that plasma tritium is present either in tritiated water or [3-^{3}H]-glucose (102). Although tritium may also be released during fructose-6-phosphate and/or pentose phosphate cycling, these pathways account for only a small percentage of glucose turnover. Additionally, some of the glucose carbons from pentose phosphate pathway will re-enter the glycolysis through glyceraldehydes. Thus, the rate of whole-body glycolysis was estimated from the appearance of the tritiated water in plasma water during the last hour of the clamp. Plasma water was assumed to be 93% of the total plasma volume and the total body water mass was assumed to be 65% of the body mass (103). The final formula to calculate the whole-body glycolysis was:

$$Glycolysis = \frac{[^3H]H_2O}{SA_g} \times 0.93 \times 0.65 \quad [\mu mol \cdot kg^{-1} \cdot \min^{-1}]$$

$[^3H]H_2O$ represents the increment per unit time in tritiated water. The calculation of glycolytic flux using the above approach assumes that the appearance of $[^3H]H_2O$ in the plasma is representative of the appearance in the whole body and the loss of $[^3H]H_2O$ during the 3h experiment is negligible. Both of these assumptions were previously experimentally validated (103). Concerning that glycolysis and glycogen synthesis account for the majority of the insulin-stimulated glucose turnover (Figure 3.12-2), the rate of whole-body glycogen synthesis can be calculated by subtracting the whole-body rate of glycolysis from the glucose turnover rate:

$$Glycogen\ synthesis = GTO - Glycolysis \quad [\mu mol \cdot kg^{-1} \cdot \min^{-1}]$$

The rate of glycogen synthesis in individual tissues (liver, quadriceps and gastrocnemius skeletal muscle) was quantitated by measuring the incorporation of D-[3-^{3}H]glucose into glycogen. It was obtained by dividing the radioactivity of D-[3-^{3}H]glucosyl units in glycogen (dpm.kg^{-1}) by the mean specific activity of D-[3-^{3}H]glucose in plasma during the last hour of the clamp:

$$Tissue\ glycogen\ synthesis = \frac{[3-^3H]glucose(glycogen)}{SA_g} \quad [\mu mol \cdot kg^{-1} \cdot \min^{-1}]$$

3.13 *Ex vivo* glucose uptake by muscle

Ex vivo glucose uptake by extensor digitorum longus (EDL) muscle was assessed in overnight fasted mice (15 h). Mice were anesthetized with pentobarbital, and their EDL muscles were removed. The muscles were pre-incubated for 10 min at 37 °C in 1.5 ml of basal medium consisted of 0.1% BSA, 8 mM mannitol, and 2 mM pyruvate in Krebs-Ringer-Bicarbonate buffer (118 mM NaCl, 4.7 mM KCl, 2.7 mM $CaCl_2$, 1.2 mM KH_2PO_4, 1.1 mM $MgSO_4$, 25 mM $NaHCO_3$, pH = 7.4). At the end of pre-incubation period, muscles were transferred to 1.5 ml of media containing 1 mM 2-deoxy D-

glucose and 500 μU/ml insulin (Actrapid, Novo Nordisk A/S, Bagsvær, Denmark) and incubated for 15 min at 37°C. Measurements of 2-deoxy-D-glucose uptake were initiated by incubation in 1.5 ml of media without or with 500 μU /ml insulin, 2-[1,2-^{3}H] deoxy-D-glucose (PerkinElmer, Shelton, USA) with a specific activity in the media of 0.25 mCi/ml, and [1-^{14}C] mannitol (PerkinElmer, Shelton, USA) with a specific activity in the media of 0.16 mCi/ml. Uptake was measured for 15 minutes. All the buffers were continuously gassed with 95% O_2–5% CO_2. To terminate the transport, muscles were taken out, washed in basal media, blotted on a filter paper, trimmed, and quickly frozen and stored at −20 °C. Muscles were processed by incubating in 200 μl 1N NaOH at 80°C for 10 min, neutralized with 0.2 ml 1N HCl, and centrifuged at 13,000 × g for 2 min. Radioactivity in the supernatant was measured using liquid scintillation counting for dual labels.

3.14 *In vivo* VLDL-triacylglycerol synthesis: Tyloxapol test

The rate of liver VLDL-triacylglycerol synthesis was evaluated according to a standard protocol (104) using Triton WR1339, an inhibitor of tissue lipoprotein lipase (LPL). Mice were fasted for 6 h and anesthetized with Pentobarbital (107 mg/kg of body weight). Triton WR1339 (15 g/dl in 0.9% NaCl; Sigma) was injected intravenously in a dose of 500 mg/kg of body weight. Blood samples were taken before injection of Triton WR1339 and 1, 2, 3 and 4 h after injection. The level of triacylglycerols in plasma was determined using enzymatic kit (Triacylglycerol liquid, BioLaTest, Lachema). The rate of hepatic VLDL-TG production was calculated from the slope of the curve of the increase in plasma triacylglycerols and expressed as mmol.l^{-1}.h^{-1}.

3.15 Indirect calorimetry measurement

Energy expenditure was evaluated in 30°C using the indirect calorimetry system INCA (Somedic, Horby, Sweden) as described before (105). Mice were transferred into sealed chambers equipped with thermostatically controlled heat exchangers. Calibration of oxygen sensors was performed before each measurement. Measurements proceeded under a constant airflow rate (1,000 ml/min). Oxygen consumption (VO_2) and carbon dioxide production (VCO_2) were recorded every 2 min. The system allowed for 4

individually housed mice to be monitored simultaneously. The overall measurement lasted for 46 h and started at 3 p.m. (12-h light-dark cycle; light from 6 a.m.). Animals were measured at 3 different metabolic conditions: 1) *ad libitum* access to their respective diets from 3 p.m. until 8 a.m. (17 h); 2) fasted state from 8 a.m. until 7 p.m. (11 h); and 3) glucose re-fed state with a free access to chow diet from 7 p.m. until 1 p.m. next day (18 h). The level of substrate partitioning was estimated by calculating respiratory exchange ratio (RER; i.e. VCO_2/VO_2 ratio).

3.16 Nor-epinephrine stimulated lipolysis

Firstly, the adipocytes were isolated from the white epididymal adipose tissue according to Rodbell et al. (106). Tissues collected from mice were firstly incubated in KRB buffer (118.5 mM NaCl, 4.8 mM KCl, 2.7 mM $CaCl_2$, 1.2 mM KH_2PO_4, 1.1 mM $MgSO_4$,$7H_2O$, 25 mM $NaHCO_3$) with 5mM glucose. Minced tissues were digested in the KRB buffer with glucose, containing 4% (w/v) BSA and 3 mg/ml type II collagenase (Sigma) while shaking at 37 °C for 45 min. The digested tissue was then filtered (250 μm) and floating adipocytes were washed three times in the KRB buffer in the absence of collagenase and centrifuged (1 min, 400 *g*, 20 °C). Isolated adipocytes were used for the measurement of lipolysis and DNA content. Lipolysis was estimated by following the rate of glycerol release from isolated adipocytes. Aliquots (50 μl) of cell suspension (10%, v/v) in KRB buffer (see above) were incubated in a 96- well dish for 60 min at 37 °C in 10% CO_2/90% air with nor-epinephrine (1 μM) or with nor-epinephrine and insulin (1 μM and 500 pM, respectively). Infranatant (60 μl) was collected and heated for 15 min at 70 °C to inactivate any enzyme released from the cells. Glycerol was assayed spectrophotometrically using a Free Glycerol Reagent kit (Sigma-Aldrich, USA). The DNA content of isolated adipocytes was measured fluorometrically after digestion (at 56 °C, overnight) in 150 μl of a medium containing 20 mM Tris, 10 mM EDTA, 1% (w/v) SDS and 50 μg/ml proteinase K (107).

3.17 Statistics

Data were analyzed by two-way ANOVA using the SigmaStat software. All values are presented as means±SE. Comparisons were judged to be significant at $p \leq 0.05$.

4 RESULTS

4.1 The involvement of α2-AMPK in the beneficial effects of *n*-3 LC-PUFA

My contribution to this work was coordination of the experiments, mice genotyping, measurement of insulin sensitivity by the hyperinsulinemic-euglycemic clamp technique, assessment of glucose tolerance by glucose tolerance test, assessment of VLDL-TAG synthesis, measurement of plasma and tissue metabolites and isolation of RNA and real-time PCR quantitative analysis.

The other contributors are:

Zuzana Macek Jílková	*(insulin measurement, adipose tissue and liver histology)*
Daša Medříková	*(adiponectin measurement)*
Vladimír Kůs	*(glucose uptake, indirect calorimetry)*
Petra Janovská	*(rate of lipolysis, indirect calorimetry)*
Ondřej Kuda	*(glucose uptake)*
Ivan Mikšík	*(assessment of nucleotides)*
Marcin Baranowski	*(fatty acid composition).*

We sought to determine, which of the beneficial effects of *n*-3 LC-PUFA in the prevention of high-fat diet-induced obesity and insulin resistance are mediated through α2-AMPK catalytic subunit. To accomplish this, we used a model of α2-AMPK knock-out mice (α2-AMPK KO) and their littermate controls (WT) fed chow, cHF and cHF+F diet for 8 weeks (see Chapter 3.2.3).

4.1.1 α1-AMPK and α2-AMPK activity profile in tissues

Specific activities of α1-AMPK and α2-AMPK were evaluated in the liver, gonadal adipose tissue and skeletal muscle (quadriceps) of female α2-AMPK KO and WT mice analyzed in ad libitum ('random-fed') state after 9 weeks of the differential dietary treatment. No significant differences in diet- or genotype-induced α1-AMPK activity

were detected in any of the tissues. α2-AMPK activity, if measured, was detected only in low residual levels in α2-AMPK KO mice (Table 4.1-1). The only significant change of α2-AMPK activity was observed in the liver of WT mice in response to the cHF+F diet rich in n-3 LC-PUFA.

Table 4.1-1 α1- and α2-AMPK activities in various tissues

	WT		
	Chow	**cHF**	**cHF+F**
Liver			
α1-AMPK	0.027 ± 0.008	0.040 ± 0.009	0.039 ± 0.011
α2-AMPK	0.033 ± 0.004	0.042 ± 0.006	0.057 ± 0.005†
Gon WAT			
α1-AMPK	0.065 ± 0.009	0.088 ± 0.001	0.066 ± 0.007
α2-AMPK	ND	ND	ND
Quadriceps SM			
α1-AMPK	0.078 ± 0.016	0.102 ± 0.012	0.070 ± 0.024
α2-AMPK	0.070 ± 0.014	0.077 ± 0.008	0.086 ± 0.011
	α2-AMPK KO		
	Chow	**cHF**	**cHF+F**
Liver			
α1-AMPK	0.064 ± 0.022	0.062 ± 0.013	0.058 ± 0.009
α2-AMPK	0.004 ± 0.001‡	0.009 ± 0.003‡	0.003 ± 0.002‡
Gon WAT			
α1-AMPK	0.072 ± 0.010	0.089 ± 0.017	0.073 ± 0.008
α2-AMPK	ND	ND	ND
Quadriceps SM			
α1-AMPK	0.108 ± 0.018	0.095 ± 0.016	0.087 ± 0.017
α2-AMPK	0.011 ± 0.005‡	0.005 ± 0.002‡	0.004 ± 0.002‡

Data are presented as means ± SE (n = 5-8). *$P < 0.05$ vs. genotype chow; †$P < 0.05$ vs. genotype cHF; ‡$P < 0.05$ vs. WT on respective diet. Gon WAT- gonadal adipose tissue; SM-skeletal muscle.

4.1.2 Tissue concentrations of AMP,ADP, ATP, and the AMP:ATP ratio

Liver content of adenosine nucleotides was measured. The only significant difference observed was the decrease of ADP content in WT mice fed cHF diet (Figure 4.1-1, B). Evaluation of the AMP:ATP ratio, which is related to the activity of AMPK, showed similar levels in all experimental subgroups (Figure 4.1-1, D).

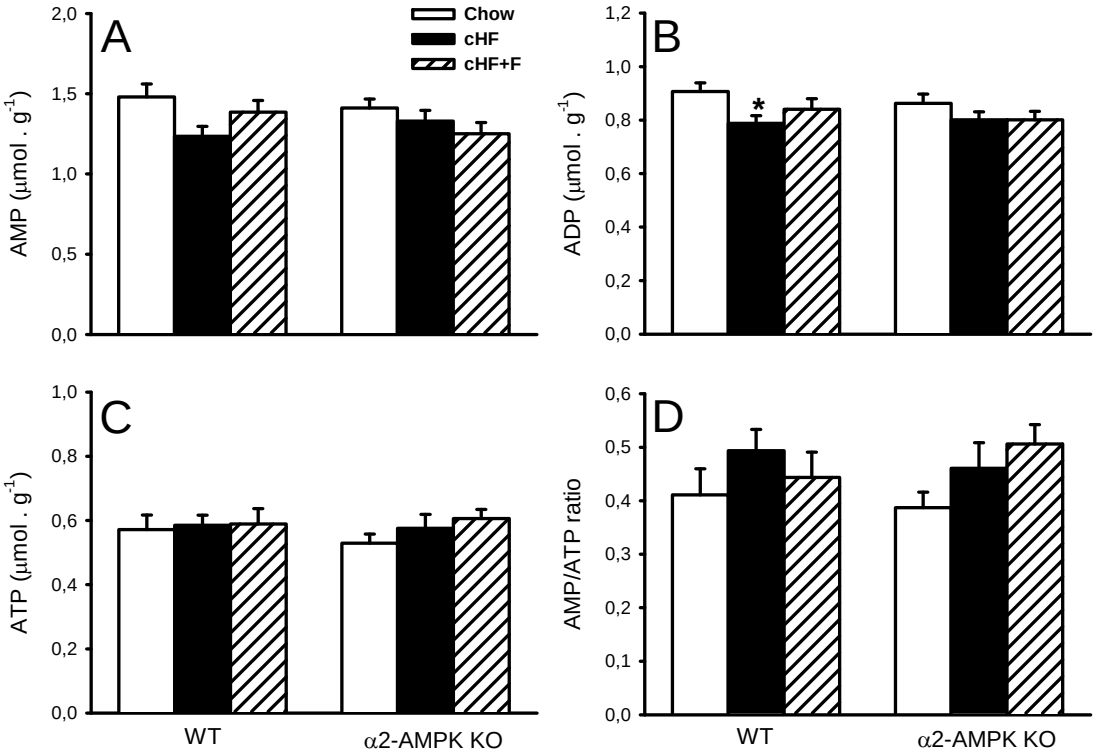

Figure 4.1-1 The content of adenosine nucleotides in the liver: AMP (A), ADP (B), ATP (C) and AMP/ATP ratio (D). Livers were collected in random-fed state from α2-AMPK KO and WT female mice fed for 9 weeks with control low-fat diet (Chow), control high-fat diet (cHF) or high-fat diet, in which 15% of lipids were replaced by n-3 LC-PUFA concentrate (cHF+F). Data are presented as means ± SE (n = 8-14). **P* < 0.05 vs. genotype chow; †*P* < 0.05 vs. genotype cHF; ‡*P* < 0.05 vs. WT on respective diet.

4.1.3 Regulation of glucose homeostasis

4.1.3.1 *In vivo* glucose tolerance

Glucose tolerance was investigated in female mice by the intraperitoneal glucose tolerance test. Firstly, blood glucose levels were not significantly changed in any of the experimental subgroups (Figure 4.1-2 A). The level of glucose tolerance is inversely related to the total area under the curve (AUC) of blood glucose appearance. As can be seen from the Figure 4.1-2 B, there was a tendency in WT female mice fed cHF diet for impaired glucose tolerance. On the other hand, mice fed the cHF+F diet seemed to be protected from this impairment and their glucose tolerance was comparable to mice fed chow diet. In contrast to WT mice, glucose tolerance in α2-AMPK KO mice fed cHF did

not change compared to chow-fed counterparts. Importantly, cHF containing n3-LC PUFA did not improve glucose tolerance in α2-AMPK KO mice as compared to their counterparts fed the cHF diet.

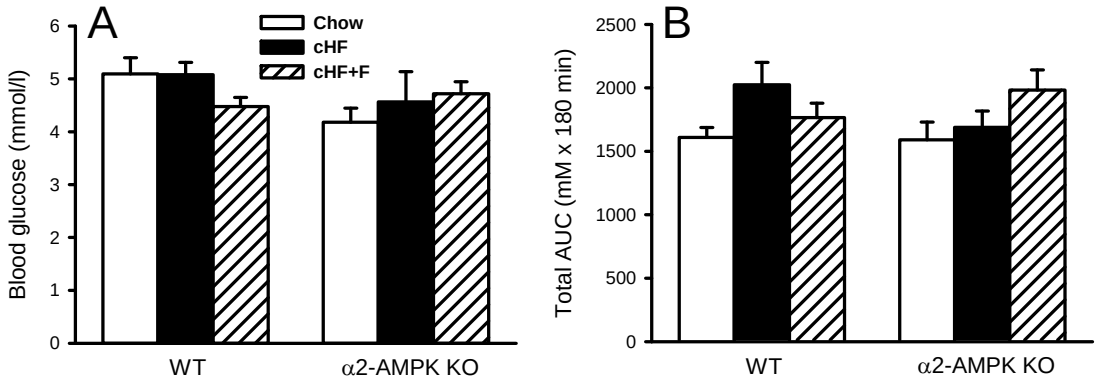

Figure 4.1-2 Glucose tolerance of female mice. Intraperitoneal glucose tolerance test was performed in α2-AMPK KO and WT female mice fed for 9 weeks with control low-fat diet (Chow), control high-fat diet (cHF) or high-fat diet, in which 15% of lipids were replaced by n-3 LC-PUFA concentrate (cHF+F). Fasting blood glucose levels at the start of the test (A), and area under the glycemic curve (B) are shown. Data are presented as means ± SE (n = 5-8). AUC, area under the curve.

4.1.3.2 *In vivo* insulin sensitivity

Insulin sensitivity was further measured in male mice by using more sensitive technique of hyperinsulinemic-euglycemic clamp. The steady state of euglycemia was accomplished, as it is obvious from the mean blood glucose levels, which remained unchanged during the last two hours of the clamp (Figure 4.1-3 A). WT and α2-AMPK KO mice fed cHF diet manifested whole-body insulin resistance as indicated by lower glucose infusion rates compared to mice fed the low-fat chow diet (Figure 4.1-3 B). This was due to both: 1) decreased insulin sensitivity of peripheral tissues (decreased glucose turnover rates (Figure 4.1-3 C) and 2) impaired suppression of hepatic glucose production by insulin (Figure 4.1-3 D). Feeding WT mice with cHF+F improved whole-body insulin sensitivity and this was due to an improvement of insulin action to suppress glucose output in the liver (an effect, which we have observed in C57BL/6N mice, Study 2, (92)). As in the case of glucose tolerance in female mice, this beneficial effect of cHF+F diet was observed only in WT mice with functional α2-AMPK. cHF+F diet was not sufficient to restore impaired liver insulin sensitivity in α2-AMPK deficient mice

(Figure 4.1-3 D). Insulin sensitivity in peripheral tissues was not significantly influenced by cHF+F feeding. There were no significant differences in whole-body glycolysis between any of the experimental subgroups (Figure 4.1-3 E), however, glycogen synthesis was decreased in WT mice fed cHF diet and improved by feeding with cHF+F diet (Figure 4.1-3 F). The effect of cHF+F diet was not observed in α2-AMPK KO mice.

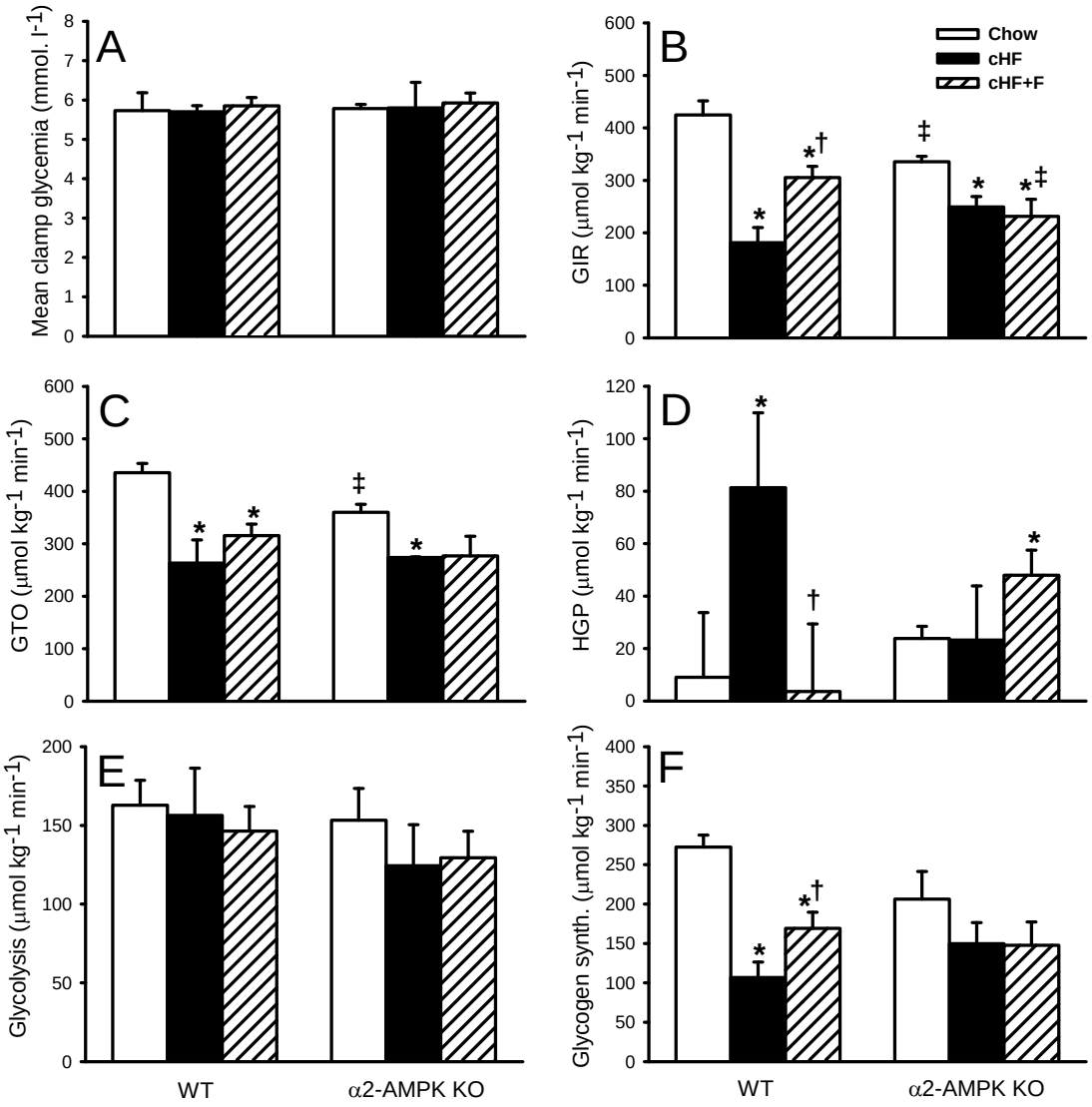

Figure 4.1-3 Insulin sensitivity of male mice. Mean clamp glucose (A), glucose infusion rate (GIR) (B), glucose turn-over rates (GTO) (C), hepatic glucose production (HGP) (D), whole-body glycolysis (E) and glycogen synthesis (F) assessed by hyperinsulinemic-euglycemic clamp in α2-AMPK KO and WT male mice fed for 9 weeks with control low-fat diet (Chow), control high-fat diet (cHF) or high-fat diet, in which 15% of lipids were replaced by n-3 LC-PUFA concentrate (cHF+F). Data are presented as means ± SE (n = 5-8). *$P < 0.05$ vs. genotype chow; †$P < 0.05$ vs. genotype cHF; ‡$P < 0.05$ vs. WT on respective diet.

The effects of diets and genotypes on glycogen synthesis in the individual tissues (Figure 4.1-4) (liver (A), quadriceps (C) and gastrocnemius (E) skeletal muscle) were similar to the effects on the whole body glycogen synthesis (Figure 4.1-3 F).

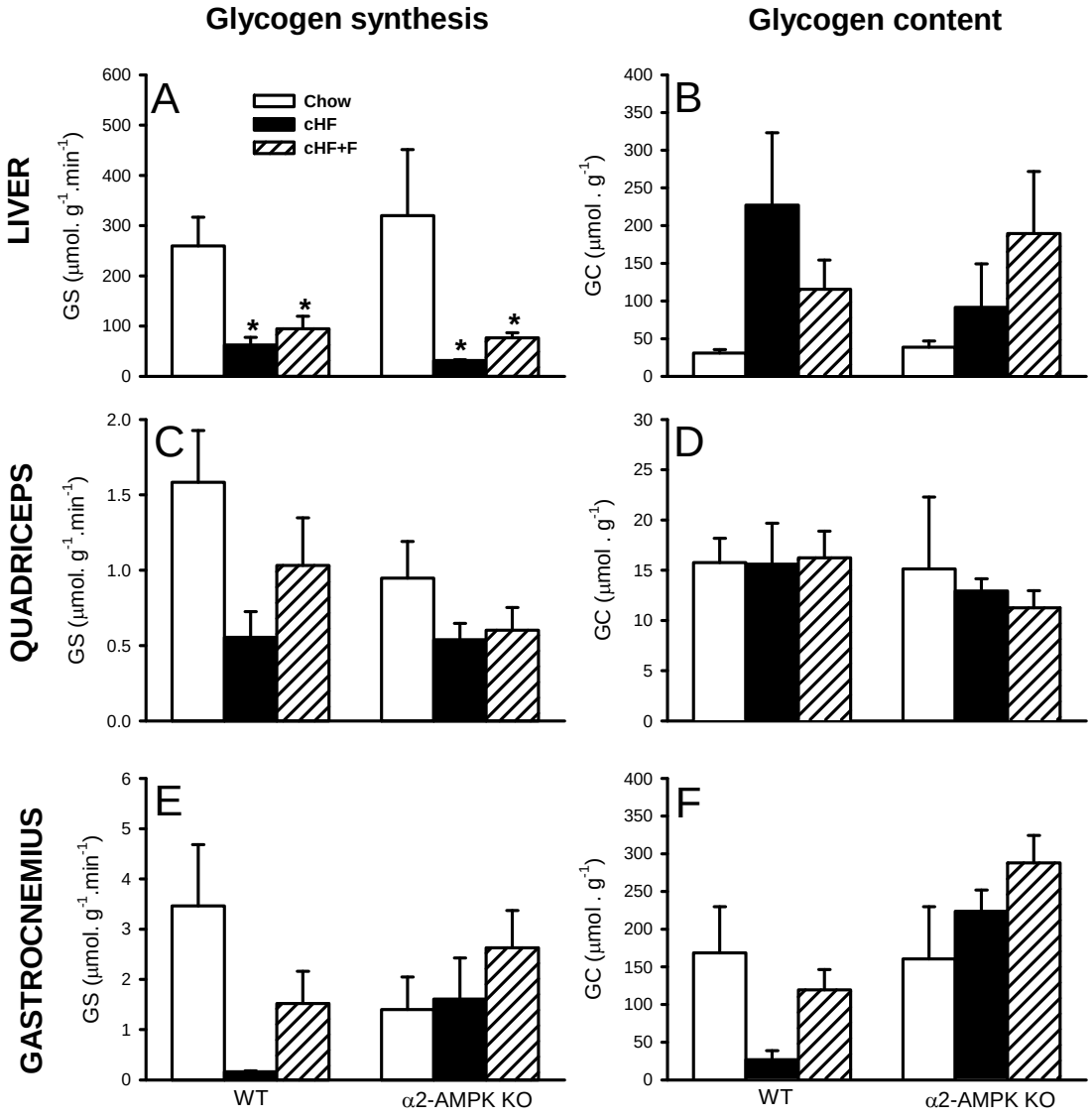

Figure 4.1-4 Tissue glycogen synthesis and content. Glycogen synthesis (A, C, E) and glycogen content (B, D, F) in the liver (A, B), quadriceps (C, D) and gastrocnemius (E, F) of α2-AMPK KO and WT male mice fed for 9 weeks with control low-fat diet (Chow), control high-fat diet (cHF) or high-fat diet, in which 15% of lipids were replaced by n-3 LC-PUFA concentrate (cHF+F). Data are presented as means ± SE (n = 5-8). **P* < 0.05 vs. genotype chow; †*P* < 0.05 vs. genotype cHF; ‡*P* < 0.05 vs. WT on respective diet.

However, the content of glycogen at the end of the clamp differed between the individual tissues. In the liver, cHF feeding tended to increase glycogen content in both genotypes while cHF+F diet suppressed this increase only in WT mice, even though insignificantly (Figure 4.1-4 B). The level of glycogen in both skeletal muscles was similar in all subgroups, nevertheless in gastrocnemius of WT mice fed cHF diet tended to be decreased.

4.1.3.3 *Ex vivo* glucose uptake by skeletal muscle

Muscle insulin sensitivity was assessed by its capacity to absorb glucose after stimulation by insulin in *ex vivo* explants of extensor digitorum longus (EDL) muscle. It is evident, that there were no significant diet-induced changes in EDL glucose uptake, neither in basal, nor in insulin stimulated conditions (Figure 4.1-5). There was a tendency in the α2-AMPK KO mice for a small decrease in muscle glucose uptake.

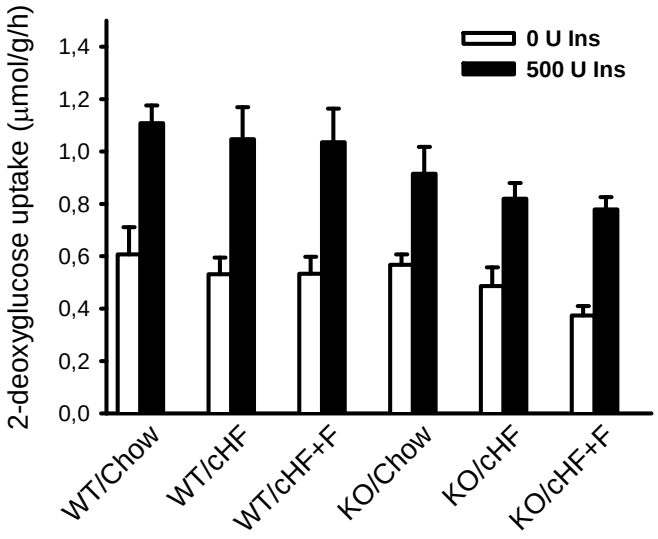

Figure 4.1-5 *Ex vivo* 2-deoxyglucose uptake by EDL muscle in female α2-AMPK KO and WT mice. Mice were fed for 9 weeks with control low-fat diet (Chow), control high-fat diet (cHF) or high-fat diet, in which 15% of lipids were replaced by n-3 LC-PUFA concentrate (cHF+F). WT-wild type; KO- α2-AMPK knock-out; Ins-insulin.

4.1.4 Obesity and white adipose tissue characteristics

It was determined whether the protective effects of n-3 LC-PUFA on high-fat diet-induced obesity and adiposity are mediated through α2-AMPK. Importantly, our experimental groups did not differ in the average food consumption (see Table 4.1-2, page 48). Feeding mice with cHF diet induced obesity in both genders and both genotypes, as it is obvious from the body weight gains (BWGs). cHF+F diet partially prevented development of high-fat diet induced obesity independently of genotype. Interestingly, in female mice, the efficiency of cHF+F diet to prevent weight gain was weaker but still significant. Furthermore, adiposity (the amount of body fat) was examined in male mice. The weight of both epididymal and dorsolumbar adipose tissue was increased by cHF feeding (Table 4.1-2). cHF+F diet significantly lowered cHF-induced increase in adiposity independently of genotype. Surprisingly, both adipose tissue depots of α2-AMPK KO mice fed either cHF or cHF+F were significantly decreased compared to the wild-type mice.

The size of adipocytes was also increased by cHF diet. However, the effect of cHF+F diet differed between the two fat depots. It effectively decreased hypertrophic adipocytes only in epididymal adipose tissue (Table 4.1-2, Figure 4.1-6), while dorsolumbar adipose tissue remained unaffected. However, the effects of cHF+F diet were independent of genotype (not shown).

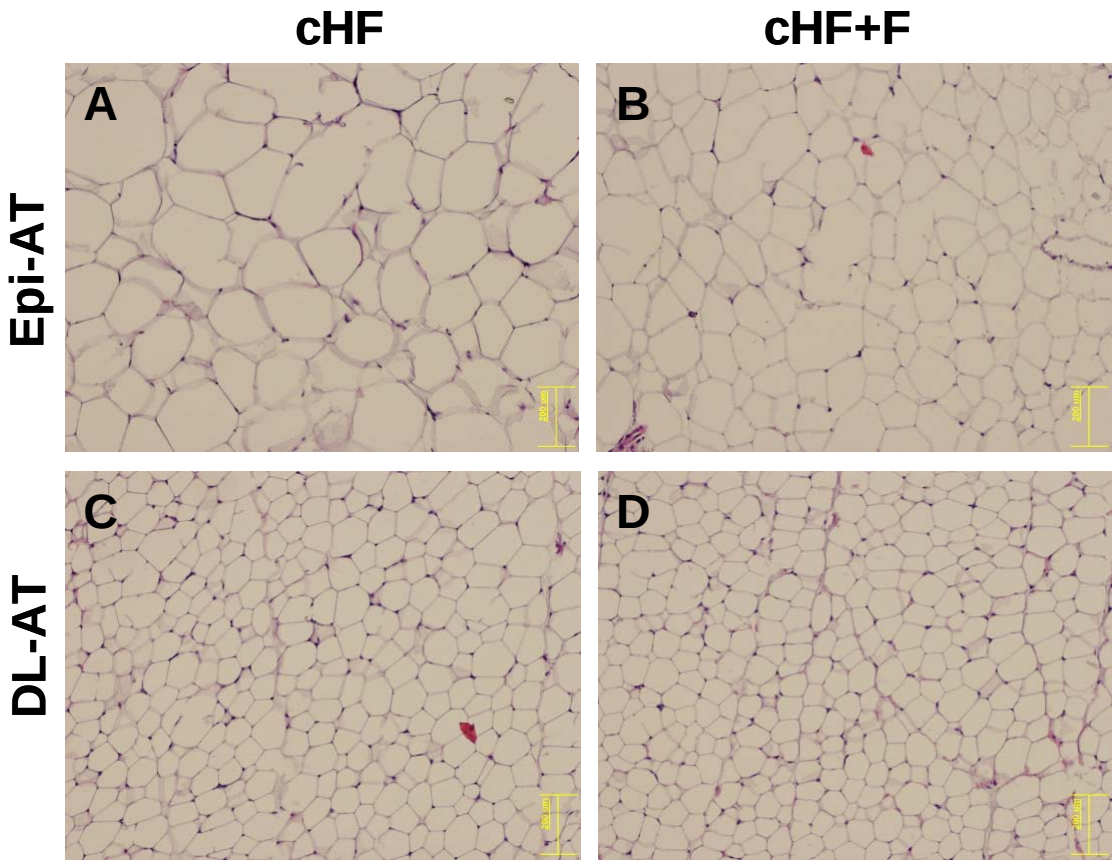

Figure 4.1-6 Differential effects of cHF+F diet on cHF-induced hypertrophy of adipocytes from edpididymal (Epi-AT) (A,B) and dorsolumbar (DL-AT) (C,D) fat depot in WT mice. Similar changes were observed in α2-AMPK KO mice. Mice were fed with control high-fat diet (cHF) (A,C) or high-fat diet, in which 15% of lipids were replaced by n-3 LC-PUFA concentrate (cHF+F) (B,D). Histological sections were counterstained with hematoxylin-eosin.

The level of macrophage infiltration assessed by the number of crown-like structures (CLS) was measured in the epididymal adipose tissue of cHF and cHF+F fed male mice (Figure 4.1-7). Chow diet-fed mice were not analyzed and the number of samples in other groups ranged from 2 to 3 due to the lack of tissue material. Macrophage infiltration tended to be decreased by cHF+F diet and also in α2-AMPK KO mice fed both diets (in cHF-fed mice significantly). The profile of the macrophage infiltration was similar to the size of adipocytes in epididymal adipose tissue (Table 4.1-2).

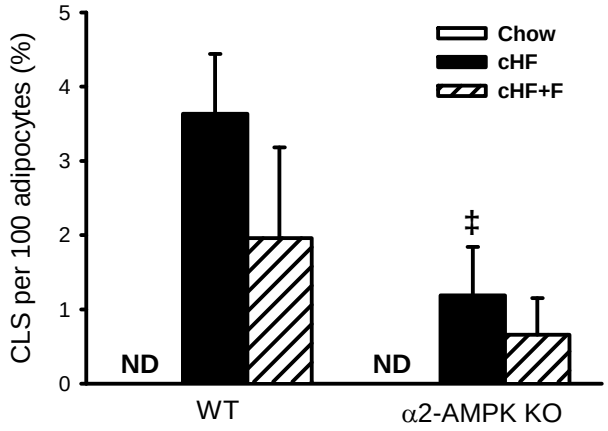

Figure 4.1-7 Macrophage infiltration in the epididymal tissue assessed by the detection of macrophage marker MAC-2 and expressed as the number of CLS. Male mice were fed with control high-fat diet (cHF) or high-fat diet, in which 15% of lipids were replaced by n-3 LC-PUFA concentrate (cHF+F). Data are presented as means ± SE (n = 2-3). **P* < 0.05 vs. genotype chow; †*P* < 0.05 vs. genotype cHF; ‡*P* < 0.05 vs. WT on respective diet. CLS – crown-like structures, ND- not determined.

Table 4.1-2 Metabolic and plasma parameters of male and female WT and α2-AMPK KO mice

		WT			α2-AMPK KO		
	Sex	**Chow**	**cHF**	**cHF+F**	**Chow**	**cHF**	**cHF+F**
Metabolic parameters							
Food consumption (kJ . g^{-1} .day^{-1})	M	2.0 ± 0.1	1.8 ± 0.1	1.9 ± 0.0	2.0 ± 0.1	1.8 ± 0.1	2.0 ± 0.1
	F	2.2 ± 0.0	2.4 ± 0.1	2.3 ± 0.1	2.2 ± 0.0	2.4 ± 0.1	2.2 ± 0.1
Initial body weight (g)	M	27.8 ± 0.5	27.9 ± 0.5	27.7 ± 0.5	27.1 ± 0.3	27.7 ± 0.4	27.3 ± 0.4
	F	21.2 ± 0.2	21.1 ± 0.2	20.9 ± 0.3	21.3 ± 0.3	21.6 ± 0.3	21.7 ± 0.4
Body weight gain (g)	M	1.4 ± 0.2	7.0 ± 1.1*	2.8 ± 0.7†	1.8 ± 0.3	4.6 ± 0.7*‡	1.2 ± 0.4†
	F	1.5 ± 0.1	7.1 ± 0.8*	5.6 ± 0.6*†	1.5 ± 0.1	8.3 ± 0.7*	6.0 ± 0.7*†
Adiposity							
Epididymal AT (g)	M	0.43 ± 0.02	1.52 ± 0.19*	1.12 ± 0.14*†	0.37 ± 0.03	1.19 ± 0.16*‡	0.64 ± 0.07*†‡
Dorsolumbar AT (g)	M	0.20 ± 0.01	0.54 ± 0.05*	0.42 ± 0.04*†	0.17 ± 0.01	0.34 ± 0.03*‡	0.23 ± 0.01†‡
Adipocyte size (μm^2)-epididymal	M	ND	15 971 ± 1 784	10 232 ± 185†	ND	13 298 ± 1 632	8 593 ± 896†
Adipocyte size (μm^2)-dorsolumbar	M	2 916 ± 610	6 775 ± 1 718*	7 311 ± 1 308*	3 395 ± 139	6 625 ± 926*	5 432 ± 648*
Plasma metabolites							
Triacylglycerol (mmol/l)	M	1.17 ± 0.08	1.23 ± 0.11	0.62 ± 0.07*†	1.04 ± 0.06	1.22 ± 0.08	0.73 ± 0.06*†
	F	0.75 ± 0.07	0.76 ± 0.02	0.48 ± 0.03*†	0.63 ± 0.16	0.79 ± 0.10	0.60 ± 0.05
Non-esterified fatty acids (mmol/l)	M	0.90 ± 0.05	0.94 ± 0.05	0.59 ± 0.04*†	0.88 ± 0.04	0.99 ± 0.06	0.68 ± 0.04*†
	F	0.53 ± 0.03	0.53 ± 0.02	0.39 ± 0.03*†	0.60 ± 0.05	0.57 ± 0.04	0.50 ± 0.02
Cholesterol (mmol/l)	M	2.25 ± 0.08	4.12 ± 0.25*	3.10 ± 0.20*†	2.10 ± 0.06	3.94 ± 0.18*	2.75 ± 0.14*†
	F	1.51 ± 0.09	2.72 ± 0.12*	2.44 ± 0.10*	1.42 ± 0.06*	2.63 ± 0.16*	2.65 ± 0.17*
Glucose (mmol/l)	M	9.9 ± 0.4	10.7 ± 0.5	10.4 ± 0.3	9.7 ± 0.4	10.0 ± 0.4	9.4 ± 0.4
	F	10.1 ± 0.7	11.3 ± 0.6	11.9 ± 0.4	10.6 ± 1.2	10.4 ± 0.5	12.3 ± 0.7
Plasma hormones							
Insulin in random fed state (ng/ml)	M	0.66 ± 0.11	1.73 ± 0.29*	1.47 ± 0.28*	0.60 ± 0.07	1.34 ± 0.20*	0.95 ± 0.12*
	F	0.15 ± 0.01	0.67 ± 0.28	0.15 ± 0.03	0.84 ± 0.48	0.47 ± 0.30	0.46 ± 0.20
Total adiponectin (A.U.)	M	1.15 ± 0.09	0.97 ± 0.10	1.33 ± 0.09†	0.82 ± 0.09‡	0.80 ± 0.07	0.97 ± 0.08‡
	F	1.02 ± 0.09	0.83 ± 0.05*	1.10 ± 0.04†	1.00 ± 0.07	0.79 ± 0.05*	1.01 ± 0.04†
HMW:total adiponectin	M	0.38 ± 0.02	0.36 ± 0.02	0.44 ± 0.02†	0.35 ± 0.02	0.34 ± 0.02	0.39 ± 0.02
	F	0.42 ± 0.03	0.43 ± 0.02	0.53 ± 0.02*†	0.45 ± 0.01	0.44 ± 0.03	0.49 ± 0.03

Data are the means ± SE of 27-30 mice for metabolic parameters or 13-15 for other measures. Food consumption was measured weekly during 9 weeks of the differential dietary treatment. Body weight gain and plasma parameters were assessed after 9 weeks of feeding with experimental diets in random-fed mice. AT, adipose tissue A.U., arbitary units; HMW: total adiponectin, ratio of high molecular weight to total adiponectin; F, female; M, male; ND, not determined. *$P < 0.05$ vs. genotype chow; †$P < 0.05$ vs. genotype cHF; ‡$P < 0.05$ vs. WT on respective diet.

4.1.5 Plasma metabolic markers

It was aimed to establish the relevance of AMPK in the mechanism of hypolipidemic and hypocholesterolemic effects of n-3 LC-PUFA. We studied basic plasma metabolic markers under various metabolic conditions, i.e. in the fasted, re-fed and random-fed state, as well as after hyperinsulinemic-euglycemic clamp. Concerning the results from random-fed state, there were no differences in blood glucose levels between any of the experimental groups (Table 4.1-2). Under random-fed conditions, triacylglycerol and NEFA levels remained unchanged after cHF feeding. In WT mice, cHF+F effectively decreased triacylglycerols and NEFA in both genders. In knock-out mice, this effect was preserved only in male mice. Furthermore, *in vivo* measurement of VLDL-triacylglycerol synthesis in female mice showed that cHF+F decreased VLDL production independently of genotype (Figure 4.1-8). Plasma cholesterol was increased in all cHF-fed groups (Table 4.1-2). Feeding cHF+F diet protected mice from cHF-induced hypercholesterolemia independently of genotype. This beneficial effect of cHF+F diet was not present in female mice but it could be explained, at least partially, by weaker hypercholesterolemic effects of cHF diet in females compared to males (Table 4.1-2).

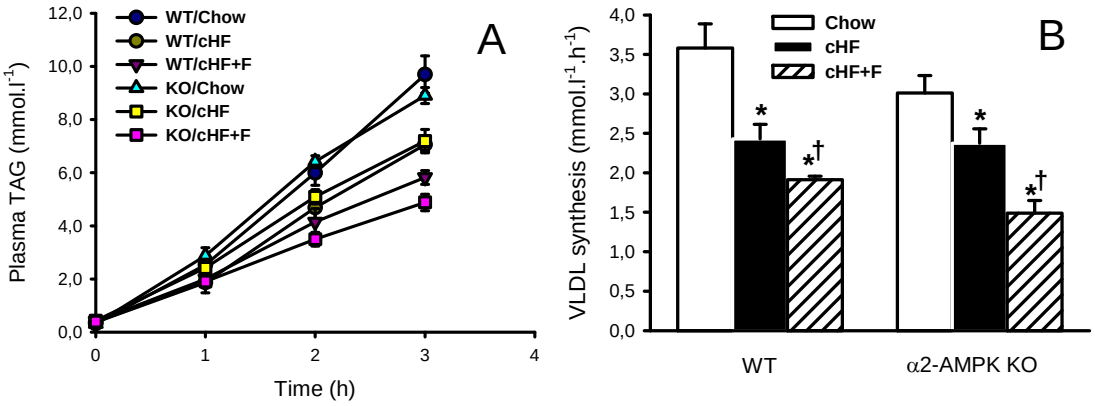

Figure 4.1-8 Rate of VLDL-triacylglycerol synthesis in female WT and α2-AMPK KO mice assessed by Tyloxapol test. Mice were fed with control low-fat diet (Chow), control high-fat diet (cHF) or high-fat diet, in which 15% of lipids were replaced by n-3 LC-PUFA concentrate (cHF+F). Data are presented as means ± SE (n = 5-8). **P* < 0.05 vs. genotype chow; †*P* < 0.05 vs. genotype cHF; ‡*P* < 0.05 vs. WT on respective diet.

The impact of nutritional status on the potency of n-3 LC-PUFA to exert measurable effects on plasma triacylglycerols and NEFA levels and the involvement of α2-AMPK in these processes are depicted in Figure 4.1-9. The data are expressed as the percentage change in the individual metabolite induced by cHF+F as compared to cHF diet. There were no significant changes in any of the metabolites during fasted state. A decrease of plasma lipids induced by cHF+F diet was amplified with a prolonged time of satiety. This effect was observed in both genotypes. Importantly, α2-AMPK was necessary to preserve the beneficial effect of n-3 LC-PUFA during the hyperinsulinemic-euglycemic clamp, when glucose was the main (exogenous) substrate and physiological hyperinsulinemia was achieved.

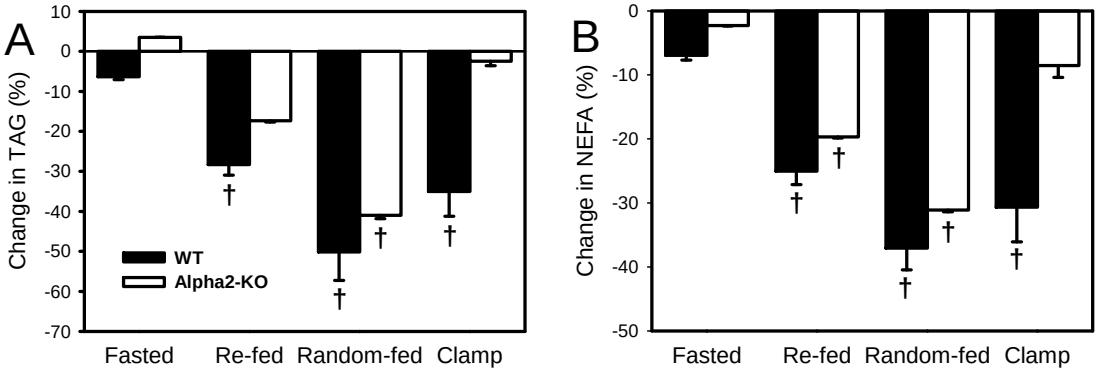

Figure 4.1-9 The impact of nutritional state on the potency of n-3 LC-PUFA to beneficially affect triacylglycerol (TAG; A) and non-esterified fatty acids (NEFA; B) plasma levels in α2-AMPK KO and WT male mice. The columns express the percent change in the individual marker by cHF+F relatively to cHF. Data are presented as means ± SE (n = 8-14). †$P < 0.05$ vs. genotype cHF.

The absolute values of plasma triacylglycerol, NEFA and cholesterol levels under different metabolic conditions are displayed in the Table 4.1-3.

A relatively small elevation of plasma insulin levels induced by cHF feeding could be observed in both genders and genotypes (Table 4.1-2). Compared to cHF-fed mice, in mice fed the cHF+F diet insulin levels tended to be decreased. The ratio of high-molecular weight (HMW) to total adiponectin, which positively correlates with insulin sensitivity (108), was not influenced by cHF feeding. However, cHF+F increased the ratio in both genders of WT mice as compared to α2-AMPK KO mice, which resisted this beneficial effect of cHF+F feeding (Table 4.1-2).

Table 4.1-3 Triacylglycerol, NEFA and cholesterol levels in male WT and α2-AMPK KO mice under different metabolic conditions

	WT			α2-AMPK KO		
	Chow	cHF	cHF+F	Chow	cHF	cHF+F
Triacylglycerols (mmol/l)						
Fasted	0.46 ± 0.03	0.49 ± 0.03	0.46 ± 0.04	0.57 ± 0.05	0.44 ± 0.02	0.46 ± 0.02
Re-fed	0.57 ± 0.05	0.50 ± 0.04	0.36 ± 0.02*†	0.53 ± 0.04	0.48 ± 0.03	0.40 ± 0.03*
Random-fed	1.17 ± 0.08	1.24 ± 0.11	0.62 ± 0.07*†	1.04 ± 0.06	1.22 ± 0.08	0.73 ± 0.07*†
Clamp	0.44 ± 0.05	0.64 ± 0.09	0.41 ± 0.04†	0.38 ± 0.06	0.55 ± 0.05	0.53 ± 0.08
NEFA (mmol/l)						
Fasted	1.16 ± 0.07	0.84 ± 0.08*	0.78 ± 0.05*	1.34 ± 0.05‡	0.89 ± 0.06*	0.87 ± 0.05*
Re-fed	0.41 ± 0.02	0.66 ± 0.05*	0.50 ± 0.02*†	0.38 ± 0.02	0.68 ± 0.04*	0.55 ± 0.04*†
Random-fed	0.90 ± 0.05	0.94 ± 0.05	0.59 ± 0.05*†	0.88 ± 0.04	0.99 ± 0.06	0.68 ± 0.04*†
Clamp	0.25 ± 0.02	0.39 ± 0.05	0.27 ± 0.03†	0.21 ± 0.03	0.41 ± 0.11	0.37 ± 0.07
Cholesterol (mmol/l)						
Fasted	1.77 ± 0.07	2.81 ± 0.22	2.00 ± 0.15†	1.78 ± 0.04	2.67 ± 0.12	2.02 ± 0.08†
Re-fed	1.85 ± 0.06	3.01 ± 0.24*	2.21 ± 0.07*†	1.85 ± 0.08	2.98 ± 0.16*	2.46 ± 0.10*†
Random-fed	2.25 ± 0.08	4.12 ± 0.25*	3.10 ± 0.20*†	2.10 ± 0.06	3.94 ± 0.18*	2.75 ± 0.14*†
Clamp	2.26 ± 0.13	2.98 ± 0.22	2.51 ± 0.15	1.83 ± 0.09	2.99 ± 0.24	2.63 ± 0.22

Data are the means ± SE (n = 8-14). Plasma parameters were assessed after 9 weeks of feeding with experimental diets.
*P < 0.05 vs. genotype chow; †P < 0.05 vs. genotype cHF; ‡P < 0.05 vs. WT on respective diet.

4.1.6 The weight of non-adipose tissues

The weight of non-adipose tissues including liver, quadriceps, gastrocnemius and soleus skeletal muscles, heart and brain was analyzed. There were no significant diet- or genotype-induced changes in the weight of any of these tissues (not shown).

4.1.7 Liver and muscle glycerolipid content

The total content of glycerolipids in liver and muscle of male mice in random-fed and post-clamp conditions was determined (Figure 4.1-10). Feeding mice with cHF diet induced hepatic steatosis in mice of both genotypes and under both nutritional conditions (Figure 4.1-10 A, C).

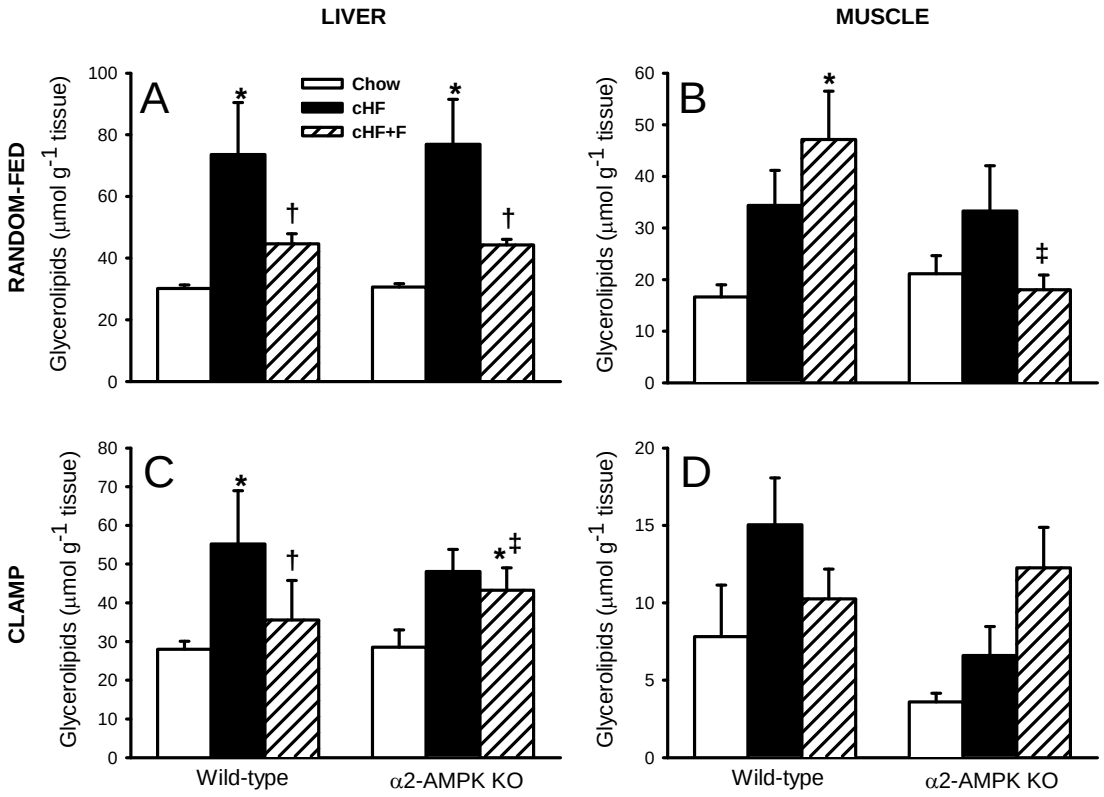

Figure 4.1-10 Liver (A, C) and muscle (B, D) glycerolipid content in random-fed (A, B) and post-clamp (C, D) mice. α2-AMPK KO and WT male mice fed for 9 weeks with control low-fat diet (Chow), control high-fat diet (cHF) or high-fat diet, in which 15% of lipids were replaced by n-3 LC-PUFA concentrate (cHF+F). Data are presented as means ± SE (n = 8-14). **P* < 0.05 vs. genotype chow; †*P* < 0.05 vs. genotype cHF; ‡*P* < 0.05 vs. WT on respective diet.

The effects of cHF+F on liver glycerolipid content in random-fed male mice were similar as those seen on plasma levels of triacylglycerols (Table 4.1-2); n-3 LC PUFA administred as cHF+F diet decreased liver glycerolipid content independently of genotype (Figure 4.1-10 C). These results were confirmed by the liver histology (Figure 4.1-11)). However, in mice subjected to hyperinsulinemic-euglycemic clamp, the deletion of α2-AMPK resulted in a failure of n-3 LC-PUFA to exert their beneficial effects (Figure 4.1-10 C).

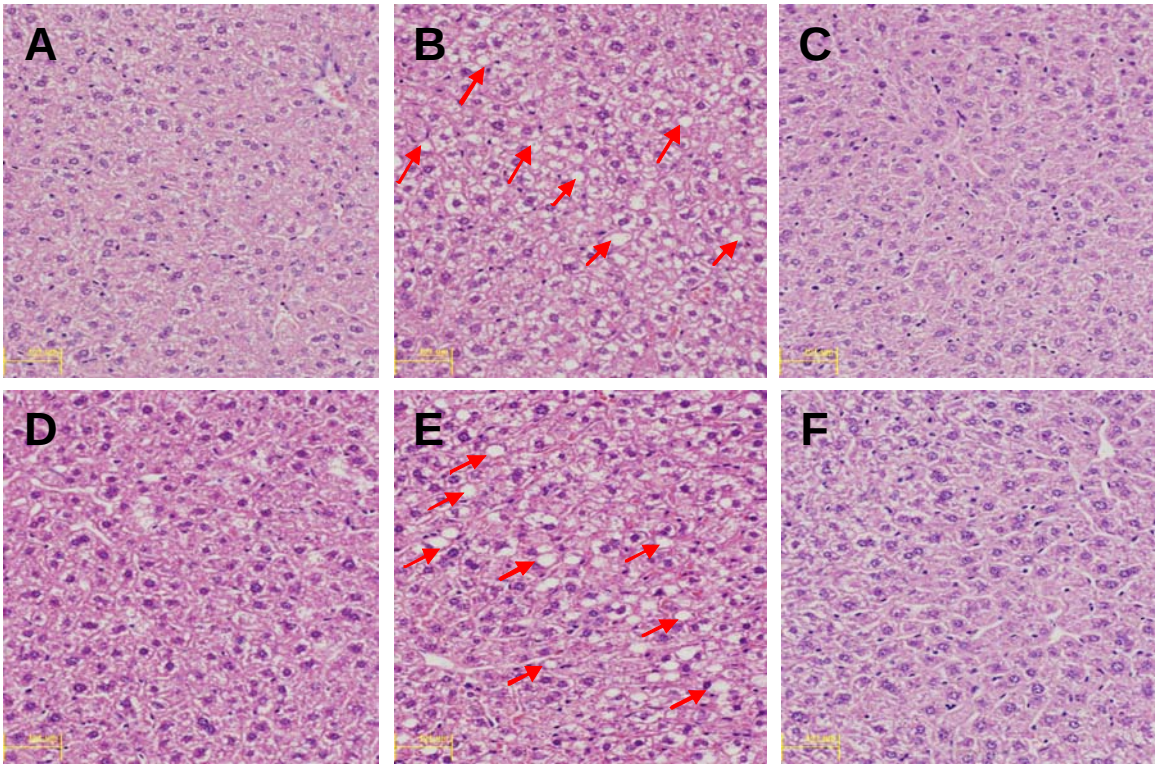

Figure 4.1-11 Liver morphology assessed by hematoxylin-eosin staining of liver sections. α2-AMPK KO (A-C) and WT (D-F) male mice fed for 9 weeks with control low-fat diet (Chow) (A, D), control high-fat diet (cHF) (B, E) or high-fat diet, in which 15% of lipids were replaced by n-3 LC-PUFA concentrate (cHF+F) (C, F). Red arrows highlight the occurence of lipid droplets in liver cells.

Concerning the effect of nutritional state on total glycerolipid levels in the quadriceps muscle, the results were relatively inconsistent. However, there were no significant differences in muscle glycerolipid content between the cHF and cHF+F fed mice irrespective of the genotype or nutritional state (Figure 4.1-10 B,D).

Next, total liver and muscle ceramides as well as the content of fatty acids in diacylglycerol, triacylglycerol and phospholipid fraction of random-fed mice was assessed. There were no effects of diet or genotype on the total liver ceramide content

(Figure 4.1-12 A). cHF+F feeding lowered liver diacylglycerol levels in WT mice, while it failed to lower diacylglycerol content in α2-AMPK KO mice (Figure 4.1-12 B). Phospholipids were slightly but significantly increased by cHF+F in both genotypes (Figure 4.1-12 C). Concerning the skeletal muscle, there were no significant differences in ceramide or diacylglycerol levels (Figure 4.1-12 D,E). In contrast to the liver, muscle phospholipids were decreased by cHF+F diet (Figure 4.1-12 D).

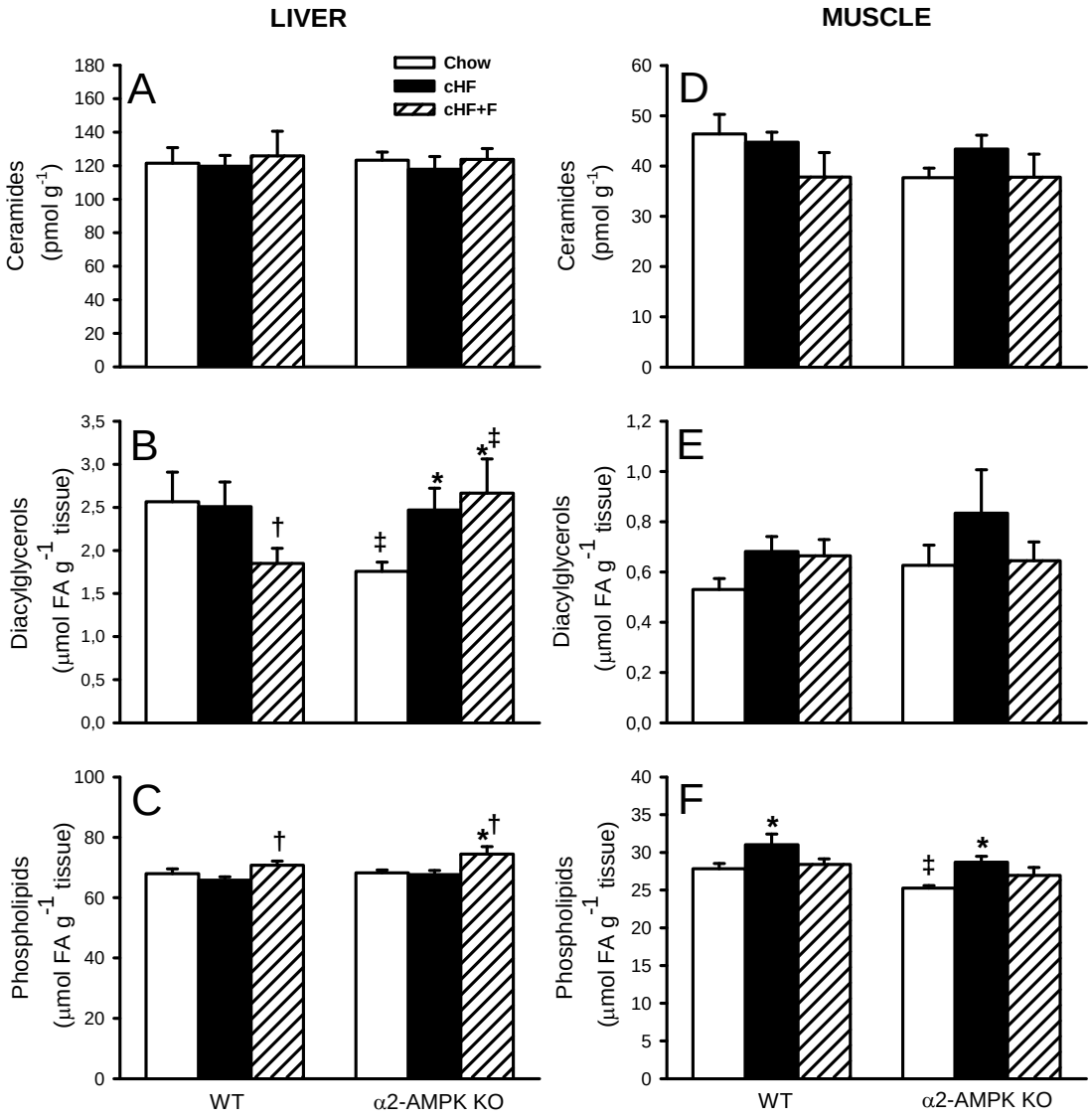

Figure 4.1-12 Liver (A-C) and muscle (D-F) content of ceramides (A, D), diacylglycerols (B, E) and phospholipids (C, F) in random-fed male α2-AMPK KO and WT mice. Mice were fed for 9 weeks with control low-fat diet (Chow), control high-fat diet (cHF) or high-fat diet, in which 15% of lipids were replaced by n-3 LC-PUFA concentrate (cHF+F). Data are presented as means ± SE (n = 8-14). *$P < 0.05$ vs. genotype chow; †$P < 0.05$ vs. genotype cHF; ‡$P < 0.05$ vs. WT on respective diet.

4.1.8 Fatty acid composition of lipid fractions

Fatty acid composition of liver and muscle triacylglycerol, diacylglycerol and phospholipid fraction in random-fed male mice was assessed (Table 4.1-4 and Table 4.1-5). Principal component analysis was performed to reveal the main factor determining the structure of lipid profiles. However, such factor could not be found by using this statistical tool. Further, since liver diacylglycerols were affected by cHF+F diet in the genotype-dependent manner, the fatty acid composition of liver diacylglycerol fraction was examined. Table 4.1-4 shows, that palmitic and α-linolenic fatty acids are mainly responsible for the changes in total liver diacylglycerols.

Table 4.1-4 Fatty acid composition of liver lipid fractions in random-fed WT and α2-AMPK KO mice (continuing on the next page)

	WT			α2-AMPK KO		
	Chow	cHF	cHF+F	Chow	cHF	cHF+F
Total ceramide (nmol/g)	121.45 ± 9.33	119.71 ± 6.43	125.89 ± 14.66	123.34 ± 4.84	117.91 ± 7.53	123.82 ± 6.42
Triacylglycerol species						
Total fatty acids (μmol/g)	38.10 ± 3.18	116.55 ± 14.51*	80.35 ± 8.80†	50.31 ± 4.60	128.04 ± 18.59*	76.80 ± 6.63†
Myristic (14:0) (μmol/g)	0.38 ± 0.05	1.25 ± 0.22*	0.63 ± 0.08†	0.44 ± 0.04	1.27 ± 0.25*	0.59 ± 0.06†
Palmitic (16:0) (μmol/g)	11.12 ± 0.94	30.39 ± 4.10*	20.27 ± 2.88†	14.44 ± 1.06	35.25 ± 6.10*	17.17 ± 1.86†
Palmitoleic (16:1n7) (μmol/g)	2.82 ± 0.35	1.54 ± 0.46*	0.54 ± 0.10*	3.01 ± 0.37	1.35 ± 0.41*	0.81 ± 0.41*
Stearic (18:0) (μmol/g)	0.85 ± 0.09	1.90 ± 0.15*	1.60 ± 0.08*	0.98 ± 0.08	2.52 ± 0.31*‡	1.83 ± 0.14*†
Oleic (18:1n9) (μmol/g)	13.23 ± 1.22	27.05 ± 3.33	15.08 ± 1.72*†	16.68 ± 1.18	30.81 ± 5.84	15.52 ± 1.60*†
Linoleic (18:2n6) (μmol/g)	7.68 ± 0.61	47.52 ± 5.98*	25.98 ± 2.67*†	12.16 ± 2.60	49.22 ± 5.78*	25.81 ± 2.43*†
Arachidic (20:0) (μmol/g)	0.08 ± 0.01	0.23 ± 0.04*	0.18 ± 0.01*	0.12 ± 0.02	0.28 ± 0.05*	0.19 ± 0.02†
α-Linolenic (C18:3n3) (μmol/g)	0.43 ± 0.03	1.42 ± 0.24*	0.81 ± 0.09†	0.56 ± 0.06	1.52 ± 0.28*	0.79 ± 0.07†
Behenic (22:0) (nmol/g)	71.89 ± 5.67	89.37 ± 11.63	31.13 ± 2.65*†	81.32 ± 3.67	98.81 ± 15.97	43.53 ± 7.20*†
Arachidonic (20:4n6) (μmol/g)	0.56 ± 0.04	3.15 ± 0.58*	0.41 ± 0.04†	0.84 ± 0.12	3.72 ± 0.79*	0.47 ± 0.06†
Lignoceric (24:0) (nmol/g)	7.30 ± 0.80	10.28 ± 1.07	9.93 ± 1.04	8.14 ± 0.70	14.66 ± 3.10*	11.19 ± 0.89
Eicosapentaenoic (20:5n3) (μmol/g)	0.13 ± 0.01	0.25 ± 0.04	1.91 ± 0.21*†	0.13 ± 0.01	0.23 ± 0.05	1.33 ± 0.13*†‡
Nervonic (24:1n9) (nmol/g)	7.43 ± 1.01	8.23 ± 0.58	10.01 ± 0.89	6.94 ± 0.28	10.04 ± 1.30*	12.30 ± 1.17*
Docosahexaenoic (22:6n3) (μmol/g)	0.73 ± 0.06	1.74 ± 0.29	12.90 ± 1.08*†	0.84 ± 0.05	1.75 ± 0.31	12.21 ± 1.21*†
Diacylglycerol species						
Total fatty acids (μmol/g)	2.57 ± 0.34	2.51 ± 0.29	1.85 ± 0.18†	1.76 ± 0.11‡	2.47 ± 0.25*	2.66 ± 0.40*†
Myristic (14:0) (μmol/g)	0.08 ± 0.01	0.08 ± 0.01	0.06 ± 0.01	0.06 ± 0.00	0.06 ± 0.01	0.06 ± 0.01
Palmitic (16:0) (μmol/g)	1.02 ± 0.13	0.95 ± 0.13	0.70 ± 0.06	0.69 ± 0.05	0.90 ± 0.09	1.12 ± 0.22‡
Palmitoleic (16:1n7) (μmol/g)	0.09 ± 0.01	0.03 ± 0.00*	0.01 ± 0.00*	0.06 ± 0.01‡	0.02 ± 0.00*	0.02 ± 0.01*
Stearic (18:0) (μmol/g)	0.70 ± 0.18	0.54 ± 0.10	0.48 ± 0.11	0.31 ± 0.02	0.40 ± 0.04	0.65 ± 0.16
Oleic (18:1n9) (μmol/g)	0.28 ± 0.02	0.25 ± 0.03	0.13 ± 0.01*†	0.24 ± 0.02	0.25 ± 0.04	0.19 ± 0.03
Linoleic (18:2n6) (μmol/g)	0.23 ± 0.02	0.49 ± 0.07*	0.27 ± 0.03†	0.24 ± 0.02	0.57 ± 0.07*	0.36 ± 0.05†
Arachidic (20:0) (nmol/g)	15.23 ± 4.54	11.84 ± 1.95	11.87 ± 2.85	7.67 ± 0.56	9.47 ± 0.62	10.94 ± 0.92
α-Linolenic (C18:3n3) (nmol/g)	12.61 ± 1.52	12.60 ± 1.88	6.55 ± 0.50*†	7.64 ± 0.64‡	10.73 ± 1.52	13.23 ± 2.62‡
Arachidonic (20:4n6) (nmol/g)	72.11 ± 3.89	83.54 ± 5.32	30.86 ± 4.35*†	65.43 ± 4.89	100.95 ± 16.46*	37.75 ± 4.28*†

Eicosapentaenoic (20:5n3) (nmol/g)	10.43 ± 0.75	8.59 ± 0.89	19.97 ± 1.62*†	8.58 ± 0.58	8.37 ± 8.84	20.29 ± 1.27*†
Nervonic (24:1n9) (nmol/g)	0.80 ± 0.10	1.36 ± 0.32	1.18 ± 0.12	0.83 ± 0.06	1.38 ± 0.37	1.38 ± 0.21
Docosahexaenoic (22:6n3) (µmol/g)	0.05 ± 0.00	0.06 ± 0.01	0.13 ± 0.01	0.06 ± 0.01	0.14 ± 0.05	0.17 ± 0.02
Phospholipid species						
Total fatty acids (µmol/g)	67.96 ± 1.61	65.83 ± 1.09	70.75 ± 1.39†	68.20 ± 0.97	67.62 ± 1.40	74.45 ± 2.44*†
Myristic (14:0) (µmol/g)	0.14 ± 0.01	0.22 ± 0.08	0.16 ± 0.01	0.26 ± 0.08	0.15 ± 0.02	0.15 ± 0.01
Palmitic (16:0) (µmol/g)	18.38 ± 0.46	13.80 ± 0.24*	17.38 ± 0.21†	18.16 ± 0.30	14.18 ± 0.34*	18.20 ± 0.87†
Palmitoleic (16:1n7) (µmol/g)	1.40 ± 0.12	0.17 ± 0.01*	0.25 ± 0.11*	1.36 ± 0.06	0.17 ± 0.01*	0.33 ± 0.19*
Stearic (18:0) (µmol/g)	11.21 ± 0.36	14.39 ± 0.28*	13.53 ± 0.47*	11.56 ± 0.25	14.81 ± 0.33*	14.30 ± 0.36*
Oleic (18:1n9) (µmol/g)	5.23 ± 0.21	3.34 ± 0.14*	3.80 ± 0.21*	5.02 ± 0.14	3.42 ± 0.14*	4.11 ± 0.36*†
Linoleic (18:2n6) (µmol/g)	12.37 ± 0.29	14.27 ± 0.39*	14.89 ± 0.42*	12.00 ± 0.21	14.38 ± 0.45*	15.91 ± 0.41*†
Arachidic (20:0) (µmol/g)	0.10 ± 0.01	0.11 ± 0.01	0.15 ± 0.01*†	0.10 ± 0.00	0.11 ± 0.01	0.15 ± 0.01*†
α-Linolenic (C18:3n3) (µmol/g)	0.07 ± 0.01	0.04 ± 0.00*	0.05 ± 0.00	0.07 ± 0.01	0.05 ± 0.00*	0.06 ± 0.01
Behenic (22:0) (µmol/g)	0.13 ± 0.01	0.03 ± 0.01*	0.04 ± 0.01*	0.13 ± 0.01	0.02 ± 0.00*	0.04 ± 0.02*
Arachidonic (20:4n6) (µmol/g)	11.83 ± 0.66	13.70 ± 0.30*	5.60 ± 0.47*†	12.85 ± 0.18	13.75 ± 0.79*	6.62 ± 0.80†
Lignoceric (24:0) (nmol/g)	9.90 ± 1.00	15.69 ± 6.14	11.32 ± 0.70	13.82 ± 3.82	10.46 ± 0.72	10.29 ± 0.83
Eicosapentaenoic (20:5n3) (µmol/g)	0.44 ± 0.08	0.08 ± 0.01*	2.01 ± 0.17*†	0.27 ± 0.01	0.16 ± 0.10	1.78 ± 0.19*†
Docosahexaenoic (22:6n3) (µmol/g)	6.64 ± 0.39	5.64 ± 0.18	12.88 ± 0.65*†	6.42 ± 0.13	6.40 ± 0.53	12.80 ± 0.75*†

Data are the means ± SE (n = 8-14). Male WT and α2-AMPK KO mice were fed for 9 weeks with control low-fat diet (Chow), control high-fat diet (cHF) or high-fat diet, in which 15% of lipids were replaced by n-3 LC-PUFA concentrate (cHF+F). Data are presented as means ± SE (n = 8-14). *$P < 0.05$ vs. genotype chow; †$P < 0.05$ vs. genotype cHF; ‡$P < 0.05$ vs. WT on respective diet.

Table 4.1-5 Fatty acid composition of muscle lipid fractions in random-fed WT and α2-AMPK KO mice (continuing on the next page)

	Wild-type			α2-AMPK KO		
	Chow	cHF	cHF+F	Chow	cHF	cHF+F
Total ceramide (nmol/g)	46.38 ± 3.90	44.73 ± 2.00	37.82 ± 4.86	37.71 ± 1.90	43.37 ± 2.76	37.78 ± 4.57
Triacylglycerol species						
Total fatty acids (μmol/g)	32.36 ± 4.67	67.00 ± 13.26	91.84 ± 18.29*	41.20 ± 6.77	75.66 ± 15.71	35.14 ± 5.59‡
Myristic (14:0) (μmol/g)	0.62 ± 0.08	1.19 ± 0.21	1.83 ± 0.38*	1.02 ± 0.30	1.35 ± 0.28	0.66 ± 0.10‡
Palmitic (16:0) (μmol/g)	8.25 ± 1.19	12.57 ± 2.39	18.78 ± 3.88*	11.02 ± 2.18	14.66 ± 3.11	6.88 ± 1.00‡
Palmitoleic (16:1n7) (μmol/g)	3.56 ± 0.62	2.76 ± 0.44	2.61 ± 0.54	5.40 ± 0.95	3.68 ± 1.08*	0.91 ± 0.23†
Stearic (18:0) (μmol/g)	0.71 ± 0.10	1.19 ± 0.18	1.82 ± 0.21*†	1.00 ± 0.23	1.20 ± 0.23	0.94 ± 0.09‡
Oleic (18:1n9) (μmol/g)	9.88 ± 1.54	20.32 ± 4.21	25.91 ± 5.21*	11.34 ± 1.81	22.58 ± 4.64	10.26 ± 1.79‡
Linoleic (18:2n6) (μmol/g)	8.69 ± 1.37	27.69 ± 5.63*	35.11 ± 7.11*	10.31 ± 1.63	30.57 ± 6.41*	13.39 ± 2.16†‡
Arachidic (20:0) (nmol/g)	18.59 ± 2.61	31.30 ± 5.44	47.40 ± 8.91*	35.15 ± 12.11	33.74 ± 4.54	21.94 ± 2.72‡
α-Linolenic (C18:3n3) (μmol/g)	0.42 ± 0.06	0.76 ± 0.15	1.01 ± 0.21*	0.68 ± 0.18	0.95 ± 0.24	0.36 ± 0.06†‡
Behenic (22:0) (nmol/g)	19.27 ± 2.12	18.08 ± 1.74	28.80 ± 3.83	29.26 ± 5.60‡	20.55 ± 2.90	16.18 ± 1.74*‡
Arachidonic (20:4n6) (μmol/g)	0.10 ± 0.01	0.27 ± 0.06	0.18 ± 0.03	0.17 ± 0.03	0.37 ± 0.11*	0.07 ± 0.01†
Lignoceric (24:0) (nmol/g)	2.48 ± 0.39	3.31 ± 0.39	5.04 ± 0.75	4.14 ± 1.62	3.80 ± 0.58	3.00 ± 0.46
Eicosapentaenoic (20:5n3) (μmol/g)	0.02 ± 0.01	0.03 ± 0.01	0.49 ± 0.11*†	0.03 ± 0.00	0.02 ± 0.01	0.17 ± 0.03‡
Nervonic (24:1n9) (nmol/g)	3.49 ± 0.65	3.24 ± 0.39	13.14 ± 3.13*†	5.88 ± 1.97	3.45 ± 0.26	6.62 ± 0.81‡
Docosahexaenoic (22:6n3) (μmol/g)	0.08 ± 0.01	0.17 ± 0.04	4.00 ± 0.75*†	0.16 ± 0.02	0.22 ± 0.06	1.45 ± 0.24*†‡
Diacylglycerol species						
Total fatty acids (μmol/g)	0.53 ± 0.04	0.68 ± 0.06	0.66 ± 0.06	0.63 ± 0.08	0.83 ± 0.17	0.64 ± 0.07
Palmitic (16:0) (nmol/g)	249.17 ± 16.49	286.90 ± 23.91	244.38 ± 14.93	297.56 ± 47.52	328.17 ± 48.10	227.16 ± 33.41
Stearic (18:0) (nmol/g)	169.34 ± 31.95	222.02 ± 38.71	205.02 ± 32.31	197.57 ± 39.62	341.59 ± 115.32	274.89 ± 42.99
Oleic (18:1n9) (nmol/g)	47.57 ± 2.40	59.52 ± 4.48	60.76 ± 9.76	58.90 ± 9.63	59.86 ± 10.03	40.27 ± 2.73
Linoleic (18:2n6) (nmol/g)	41.43 ± 3.22	82.56 ± 7.29*	85.02 ± 17.89*	49.47 ± 11.24	76.44 ± 13.01	47.38 ± 4.07‡
Arachidic (20:0) (nmol/g)	4.35 ± 0.91	6.09 ± 1.10	5.19 ± 0.97	4.22 ± 0.62	8.72 ± 3.23	7.36 ± 1.04
Arachidonic (20:4n6) (nmol/g)	6.81 ± 0.34	8.11 ± 0.67	4.18 ± 0.36*†	7.54 ± 0.33	7.23 ± 0.93	3.58 ± 0.35*†
Eicosapentaenoic (20:5n3) (nmol/g)	3.90 ± 0.73	4.68 ± 1.03	5.54 ± 0.58	4.30 ± 0.67	4.10 ± 0.62	5.08 ± 1.04
Docosahexaenoic (22:6n3) (nmol/g)	8.11 ± 0.52	11.60 ± 1.29	54.43 ± 3.95*†	7.25 ± 0.60	8.14 ± 0.92	39.18 ± 3.09*†‡
Phospholipid species						

Total fatty acids (µmol/g)	27.85 ± 0.68	31.03 ± 1.41*	28.39 ± 0.74	25.27 ± 0.34‡	28.72 ± 0.76*	26.96 ± 1.05
Myristic (14:0) (µmol/g)	0.25 ± 0.01	0.35 ± 0.01*	0.36 ± 0.01*	0.22 ± 0.01	0.36 ± 0.02*	0.38 ± 0.04*
Palmitic (16:0) (µmol/g)	8.44 ± 0.17	8.44 ± 0.29	8.49 ± 0.15	7.62 ± 0.15‡	7.79 ± 0.22‡	7.43 ± 0.30‡
Palmitoleic (16:1n7) (µmol/g)	0.73 ± 0.04	0.16 ± 0.01*	0.11 ± 0.01*	0.77 ± 0.04	0.16 ± 0.01*	0.09 ± 0.01*
Stearic (18:0) (µmol/g)	3.68 ± 0.17	4.44 ± 0.30*	3.24 ± 0.18†	3.35 ± 0.13	4.15 ± 0.24*	3.33 ± 0.12†
Oleic (18:1n9) (µmol/g)	1.44 ± 0.04	1.69 ± 0.06*	1.28 ± 0.05†	1.73 ± 0.08‡	1.90 ± 0.05‡	1.57 ± 0.05†‡
Linoleic (18:2n6) (µmol/g)	3.90 ± 0.20	6.50 ± 0.29*	2.55 ± 0.20*†	3.57 ± 0.10	5.55 ± 0.26*	2.66 ± 0.12*†
Arachidic (20:0) (µmol/g)	0.01 ± 0.00	0.02 ± 0.00*	0.01 ± 0.00	0.01 ± 0.00	0.01 ± 0.00*	0.02 ± 0.00*
α-Linolenic (C18:3n3) (µmol/g)	0.06 ± 0.00	0.06 ± 0.00*	0.03 ± 0.00*†	0.05 ± 0.00‡	0.04 ± 0.00*‡	0.03 ± 0.00*†‡
Behenic (22:0) (µmol/g)	0.03 ± 0.00	0.02 ± 0.00*	0.01 ± 0.00*†	0.03 ± 0.00	0.02 ± 0.00*	0.01 ± 0.00*
Arachidonic (20:4n6) (µmol/g)	3.34 ± 0.09	3.45 ± 0.14	0.62 ± 0.03*†	3.12 ± 0.06	3.26 ± 0.10	0.54 ± 0.02*†
Lignoceric (24:0) (µmol/g)	0.01 ± 0.00	0.02 ± 0.00	0.01 ± 0.00	0.02 ± 0.00	0.02 ± 0.00	0.01 ± 0.00
Eicosapentaenoic (20:5n3) (µmol/g)	0.03 ± 0.00	0.02 ± 0.00	0.12 ± 0.00*†	0.04 ± 0.00	0.02 ± 0.00*	0.14 ± 0.01*†‡
Docosahexaenoic (22:6n3) (µmol/g)	5.93 ± 0.12	5.87 ± 0.57	11.54 ± 0.25*†	4.75 ± 0.13‡	5.43 ± 0.22	10.74 ± 0.43*†

Data are the means ± SE (n = 8-14). Male WT and α2-AMPK KO mice were fed for 9 weeks with control low-fat diet (Chow), control high-fat diet (cHF) or high-fat diet, in which 15% of lipids were replaced by n-3 LC-PUFA concentrate (cHF+F). Data are presented as means ± SE (n = 8-14). *$P < 0.05$ vs. genotype chow; †$P < 0.05$ vs. genotype cHF; ‡$P < 0.05$ vs. WT on respective diet.

4.1.9 Liver and muscle SCD1 activity expressed by the Δ^9 desaturation index

The activity of stearoyl-CoA desaturase 1 (SCD1), the rate limiting enzyme with Δ^9 desaturation activity involved in the biosynthesis of monounsaturated fatty acids (MUFAs), was evaluated. The ratio of palmitoleate/palmitate (16:1/16:0) and oleate/stearate (18:1/18:0) was used to estimate the activity of SCD-1. Using the 16:1/16:0 index, we could observe a global decrease of SCD-1 activity in all lipid fractions from the liver and muscle of mice fed cHF or cHF+F diets (Table 4.1-6). In general, cHF+F seemed to potentiate the decrease in the SCD-1 activity, but the effect was not significant. There were no genotype differences in this parameter. The 18:1/18:0 index revealed that cHF+F feeding significantly decreased the activity of SCD-1 in triacylglycerol fraction when compared to cHF and this effect was independent of the presence of α2-AMPK subunit.

Table 4.1-6 The activity of SCD1 in different lipid fractions from the liver and skeletal muscle

	WT			α2-AMPK KO		
	Chow	cHF	cHF+F	Chow	cHF	cHF+F
16:1/16:0						
Liver						
Triacylglycerol fraction	0.25 ± 0.01	0.06 ± 0.02*	0.03 ± 0.00*	0.21 ± 0.02	0.03 ± 0.00*	0.04 ± 0.02*
Diacylglycerol fraction	0.10 ± 0.01	0.03 ± 0.01*	0.02 ± 0.00*	0.09 ± 0.01	0.02 ± 0.00*	0.02 ± 0.01*
Phospholipid fraction	0.08 ± 0.01	0.01 ± 0.00*	0.01 ± 0.01*	0.08 ± 0.00	0.01 ± 0.00*	0.01 ± 0.01*
Skeletal muscle						
Triacylglycerol fraction	0.43 ± 0.05	0.23 ± 0.01*	0.14 ± 0.01*	0.52 ± 0.06	0.23 ± 0.03*	0.13 ± 0.02*
Diacylglycerol fraction	ND, The level of 16:1 under detection limit					
Phospholipid fraction	0.09 ± 0.00	0.02 ± 0.00*	0.01 ± 0.00*	0.10 ± 0.00	0.02 ± 0.00*	0.01 ± 0.00*
18:1/18:0						
Liver						
Triacylglycerol fraction	16.08 ± 0.85	14.17 ± 1.17	9.21 ± 0.74*†	17.40 ± 0.97	13.31 ± 2.28*	8.74 ± 1.02*†
Diacylglycerol fraction	0.66 ± 0.11	0.61 ± 0.13	0.37 ± 0.06*	0.80 ± 0.08	0.64 ± 0.09	0.46 ± 0.12 *
Phospholipid fraction	0.47 ± 0.03	0.23 ± 0.01*	0.29 ± 0.03*	0.44 ± 0.02	0.23 ± 0.01*	0.29 ± 0.03*
Skeletal muscle						
Triacylglycerol fraction	14.05 ± 1.65	16.23 ± 1.43	13.54 ± 1.45	13.29 ± 2.05	20.28 ± 3.80	11.23 ± 1.96†
Diacylglycerol fraction	0.33 ± 0.06	0.31 ± 0.06	0.32 ± 0.06	0.37 ± 0.10	0.27 ± 0.07	0.17 ± 0.04
Phospholipid fraction	0.39 ± 0.01	0.39 ± 0.03	0.40 ± 0.02	0.52 ± 0.03‡	0.46 ± 0.02‡	0.47 ± 0.01‡

Data are the means ± SE of 13-15 values. The Δ9 desaturation activity of SCD1 was estimated by the ratio of palmitoleate/palmitate (16:1/16:0) and oleate:stearate (18:1/18:0). ND, not determined. *$P < 0.05$ vs. genotype chow; †$P < 0.05$ vs. genotype cHF; ‡$P < 0.05$ vs. WT on respective diet.

4.1.10 The expression of genes involved in lipid metabolism in the liver

The mRNA levels of several genes involved in lipogenesis and lipid catabolism were measured by the real-time quantitative analysis. The liver samples of mice in random-fed or post-clamp conditions were analyzed. A representative sample for each experimental group was prepared by pooling the products of reverse transcription obtained for each individual mouse from a given subgroup. There were only a minute changes in SREBP-1c, ChREBP and FAS gene expression in random-fed mice (Figure 4.1-13 A). However, the expression of SCD1 gene was decreased by cHF feeding and cHF+F diet potentiated this decrease. This effect did not depend on the genotype. Among the genes of lipid catabolism, PPARα was induced solely in cHF+F fed α2-AMPK KO mice, CPT1α did not change in any of the subgroup and AOX levels were suppressed by cHF and induced by cHF+F to a similar extent in both genotypes. Different results were observed in the livers of mice analyzed after hyperinsulinemic-euglycemic clamp (Figure 4.1-13 B). Only small changes in the level of ChREBP and FAS genes were observed. SCD1 was down-regulated by cHF feeding in both genotypes. cHF+F reversed the effect of cHF diet on SCD1 expression levels only in WT mice. Similarly, the levels of SREBP-1c mRNA were induced in the livers of WT mice fed cHF+F but not in α2-AMPK KO mice. The levels of genes involved in lipid catabolism did not change in mice analyzed after the clamp.

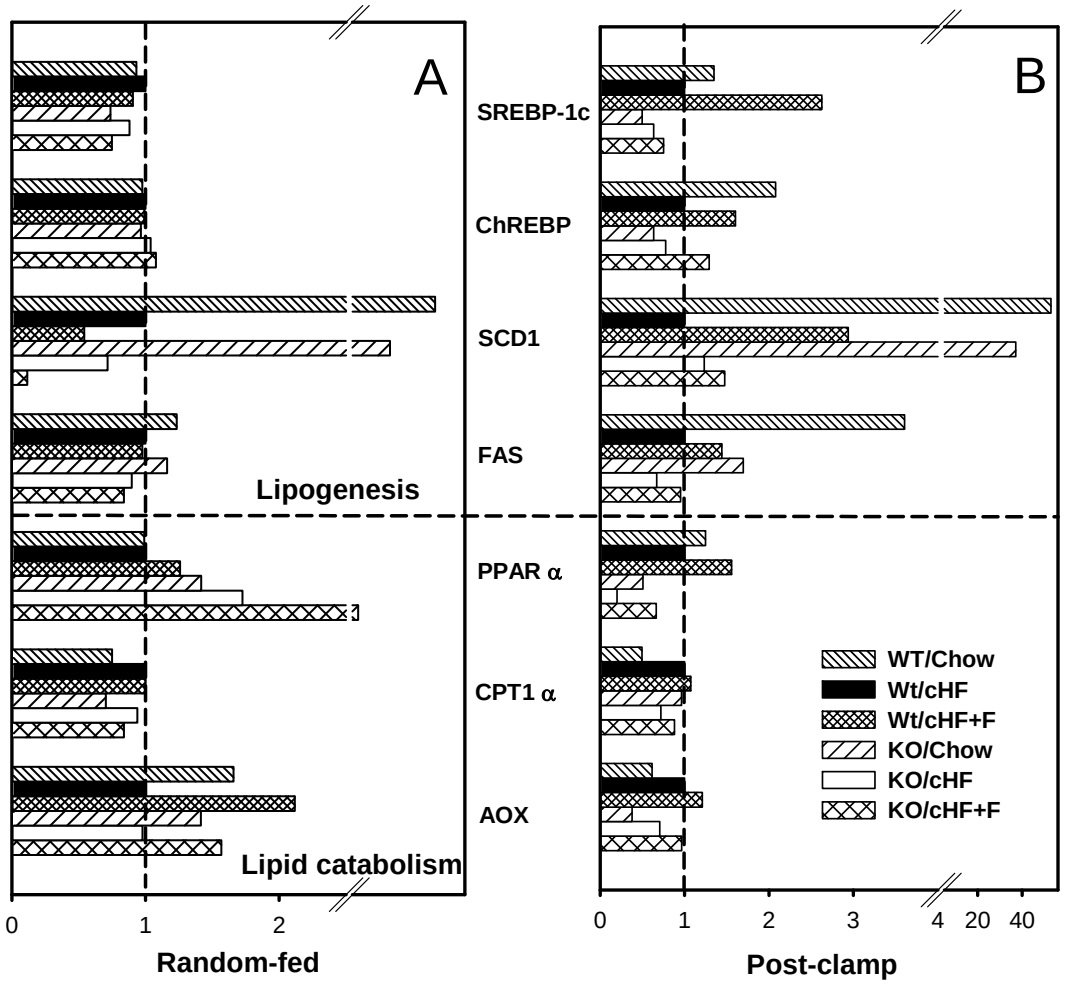

Figure 4.1-13 mRNA levels in arbitrary units of genes involved in lipogenesis and lipid catabolism from livers of male WT and α2-AMPK KO mice in in random-fed (A) and post clamp (B) conditions. Mice were fed for 9 weeks with control low-fat diet (Chow), control high-fat diet (cHF) or high-fat diet, in which 15% of lipids were replaced by n-3 LC-PUFA concentrate (cHF+F). The columns represent the expression level in one sample, obtained by pooling cDNA samples from individual mice with the given subgroup (n = 8-14).

4.1.11 Whole body energy expenditure in awake mice

To characterize whole body energy expenditure and its changes in response to diet in mice of both genotypes, indirect calorimetry was used to analyze oxygen consumption and respiratory quotient in random-fed, fasted, and mice re-fed by chow diet (see Methods 3.15). Oxygen consumption was decreased during fasting; however, there were no changes in this parameter between any of the subgroups irrespective of the nutritional conditions (Table 4.1-7).

Table 4.1-7 Results from indirect calorimetry measurement

	WT			α2-AMPK KO		
	Chow	cHF	cHF+F	Chow	cHF	cHF+F
O_2 consumption [ml . kg-1 . min-1]						
Random-fed	41,76 ± 1,71	37,75 ± 2,64	39,09 ± 1,72	42,44 ± 1,06	41,07 ± 1,76	41,95 ± 1,94
Fasting	31,15 ± 1,09	30,41 ± 0,39	30,38 ± 1,59	30,57 ± 0,93	33,01 ± 2,01	31,83 ± 1,36
Chow re-fed	40,86 ± 0,99	35,42 ± 2,49	38,68 ± 1,70	40,65 ± 1,16	40,39 ± 1,59	41,02 ± 1,21
Respiratory quocient (RQ) [%]						
Random-fed	87,87 ± 2,15	79,74 ± 1,35*	80,08 ± 0,54*	85,89 ± 1,73	80,58 ± 0,92*	80,66 ± 1,59*
Fasting	87,10 ± 1,87	85,09 ± 1,06	84,89 ± 1,74	86,70 ± 1,62	83,34 ± 1,71	83,57 ± 2,21
Chow re-fed	92,23 ± 2,04	83,85 ± 1,80*	84,34 ± 1,01*	89,83 ± 1,23	85,55 ± 1,01*	87,19 ± 1,86
Shift of RQ	4,37 ± 0,20	4,11 ± 0,16	4,26 ± 0,08	3,94 ± 0,13	4,97 ± 0,11	6,52 ± 0,27

Data are the means ± SE of 8 mice. *$P < 0.05$ vs. genotype chow; †$P < 0.05$ vs. genotype cHF; ‡$P < 0.05$ vs. WT on respective diet. Shift of RQ is the difference between the RQs corresponding to re-fed and random-fed mice.

Both, WT and α2-AMPK KO mice on the cHF or cHF+F diet preferentially oxidized lipids when compared to the chow-fed mice, as evidenced by the decreased respiratory quotient (RQ). Fasting diminished the differences between experimental groups and shifted the RQ of cHF- and cHF+F- fed mice towards increased glucose utilization. Administration of chow diet rich in carbohydrate resulted in the increase of glucose oxidation to a level similar in all subgroups (as expressed by the shift of RQ, see Table 4.1-7). However, the ability of chow re-fed mice, which were chronically treated with cHF and cHF+F diets to oxidize glucose was lower than in chow-fed mice. There was no effect of cHF+F feeding compared to cHF- fed mice in any of the genotype.

4.1.12 Norepinephrine-stimulated lipolysis in adipocytes

Basal and norepinephrine(NE)-stimulated lipolysis and the suppression of NE-stimulated lipolysis by insulin were analyzed in the adipocytes isolated from the epididymal white adipose tissue of male mice. The level of lipolysis in different conditions was estimated by following the rate of glycerol release from isolated adipocytes. Feeding mice with cHF diet decreased the level of basal, non-stimulated lipolysis in both genotypes (Figure 4.1-14 A). cHF+F diet tended to increase basal lipolysis in WT mice, while significantly increasing lipolysis in α2-AMPK KO mice when compared to cHF-fed mice. Addition of NE into adipocytes stimulated lipolysis in all experimental groups (Figure 4.1-14 B). α2-AMPK KO mice fed chow diet had significantly increased NE-stimulated lipolysis compared to the WT mice fed the same diet. The level of NE-stimulated lipolysis in mice fed with cHF or cHF+F diets was similar in both genotypes, while being decreased compared to chow diet (significant effect in α2-AMPK KO). Addition of insulin caused only negligible suppression of NE-stimulated lipolysis in this experimental setup, except of α2-AMPK KO mice fed a chow diet (~30%).

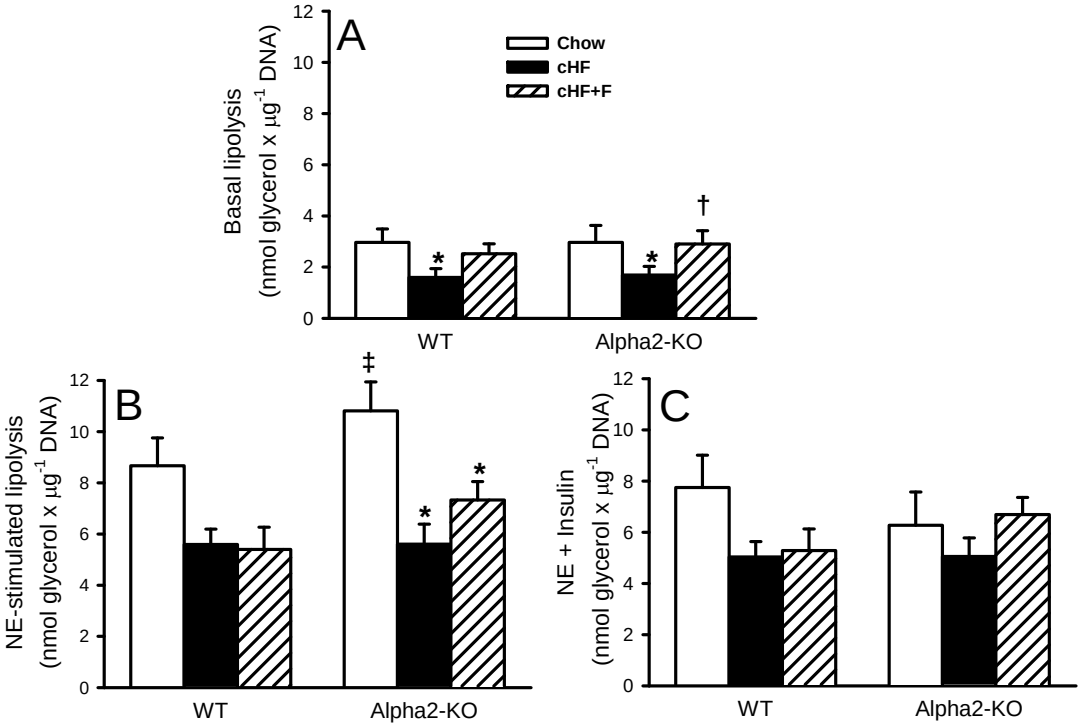

Figure 4.1-14 The level of lipolysis in adipocytes under different experimental conditions. Basal lipolysis (A), norepinephrine (NE)-stimulated lipolysis (B) and suppression of norepinephrine-stimulated lipolysis by insulin (C) in mice fed for 9 weeks with control low-fat diet (Chow), control high-fat diet (cHF) or high-fat diet, in which 15% of lipids were replaced by n-3 LC-PUFA concentrate (cHF+F). Data are presented as means ± SE (n = 8-14). **P* < 0.05 vs. genotype chow; †*P* < 0.05 vs. genotype cHF; ‡*P* < 0.05 vs. WT on respective diet.

4.2 Beneficial effects of DHA derivatives

My contribution to this work was the isolation of RNA and measurement of mRNA levels by the real-time PCR quantitative analysis.

The efficacy of n-3 LC-PUFA in the treatment of insulin resistance is relatively low in humans, especially in obese, insulin resistant objects. The aim of this study was to determine the efficacy of α-substituted DHA derivatives to prevent and reverse obesity, glucose intolerance, dyslipidemia, white-adipose tissue inflammation and lipid accumulation in nonadipose tissues in a mouse model of high-fat feeding. Among the DHA derivatives examined, Substance-2 displayed the most efficient effects in the prevention and reversal of obesity, glucose intolerance, and accumulation of lipids in the liver and skeletal muscle, as well as in the prevention of dyslipidemia and inflammation of adipose tissue (data not shown, see Paper 1, Chapter 9).

To better understand the mechanism of the effects of Substance-2, the expression of metabolic genes was measured in adipose tissue, liver and skeletal muscle by the real-time quantitative PCR analysis. Substance-2 prevented and reversed obesity-associated macrophage infiltration of epididymal WAT, as revealed by immunohistochemical detection of MAC-2 (data not shown, see Paper 1, Chapter 9). In line with this, mRNA levels of CD68 and MCP-1, the two factors that are closely linked to macrophage function, were decreased by 91% and 56% in the prevention and by 32% and 50% in the reversal study, respectively (Table 4.2-1). mRNA levels of PGC-1α and GLUT-4 did not change by Substance-2 when compared to cHF diet.

The expression of genes involved in fatty acid oxidation in the liver, such as AOX-1 and CPT-1α, was induced by Substance-2 in both, the prevention and reversal study, with a stronger induction in the latter. The activation of the peroxisomal oxidation through AOX-1 seemed to be stronger than the induction of mitochondrial oxidation (CPT-1α) in both studies. The expression of PPAR-α, the regulatory transcription factor for AOX-1 and CPT-1α, correlated well with mRNA levels of its target genes. In the reversal study, cHF+F diet (enriched with EPA and DHA) and to a lesser extent also DHA diet upregulated CPT-1α (but not AOX-1). However, these changes were

relatively small compared to the effects of Substance-2 admixed at a 10-fold lower dose to the cHF diet. n-3 LC-PUFA are known to decrease expression of lipogenic genes including stearoyl-coenzyme A desaturase-1 (SCD-1), as well as SPOT 14 and farnesyl diphosphate synthase (FDPS); (76). Expression of SCD-1, SPOT 14, and FDPS was down-regulated by cHF when compared with Chow diet. In the reversal study, expression of SCD-1 and SPOT 14 was decreased by both EPA/DHA and DHA alone. In contrast, expression of SCD-1 and FDPS was markedly induced by Substance-2, namely in the reversal study.

In the skeletal muscle, Substance-2 exerted negligible effects on gene expression except for a down-regulation of SCD-1 in the prevention study.

Table 4.2-1 The effect of Substance-2 on mRNA levels of selected genes

	Prevention study			*Reversal study*				
	Chow	cHF	Substance-2	Chow	cHF	Substance-2	cHF+F	DHA
Adipose tissue								
CD68	7 ± 1*	100 ± 24	9 ± 3*	17 ± 2*	100 ± 16	68 ± 16	NM	NM
MCP-1	20 ± 3*	100 ± 15	44 ± 19*	33 ± 3*	100 ± 13	50 ± 14*	NM	NM
PGC-1α	109 ± 3*	100 ± 2	100 ± 2	99 ± 8	100 ± 3	101 ± 4	NM	NM
GLUT-4	647 ± 61*	100 ± 24	193 ± 45	229 ± 72*	100 ± 16	68 ± 16	NM	NM
Liver								
CPT-1α	52 ± 6*	100 ± 7	140 ± 13*	14 ± 2*	100 ± 24	563 ± 203*	196 ± 54*	145 ± 49
AOX-1	68 ± 10	100 ± 8	308 ± 23*	12 ± 5*	100 ± 27	1477 ± 500*	88 ± 35	114 ± 33
PPAR-α	73 ± 8*	100 ± 8	135 ± 10*	6 ± 2*	100 ± 19	296 ± 100*	113 ± 31	78 ± 15
SCD-1	243 ± 39*	100 ± 7	410 ± 34*	293 ± 71*	100 ± 15	1004 ± 98*	44 ± 19	23 ± 11*
SPOT 14	155 ± 49	100 ± 17	65 ± 17	132 ± 22	100 ± 14	149 ± 31	49 ± 18	43 ± 10*
FDPS	211 ± 24*	100 ± 13	260 ± 28*	174 ± 43	100 ± 13	452 ± 46*	84 ± 21	81 ± 23
Skeletal muscle								
GLUT-4	139 ± 6*	100 ± 15	109 ± 13	83 ± 9	100 ± 6	79 ± 5	NM	NM
PDK-4	31 ± 6*	100 ± 13	96 ± 12	23 ± 10*	100 ± 14	89 ± 10	NM	NM
SCD-1	319 ± 151	100 ± 25	49 ± 6*	79 ± 12	100 ± 8	87 ± 5	NM	NM

Data are the means ± SE of 7-9 except for Chow-fed mice in the „*reversal study*“ ($n = 4$).
Gene expression data were expressed as a percentage of the cHF-fed controls. 1,5% of dietary lipids was replaced by Substance-2, while 15% of dietary lipids was replaced by EPA/DHA concentrate (cHF+F diet) or DHA.
AOX-1, acyl-CoA oxidase-1; CPT-1α, carnitine palmitoyltransferase-1α; FDPS, farnesyl diphosphate synthetase; GLUT-4, glucose transporter-4; MCP-1, monocyte chemoattractant protein-1; PDK-4, pyruvate dehydrogenase kinase-4; PGC-1α, peroxisome proliferator-activated receptor-γ coactivator-1α; PPAR-α, peroxisome proliferator-activated receptor-α; SCD-1, stearoyl-coenzyme A desaturase-1; SPOT 14, thyroid hormone responsive SPOT 14; NM, not measured. *$P < 0.05$ vs. cHF (ANOVA).

4.3 Additive beneficial effects of combination treatments

My contribution to this work was the measurement of insulin sensitivity by the hyperinsulinemic-euglycemic clamp technique, evaluation of VLDL-TAG synthesis, measurement of plasma metabolites and management and coordination of this part of the experiment.

Another approach how to improve the efficiency of n-3 LC-PUFA treatment in the prevention and reversal of obesity-induced metabolic diseases could be the combination treatment with other potent anti-diabetic drugs. We hypothesised that partially overlapping mechanisms of action of n–3 PUFA and rosiglitazone, an anti-diabetic drug in the thiazolidinedione (TZD) class, could have synergistic effects in a combination treatment, leading to an improved of glycemic profile.

Combined treatment using n–3 LC-PUFA and a low-dose rosiglitazone generated additive effects in the prevention as well as reversal of obesity, adipose tissue hypertrophy, hyperlipidemia and impaired glycemic control in mice fed an obesogenic cHF diet (data not shown, see Paper 2, Chapter 9). To evaluate precisely the changes in whole-body insulin sensitivity brought about by various treatments, hyperinsulinemic-euglycemic clamps were performed in awake mice after 8 weeks of feeding with cHF, cHF+F, cHF+TZD and cHF+F+TZD diets (see Methods, Table 3.1-1). In the hyperinsulinemic conditions, the amount of exogenous glucose required to maintain euglycemia, i.e. glucose infusion rate (GIR), was significantly (~1.7-fold) higher in mice treated by either cHF+F or cHF+TZD as compared with the cHF mice (Figure 4.3-1 B), suggesting improvements in insulin sensitivity. Importantly, cHF+F+TZD resulted in a ~2.4-fold higher GIR compared with the cHF-fed mice, which represented the strongest effect among all the treatments. Hepatic glucose production (HGP) in the hyperinsulinemic conditions was decreased in the cHF+F mice, and significantly lower as compared with the other subgroups (Figure 4.3-1 C), suggesting improvements in hepatic insulin sensitivity by n-3 LC-PUFA. The cHF+F+TZD and cHF+TZD (but not cHF+F) treatments also significantly improved whole-body glucose turnover (GTO), while cHF+F+TZD showed the most dramatic effect (Figure 4.3-1 D). The rate of whole-body glycolysis was not significantly affected by the treatments (Figure 4.3-1 E).

Whole-body glycogen synthesis was strongly stimulated by cHF+F+TZD, while cHF+F and cHF+TZD had nosignificant effects (Figure 4.3-1 F).

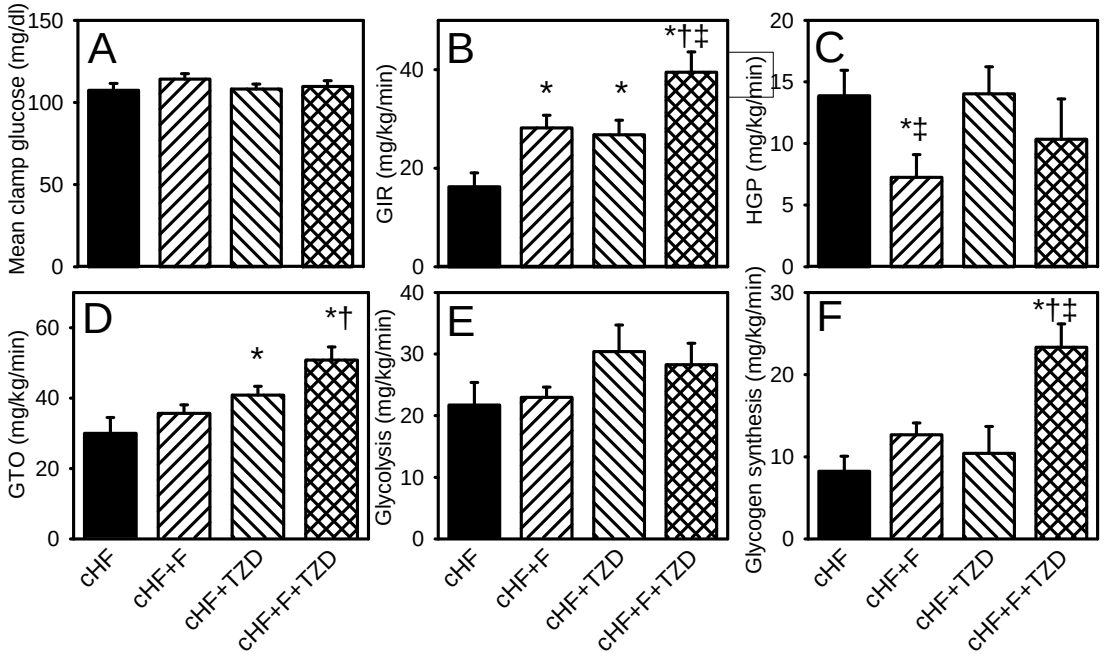

Figure 4.3-1 Insulin sensitivity of male mice. Mean clamp glucose (A), glucose infusion rate (GIR) (B), hepatic glucose production (HGP) (C), glucose turn-over rates (GTO) (D), , whole-body glycolysis (E) and glycogen synthesis (F) assessed by hyperinsulinemic-euglycemic clamp in C57BL/6J male mice fed for 8 weeks with control high-fat diet (cHF), high-fat diet, in which 15% of lipids were replaced by n-3 LC-PUFA concentrate (cHF+F), or high-fat diet supplemented with 10 mg/kg diet of rosiglitazone (cHF+TZD) or both, n-3 LC-PUFA and rosiglitazone supplemented (cHF+F+TZD). Data are presented as means ± SE (n = 6-9). *$P < 0.05$ for difference from cHF; †$P < 0.05$ for difference from cHF+F; ‡$P < 0.05$ for difference from cHF+TZD (ANOVA).

Individual treatments exerted hypolipidemic effects with the most potent reduction observed in the combination (cHF+F+TZD) treatment (data not shown). Therefore, liver VLDL-triacylglycerol synthesis was investigated after 8 weeks of treatment. All the treatments significantly decreased the rate of VLDL-triacylglycerol synthesis, while the strongest reduction (approximately twofold) was observed in the cHF+F+TZD treatment (Figure 4.3-2).

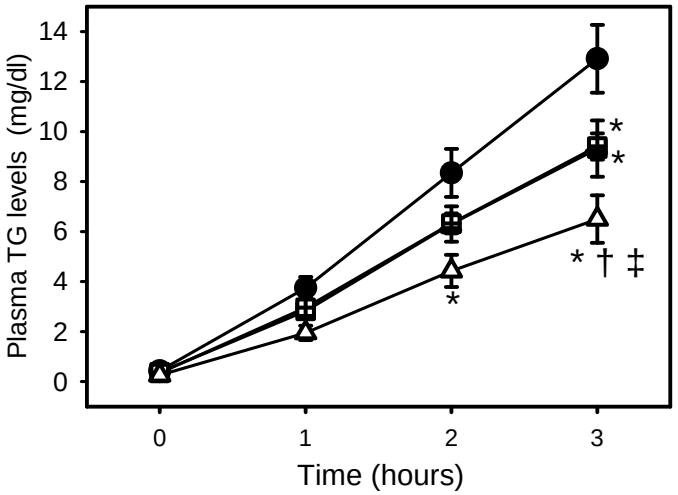

Figure 4.3-2 Hepatic VLDL-triacylglycerol production. At 3 months of age, mice were randomly assigned to various diets, and after 8 weeks of treatment, mice were fasted for 6 h, anesthetized, injected with Triton WR1339, and plasma triacylglycerol levels were measured before (time 0), and at 1,2, and 3 hour after injection in the cHF (black circles), cHF+F (empty squares), cHF+TZD (crossed squares), and cHF+F+TZD (empty triangles)-fed mice. Data are presented as means ± SE (n=5-8). *Significantly different from cHF; †significantly different from cHF+F; ‡significantly different from cHF+TZD (ANOVA).

5 DISCUSSION

5.1 The involvement of α2-AMPK in the beneficial effects of *n*-3 LC-PUFA

To date, many studies and clinical investigations have reported beneficial effects of n-3 LC-PUFA, namely EPA and DHA, in both healthy as well as diseased organisms. These naturally occurring compounds, essential for humans, have pleiotropic effects in the organism. The aim of this study was: 1) to characterize the effects of n-3 LC-PUFA on the development of obesity-related metabolic disorders in the mouse model of high-fat diet-induced obesity and insulin resistance; and 2) to verify the hypothesis that n-3 LC-PUFA could act through the pathways that involve α2 catalytic subunit of AMPK by using knock-out mice with a targeted deletion of α2-AMPK.

In this study, the diet with a high fat content (cHF, ~35% wt/wt) was used to induce obesity, insulin resistance and related metabolic disorders. The obesogenic and diabetogenic effects of high-fat diets are well-known [(109); (110); (111)], however the occurrence and severity of high-fat diet-induced metabolic disorders may vary depending on the ratio of fat/carbohydrate, saturated/monounsaturated/polyunsaturated fatty acids, and the model organism. Nevertheless, the heterogeneity in response to a high-fat diet in genetically homogeneous mice has been also observed (101). Therefore, it is extremely important to characterize in detail any experimental model of diet-induced metabolic disorders. In this study, the whole-body α2-AMPK knock-out mice, generated on a hybrid C57BL/6J and 129/Sv genetic background and subsequently backcrossed to C57BL/6J genetic background for 9 generations, were used. C57BL/6J mouse strain is known to carry a genetic predisposition to develop diet-induced obesity and insulin resistance (112). Indeed, 9 weeks of cHF feeding induced obesity and adiposity in male WT mice characterized by the increased body weight gain, increased epididymal and dorsolumbar white adipose tissue mass and hypertrophy of adipocytes when compared to chow-fed controls, whereas the average food consumption did not significantly change. The weight of non-adipose tissues remained unaffected.

cHF-feeding proved to have detrimental effects on the whole-body insulin sensitivity as assessed by the hyperinsulinemic-euglycemic clamp. This was due to impaired whole-body glucose turnover rates and glycogen synthesis, and a lower potency of insulin to suppress hepatic glucose production. The decline in glycogen synthesis in individual tissues corresponded to the overall decline in whole-body glycogen synthesis. Another signs of impaired metabolism are changes in plasma levels of metabolites and hormones, such as glucose, insulin, triacylglycerols, NEFA, cholesterol and adiponectin. Mice fed cHF-diet had normal blood glucose levels, while insulin levels were increased. Normoglycemia together with hyperinsulinemia in cHF-fed mice indicated the presence of insulin resistance, which was confirmed by the clamp studies. As shown in first-degree relatives of patients with type 2 diabetes, insulin resistance precedes and predicts the development of glucose intolerance and type 2 diabetes (113). Indeed, as shown in female mice, glucose intolerance was not yet developed after 9 month of cHF feeding in this study.

Elevated plasma triacylglycerol concentrations have been identified as one of the primary components of the insulin resistance syndrome (114). However, in our model, plasma triacylglycerol levels remained normal in response to high-fat feeding under all nutritional conditions. The overall concentration of plasma triacylglycerols is the result of the exogenous intake of dietary lipids, the synthesis and secretion of VLDL-triacylglycerols from the liver and their uptake in the peripheral tissues. Mice fed the cHF diet with a high content of lipids had a decreased secretion of VLDL-triacylglycerols from the liver, while preferentially oxidizing lipids at the whole-body level. These effects could maintain homeostasis of plasma triacylglycerol levels. Feeding mice with the cHF diet also resulted in elevated plasma NEFA levels in the fasted and re-fed state. Hypertrophied adipocytes are characterized by an increased rate of lipolysis (115). However, the basal lipolysis, norepinephrine-stimulated lipolysis as well as lipolysis suppressed by insulin were all decreased in isolated adipocytes from cHF-fed mice compared to those from the chow-fed mice. Thus, a decreased uptake of fatty acids by the liver and/or by peripheral tissues could be responsible for the elevated levels of plasma NEFA, but this is not supported by any experimental data. On the contrary, the livers of mice fed the cHF diet had increased levels of triacylglycerols, and

hepatic steatosis was observed. The excessive accumulation of triacylglycerols in the liver can occur as the result of increased lipid delivery (exogenously from the diet in the form of chylomicrons or from increased lipolysis in the form of NEFA), increased lipid synthesis, reduced oxidation and/or reduced VLDL-triacylglycerols secretion. The lipolysis in adipocytes was decreased by cHF diet and lipogenesis, as assessed by the expression levels of key lipogenic enzymes, was unchanged (SREBP-1c, ChREBP, FAS) or even decreased (based on SCD1 mRNA expression and Δ9 desaturation activity of SCD1). Mitochondrial β-oxidation seemed to be unchanged (PPARα, CPT1α) and peroxisomal oxidation seemed to be slightly decreased (AOX). Therefore, increased delivery of lipids from the diet and a decreased VLDL-triacylglycerols secretion, which could protect the mice from the hypertriacylglycerolemia, are possibly responsible for the development of hepatic steatosis by cHF feeding. Plasma cholesterol levels were increased under all nutritional conditions by cHF feeding. Finally, the level of insulin-sensitizing hormone adiponectin tended to decrease by cHF diet. This effect was in agreement with the previous studies which showed decreased adiponectin secretion in obese people (116) and increased pro-inflammatory secretion profile of adipose tissue in hypertrophied adipocytes (9). To summary, high-fat diet induced obesity, insulin resistance, hypercholesterolemia, increased NEFA levels, hepatic steatosis and tended to decrease plasma adiponectin while plasma triacylglycerols levels remained unchanged in wild-type mice.

The next question was, how the above mentioned parameters changed after replacing 15 % of fat in cHF diet with n-3 LC-PUFA concentrate and whether α2-AMPK was involved in these effects. Wild type mice treated with cHF+F diet for 9 weeks were protected against high-fat diet-induced obesity and adiposity, as documented by a significantly lower body weight gain and the weight of epididymal and dorsolumbar white adipose tissue mass. The average food consumption was unaffected. The anti-obesity effects of n-3 LC-PUFA in animal models and human subjects are well-documented [(70); (66); (86)]. Adipose tissue mass can increase either by hyperplasia or hypertrophy. n-3 LC-PUFA have been shown to decrease the number of adipocytes by inhibiting adipocyte differentiation and by the induction of apoptosis of preadipocytes (81). However, in this experiment, the anti-obesity effects of cHF+F diet rich in n-3 LC-

PUFA was primarily due to a reduction in the epididymal adipocyte size. The increased basal lipolysis in epididymal adipose tissue of cHF+F fed mice could explain the potency of cHF+F to decrease epididymal adipocyte size. There was a differential effect of cHF+F on the size of dorsolumbar adipocytes. The size of these adipocytes remained unaffected, even though the mass of this fat depot was reduced. The lipolysis in this depot was not measured and probably other mechanisms are involved in the effects of cHF+F on the mass of dorsolumbar adipose tissue. Importantly, any of these effects of cHF+F were independent of the α2-AMPK, since a similar phenotype was observed in α2-AMPK KO mice. In agreement with its effect on epididymal adipose tissue mass and adipocyte size, cHF+F diet affected the properties of the epididymal depot. Adipocyte size is an important factor linked to inflammation, insulin sensitivity and adipokine secretion profile. Increasing adipocyte size resulted in a higher propensity to a cell death and subsequent macrophage infiltration (18) resulting in a shift towards pro-inflammatory secretion profile (9). The level of macrophage infiltration evaluated by the immunohistochemical detection of MAC-2 tended to be reduced by cHF+F diet together with the decreased adipocyte size. Moreover, the secretion of HMW form of adiponectin, the adipokine with insulin sensitizing properties, was increased. The ability of adiponectin to reverse obesity-induced insulin resistance was due to a reduction in hepatic glucose production (15) and was mediated through the activation of AMPK in the liver. In our study, the beneficial effect of cHF+F on adiponectin secretion was not observed in mice without α2-AMPK subunit. The reason for this observation is not clear, since the predominant form of AMPK in adipose tissue is represented by α1-catalytic subunit and adiponectin lies upstream in the activation cascade of AMPK. For instance, AICAR induced adiponectin secretion from adipose tissue, but this effect was indirect via a decrease in TNFα (34).

The insulin sensitivity measured by hyperinsulinemic-euglycemic clamp was improved by cHF+F diet rich in n-3 LC-PUFA. Mice on this diet had better suppression of hepatic glucose production by insulin. The insulin sensitivity of peripheral tissues, assessed by the rate of glucose turnover, was only slightly and non-significantly improved. On the other hand, whole-body glycogen synthesis was ameliorated by cHF+F. The beneficial effects of n-3 LC-PUFA in the prevention of obesity-induced

insulin resistance in rodent models are known (72). However, it has been shown for the first time in this study, that n-3 LC-PUFA mediate their beneficial effects on the prevention of obesity-induced insulin resistance in α2-AMPK-dependent manner. First of all, insulin inefficiently suppressed hepatic glucose production in α2-AMPK KO mice fed the cHF+F, while whole-body glycogen synthesis was not improved. The question is what is the mechanism of AMPK action in the beneficial effects of n-3 LC-PUFA? The activation of AMPK in animals fed n-3 LC-PUFA rich diet was demonstrated before [(87); (88)], even though another work argued against the involvement of AMPK in n-3 LC-PUFA effects (117). In our study, the α2-AMPK activity in the liver measured *ex vivo* was increased by cHF+F diet supplemented with n-3 LC-PUFA. Activation of liver AMPK by various treatments, for example by AICAR (the AMP mimetic) or metformin, led to a suppression of liver gluconeogenesis [(118); (43)]. Thus, the activation of liver AMPK by n-3 LC-PUFA could be responsible for the improved suppression of hepatic glucose production and whole-body insulin sensitivity.

It has been described that liver steatosis is associated with insulin resistance, and that lowering of liver triacylglycerols pools in several rodent models correlated with improved insulin sensitivity (22). Also in this study, improved liver insulin sensitivity in wild-type mice in response to cHF+F was accompanied by decreased liver triacylglycerol levels and by reduced plasma triacylglycerol, NEFA, and cholesterol levels. However, this was not the case in cHF+F-fed α2-AMPK KO mice, which exhibited decreased liver steatosis and plasma lipids but insulin resistance was still present. The question of causal relationship between liver triacylglycerol levels and insulin sensitivity still remains controversial (20). There are several lines of evidence, that diacylglycerols determine the development of insulin resistance (see chapter 1.1.2, (27)). Diacylglycerols activate protein kinase C-ε (PKCε), which in turn inhibits insulin signaling pathways (28). In our study, wild-type mice fed cHF+F diet had decreased levels of liver diacylglycerols, and this was accompanied by improved insulin sensitivity. The effects of cHF+F on both liver diacylglycerol content and liver insulin sensitivity were abolished in α2-AMPK KO mice. In agreement with our observations, mice with a targeted deletion of PPAR-α, the transcription factor which is downstream of AMPK (119), did not improve liver insulin sensitivity by n-3 LC-PUFA feeding,

while the effect of n-3 LC-PUFA in reducing liver triacylglycerol content was still present; in contrast, liver diacylglycerols were increased (73). Furthermore, it was also observed that the onset of insulin resistance correlated with increased diacylglycerol content and reduced AMPK activity in the liver (120). Therefore, in our model, n-3 LC-PUFA could improve insulin sensitivity by activating AMPK, which could in turn result in a decrease of liver diacylglycerol levels. How the stimulation of AMPK axis would affect diacylglycerol levels in the liver remains to be elucidated.

Another interesting observation of this study was an interaction between the diet and genotype concerning the effects on liver lipogenesis assessed by the measurement of mRNA levels for the SREBP-1c transcription factor. There was no suppression of liver SREBP-1c mRNA levels by cHF+F diet, neither in wild type nor in α2-AMPK KO mice analyzed in random-fed state. This is in contrast to the earlier studies, in which n-3 LC-PUFA suppressed liver lipogenesis through a downregulation of SREBP-1c expression (121). This discrepancy might be explained by the differences in experimental models, such as the use of high-fat diet vs. the low fat/high sucrose diet, which has a high lipogenic potency. High-fat diet used in our study strongly repressed lipogenesis and therefore the possibility to detect additional inhibitory effect of n-3 LC-PUFA diet was quite low. On the other hand, liver SREBP-1c was induced by cHF+F in wild type mice during the clamp study, i.e. during the conditions of hyperinsulinemia and glucose being the only exogenous substrate. Increased ability of insulin to convert glucose from circulation into lipids by inducing *de novo* lipogenesis could imply increased liver sensitivity to insulin. Accordingly, this effect was not observed in mice lacking α2-AMPK, which failed to improve liver insulin sensitivity in response to cHF+F diet. Our results are controversial when data from the literature are taken into account. Firstly, it was shown in primary hepatocytes, that n-3 LC-PUFA suppressed insulin-induced SREBP-1c transcription by the mechanism involving lower capacity of liver X receptor alpha (LXRα) to activate SREBP-1c (122). Secondly, the increase of SREBP-1c in the liver of cHF+F-fed mice and absence of this effect in mice lacking α2-AMPK is not in agreement with the known function of AMPK, which down-regulates anabolic pathways such as lipogenesis by decreasing the SREBP-1c (123). Probably the use of *in vivo* model and specific conditions of hyperinsulinemic-euglycemis clamp could explain

these discrepancies. Other measurements, for example the nuclear content of SREBP-1c or biochemical measurement of lipogenesis in liver explants could answer these questions.

The gender differences in several metabolic parameters were observed. For instance, the potency of n-3 LC-PUFA to protect against high-fat diet-induced obesity was lower in female mice, compared to male mice. Interestingly, while the effects of n-3 LC-PUFA to decrease plasma triacylglycerol, NEFA and cholesterol levels in random-fed state were genotype-independent in male mice, in females, the lack of functional α2-AMPK led to a disappearance of these beneficial effects. This study was primarily aimed to study the male mice, and therefore more experiments would be needed to resolve the mechanisms responsible for these gender differences.

5.2 Beneficial effects of DHA derivatives

The efficiency of n-3 LC-PUFA to treat insulin resistance in obese humans is relatively low. We showed that replacement of 1.5% of dietary lipids by various chemical DHA-derivatives affected the development of diet-induced obesity and associated metabolic traits in C57BL/6 mice fed a high-fat diet (93). Substance-2 (α-ethyl DHA ethyl ester) completely prevented and even partially reversed the development of obesity, fat accumulation, impaired glucose tolerance, dyslipidemia and white adipose tissue inflammation.

The assessment of mRNA levels of various metabolic genes revealed some information on the mechanisms of action of these DHA-derivatives, namely Substance-2. The properties of epididymal white adipose tissue (tissue cellularity, the size of adipocytes, macrophage infiltration) were profoundly affected by Substance-2. The expression of CD68 and MCP-1, two factors that are closely linked to the function of macrophages, was decreased by Substance-2. In line with this observation, histological analysis of epididymal white adipose tissue revealed that Substance-2 completely prevented obesity-associated macrophage infiltration of adipose tissue. The reduction of macrophage infiltration should have beneficial systemic effects, since macrophages represent an additional source of pro-inflammatory cytokines, which induce insulin resistance and contribute to a state of chronic low-level inflammation in obesity (124). Similar to the effects of n-3 LC-PUFA, Substance-2 also partially prevented down-regulation of GLUT4 in white adipose tissue, otherwise induced by high-fat diet. In the liver, Substance-2 induced lipid oxidation as documented by the upregulation of PPARα and its target genes AOX1 and CPT1α. Moreover, lipogenic genes such as SCD1 and FDPS were also induced. This simultaneous stimulation of *in situ* lipogenesis and lipid oxidation by Substance 2 in the liver suggests induction of futile substrate cycling, which may be responsible for the reduced accumulation of triacylglycerols in the tissues.

5.3 Additive beneficial effects of combination treatments

Combination of life style changes with pharmacological interventions is required for treatment of diabetes and other metabolic diseases associated with obesity. We showed that long-term treatment combining partial replacement of dietary lipids by n-3 LC-PUFA and a low dose of thiazolidinedione rosiglitazone markedly and in additive manner prevented development of dyslipidemia and insulin resistance, reduced accumulation of body fat and adipocyte hypertrophy, while inducing adiponectin in mice fed a high-fat diet. Importantly, this treatment also reverted impaired glucose tolerance in obese mice.

Hyperinsulinemic-euglycemic clamps in mice showed synergistic induction of glycogen synthesis at the insulin-stimulated conditions by the combination treatment, indicating that skeletal muscle was the major organ responsible for the additive effects of n-3 LC-PUFA and rosiglitazone combination on whole-body glycemic control. Interestingly, and in accordance with the previous studies, neither the treatment by n-3 LC-PUFA [(72); (73); (125)] nor rosiglitazone alone (at the relatively low dose used; (126)) significantly affected the rate of glycogen synthesis. n-3 LC-PUFA but not rosiglitazone were able to depress hepatic glucose production under hyperinsulinemic conditions, suggesting improvement of hepatic insulin sensitivity by the former treatment. Given the ability of n-3 LC-PUFA to prevent development of impaired glucose tolerance, the above data also suggest that the effect on hepatic glucose production may dominate in the effect of n-3 LC-PUFA. On the other hand, the reversal of impaired glucose tolerance and insulin resistance by thiazolidinedione may depend more on the enhancement of insulin action in skeletal muscle. This effect could be mediated either by TZD, or, according to our results, even more potently by the combination of n-3 LC-PUFA and TZD. A putative mechanism behind the synergistic effect of the combination treatment might involve reductions of muscle ceramide content.

The additive improvements of insulin sensitivity correlated with the hypolipidemic effect of the treatments. The suppresion of plasma triacylglycerol levels possibly resulted either from an increased triacylglycerol uptake by muscle and other tissues induced by both TZD (127) and n-3 LC-PUFA (128), or from a decreased hepatic

VLDL-triacylglycerol production. The former mechanism has not been studied in our experiments, however, we have demonstrated the inhibition of hepatic VLDL-triacylglycerol production by either n-3 LC-PUFA or rosiglitazone, while the strongest effect was observed in the combination treatment. The decrease of hepatic triacylglycerol production by n-3 LC-PUFA may represent a functional outcome of the coordinated suppression of lipogenic genes by n-3 LC-PUFA (76). In addition, a stimulation of AMP-activated protein kinase by n-3 LC-PUFA, resulting in a metabolic switch from lipogenesis to lipid catabolism, may be also involved (87).

In contrast, the mechanism of suppression of VLDL-triacylglycerol formation by rosiglitazone must be different, since rosiglitazone increased both SCD1 expression and triacylglycerol content in the liver. The mechanism may reflect increased rate of fatty acid re-esterification induced by rosiglitazone (129) rather than suppresion of de novo lipogenesis in hepatocytes. These data, in accordance with the effects of the treatments on muscle SCD1, document differential modulation of the genes involved in de novo fatty acid synthesis (FAS) and desaturation (SCD1) by n-3 LC-PUFA and rosiglitazone. That rosiglitazone treatment induced expression and activity of SCD1 in association with insulin sensitization has been observed before (130), but the underlying mechanism remains unknown.

6 CONCLUSIONS

With respect to the specific aims of the thesis, the following conclusions could be drawn:

1. Among the beneficial effects of n-3 LC-PUFA, it is primarily the effect on hepatic insulin sensitivity, which shows a clear α2-AMPK dependency. Moreover, there is an association between the improvement in hepatic insulin sensitivity and hepatic levels of diacylglycerols, but not triacylglycerols. The precise mechanism of AMPK action in the beneficial effects of n-3 LC-PUFA remains to be elucidated.

2. Among the four DHA-derivatives tested, Substance-2 (α-ethyl DHA ethyl ester) appeared to exhibit a similar range of beneficial effects on obesity and associated metabolic disorders as naturally occurring n-3 LC-PUFA, but with a higher efficacy. Therefore, this compound could qualify as a novel drug for the treatment of obesity, dyslipidemia and insulin resistance.

3. Combined use of n-3 LC-PUFA and a low dose rosiglitazone generated additive effects in the prevention as well as reversal of adipose tissue hypertrophy, hyperlipidemia and impaired glycemic control in mice fed an obesogenic diet. Multiple mechanisms underlined the beneficial effects of the combination treatment with a prominent synergistic stimulation of muscle glycogen synthesis in response to insulin. The combined use of n-3 LC-PUFA and thiazolidinedions thus represents a prospective strategy in the treatment of type 2 diabetes and other obesity-associated metabolic disorders. The inclusion of n-3 LC-PUFA in the pharmacological treatment may reduce the dose requirements and the incidence of adverse side-effects associated with the thiazolidinedione-based therapy.

7 SUMMARY

It is well established that n-3 LC-PUFA have beneficial effects on the obesity-induced metabolic disorders in mice. However, in obese humans, the potency of these fatty acids to positively affect obesity and insulin resistance has been shown to be lower. The aim of the studies described in this thesis was to verify various approaches aimed at increasing efficiency of n-3 LC-PUFA and to study their mechanism of action.

Firstly, various chemical derivatives of DHA were tested in mice. Substance-2, the α-ethyl ester of DHA, completely prevented and even partially reversed the development of obesity, fat accumulation, impaired glucose tolerance, dyslipidemia and white adipose tissue inflammation, even though the dose was only 10 % of that normally used in mice for the treatment with n-3 LC-PUFA. Secondly, the combination of n-3 LC-PUFA and a low-dose of anti-diabetic rosiglitazone prevented, in additive manner, development of dyslipidemia and insulin resistance, reduced the accumulation of body fat and adipocyte hypertrophy, while inducing adiponectin in mice fed a high-fat diet. This treatment also reversed impaired glucose tolerance in obese mice.

The major part of this thesis was aimed to study the mechanism of n-3 LC-PUFA action and the possible involvement of α2-AMPK. We found, by using the model of α2-AMPK knockout mice, that beneficial effects of n-3 LC-PUFA on the prevention of insulin resistance were mediated by α2-AMPK. The liver appeared to be the site of a dominant effect of n-3 LC-PUFA, since their inclusion in the diet resulted in the activation of α2-AMPK primarily in the liver and improved hepatic insulin sensitivity in the α2-AMPK-dependent manner. The improvement of liver insulin sensitivity was not associated with the changes in liver triacylglycerol levels; however, it was closely related to the content of diacylglycerols that are known to affect insulin sensitivity. Similarly to hepatic insulin sensitivity, also the effect of n-3 LC-PUFA on diacylglycerol levels was α2-AMPK-dependent. The precise mechanisms of α2-AMPK activation by n-3 LC-PUFA as well as downstream effectors of α2-AMPK activation in this context remain to be elucidated

8 REFERENCES

1. Despres,JP, Lemieux,I: Abdominal obesity and metabolic syndrome. *Nature* 444:881-887, 2006

2. Kahn,SE, Hull,RL, Utzschneider,KM: Mechanisms linking obesity to insulin resistance and type 2 diabetes. *Nature* 444:840-846, 2006

3. Cao,H, Gerhold,K, Mayers,JR, Wiest,MM, Watkins,SM, Hotamisligil,GS: Identification of a lipokine, a lipid hormone linking adipose tissue to systemic metabolism. *Cell* 134:933-944, 2008

4. Galic,S, Oakhill,JS, Steinberg,GR: Adipose tissue as an endocrine organ. *Mol.Cell Endocrinol.* 316(2):129-39, 2010

5. Farnier,C, Krief,S, Blache,M, Diot-Dupuy,F, Mory,G, Ferre,P, Bazin,R: Adipocyte functions are modulated by cell size change: potential involvement of an integrin/ERK signalling pathway. *Int.J.Obes.Relat Metab Disord.* 27:1178-1186, 2003

6. Yki-Jarvinen,H: Ectopic fat accumulation: an important cause of insulin resistance in humans. *Journal of the Royal Society of Medicine* 95:39-45, 2002

7. Campbell,PJ, Carlson,MG, Hill,JO, Nurjhan,N: Regulation of free fatty acid metabolism by insulin in humans: role of lipolysis and reesterification. *Am.J.Physiol* 263:E1063-E1069, 1992

8. Boden,G: Role of fatty acids in the pathogenesis of insulin resistance and NIDDM. *Diabetes* 46:3-10, 1997

9. Skurk,T, Alberti-Huber,C, Herder,C, Hauner,H: Relationship between adipocyte size and adipokine expression and secretion. *J.Clin.Endocrinol.Metab* 92:1023-1033, 2007

10. Pelleymounter,MA, Cullen,MJ, Baker,MB, Hecht,R, Winters,D, Boone,T, Collins,F: Effects of the obese gene product on body weight regulation in ob/ob mice. *Science* 269:540-543, 1995

11. Shimizu,H, Shimomura,Y, Hayashi,R, Ohtani,K, Sato,N, Futawatari,T, Mori,M: Serum leptin concentration is associated with total body fat mass, but not abdominal fat distribution. *Int.J.Obes.* 21:536-541, 1997

12. Steinberg,GR, Dyck,DJ: Development of leptin resistance in rat soleus muscle in response to high-fat diets. *Am.J Physiol Endocrinol.Metab* 279:E1374-E1382, 2000

13. Hu,E, Liang,P, Spiegelman,BM: AdipoQ is a novel adipose-specific gene dysregulated in obesity. *J.Biol.Chem.* 271:10697-10703, 1996

14. Yamauchi,T, Kamon,J, Waki,H, Terauchi,Y, Kubota,N, Hara,K, Mori,Y, Ide,T, Murakami,K, Tsuboyama-Kasaoka,N, Ezaki,O, Akanuma,Y, Gavrilova,O, Vinson,C, Reitman,ML, Kagechika,H, Shudo,K, Yoda,M, Nakano,Y, Tobe,K, Nagai,R, Kimura,S, Tomita,M, Froguel,P, Kadowaki,T: The fat-derived hormone adiponectin reverses insulin resistance associated with both lipoatrophy and obesity. *Nature Medicine* 7:941-946, 2001

15. Yamauchi,T, Kamon,J, Minokoshi,Y, Ito,Y, Waki,H, Uchida,S, Yamashita,S, Noda,M, Kita,S, Ueki,K, Eto,K, Akanuma,Y, Froguel,P, Foufelle,F, Ferre,P, Carling,D, Kimura,S, Nagai,R, Kahn,BB, Kadowaki,T: Adiponectin stimulates glucose utilization and fatty-acid oxidation by activating AMP-activated protein kinase. *Nat.Med.* 8:1288-1295, 2002

16. Wu,X, Motoshima,H, Mahadev,K, Stalker,TJ, Scalia,R, Goldstein,BJ: Involvement of AMP-Activated Protein Kinase in Glucose Uptake Stimulated by the Globular Domain of Adiponectin in Primary Rat Adipocytes. *Diabetes* 52:1355-1363, 2003

17. Yokota,T, Oritani,K, Takahashi,I, Ishikawa,J, Matsuyama,A, Ouchi,N, Kihara,S, Funahashi,T, Tenner,AJ, Tomiyama,Y, Matsuzawa,Y: Adiponectin, a new member of the family of soluble defense collagens, negatively regulates the growth of myelomonocytic progenitors and the functions of macrophages. *Blood* 96:1723-1732, 2000

18. Monteiro,R, de Castro,PMST, Calhau,C, Azevedo,I: Adipocyte size and liability to cell death. *Obesity Surgery* 16:804-806, 2006

19. Tilg,H, Moschen,AR: Adipocytokines: mediators linking adipose tissue, inflammation and immunity. *Nat.Rev.Immunol.* 6:772-783, 2006

20. Postic,C, Girard,J: Contribution of de novo fatty acid synthesis to hepatic steatosis and insulin resistance: lessons from genetically engineered mice. *J.Clin.Invest* 118:829-838, 2008

21. Sakurai,M, Takamura,T, Ota,T, Ando,H, Akahori,H, Kaji,K, Sasaki,M, Nakanuma,Y, Miura,K, Kaneko,S: Liver steatosis, but not fibrosis, is associated

with insulin resistance in nonalcoholic fatty liver disease. *Journal of Gastroenterology* 42:312-317, 2007

22. Savage,DB, Choi,CS, Samuel,VT, Liu,ZX, Zhang,DY, Wang,A, Zhang,XM, Cline,GW, Yu,XX, Geisler,JG, Bhanot,S, Monia,BP, Shulman,GI: Reversal of diet-induced hepatic steatosis and hepatic insulin resistance by antisense oligonucleotide inhibitors of acetyl-CoA carboxylases 1 and 2. *J.Clin.Invest.* 116:817-824, 2006

23. Petersen,KF, Dufour,S, Befroy,D, Lehrke,M, Hendler,RE, Shulman,GI: Reversal of nonalcoholic hepatic steatosis, hepatic insulin resistance, and hyperglycemia by moderate weight reduction in patients with type 2 diabetes. *Diabetes* 54:603-608, 2005

24. Dentin,R, Benhamed,F, Pegorier,JP, Foufelle,F, Viollet,B, Vaulont,S, Girard,J, Postic,C: Polyunsaturated fatty acids suppress glycolytic and lipogenic genes through the inhibition of ChREBP nuclear protein translocation. *J.Clin.Invest* 115:2843-2854, 2005

25. Monetti,M, Levin,MC, Watt,MJ, Sajan,MP, Marmor,S, Hubbard,BK, Stevens,RD, Bain,JR, Newgard,CB, Farese,RV, Hevener,AL, Farese,RV: Dissociation of hepatic steatosis and insulin resistance in mice overexpressing DGAT in the liver. *Cell Metabolism* 6:69-78, 2007

26. Listenberger,LL, Han,XL, Lewis,SE, Cases,S, Farese,RV, Ory,DS, Schaffer,JE: Triglyceride accumulation protects against fatty acid-induced lipotoxicity. *Proceedings of the National Academy of Sciences of the United States of America* 100:3077-3082, 2003

27. Neschen,S, Morino,K, Hammond,LE, Zhang,DY, Liu,ZX, Romanelli,AJ, Cline,GW, Pongratz,RL, Zhang,XM, Choi,CS, Coleman,RA, Shulman,GI: Prevention of hepatic steatosis and hepatic insulin resistance in mitochondrial acyl-CoA : glycerol-sn-3-phosphate acyltransferase 1 knockout mice. *Cell Metabolism* 2:55-65, 2005

28. Samuel,VT, Liu,ZX, Wang,A, Beddow,SA, Geisler,JG, Kahn,M, Zhang,XM, Monia,BP, Bhanot,S, Shulman,GI: Inhibition of protein kinase C epsilon prevents hepatic insulin resistance in nonalcoholic fatty liver disease. *J.Clin.Invest.* 117:739-745, 2007

29. Koves,TR, Ussher,JR, Noland,RC, Slentz,D, Mosedale,M, Ilkayeva,O, Bain,J, Stevens,R, Dyck,JR, Newgard,CB, Lopaschuk,GD, Muoio,DM: Mitochondrial overload and incomplete fatty acid oxidation contribute to skeletal muscle insulin resistance. *Cell Metab* 7:45-56, 2008

30. Kelley,DE: Skeletal muscle fat oxidation: timing and flexibility are everything. *J Clin.Invest* 115:1699-1702, 2005

31. Golay,A, Munger,R, Assimacopoulos-Jeannet,F, Bobbioni-Harsch,E, Habicht,F, Felber,JP: Progressive defect of insulin action on glycogen synthase in obesity and diabetes. *Metabolism-Clinical and Experimental* 51:549-553, 2002

32. Woods,A, Cheung,PCF, Smith,FC, Davison,MD, Scott,J, Beri,RK, Carling,D: Characterization of AMP-activated protein kinase beta and gamma subunits - Assembly of the heterotrimeric complex in vitro. *J.Biol.Chem.* 271:10282-10290, 1996

33. Cheung,PC, Salt,IP, Davies,SP, Hardie,DG, Carling,D: Characterization of AMP-activated protein kinase gamma-subunit isoforms and their role in AMP binding. *Biochem.J.* 346 Pt 3:659-669, 2000

34. Lihn,AS, Jessen,N, Pedersen,SB, Lund,S, Richelsen,B: AICAR stimulates adiponectin and inhibits cytokines in adipose tissue. *Biochem.Biophys.Res.Commun.* 316:853-858, 2004

35. Stapleton,D, Mitchelhill,KI, Gao,G, Widmer,J, Michell,BJ, Teh,T, House,CM, Fernandez,CS, Cox,T, Witters,LA, Kemp,BE: Mammalian AMP-activated protein kinase subfamily. *J.Biol.Chem.* 271:611-614, 1996

36. Shaw,RJ, Lamia,KA, Vasquez,D, Koo,SH, Bardeesy,N, DePinho,RA, Montminy,M, Cantley,LC: The kinase LKB1 mediates glucose homeostasis in liver and therapeutic effects of metformin. *Science* 310:1642-1646, 2005

37. Hawley,SA, Pan,DA, Mustard,KJ, Ross,L, Bain,J, Edelman,AM, Frenguelli,BG, Hardie,DG: Calmodulin-dependent protein kinase kinase-beta is an alternative upstream kinase for AMP-activated protein kinase. *Cell Metab* 2:9-19, 2005

38. Jensen,TE, Rose,AJ, Jorgensen,SB, Brandt,N, Schjerling,P, Wojtaszewski,JFP, Richter,EA: Possible CaMKK-dependent regulation of AMPK phosphorylation and glucose uptake at the onset of mild tetanic skeletal muscle contraction. *American Journal of Physiology-Endocrinology and Metabolism* 292:E1308-E1317, 2007

39. Suter,M, Riek,U, Tuerk,R, Schlattner,U, Wallimann,T, Neumann,D: Dissecting the role of 5 '-AMP for allosteric stimulation, activation, and deactivation of AMP-activated protein kinase. *J.Biol.Chem.* 281:32207-32216, 2006

40. Zhou,LJ, Deepa,SS, Etzler,JC, Ryu,JY, Mao,XM, Fang,QC, Liu,DD, Torres,JM, Jia,WP, Lechleiter,JD, Liu,F, Dong,LQ: Adiponectin Activates AMP-activated Protein Kinase in Muscle Cells via APPL1/LKB1-dependent and Phospholipase C/Ca2+/Ca2+/Calmodulin-dependent Protein Kinase Kinase-dependent Pathways. *J.Biol.Chem.* 284:22426-22435, 2009

41. Salt,I, Celler,JW, Hawley,SA, Prescott,A, Woods,A, Carling,D, Hardie,DG: AMP-activated protein kinase: greater AMP dependence, and preferential nuclear localization, of complexes containing the alpha 2 isoform. *Biochem.J.* 334:177-187, 1998

42. Hardie,DG: The AMP-activated protein kinase pathway--new players upstream and downstream. *J.Cell Sci.* 117:5479-5487, 2004

43. Zhou,G, Myers,R, Li,Y, Chen,Y, Shen,X, Fenyk-Melody,J, Wu,M, Ventre,J, Doebber,T, Fujii,N, Musi,N, Hirshman,MF, Goodyear,LJ, Moller,DE: Role of AMP-activated protein kinase in mechanism of metformin action. *J.Clin.Invest* 108:1167-1174, 2001

44. Foretz,M, Ancellin,N, Andreelli,F, Saintillan,Y, Grondin,P, Kahn,A, Thorens,B, Vaulont,S, Viollet,B: Short-term overexpression of a constitutively active form of AMP-activated protein kinase in the liver leads to mild hypoglycemia and fatty liver. *Diabetes* 54:1331-1339, 2005

45. Velasco,G, Geelen,MJH, Guzman,M: Control of hepatic fatty acid oxidation by 5'-AMP-activated protein kinase involves a malonyl-CoA-dependent and a malonyl-CoA-independent mechanism. *Arch.Biochem.Biophys.* 337:169-175, 1997

46. Baur,JA, Pearson,KJ, Price,NL, Jamieson,HA, Lerin,C, Kalra,A, Prabhu,VV, Allard,JS, Lopez-Lluch,G, Lewis,K, Pistell,PJ, Poosala,S, Becker,KG, Boss,O, Gwinn,D, Wang,M, Ramaswamy,S, Fishbein,KW, Spencer,RG, Lakatta,EG, Le Couteur,D, Shaw,RJ, Navas,P, Puigserver,P, Ingram,DK, de Cabo,R, Sinclair,DA: Resveratrol improves health and survival of mice on a high-calorie diet. *Nature* 444:337-342, 2006

47. Guigas,B, Taleux,N, Foretz,M, Detaille,D, Andreelli,F, Viollet,B, Hue,L: AMP-activated protein kinase-independent inhibition of hepatic mitochondrial oxidative phosphorylation by AICA riboside. *Biochem.J.* 404:499-507, 2007

48. Bergeron,R, Previs,SF, Cline,GW, Perret,P, Russell,RR, Young,LH, Shulman,GI: Effect of 5-aminoimidazole-4-carboxamide-1-beta-D-ribofuranoside infusion on in vivo glucose and lipid metabolism in lean and obese Zucker rats. *Diabetes* 50:1076-1082, 2001

49. Andreelli,F, Foretz,M, Knauf,C, Cani,PD, Perrin,C, Iglesias,MA, Pillot,B, Bado,A, Tronche,F, Mithieux,G, Vaulont,S, Burcelin,R, Viollet,B: Liver AMPKalpha2 catalytic subunit is a key target for the control of hepatic glucose production by adiponectin and leptin but not by insulin. *Endocrinology* 147:2432-2441, 2006

50. Habinowski,SA, Witters,LA: The effects of AICAR on adipocyte differentiation of 3T3-L1 cells. *Biochem.Biophys.Res.Commun.* 286:852-856, 2001

51. Sullivan,JE, Brocklehurst,KJ, Marley,AE, Carey,F, Carling,D, Beri,RK: Inhibition of lipolysis and lipogenesis in isolated rat adipocytes with AICAR, a cell-permeable activator of AMP-activated protein kinase. *FEBS Lett.* 353:33-36, 1994

52. Daval,M, Diot-Dupuy,F, Bazin,R, Hainault,I, Viollet,B, Vaulont,S, Hajduch,E, Ferre,P, Foufelle,F: Anti-lipolytic action of AMP-activated protein kinase in rodent adipocytes. *J Biol.Chem.* 280:25250-25257, 2005

53. Merrill,GF, Kurth,EJ, Hardie,DG, Winder,WW: AICA riboside increases AMP-activated protein kinase, fatty acid oxidation, and glucose uptake in rat muscle. *American Journal of Physiology-Endocrinology and Metabolism* 36:E1107-E1112, 1997

54. Breen,DM, Sanli,T, Giacca,A, Tsiani,E: Stimulation of muscle cell glucose uptake by resveratrol through sirtuins and AMPK. *Biochem.Biophys.Res.Commun.* 374:117-122, 2008

55. McBride,A, Ghilagaber,S, Nikolaev,A, Hardie,DG: The Glycogen-Binding Domain on the AMPK beta Subunit Allows the Kinase to Act as a Glycogen Sensor. *Cell Metabolism* 9:23-34, 2009

56. Bavenholm,PN, Pigon,J, Saha,AK, Ruderman,NB, Efendic,S: Fatty acid oxidation and the regulation of malonyl-CoA in human muscle. *Diabetes* 49:1078-1083, 2000

57. Kelley,DE, Goodpaster,B, Wing,RR, Simoneau,JA: Skeletal muscle fatty acid metabolism in association with insulin resistance, obesity, and weight loss. *American Journal of Physiology-Endocrinology and Metabolism* 277:E1130-E1141, 1999

58. Boon,H, Bosselaar,M, Praet,SF, Blaak,EE, Saris,WH, Wagenmakers,AJ, McGee,SL, Tack,CJ, Smits,P, Hargreaves,M, van Loon,LJ: Intravenous AICAR administration reduces hepatic glucose output and inhibits whole body lipolysis in type 2 diabetic patients. *Diabetologia* 51:1893-1900, 2008

59. Burdge,GC, Calder,PC: Conversion of alpha-linolenic acid to longer-chain polyunsaturated fatty acids in human adults. *Reproduction Nutrition Development* 45:581-597, 2005

60. Kromann,N, Green,A: Epidemiological-Studies in the Upernavik District, Greenland - Incidence of Some Chronic Diseases 1950-1974. *Acta Medica Scandinavica* 208:401-406, 1980

61. Nestel,PJ, Connor,WE, Reardon,MF, Connor,S, Wong,S, Boston,R: Suppression by Diets Rich in Fish Oil of Very Low-Density Lipoprotein Production in Man. *J.Clin.Invest.* 74:82-89, 1984

62. Ruxton,CH, Reed,SC, Simpson Double Dagger,MJ, Millington,KJ: The health benefits of omega-3 polyunsaturated fatty acids: a review of the evidence. *J Hum.Nutr.Diet.* 17:449-459, 2004

63. MacLean, C. H., Konica, W. A., Morton, S. C., Pencharz, J., and et al. Effects of Omega-3 Fatty Acids on Lipids and Glycemic Control in Type II Diabetes and the Metabolic Syndrome and on Inflammatory Bowel Disease, Rheumatoid Arthritis, Renal Disease, Systemic Lupus Erythrematousus, and Osteoporosis. Summary, Evidence Report/Technology Assessment No. 89. AHRQ Publication No. 04-E012-1. 2004. Agency for Healthcare Research and Quality. Ref Type: Report

64. Nettleton,JA, Katz,R: n-3 long-chain polyunsaturated fatty acids in type 2 diabetes: a review. *J Am.Diet.Assoc.* 105:428-440, 2005

65. Mori,TA, Bao,DQ, Burke,V, Puddey,IB, Watts,GF, Beilin,LJ: Dietary fish as a major component of a weight-loss diet: effect on serum lipids, glucose, and insulin metabolism in overweight hypertensive subjects. *Am.J.Clin.Nutr.* 70:817-825, 1999

66. Couet,C, Delarue,J, Ritz,P, Antoine,J-M, Lamisse,F: Effect of dietary fish oil on body fat mass and basal fat oxidation in healthy adults. *Int.J Obes.* 21:637-643, 1997

67. Fasching,P, Ratheiser,K, Waldhausl,W, Rohac,M, Osterrode,W, Nowotny,P, Vierhapper,H: Metabolic effects of fish-oil supplementation in patients with impaired glucose tolerance. *Diabetes* 40:583-589, 1991

68. Pelikanova,T, Kohout,M, Valek,J, Kazdova,L, Base,J: Metabolic effects of omega-3 fatty acids in type 2 (non-insulin-dependent) diabetic patients. *Ann.N.Y.Acad.Sci.* 683:272-278, 1993

69. Ikemoto,S, Takahashi,M, Tsunoda,N, Maruyama,K, Itakura,H, Ezaki,O: High-fat diet-induced hyperglycemia and obesity in mice: Differential effects of dietary oils. *Metabolism* 45:1539-1546, 1996

70. Ruzickova,J, Rossmeisl,M, Prazak,T, Flachs,P, Sponarova,J, Vecka,M, Tvrzicka,E, Bryhn,M, Kopecky,J: Omega-3 PUFA of marine origin limit diet-induced obesity in mice by reducing cellularity of adipose tissue. *Lipids* 39:1177-1185, 2004

71. Flachs,P, Horakova,O, Brauner,P, Rossmeisl,M, Pecina,P, Franssen-van Hal,NL, Ruzickova,J, Sponarova,J, Drahota,Z, Vlcek,C, Keijer,J, Houstek,J, Kopecky,J: Polyunsaturated fatty acids of marine origin upregulate mitochondrial biogenesis and induce beta-oxidation in white fat. *Diabetologia* 48:2365-2375, 2005

72. Storlien,LH, Kraegen,EW, Chisholm,DJ, Ford,GL, Bruce,DG, Pascoe,WS: Fish oil prevents insulin resistance induced by high-fat feeding in rats. *Science* 237:885-888, 1987

73. Neschen,S, Morino,K, Dong,J, Wang-Fischer,Y, Cline,GW, Romanelli,AJ, Rossbacher,JC, Moore,IK, Regittnig,W, Munoz,DS, Kim,JH, Shulman,GI: N-3 Fatty Acids Preserve Insulin Sensitivity In Vivo in a PPAR{alpha}-Dependent Manner. *Diabetes* 56:1034-1041, 2007

74. Tsuchida,A, Yamauchi,T, Takekawa,S, Hada,Y, Ito,Y, Maki,T, Kadowaki,T: Peroxisome proliferator-activated receptor (PPAR)alpha activation increases adiponectin receptors and reduces obesity-related inflammation in adipose tissue: comparison of activation of PPARalpha, PPARgamma, and their combination. *Diabetes* 54:3358-3370, 2005

75. Neschen,S, Morino,K, Rossbacher,JC, Pongratz,RL, Cline,GW, Sono,S, Gillum,M, Shulman,GI: Fish Oil Regulates Adiponectin Secretion by a Peroxisome Proliferator-Activated Receptor--Dependent Mechanism in Mice. *Diabetes* 55:924-928, 2006

76. Teran-Garcia,M, Adamson,AW, Yu,G, Rufo,C, Suchankova,G, Dreesen,TD, Tekle,M, Clarke,SD, Gettys,TW: Polyunsaturated fatty acid suppression of fatty acid synthase (FASN): evidence for dietary modulation of NF-Y binding to the Fasn promoter by SREBP-1c. *Biochem.J* 402:591-600, 2007

77. Xu,J, Teran-Garcia,M, Park,JHY, Nakamura,MT, Clarke,SD: Polyunsaturated fatty acids suppress hepatic sterol regulatory element-binding protein-1 expression by accelerating transcript decay. *J.Biol.Chem.* 276:9800-9807, 2001

78. Wilson,MD, Blake,WL, Salati,LM, Clarke,SD: Potency of Polyunsaturated and Saturated Fats As Short-Term Inhibitors of Hepatic Lipogenesis in Rats. *Journal of Nutrition* 120:544-552, 1990

79. Sanderson,LM, de Groot,PJ, Hooiveld,GJ, Koppen,A, Kalkhoven,E, Muller,M, Kersten,S: Effect of synthetic dietary triglycerides: a novel research paradigm for nutrigenomics. *PLoS.ONE.* 3:e1681, 2008

80. Neschen,S, Moore,I, Regittnig,W, Yu,CL, Wang,Y, Pypaert,M, Petersen,KF, Shulman,GI: Contrasting effects of fish oil and safflower oil on hepatic peroxisomal and tissue lipid content. *Am.J Physiol Endocrinol.Metab* 282:E395-E401, 2002

81. Kim,HK, Della-Fera,M, Lin,J, Baile,CA: Docosahexaenoic acid inhibits adipocyte differentiation and induces apoptosis in 3T3-L1 preadipocytes. *J Nutr* 136:2965-2969, 2006

82. Flachs,P, Mohamed-Ali,V, Horakova,O, Rossmeisl,M, Hosseinzadeh-Attar,MJ, Hensler,M, Ruzickova,J, Kopecky,J: Polyunsaturated fatty acids of marine origin induce adiponectin in mice fed high-fat diet. *Diabetologia* 49:394-397, 2006

83. Toruner,F, Akbay,E, Cakir,N, Sancak,B, Elbeg,S, Taneri,F, Akturk,M, Karakoc,A, Ayvaz,G, Arslan,M: Effects of PPARgamma and PPARalpha agonists on serum leptin levels in diet-induced obese rats. *Horm.Metab Res.* 36:226-230, 2004

84. Peyron-Caso,E, Fluteau-Nadler,S, Kabir,M, Guerre-Millo,M, Quignard-Boulange,A, Slama,G, Rizkalla,SW: Regulation of glucose transport and transporter 4 (GLUT-4) in muscle and adipocytes of sucrose-fed rats: effects of N-3 poly- and monounsaturated fatty acids. *Horm.Metab Res.* 34:360-366, 2002

85. Serhan,CN: Novel omega -- 3-derived local mediators in anti-inflammation and resolution. *Pharmacol.Ther.* 105:7-21, 2005

86. Gregoire,FM, Smas,CM, Sul,HS: Understanding adipocyte differentiation. *Physiol Rev.* 78:783-809, 1998

87. Suchankova,G, Tekle,M, Saha,AK, Ruderman,NB, Clarke,SD, Gettys,TW: Dietary polyunsaturated fatty acids enhance hepatic AMP-activated protein kinase activity in rats. *Biochem.Biophys.Res.Commun.* 326:851-858, 2005

88. Gabler,NK, Radcliffe,JS, Spencer,JD, Webel,DM, Spurlock,ME: Feeding long-chain n-3 polyunsaturated fatty acids during gestation increases intestinal glucose

absorption potentially via the acute activation of AMPK. *J.Nutr.Biochem.* 20:17-25, 2009

89. Gonzalez-Periz,A, Horrillo,R, Ferre,N, Gronert,K, Dong,B, Moran-Salvador,E, Titos,E, Martinez-Clemente,M, Lopez-Parra,M, Arroyo,V, Claria,J: Obesity-induced insulin resistance and hepatic steatosis are alleviated by {omega}-3 fatty acids: a role for resolvins and protectins. *FASEB J.* 2009

90. Kopecky,J, Rossmeisl,M, Flachs,P, Kuda,O, Brauner,P, Jilkova,Z, Stankova,B, Tvrzicka,E, Bryhn,M: n-3 PUFA: bioavailability and modulation of adipose tissue function. *Proc.Nutr.Soc.*1-9, 2009

91. Viollet,B, Andreelli,F, Jorgensen,SB, Perrin,C, Geloen,A, Flamez,D, Mu,J, Lenzner,C, Baud,O, Bennoun,M, Gomas,E, Nicolas,G, Wojtaszewski,JF, Kahn,A, Carling,D, Schuit,FC, Birnbaum,MJ, Richter,EA, Burcelin,R, Vaulont,S: The AMP-activated protein kinase alpha2 catalytic subunit controls whole-body insulin sensitivity. *J Clin.Invest* 111:91-98, 2003

92. Kuda,O, Jelenik,T, Jilkova,Z, Flachs,P, Rossmeisl,M, Hensler,M, Kazdova,L, Ogston,N, Baranowski,M, Gorski,J, Janovska,P, Kus,V, Polak,J, Mohamed-Ali,V, Burcelin,R, Cinti,S, Bryhn,M, Kopecky,J: n-3 Fatty acids and rosiglitazone improve insulin sensitivity through additive stimulatory effects on muscle glycogen synthesis in mice fed a high-fat diet. *Diabetologia* 2009

93. Rossmeisl,M, Jelenik,T, Jilkova,Z, Slamova,K, Kus,V, Hensler,M, Medrikova,D, Povysil,C, Flachs,P, Mohamed-Ali,V, Bryhn,M, Berge,K, Holmeide,AK, Kopecky,J: Prevention and reversal of obesity and glucose intolerance in mice by DHA-derivatives. *Obesity (Silver.Spring)* 2009

94. Polak,J, Kovacova,Z, Jacek,M, Klimcakova,E, Kovacikova,M, Vitkova,M, Kuda,O, Sebela,M, Samcova,E, Stich,V: An increase in plasma adiponectin multimeric complexes follows hypocaloric diet-induced weight loss in obese and overweight pre-menopausal women. *Clin.Sci.(Lond)* 112:557-565, 2007

95. Roemen,TH, Van der Vusse,GJ: Application of silica gel column chromatography in the assessment of non-esterified fatty acids and phosphoglycerides in myocardial tissue. *J.Chromatogr.* 344:304-308, 1985

96. Nawrocki,AR, Rajala,MW, Tomas,E, Pajvani,UB, Saha,AK, Trumbauer,ME, Pang,Z, Chen,AS, Ruderman,NB, Chen,H, Rossetti,L, Scherer,PE: Mice lacking adiponectin show decreased hepatic insulin sensitivity and reduced responsiveness to peroxisome proliferator-activated receptor gamma agonists. *J Biol.Chem.* 281:2654-2660, 2006

97. Baranowski,M, Zabielski,P, Blachnio,A, Gorski,J: Effect of exercise duration on ceramide metabolism in the rat heart. *Acta Physiol (Oxf)* 192:519-529, 2008

98. Hawley,SA, Gadalla,AE, Olsen,GS, Hardie,DG: The antidiabetic drug metformin activates the AMP-activated protein kinase cascade via an adenine nucleotide-independent mechanism. *Diabetes* 51:2420-2425, 2002

99. Matejkova,O, Mustard,KJ, Sponarova,J, Flachs,P, Rossmeisl,M, Miksik,I, Thomason-Hughes,M, Hardie,DG, Kopecky,J: Possible involvement of AMP-activated protein kinase in obesity resistance induced by respiratory uncoupling in white fat. *FEBS Lett.* 569:245-248, 2004

100. Cinti,S, Mitchell,G, Barbatelli,G, Murano,I, Ceresi,E, Faloia,E, Wang,S, Fortier,M, Greenberg,AS, Obin,MS: Adipocyte death defines macrophage localization and function in adipose tissue of obese mice and humans. *J Lipid Res.* 46:2347-2355, 2005

101. Burcelin,R, Crivelli,V, Dacosta,A, Roy-Tirelli,A, Thorens,B: Heterogeneous metabolic adaptation of C57BL/6J mice to high-fat diet. *Am J Physiol Endocrinol.Metab* 282:E834-E842, 2002

102. Young,AA, Bogardus,C, Wolfelopez,D, Mott,DM: Muscle Glycogen-Synthesis and Disposition of Infused Glucose in Humans with Reduced Rates of Insulin-Mediated Carbohydrate Storage. *Diabetes* 37:303-308, 1988

103. Rossetti,L, Giaccari,A: Relative contribution of glycogen synthesis and glycolysis to insulin-mediated glucose uptake. A dose-response euglycemic clamp study in normal and diabetic rats. *J Clin.Invest* 85:1785-1792, 1990

104. Kuipers,F, Jong,MC, Lin,YG, van Eck,M, Havinga,R, Bloks,V, Verkade,HJ, Hofker,MH, Moshage,H, van Berkel,TJC, Vonk,RJ, Havekes,LM: Impaired secretion of very low density lipoprotein triglycerides by apolipoprotein E deficient mouse hepatocytes. *J.Clin.Invest.* 100:2915-2922, 1997

105. Alberts P, Johansson BG, McArthur RA: Measurement and characterization of energy expenditure as a tool in the development of drugs for metabolic diseases, such as obesity and diabetes. In Current protocols in pharmacology. Enna SJ, Williams M, Ferkany JW, Kenakin T, Porsolt RD, Sullivan JP, Eds. John Wiley and Sons, Inc., 2005, p. 1-15

106. Rodbell,M: Metabolism of isolated fat cells. *J.Biol.Chem.* 239:375-380, 1964

107. Stefl,B, Janovska,A, Hodny,Z, Rossmeisl,M, Horakova,M, Syrovy,I, Bemova,J, Bendlova,B, Kopecky,J: Brown fat is essential for cold-induced thermogenesis but not for obesity resistance in aP2-Ucp mice. *Am.J.Physiol* 274:E527-E533, 1998

108. Waki,H, Yamauchi,T, Kamon,J, Ito,Y, Uchida,S, Kita,S, Hara,K, Hada,Y, Vasseur,F, Froguel,P, Kimura,S, Nagai,R, Kadowaki,T: Impaired multimerization of human adiponectin mutants associated with diabetes - Molecular structure and multimer formation of adiponectin. *J.Biol.Chem.* 278:40352-40363, 2003

109. Lin,S, Thomas,TC, Storlien,LH, Huang,XF: Development of high fat diet-induced obesity and leptin resistance in C57Bl/6J mice. *Int.J Obes.Relat Metab Disord.* 24:639-646, 2000

110. Kraegen,EW, Clark,PW, Jenkins,AB, Daley,EA, Chisholm,DJ, Storlien,LH: Development of muscle insulin resistance after liver insulin resistance in high-fat-fed rats. *Diabetes* 40:1397-1403, 1991

111. Kim,JY, Nolte,LA, Hansen,PA, Han,DH, Ferguson,K, Thompson,PA, Holloszy,JO: High-fat diet-induced muscle insulin resistance: relationship to visceral fat mass. *American Journal of Physiology-Regulatory Integrative and Comparative Physiology* 279:R2057-R2065, 2000

112. Surwit,RS, Kuhn,CM, Cochrane,C, McCubbin,JA, Feinglos,MN: Diet-induced type II diabetes in C57BL/6J mice. *Diabetes* 37:1163-1167, 1988

113. Eriksson,J, Franssilakallunki,A, Ekstrand,A, Saloranta,C, Widen,E, Schalin,C, Groop,L: Early Metabolic Defects in Persons at Increased Risk for Non-Insulin-Dependent Diabetes-Mellitus. *N.Engl.J.Med.* 321:337-343, 1989

114. Reaven,GM: Role of Insulin Resistance in Human-Disease. *Diabetes* 37:1595-1607, 1988

115. Wueest,S, Rapold,RA, Rytka,JM, Schoenle,EJ, Konrad,D: Basal lipolysis, not the degree of insulin resistance, differentiates large from small isolated adipocytes in high-fat fed mice. *Diabetologia* 52:541-546, 2009

116. Arita,Y, Kihara,S, Ouchi,N, Takahashi,M, Maeda,K, Miyagawa,J, Hotta,K, Shimomura,I, Nakamura,T, Miyaoka,K, Kuriyama,H, Nishida,M, Yamashita,S, Okubo,K, Matsubara,K, Muraguchi,M, Ohmoto,Y, Funahashi,T, Matsuzawa,Y: Paradoxical decrease of an adipose-specific protein, adiponectin, in obesity. *Biochem.Biophys.Res.Commun.* 257:79-83, 1999

117. Dobrzyn,A, Dobrzyn,P, Miyazaki,M, Ntambi,JM: Polyunsaturated fatty acids do not activate AMP-activated protein kinase in mouse tissues. *Biochem.Biophys.Res.Commun.* 332:892-896, 2005

118. Lochhead,PA, Salt,IP, Walker,KS, Hardie,DG, Sutherland,C: 5-aminoimidazole-4-carboxamide riboside mimics the effects of insulin on the expression of the 2 key gluconeogenic genes PEPCK and glucose-6- phosphatase. *Diabetes* 49:896-903, 2000

119. Lee,WJ, Kim,M, Park,HS, Kim,HS, Jeon,MJ, Oh,KS, Koh,EH, Won,JC, Kim,MS, Oh,GT, Yoon,M, Lee,KU, Park,JY: AMPK activation increases fatty acid oxidation in skeletal muscle by activating PPARalpha and PGC-1. *Biochem.Biophys.Res.Commun.* 340:291-295, 2006

120. Kraegen,EW, Saha,AK, Preston,E, Wilks,D, Hoy,AJ, Cooney,GJ, Ruderman,NB: Increased malonyl-CoA and diacylglycerol content and reduced AMPK activity accompany insulin resistance induced by glucose infusion in muscle and liver of rats. *American Journal of Physiology-Endocrinology and Metabolism* 290:E471-E479, 2006

121. Xu,J, Nakamura,MT, Cho,HP, Clarke,SD: Sterol regulatory element binding protein-1 expression is suppressed by dietary polyunsaturated fatty acids - A mechanism for the coordinate suppression of lipogenic genes by polyunsaturated fats. *J.Biol.Chem.* 274:23577-23583, 1999

122. Howell,G, III, Deng,X, Yellaturu,C, Park,EA, Wilcox,HG, Raghow,R, Elam,MB: N-3 polyunsaturated fatty acids suppress insulin-induced SREBP-1c transcription via reduced trans-activating capacity of LXRalpha. *Biochim.Biophys.Acta* 2009

123. Hardie,DG: Minireview: the AMP-activated protein kinase cascade: the key sensor of cellular energy status. *Endocrinology* 144:5179-5183, 2003

124. Wellen,KE, Hotamisligil,GS: Inflammation, stress, and diabetes. *J Clin Invest* 115:1111-1119, 2005

125. Jucker,BM, Cline,GW, Barucci,N, Shulman,GI: Differential effects of safflower oil versus fish oil feeding on insulin-stimulated glycogen synthesis, glycolysis, and pyruvate dehydrogenase flux in skeletal muscle: a 13C nuclear magnetic resonance study. *Diabetes* 48:134-140, 1999

126. Kim,JK, Fillmore,JJ, Gavrilova,O, Chao,L, Higashimori,T, Choi,H, Kim,HJ, Yu,C, Chen,Y, Qu,X, Haluzik,M, Reitman,ML, Shulman,GI: Differential effects

of rosiglitazone on skeletal muscle and liver insulin resistance in A-ZIP/F-1 fatless mice. *Diabetes* 52:1311-1318, 2003

127. Laplante,M, Festuccia,WT, Soucy,G, Blanchard,PG, Renaud,A, Berger,JP, Olivecrona,G, Deshaies,Y: Tissue-specific postprandial clearance is the major determinant of PPAR{gamma}-induced triglyceride lowering in the rat. *Am.J.Physiol Regul.Integr.Comp Physiol* 2008

128. Ton,MN, Chang,C, Carpentier,YA, Deckelbaum,RJ: In vivo and in vitro properties of an intravenous lipid emulsion containing only medium chain and fish oil triglycerides. *Clin.Nutr.* 24:492-501, 2005

129. Gibbons,GF, Wiggins,D, Brown,AM, Hebbachi,AM: Synthesis and function of hepatic very-low-density lipoprotein. *Biochem.Soc.Trans.* 32:59-64, 2004

130. Riserus,U, Tan,GD, Fielding,BA, Neville,MJ, Currie,J, Savage,DB, Chatterjee,VK, Frayn,KN, O'Rahilly,S, Karpe,F: Rosiglitazone increases indexes of stearoyl-CoA desaturase activity in humans: link to insulin sensitization and the role of dominant-negative mutation in peroxisome proliferator-activated receptor-gamma. *Diabetes* 54:1379-1384, 2005

9 LIST OF PAPERS

1) **Jelenik T,** Rossmeisl M, Kuda O, Macek Jilkova Z, Medrikova D, Kus V, Hensler M, Janovska P, Miksik I, Baranowski M, Gorski J, Hébrard S, Jensen TE, Flachs P, Hawley S, Viollet B, Kopecky J.
   AMP-activated protein kinase α2 subunit is required for the preservation of hepatic insulin sensitivity by n-3 polyunsaturated fatty acids.
   Diabetes (accepted in July 2010), (IF = 8,26)

2) Kuda O, Stankova B, Tvrzicka E, Hensler M, **Jelenik T,** Rossmeisl M, Flachs P, Kopecky J.
   Prominent role of liver in elevated plasma palmitoleate levels in response to rosiglitazone in mice fed high-fat diet.
   Journal of physiology and pharmacology 60(4): 135-40, 2009, (IF = 4,47)

3) Kuda O, **Jelenik T,** Jilkova Z, Flachs Z, Rossmeisl M, Hensler M, Kazdova L, Ogston N, Baranowski M, Gorski J, Janovska P, Polak J, Mohamed-Ali V, Burcelin R, Cinti S, Bryhn M, Kopecky J.
   n–3 fatty acids and rosiglitazone improve insulin sensitivity through additive stimulatory effects on muscle glycogen synthesis in mice fed high-fat diet.
   Diabetologia 52: 941-951, 2009, (IF = 6,328)

4) Rossmeisl M, **Jelenik T,** Jilkova Z, Slamova K, Kus V, Hensler M, Medrikova D, Povysil C, Flachs P, Mohamed-Ali V, Bryhn M, Berge Kristin Holmeide K, Kopecky J. *DHA-derivatives in the prevention and reversal of obesity and glucose intolerance in mice.*
   Obesity 17: 1023–1031, 2009, (IF = 3,24)

rich4/zdb-diab/zdb-diab/zdb01110/zdb6323d10z | xppws | S=1 | 8/26/10 | 9:12 | doi: 10.2337/db09-1716 | artno: 1716

ORIGINAL ARTICLE

AMP-activated Protein Kinase α2 Subunit Is Required for the Preservation of Hepatic Insulin Sensitivity by n-3 Polyunsaturated Fatty Acids

Tomas Jelenik,[1] Martin Rossmeisl,[1] Ondrej Kuda,[1] Zuzana Macek Jilkova,[1] Dasa Medrikova,[1] Vladimir Kus,[1] Michal Hensler,[1] Petra Janovska,[1] Ivan Miksik,[2] Marcin Baranowski,[3] Jan Gorski,[3] Sophie Hébrard,[4,5] Thomas E. Jensen,[6] Pavel Flachs,[1] Simon Hawley,[7] Benoit Viollet,[4,5] and Jan Kopecky[1]

OBJECTIVE—The induction of obesity, dyslipidemia, and insulin resistance by high-fat diet in rodents can be prevented by n-3 long-chain polyunsaturated fatty acids (LC-PUFAs). We tested a hypothesis whether AMP-activated protein kinase (AMPK) has a role in the beneficial effects of n-3 LC-PUFAs.

RESEARCH DESIGN AND METHODS—Mice with a whole-body deletion of the α2 catalytic subunit of AMPK (AMPKα2$^{-/-}$) and their wild-type littermates were fed on either a low-fat chow, or a corn oil-based high-fat diet (cHF), or a cHF diet with 15% lipids replaced by n-3 LC-PUFA concentrate (cHF+F).

RESULTS—Feeding a cHF diet induced obesity, dyslipidemia, hepatic steatosis, and whole-body insulin resistance in mice of both genotypes. Although cHF+F feeding increased hepatic AMPKα2 activity, the body weight gain, dyslipidemia, and the accumulation of hepatic triglycerides were prevented by the cHF+F diet to a similar degree in both AMPKα2$^{-/-}$ and wild-type mice in ad libitum-fed state. However, preservation of hepatic insulin sensitivity by n-3 LC-PUFAs required functional AMPKα2 and correlated with the induction of adiponectin and reduction in liver diacylglycerol content. Under hyperinsulinemic-euglycemic conditions, AMPKα2 was essential for preserving low levels of both hepatic and plasma triglycerides, as well as plasma free fatty acids, in response to the n-3 LC-PUFA treatment.

CONCLUSIONS—Our results show that n-3 LC-PUFAs prevent hepatic insulin resistance in an AMPKα2-dependent manner and support the role of adiponectin and hepatic diacylglycerols in the regulation of insulin sensitivity. AMPKα2 is also essential for hypolipidemic and antisteatotic effects of n-3 LC-PUFA under insulin-stimulated conditions. ***Diabetes*** **59:1–2, 2010**

From the [1]Department of Adipose Tissue Biology and the [2]Department of Analysis of Biologically Important Compounds, Institute of Physiology of the Academy of Sciences of the Czech Republic, v.v.i., Prague, Czech Republic; the [3]Department of Physiology, Medical University of Bialystok, Poland; the [4]Institut Cochin, Université Paris Descartes, CNRS (UMR 8104), Paris, France; [5]INSERM, U1016, Paris, France; the [6]Molecular Physiology Group, Copenhagen Muscle Research Centre, Department of Exercise and Sport Sciences, Section of Human Physiology, University of Copenhagen, Copenhagen, Denmark; and the [7]Division of Molecular Physiology, College of Life Sciences, University of Dundee, Scotland, U.K.

Corresponding author: Jan Kopecky, kopecky@biomed.cas.cz.

Received 20 November 2009 and accepted 26 July 2010. Published ahead of print at http://diabetes.diabetesjournals.org on 6 August 2010. DOI: 10.2337/db09-1716.

T.J. and M.R. contributed equally to this study.

Naturally occurring n-3 long-chain polyunsaturated fatty acids (LC-PUFAs)—namely, eicosapentaenoic acid (20:5n-3) and docosahexaenoic acid (22:6n-3)—which are abundant in sea fish, act as hypolipidemics, reduce cardiac events, and decrease the progression of atherosclerosis [reviewed in refs (1,2).]. Studies of obese humans have also demonstrated a reduction in adiposity after n-3 LC-PUFA supplementation (3,4). In rodents fed a high-fat diet, n-3 LC-PUFAs efficiently prevented the development of obesity, hepatic steatosis, and dyslipidemia (5–8), as well as impaired glucose tolerance (8–10). However, in diabetic patients, n-3 LC-PUFAs appear to have little effect on glycemic control (3,11,12).

The hypolipidemic and antiobesity effects of n-3 LC-PUFAs depend on both the suppression of lipogenesis and the increase in fatty acid oxidation in several tissues, including the liver (13,14), adipose tissue (6), and intestine (15). This metabolic switch may reduce the accumulation of toxic fatty acid derivatives, while protecting insulin signaling in the liver and muscle (9,10,16). Our previous work has documented that the preservation of whole-body insulin sensitivity by n-3 LC-PUFAs in mice fed a high-fat diet mainly reflects improved hepatic insulin sensitivity (8). The effects of n-3 LC-PUFAs and their active metabolites (17,18) are mediated by peroxisome proliferator-activated receptors (PPAR), with PPAR-α and PPAR-δ (-β) being the main targets (14,16), although PPAR-γ, liver X receptor-α, hepatic nuclear factor-4, sterol regulatory element binding protein-1c (SREBP-1c) and carbohydrate-responsive element-binding protein are also involved (16,19–21).

It has been demonstrated that n-3 LC-PUFAs enhanced AMP-activated protein kinase (AMPK) activity in the liver (22), intestine (23), and adipose tissue (18,24). AMPK is a heterotrimeric protein consisting of a catalytic α-subunit and regulatory β- and γ-subunits, with multiple isoforms identified for each subunit [α1, α2, β1, β2, γ1, γ2, and γ3; reviewed in ref (25)]. Experiments using whole-body AMPKα2 null [AMPKα2$^{-/-}$; ref (26)] mice showed the importance of the AMPKα2 subunit for whole-body insulin action, while liver-specific AMPKα2 knockout mice (27) as well as adenovirus-mediated activation of AMPKα2 in the liver (28) implicated the hepatic AMPKα2 isoform in the suppression of hepatic glucose production and maintenance of fasting blood glucose levels. Furthermore, AMPK controls metabolic fluxes in response to changing cellular

energy levels, namely, the partitioning between lipid oxidation and lipogenesis (29,30).

We hypothesized that the effects of n-3 LC-PUFA on insulin sensitivity and lipid metabolism in mice fed an obesogenic high-fat diet require a functional AMPKα2 isoform. To test this hypothesis in vivo, AMPKα2$^{-/-}$ and wild-type mice were fed either a low-fat chow diet (Chow), a corn oil-based high-fat (cHF) diet, or cHF diet in which 15% of the lipids were replaced by n-3 LC-PUFA concentrate (cHF+F). Our results demonstrate an AMPKα2-dependent action of n-3 LC-PUFAs, in *1*) the preservation of hepatic and muscle insulin sensitivity; *2*) the changes in hepatic diacylglycerol content and composition; and *3*) the antisteatotic effect in the liver and hypolipidemic effect under insulin-stimulated conditions, such as during hyperinsulinemic-euglycemic clamp, but not when the organism depends on lipids as substrates.

RESEARCH DESIGN AND METHODS

Four-month-old whole-body AMPKα2$^{-/-}$ mice (29) backcrossed to C57BL/6J mice for nine generations, and wild-type littermate controls were fed on either Chow, cHF, or cHF+F diet for nine weeks. Body weight and food consumption were recorded, and EDTA-plasma and tissues were collected for various analyses as described in the online appendix, available at http://diabetes.diabetesjournals.org/cgi/content/full/db09-1716/DC1. Male mice were used for all the experiments, except for the measurements of hepatic AMPK activity, which were performed on female mice (see below). The experiments were conducted under the guidelines for the use and care of laboratory animals of the Institute of Physiology and followed the "Principles of laboratory animal care" (National Institutes of Health publication no. 85-23, revised 1985).

Blood and plasma parameters. Blood glucose was measured using calibrated glucometers (LifeScan, Milpitas, CA). Nonesterified fatty acids (NEFAs), triglycerides, and total cholesterol were determined in plasma using the following enzymatic photometric tests: NEFA-C (Wako Chemicals, Neuss, Germany), triacylglycerols liquid, and cholesterol liquid (Pliva-Lachema Diagnostika, Brno, Czech Republic), respectively. Plasma insulin was measured using the Sensitive Rat Insulin RIA Kit (LINCO Research, St. Charles, MO). Total adiponectin levels and adiponectin multimeric complexes were determined using Western blotting (31).

Lipid content and gene expression in the liver. The tissue content of triglycerides was estimated in ethanolic KOH tissue solubilizes as described before (8). The content and fatty acid composition of the phospholipid, diacylglycerol, triglyceride, and ceramide fractions were assessed in tissue lipid extracts; gene expression was evaluated using real-time RT-PCR (see online appendix).

Activity of α1 and α2 AMPK isoforms. Livers were collected by freeze-clamping, AMPK was immunoprecipitated from tissue extracts, and the activity was assayed using a peptide substrate (32); see the online appendix.

Hyperinsulinemic-euglycemic clamp. Five days before the experiment, an indwelling catheter was placed into the left femoral vein under anesthesia (33). Mice were allowed to recover for 5–7 days, followed by a 6-h fast (8:00 A.M.–2:00 P.M.) prior to the experiment. The whole-body glucose turnover was determined under basal (nonstimulated) and insulin-stimulated conditions (hyperinsulinemic-euglycemic clamp), using separate groups of mice. Insulin (Actrapid, Novo Nordisk Pharma, Denmark) was infused at a constant rate of 4.8 mU/kg·min for 3 h, while D-[3-^{3}H]glucose (Perkin Elmer, Boston, MA) was infused at a rate of 15.9 kBq/min. Throughout the infusion, glucose concentration and D-[3-^{3}H]glucose specific activity (during the last hour of infusion) were determined in tail blood. Euglycemia (~5.55 mmol/l) was maintained by periodically adjusting a variable infusion of 33% glucose (33). At the end of a 3-h infusion period, mice were first anesthetized by diethylether, exsanguinated through the cervical incision, and then killed by cervical dislocation, and tissues (liver and quadriceps muscle) and EDTA-plasma were collected for biochemical analyses (see supplementary Table 1 in the online appendix) and Research Design and Methods of the online appendix for details on basic clamp parameters and methodology).

Primary cultures of hepatocytes. Hepatocytes were isolated from livers of fed mice by a modification of the collagenase method (34) and seeded at a density of 0.5×10^6 cells per each 35-mm Petri dish. Rates of basal and insulin-stimulated de novo lipogenesis and AICAR-stimulated fatty acid oxidation were measured using [1-^{14}C] acetate and [1-^{14}C] palmitate, respectively (see online appendix).

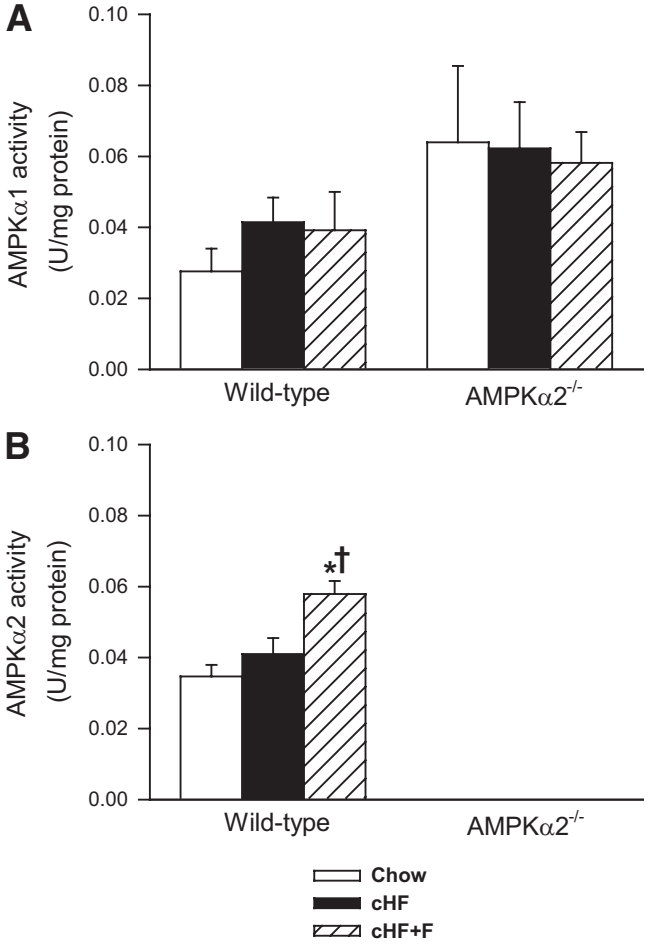

FIG. 1. Liver AMPKα1 (*A*) and AMPKα2 (*B*) activity in wild-type and AMPKα2$^{-/-}$ mice fed either a Chow diet, cHF, or cHF+F for 9 weeks. The data are the means ± SE (n = 5–8). In the AMPKα2$^{-/-}$ mice, AMPKα2 activity was below the detection limit. *P < 0.05 versus genotype Chow; †P < 0.05 versus genotype cHF.

Statistics. All values are presented as means ± SE. Data were analyzed by two-way ANOVA. Comparisons were judged to be significant at $P \leq 0.05$.

RESULTS

Enhancement of hepatic AMPKα2 activity by n-3 LC-PUFAs. Specific activities of AMPKα1 and AMPKα2 were evaluated in the liver of ad libitum-fed mice after nine weeks of the differential dietary treatment (Fig. 1). No significant effect of either diet (Chow, cHF, and cHF+F) or genotype (wild-type versus AMPKα2$^{-/-}$) on AMPKα1-specific activity was observed, although the AMPKα1 activity tended to be higher in the AMPKα2$^{-/-}$ mice (Fig. 1*A*). In contrast, AMPKα2 activity was stimulated by n-3 LC-PUFAs (cHF+F diet; Fig. 1*B*). AMPKα2 activity was not detected in the AMPKα2$^{-/-}$ mice (Fig. 1*B*). No changes were detected in the activity of AMPKα1 and AMPKα2 in the quadriceps muscle in response to n-3 LC-PUFAs (not shown).

AMPKα2 is not required for antiobesity and hypolipidemic effects of n-3 LC-PUFAs in ad libitum-fed mice. At four months of age, at the beginning of dietary treatments, wild-type and AMPKα2$^{-/-}$ mice fed the Chow diet exhibited similar body weights (Table 1). In mice of both genotypes, cHF-feeding for nine weeks resulted in greater body weight gain compared with the Chow-fed mice. However, this effect was less pronounced in AMPKα2$^{-/-}$

rich4/zdb-diab/zdb-diab/zdb01110/zdb6323d10z | xppws | S=1 | 8/26/10 | 9:12 | doi: 10.2337/db09-1716 | artno: 1716

TABLE 1
Metabolic and plasma parameters in wild-type and AMPKα2$^{-/-}$ mice

Metabolic parameters	Wild-type			AMPKα2$^{-/-}$		
	Chow	cHF	cHF+F	Chow	cHF	cHF+F
Food consumption (kJ · g^{-1} · day^{-1})	2.0 ± 0.1	1.8 ± 0.1	1.9 ± 0.0	2.0 ± 0.1	1.8 ± 0.1	2.0 ± 0.1
Initial body weight (g)	27.8 ± 0.5	27.9 ± 0.5	27.7 ± 0.5	27.1 ± 0.3	27.7 ± 0.4	27.3 ± 0.4
Body weight gain (g)	1.4 ± 0.2	7.0 ± 1.1*	2.8 ± 0.7†	1.8 ± 0.3	4.6 ± 0.7*‡	1.2 ± 0.4†
Adiposity						
Epididymal AT size (g)	0.43 ± 0.02	1.52 ± 0.19*	1.12 ± 0.14*†	0.37 ± 0.03	1.19 ± 0.16*‡	0.64 ± 0.07*†‡
Subcutaneous AT size (g)	0.20 ± 0.01	0.54 ± 0.05*	0.42 ± 0.04*†	0.17 ± 0.01	0.34 ± 0.03*‡	0.23 ± 0.01†‡
Epididymal adipocytes size (μm^2)	ND	15,971 ± 1,784	10,232 ± 185†	ND	13,298 ± 1,632	8 593 ± 896†
Subcutaneous adipocytes size (μm^2)	2,916 ± 610	6,775 ± 1,718*	7,311 ± 1,308*	3,395 ± 139	6,625 ± 926*	5,432 ± 648*
Plasma metabolites						
Triglycerides (mmol/l)	1.17 ± 0.08	1.23 ± 0.11	0.62 ± 0.07*†	1.04 ± 0.06	1.22 ± 0.08	0.73 ± 0.06*†
NEFAs (mmol/l)	0.90 ± 0.05	0.94 ± 0.05	0.59 ± 0.04*†	0.88 ± 0.04	0.99 ± 0.06	0.68 ± 0.04*†
Cholesterol (mmol/l)	2.25 ± 0.08	4.12 ± 0.25*	3.10 ± 0.20*†	2.10 ± 0.06	3.94 ± 0.18*	2.75 ± 0.14*†
Glucose (mmol/l)	9.9 ± 0.4	10.7 ± 0.5	10.4 ± 0.3	9.7 ± 0.4	10.0 ± 0.4	9.4 ± 0.4
Plasma hormones						
Insulin fed (ng/ml)	0.66 ± 0.11	1.73 ± 0.29*	1.47 ± 0.28*	0.60 ± 0.07	1.34 ± 0.20*	0.95 ± 0.12*
Insulin fasted (ng/ml)	0.13 ± 0.01	0.39 ± 0.06*	0.19 ± 0.05†	0.16 ± 0.02	0.22 ± 0.03‡	0.15 ± 0.01
Total adiponectin (A.U.)	1.15 ± 0.09	0.97 ± 0.10	1.33 ± 0.09†	0.82 ± 0.09‡	0.80 ± 0.07	0.97 ± 0.08‡
HMW: total adiponectin	0.38 ± 0.02	0.36 ± 0.02	0.44 ± 0.02†	0.35 ± 0.02	0.34 ± 0.02	0.39 ± 0.02

Data are means ± SE of 27–30 mice for metabolic parameters and 13–15 mice for other measures. AMPKα2$^{-/-}$ and wild-type mice were fed either a Chow diet, cHF, or cHF+F for nine weeks. Food consumption was measured weekly for nine weeks. Body weight gain (see also supplementary Fig. 1) and plasma parameters were assessed in ad libitum-fed mice after nine weeks. Plasma insulin levels were also assessed in fasted mice after eight weeks. AT, adipose tissue; A.U., arbitary units; HMW, total adiponectin, ratio of high molecular weight to total adiponectin (for levels of all molecular weight forms of adiponectin; ND, no data; see supplementary Fig. 2); *$P < 0.05$ vs. genotype Chow; †$P < 0.05$ vs. genotype cHF; ‡$P < 0.05$ vs. wild-type on respective diet.

mice (Table 1). In both wild-type and AMPKα2$^{-/-}$ mice, the cHF+F diet induced smaller body weight gain than the cHF diet (Table 1 and supplementary Figure 1). None of the differences in body weight gain could be explained by caloric intake, which was similar in all experimental groups (Table 1). The weight of fat depots increased in response to cHF feeding, while the cHF+F diet partially prevented this increase (Table 1). Triglycerides and NEFA levels in plasma of ad libitum-fed mice were similar in the Chow- and cHF-fed mice, while cholesterol levels were markedly and significantly elevated by the cHF diet. n-3 LC-PUFAs lowered plasma lipid levels independently of AMPKα2. Triglycerides and NEFA levels were strongly reduced, even below the levels observed in the Chow-fed mice (Table 1).

AMPKα2 is essential for the preservation of insulin sensitivity in response to n-3 LC-PUFAs. After nine weeks of dietary treatment, no change was observed in blood glucose, but elevations were observed in plasma insulin levels in response to the cHF diet in ad libitum-fed mice of both genotypes. However, the increase in plasma insulin levels was less pronounced in AMPKα2$^{-/-}$ mice, closely reflecting the genotype-dependent differences in body weight gain (Table 1). A similar pattern of changes in insulin levels was also observed in fasted mice, in which n-3 LC-PUFAs significantly reduced insulin levels only in wild-type animals (Table 1). As expected, plasma levels of total as well as high molecular weight form of adiponectin, an adipokine associated with increased insulin sensitivity (35), were increased ~1.4- and ~1.2-fold, respectively, in wild-type mice in response to n-3 LC-PUFA supplementation (Table 1 and supplementary Figure 2, available in an online appendix); however, no significant increase of plasma adiponectin by n-3 LC-PUFAs was observed in AMPKα2$^{-/-}$ mice.

In further experiments, hyperinsulinemic-euglycemic clamps were performed to evaluate whole-body insulin sensitivity. Under basal conditions, glucose turnover rate (GTO; i.e., glucose uptake in peripheral tissues) was similar in all groups of mice (supplementary Table 1). Under insulin-stimulated conditions (Fig. 2*A–F*), the amount of exogenous glucose required to maintain euglycemia during the clamp, i.e., the glucose infusion rate (GIR), was ~1.3-fold lower in AMPKα2$^{-/-}$ than in wild-type mice fed the Chow diet (Fig. 2*A*). On the other hand, GIR was decreased by the cHF diet to a similar level in mice of both genotypes, manifesting diet-induced insulin resistance. This was attributed to a decreased GTO and, in particular, to an impaired suppression of hepatic glucose production (HGP) by insulin, with HGP being ~8.5-fold higher in the cHF-fed compared with the Chow-fed wild-type mice (Fig. 2*C*). In wild-type mice, cHF+F diet feeding increased GIR and GTO (~1.9- and ~1.2-fold increase, respectively) as compared with cHF-fed mice, while HGP was lowered to a similar level as in the Chow-fed mice. These results document the protective effects of n-3 LC-PUFAs from high-fat diet-induced insulin resistance in wild-type mice, namely, at the level of HGP. In contrast, none of these beneficial effects of n-3 LC-PUFAs was observed in AMPKα2$^{-/-}$ mice, in which neither the GIR (Fig. 2*A*) nor the GTO (Fig. 2*B*) differed between the cHF+F-fed and the cHF-fed mice, whereas the rate of HGP was even higher in the cHF+F-fed than in the cHF-fed AMPKα2$^{-/-}$ mice (Fig. 2*C*). Although whole-body glycolysis was similar in all the groups (Fig. 2*D*), the rate of whole-body glycogen synthesis, which reflects insulin sensitivity of muscle glucose metabolism, was dependent on both diet and genotype (Fig. 2*E*). In the Chow-fed mice, the rate of whole-body glycogen synthesis tended to be higher in wild-type mice than in AMPKα2$^{-/-}$ mice. Only in the former mice was it significantly affected by dietary treatment. Thus, in wild-type mice, glycogen synthesis was

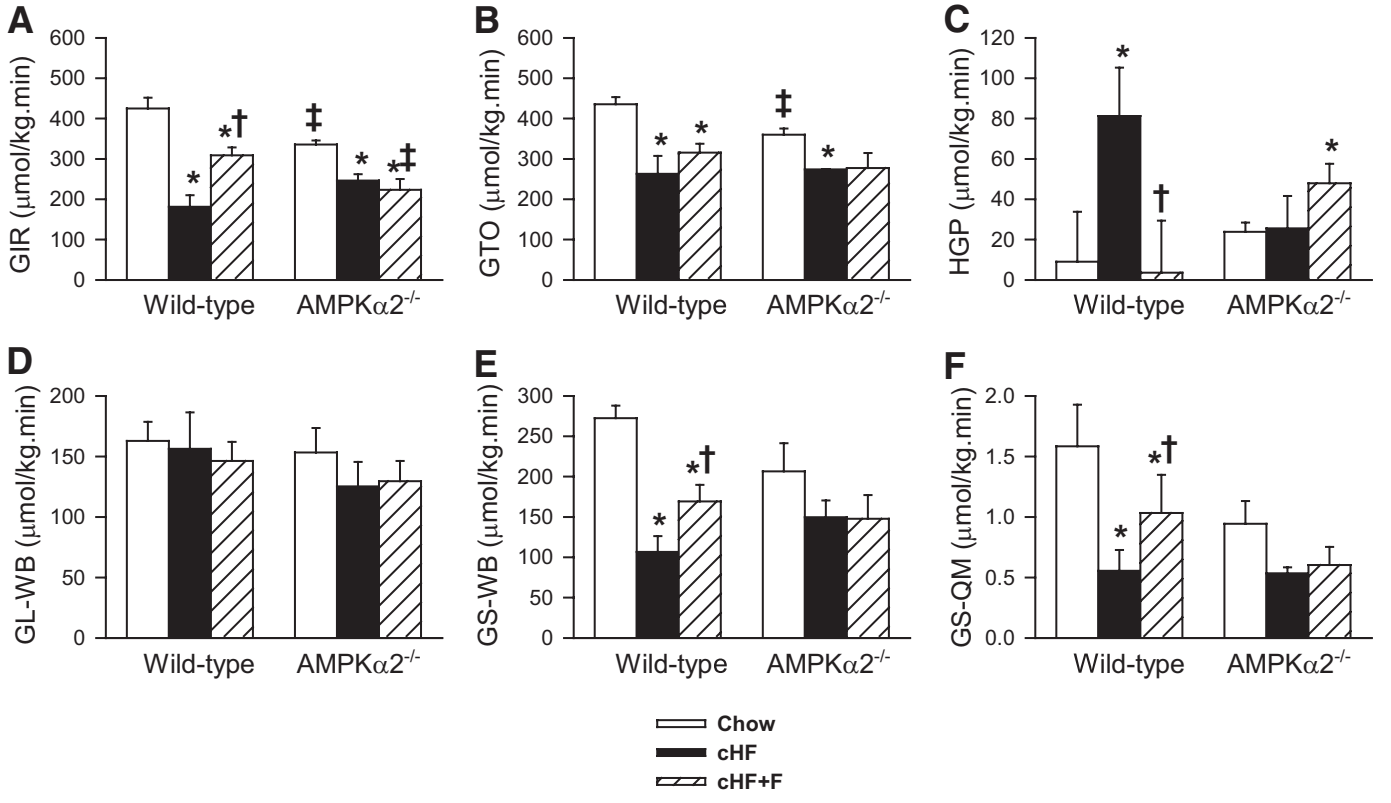

FIG. 2. Insulin sensitivity assessed by hyperinsulinemic-euglycemic clamp. GIR (*A*), GTO (*B*), HGP (*C*), whole-body glycolysis (GL-WB; *D*), whole-body glycogen synthesis (GS-WB; *E*); and glycogen synthesis in quadriceps muscle (GS-QM; *F*) were measured in wild-type and AMPKα2$^{-/-}$ mice fed either a Chow diet, cHF, or cHF+F for 9 weeks. The data are the means ± SE (n = 5–8). *P < 0.05 versus genotype Chow; †P < 0.05 versus genotype cHF; ‡P < 0.05 versus wild-type on respective diet.

decreased ~2.4-fold in response to the cHF diet, while n-3 LC-PUFAs provided a partial protection from this decrease (Fig. 2*E*). A similar pattern of changes in the glycogen synthesis rate in response to n-3 LC-PUFAs was observed when measured directly in the skeletal muscle (Fig. 2*F*). Thus, in accordance with the previous study (26), the results of clamp studies suggested impairment of insulin sensitivity in response to whole-body ablation of AMPKα2 in Chow-fed mice. However, AMPKα2$^{-/-}$ mice seemed to be partially protected against cHF-induced insulin resistance, while AMPKα2 was required for preservation of insulin sensitivity in the skeletal muscle and especially in the liver in response to n-3 LC-PUFA feeding.

Unmasking the role of AMPKα2 in the lipid-lowering effect of n-3 LC-PUFAs under hyperinsulinemic-euglycemic conditions. In addition to the ad libitum-fed mice (Table 1), plasma lipid levels were also measured in fasted mice, as well as in mice subjected to hyperinsulinemic-euglycemic clamp (supplementary Table 2). In contrast to the ad libitum-fed state, cHF+F diet did not affect either triglyceride or NEFA levels under fasting conditions. Under the hyperinsulinemic-euglycemic conditions, both triglyceride and NEFA levels were lower in the cHF+F-fed than in the cHF-fed wild-type mice (~1.6-fold and ~1.4-fold difference, respectively), but no such difference between the diets was observed in AMPKα2$^{-/-}$ mice. Cholesterol levels were consistently decreased by n-3 LC-PUFAs independently of both the metabolic state and genotype (supplementary Table 2).

In ad libitum-fed mice of both genotypes, the hepatic triglyceride content was increased ~twofold by cHF compared with the Chow diet, while triglyceride accumulation was increased only ~1.3-fold by cHF+F diet in both genotypes, documenting a protection against hepatic triglyceride accumulation by n-3 LC-PUFAs (Fig. 3*A*). Under hyperinsulinemic-euglycemic conditions, n-3 LC-PUFAs also protected livers of wild-type mice against the cHF-induced accumulation of triglycerides. However, this effect was absent in AMPKα2$^{-/-}$ mice (Fig. 3*B*). Moreover, a strong correlation was found between plasma NEFA levels and hepatic triglyceride content assessed under the clamp conditions in the cHF+F-fed AMPKα2$^{-/-}$ mice (R^2 = 0.43, P < 0.05) but not in wild-type mice (R^2 = 0.08, P = 0.395). F3

Dietary n-3 LC-PUFAs increase 5-aminoimidazole-4-carboxamide-1-β-D-ribofuranoside-stimulated fatty acid oxidation and insulin-stimulated lipogenesis in cultured hepatocytes from wild-type but not from AMPKα2$^{-/-}$ mice. We sought to determine whether the differential effect of n-3 LC-PUFAs on accumulation of liver triglycerides in wild-type and AMPKα2$^{-/-}$ mice under the clamp conditions could be explained by hepatic lipid metabolism. In cultured hepatocytes isolated from mice following the different dietary treatments, activities of both fatty acid oxidation and de novo fatty acid synthesis were evaluated. The stimulatory effects of 5-aminoimidazole-4-carboxamide-1-β-D-ribofuranoside (AICAR), an AMPK activator, and insulin on fatty acid oxidation and synthesis are shown in Fig. 4*A* and *B*, respectively (for corresponding basal metabolic activities, see supplementary Table 3, available in an online appendix). In hepatocytes from both Chow and cHF diet-fed mice, the absence of AMPKα2 was associated with a trend for lower AICAR-stimulated fatty acid oxidation. Although hepatocytes F4

rich4/zdb-diab/zdb-diab/zdb01110/zdb6323d10z | xppws | S=1 | 8/26/10 | 9:12 | doi: 10.2337/db09-1716 | artno: 1716

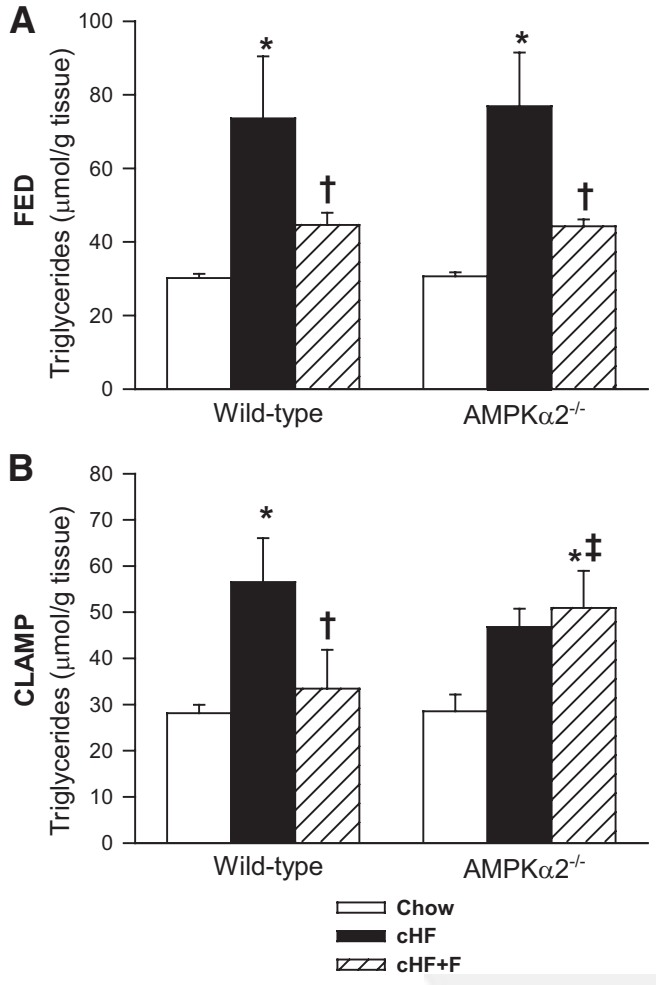

FIG. 3. Triglyceride concentration in the livers of ad libitum-fed mice (*A*) and mice killed at the end of a 3-h infusion period of the hyperinsulinemic-euglycemic clamp (*B*). Wild-type and AMPKα2$^{-/-}$ mice were fed either a Chow diet, cHF, or cHF+F for 9 weeks. The data are the means ± SE (*A*, *n* = 13–15; *B*, *n* = 8–14). **P* < 0.05 versus genotype Chow; †*P* < 0.05 versus genotype cHF; ‡*P* < 0.05 versus wild-type on respective diet. For the detailed fatty acid composition of triglyceride fractions in the livers of ad libitum-fed mice, see supplementary Table 4.

from cHF-fed mice showed reduced stimulatory effect of AICAR irrespective of the genotype, cHF+F feeding normalized this defect in wild-type but not in AMPKα2$^{-/-}$ hepatocytes (Fig. 5*A*), suggesting AMPK-dependent induction of capacity for fatty acid oxidation by n-3 LC-PUFAs in the liver. The stimulatory effect of insulin on de novo fatty acid synthesis was reduced in hepatocytes from cHF-fed wild-type mice, whereas it was retained in the hepatocytes from cHF-fed AMPKα2$^{-/-}$ mice (Fig. 4*B*). cHF+F feeding tended to restore the stimulatory effect of insulin only in wild-type hepatocytes (Fig. 4*B*).

To further characterize hepatic effects of differential dietary treatment, the expression of selected genes was quantified in total RNA isolated from the livers of mice subjected to hyperinsulinemic-euglycemic clamp (Fig. 4*C* and *D*). Feeding cHF diet suppressed expression of lipogenic genes stearoyl-CoA desaturase (SCD-1) and SREBP-1c in all groups (except for SREBP-1c in AMPKα2$^{-/-}$ mice). This suppression was partially counteracted by cHF+F diet in wild-type but not AMPKα2$^{-/-}$ mice (Fig. 4*C* and *D*). Together with the de novo fatty acid synthesis data, these results further support the AMPKα2-dependent improvement of liver insulin sensitivity by n-3 LC-PUFAs.

Changes in hepatic diacylglycerol levels are associated with insulin-sensitizing effects of n-3 LC-PUFAs. To identify factors predisposing animals to insulin resistance in an AMPKα2-dependent manner, a detailed analysis of hepatic lipids in ad libitum-fed mice was performed. No major genotype-dependent differences in the contents of either ceramides or phospholipids were observed (supplementary Table 4, available in an online appendix). In contrast, hepatic content of diacylglycerols was affected in a genotype- and diet-dependent manner (Fig. 5*A*). Wild-type mice fed the cHF+F diet had lower diacylglycerol content than genotype-matched cHF diet-fed mice, while this effect of the cHF+F diet was not observed in AMPKα2$^{-/-}$ mice. Moreover, the analysis of fatty acid composition of the diacylglycerol fraction in the liver revealed that wild-type as well as AMPKα2$^{-/-}$ mice fed cHF diet were characterized by marked increase in the level of PUFA but not monounsaturated or saturated fatty acids (Fig. 5*B*, *C*, and *D* and supplementary Table 4). The increase in the PUFA content tended to be smaller in the wild-type compared with AMPKα2$^{-/-}$ mice (~1.7-fold and ~2.2-fold, respectively). Administration of n-3 LC-PUFAs completely prevented accumulation of hepatic polyunsaturated diacylglycerols in wild-type mice, whereas their level in the AMPKα2$^{-/-}$ animals, although decreased, was still significantly higher compared with genotype-matched Chow-fed mice (Fig. 5*B*). Regarding polyunsaturated diacylglycerols, α-linolenic acid (18:3n-3) appeared to be by far the most differentially regulated PUFA in the diacylglycerol fraction in the two genotypes (supplementary Table 4). In addition, cHF+F diet markedly reduced hepatic content of monounsaturated diacylglycerols in wild-type but not in knockout animals (Fig. 5*C*). Hepatic diacylglycerol levels and their fatty acid composition were also analyzed in mice subjected to hyperinsulinemic-euglycemic clamp. No significant differences among the groups were observed in total diacylglycerols content or in their saturated or monounsaturated fatty acid fractions (supplementary Figure 3, available in an online appendix).

DISCUSSION

Previous animal studies demonstrated that n-3 LC-PUFAs could counteract the development of both hepatic steatosis (8,18,36,37) and hepatic insulin resistance (8,9,16), while suppressing lipogenesis and augmenting lipid catabolism in the liver (8,13,19,21). Using mice with a whole-body deletion of AMPKα2 and high-fat feeding, we show for the first time that AMPKα2 is required for the effect of n-3 LC-PUFAs to preserve whole-body, muscle, and especially hepatic insulin sensitivity, as well as to suppress hepatic and plasma triglycerides as well as NEFA levels under hyperinsulinemic-euglycemic clamp conditions. In contrast, AMPKα2 was not required for protection by n-3 LC-PUFAs from hepatic lipid accumulation and dyslipidemia in ad libitum-fed mice.

In addition to AMPKα2, PPARα was previously identified as an important determinant of n-3 LC-PUFA's effect on lipid metabolism, especially short-term modulation of hepatic gene expression (14) and insulin sensitivity (16). Thus, the reduction in hepatic triglyceride concentrations by fish oil feeding did not rescue insulin action in PPARα-null mice, while hepatic diacylglycerol concentrations were decreased by fish oil in a PPARα-dependent manner

rich4/zdb-diab/zdb-diab/zdb01110/zdb6323d10z | xppws | S=1 | 8/26/10 | 9:12 | doi: 10.2337/db09-1716 | artno: 1716

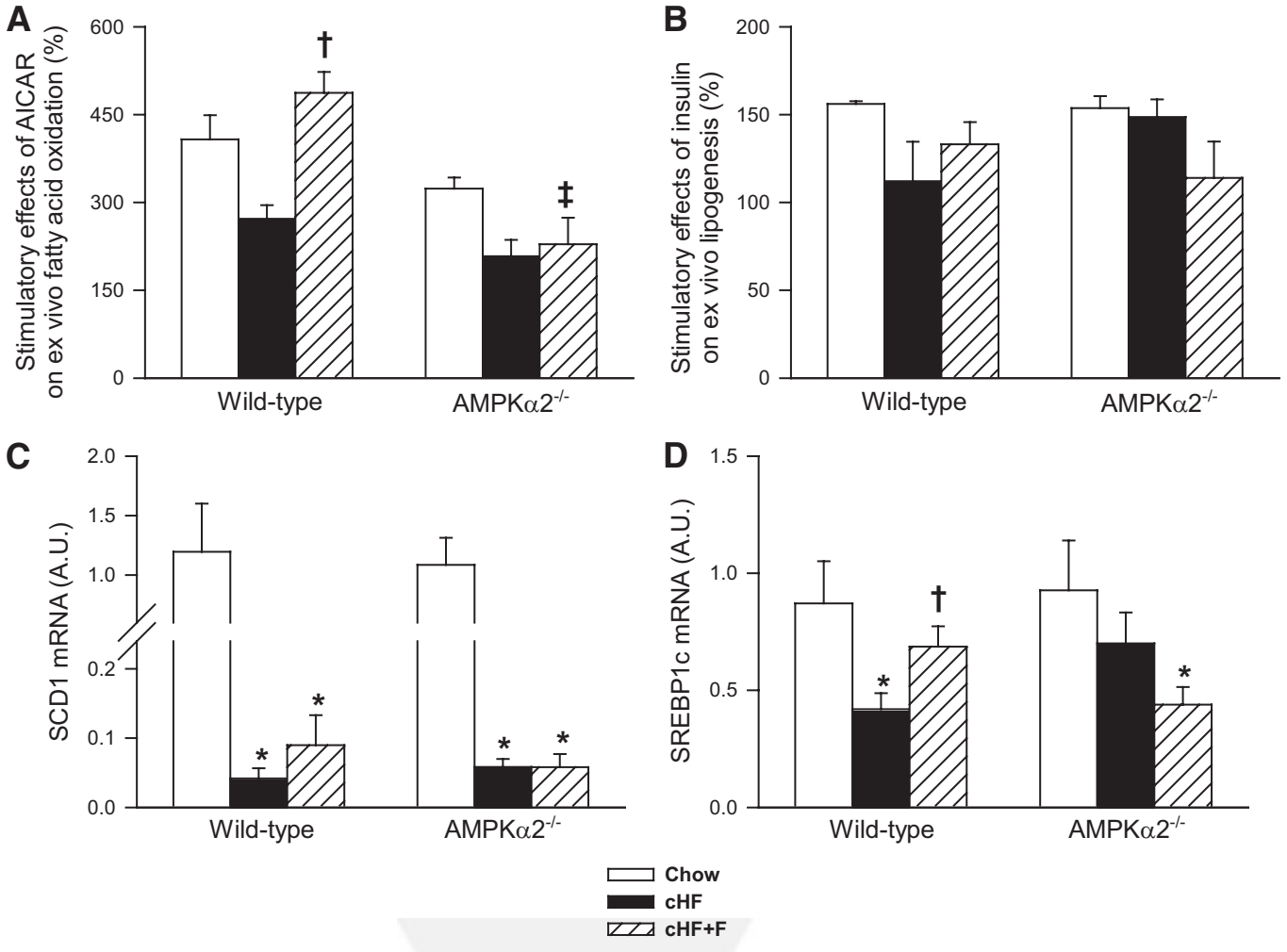

FIG. 4. The effect of differential dietary treatment on the regulation of metabolic fluxes in the liver. AICAR-stimulated fatty acid oxidation (*A*) and insulin-stimulated de novo fatty acid synthesis (*B*) in cultured hepatocytes isolated from wild-type and AMPKα2$^{-/-}$ mice fed for 9 weeks either a Chow diet, cHF, or cHF+F. For basal nonstimulated rates of lipid metabolism, see supplementary Table 3. The expression of SCD-1 (*C*) and SREBP-1c (*D*) genes was quantified in total RNA isolated from the livers of mice subjected to hyperinsulinemic-euglycemic clamp following the differential dietary treatment for 9 weeks. The data are means ± SE (isolated hepatocytes, $n = 3$ in triplets; hepatic gene expression, $n = 5–8$). *$P < 0.05$ versus genotype Chow; †$P < 0.05$ versus genotype cHF; ‡$P < 0.05$ versus wild-type on respective diet. A.U., arbitrary units.

and were associated with a preserved hepatic insulin sensitivity (16). It is generally accepted that *1*) diacylglycerols rather than triglycerides or ceramides mediate hepatic insulin resistance in mice fed a high-fat diet (19,38,39), *2*) diacylglycerol-induced insulin resistance depends on activation of protein kinase C, and *3*) that polyunsaturated diacylglycerols in particular are better protein kinase C activators than saturated diacylglycerol species [reviewed in refs (38,39)]. Also our results showed that cHF diet-induced insulin resistance was associated primarily with the accumulation of PUFA in hepatic diacylglycerols and that n-3 LC-PUFA completely prevented cHF diet-induced increase in PUFA diacylglycerols in wild-type mice, whereas in AMPKα2$^{-/-}$ animals, the content of these lipids was still significantly higher compared with the control. Moreover, it was only in ad libitum-fed mice but not in mice subjected to hyperinsulinemic-euglycemic clamps that the levels of hepatic diacylglycerols and their fatty acid compositions were associated with hepatic insulin sensitivity. It is possible that under clamp conditions AMPKα2-dependent effects of n-3 LC-PUFAs on liver diacylglycerols were masked by metabolic changes occurring during a 3-h infusion of insulin and glucose.

The failure of n-3 LC-PUFAs to decrease hepatic lipids in AMPKα2$^{-/-}$ mice under clamp conditions could be due to primary alterations in metabolic fluxes in the liver, reflecting *1*) increased de novo fatty acid synthesis, *2*) decreased secretion of VLDL triglycerides, or *3*) reduced fatty acid oxidation. De novo fatty acid synthesis was not the responsible factor, because hepatocytes of the n-3 LC-PUFA-fed AMPKα2$^{-/-}$ mice showed decreased insulin-stimulated de novo fatty acid synthesis and reduced expression of SREBP-1c and SCD-1, as compared with hepatocytes isolated from n-3 LC-PUFA-fed wild-type mice, reflecting probably low insulin sensitivity of the liver in AMPKα2$^{-/-}$ mice. Moreover, AICAR-stimulated fatty acid oxidation in hepatocytes from n-3 LC-PUFA-fed AMPKα2$^{-/-}$ mice was markedly reduced as compared with those from wild-type mice, suggesting decreased hepatic capacity for fatty acid oxidation in the absence of AMPKα2, which could contribute to enhanced lipid accumulation. Therefore, these experiments supported a major role of hepatic AMPKα2 in the regulation of both insulin sensitivity and lipid metabolism by n-3 LC-PUFAs. However, the differential modulation of lipid accumulation by n-3 LC-PUFAs in the livers of wild-type and AMPKα2$^{-/-}$

rich4/zdb-diab/zdb-diab/zdb01110/zdb6323d10z | xppws | S=1 | 8/26/10 | 9:12 | doi: 10.2337/db09-1716 | artno: 1716

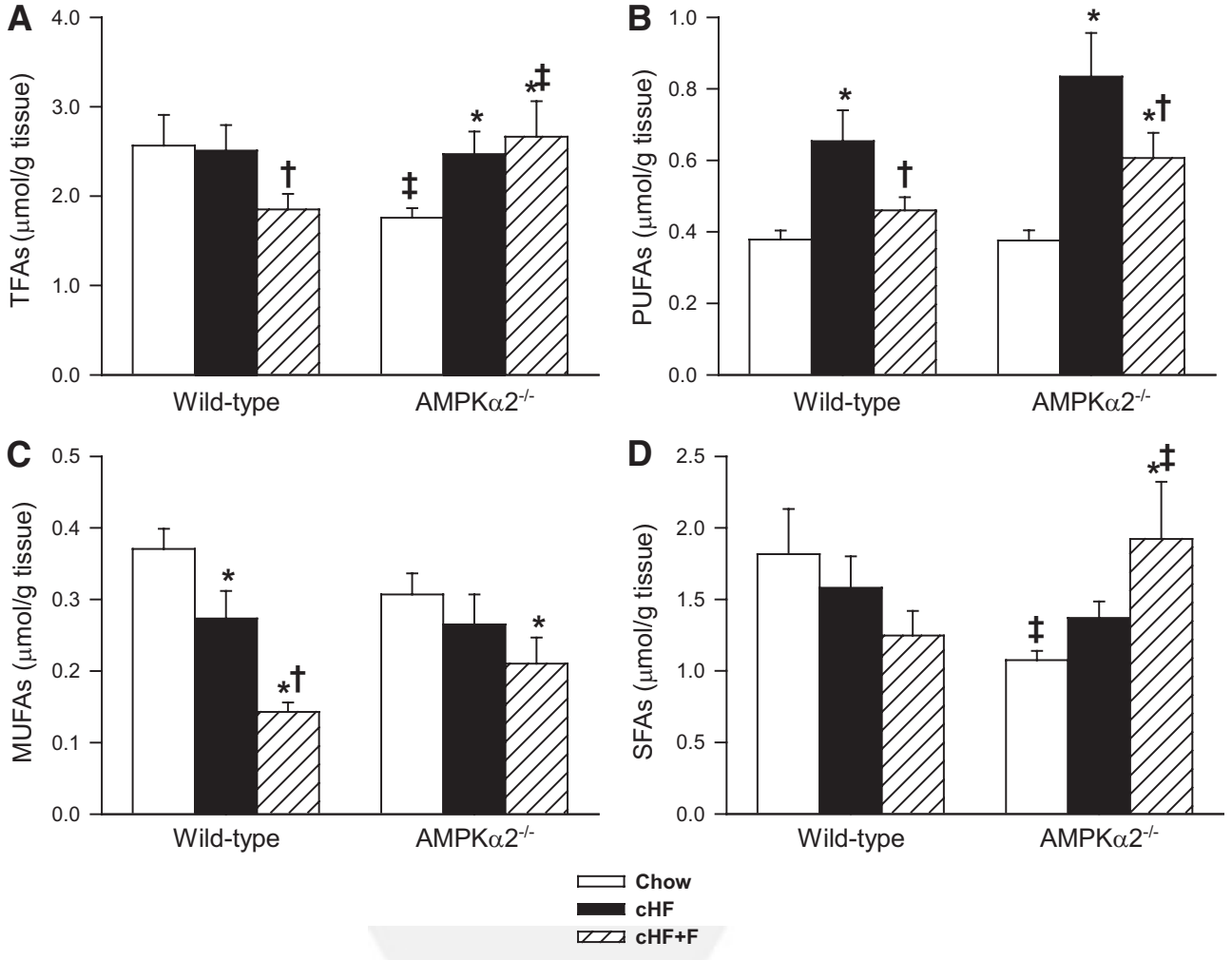

FIG. 5. The composition of fatty acids in hepatic diacylglycerol fraction in ad libitum-fed wild-type and AMPKα2$^{-/-}$ mice: total fatty acids (TFAs; *A*), PUFAs (*B*), monounsaturated fatty acids (MUFAs; *C*), and saturated fatty acids (SFAs; *D*). Animals were fed either a Chow diet, cHF, or cHF+F for 9 weeks. The data are the means ± SE (n = 13–15). *P < 0.05 versus genotype Chow; †P < 0.05 versus genotype cHF; ‡P < 0.05 versus wild-type on respective diet. For the detailed fatty acid composition of diacylglycerol fractions in the livers of ad libitum fed mice, see supplementary Table 4.

mice under clamp conditions could also be secondary to the AMPKα2-dependent effects of n-3 LC-PUFAs in other tissues, namely, due to a relatively high uptake of circulating NEFA in AMPKα2$^{-/-}$ mice. This is supported by persistently elevated plasma levels of NEFA in AMPKα2$^{-/-}$ mice, as well as by a significant correlation between plasma NEFA levels and hepatic triglyceride content observed under clamp conditions in AMPKα2$^{-/-}$ but not wild-type mice fed n-3 LC-PUFA-containing diet. Moreover, it has been shown in humans with nonalcoholic fatty liver disease that most of hepatic triglycerides arise from circulating NEFA (40). That plasma NEFA levels under clamp conditions were reduced only in wild-type but not in AMPKα2$^{-/-}$ mice fed n-3 LC-PUFAs may reflect a role of AMPKα2 in muscle lipid uptake mediated by lipoprotein lipase (41), as well as the antilipolytic effect of AMPK in adipose tissue, documented for AMPKα1 (42). In any case, decreased fatty acid oxidation in situ in the liver and, possibly even more importantly, abundant supply of circulating NEFA could be responsible for the lack of the antisteatotic effect of n-3 LC-PUFAs in AMPKα2$^{-/-}$ mice under clamp conditions (Fig. 6). F6

Previous studies reported contradictory results, showing either *1*) activation of AMPK in rat liver (22) and murine adipose tissue (24) or *2*) no changes in AMPK activity in the liver, skeletal muscle, and heart of mice (43) in response to dietary n-3 LC-PUFAs. These discrepancies could be related to differences in dietary n-3 LC-PUFA intake, nutritional state of animals, and other parameters. In accordance with the involvement of AMPKα2 in various effects of n-3 LC-PUFAs, our results document activation of AMPKα2 (but not AMPKα1) in the liver of mice by long-term n-3 LC-PUFA treatment, in the absence of significant changes in either the AMP to ATP ratio assessed in whole liver extracts [not shown and ref (44)] or the phosphorylation status of LKB1, an upstream kinase for AMPK [not shown and ref (45)]. In addition, no effect on AMPK activity in either cultured hepatocytes (21) or embryonic kidney cells (not shown) of n-3 LC-PUFAs added to the cell culture medium could be detected. Therefore, the activation of AMPKα2 by n-3 LC-PUFAs probably does not depend on a direct interaction between n-3 LC-PUFAs and AMPK. On the other hand, induction of adiponectin by n-3 LC-PUFAs [results of this study and refs (46,47)] could be involved, because adiponectin activates AMPK in both the liver and skeletal muscle (35). Adiponectin is also required for the activation of AMPK upon administration of PPARγ agonists thiazolidinedio-

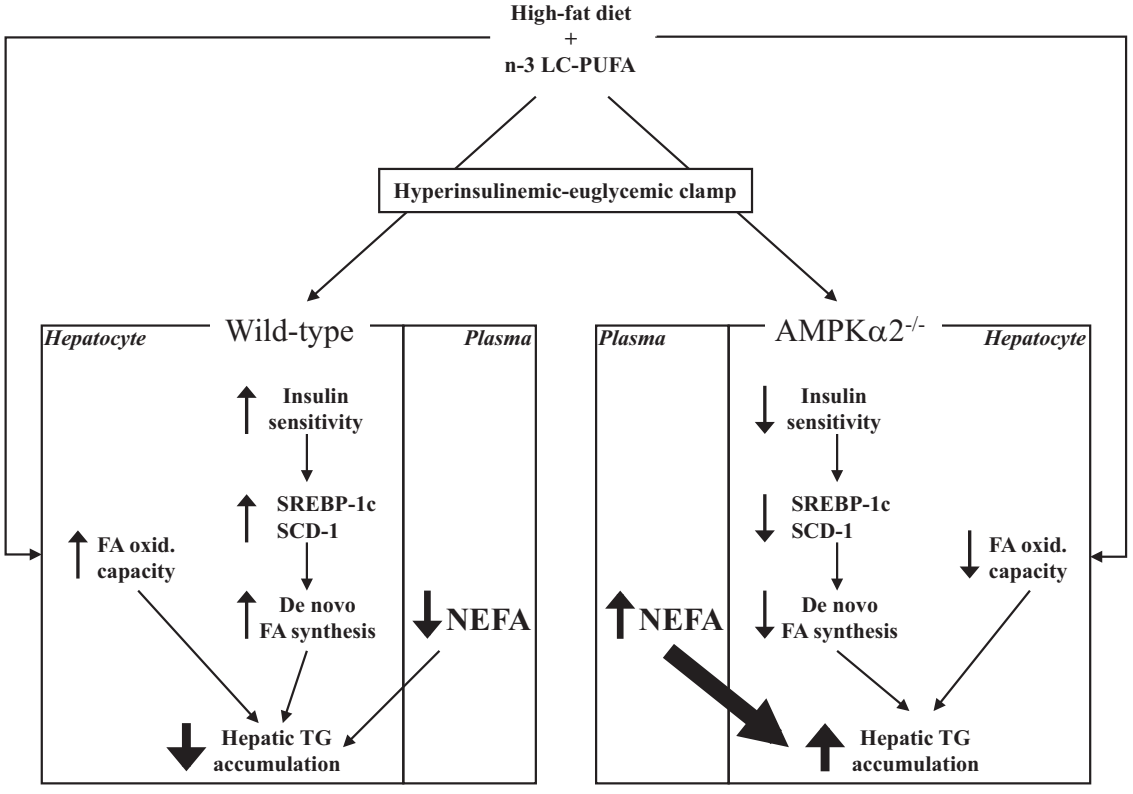

FIG. 6. Putative involvement of AMPKα2 in antisteatotic action of n-3 LC-PUFAs in the liver. Dietary intake of n-3 LC-PUFAs increases the capacity of hepatocytes to oxidize fatty acids in wild-type (left panels) but not in AMPKα2$^{-/-}$ mice (right panels). When insulin and glucose levels are high, such as during hyperinsulinemic-euglycemic clamp, wild-type mice fed n-3 LC-PUFAs exhibit improved hepatic insulin sensitivity and decreased plasma levels of NEFAs as compared with high-fat diet-fed controls. This is associated with increased expression of lipogenic genes such as SREBP-1c and SCD-1 and increased drive for de novo fatty acid synthesis. Despite the elevated lipogenic drive under clamp conditions, the livers of wild-type mice fed n-3 LC-PUFAs show reduced accumulation of triglycerides. However, in AMPKα2$^{-/-}$ mice fed n-3 LC-PUFAs, hepatic triglyceride content is markedly elevated despite reduced rates of de novo fatty acid synthesis. This effect could be secondary to persisting elevated NEFA levels in circulation and thus better substrate availability in AMPKα2$^{-/-}$ mice under clamp conditions. FA, fatty acids; TG, triglycerides.

nes, whereas mice lacking adiponectin show decreased hepatic insulin sensitivity and reduced responsiveness to these compounds (48). Thus, absence of AMPKα2 may blunt adiponectin-mediated effects of n-3 LC-PUFAs. In accordance with the previous study (49), plasma adiponectin levels tended to be reduced in AMPKα2$^{-/-}$ mice. Moreover, the induction of adiponectin by n-3 LC-PUFAs in AMPKα2$^{-/-}$ mice was compromised (Table 1 and supplementary Figure 2).

AMPKα1 and AMPKα2 contribute equally to total AMPK activity in the liver (50). In mice with liver-specific ablation of AMPKα2 (27), hepatic AMPKα2 was essential for suppressing hepatic glucose production and maintaining fasting blood glucose levels; however, the absence of AMPKα2 did not affect inhibitory action of insulin on hepatic glucose production. In our study, although fasting blood glucose levels were unaltered by whole-body ablation of AMPKα2, the beneficial effect of dietary n-3 LC-PUFAs on hepatic insulin sensitivity was clearly AMPKα2-dependent. Differential regulation of glucose homeostasis in the above transgenic models likely reflects the complexity of whole-body (26) versus liver-specific (27) deletion of AMPKα2. In contrast to the previous report, showing induction of adiposity and adipocyte hypertrophy in AMPKα2$^{-/-}$ mice fed a lard-based high-fat diet (49), our study documented a relatively low weight gain, low adiposity, and smaller fat cells in AMPKα2$^{-/-}$ mice fed a corn-oil based high-fat diet. This discrepancy could be related to the differences in the composition of experimental high-fat diets; however, our results are consistent with the elevated sympathetic tonus of AMPKα2$^{-/-}$ mice (26), which may stimulate energy dissipation in these animals. In any case, lower body weight of cHF-fed AMPKα2$^{-/-}$ mice as compared with their wild-type counterparts could be related to better insulin sensitivity of the former mice, as suggested by the differences in insulinemia, results of hyperinsulinemic-euglycemic clamp, stimulatory effect of insulin on lipogenesis, and expression of lipogenic genes in the liver.

In conclusion, the preservation of hepatic insulin sensitivity by n-3 LC-PUFAs in mice fed a high-fat diet depends on AMPKα2. The accumulation of diacylglycerols, which is regulated in an AMPKα2-dependent manner, could contribute to the modulation of hepatic insulin sensitivity in response to dietary n-3 LC-PUFAs. On the other hand, the AMPKα2-dependent acute changes in lipid metabolism and hepatic triglyceride accumulation, which are unmasked under insulin-stimulated conditions such as during hyperinsulinemic-euglycemic clamp, largely reflect the extrahepatic action of n-3 LC-PUFAs. Our results are relevant for the development of novel strategies for prevention and treatment of the metabolic syndrome. AQ: B

ACKNOWLEDGMENTS

The work was supported by grants from the Czech Science Foundation (301/10/1,420) and the Ministry of Education, Youth and Sports (1M6837805002, COST BMB0602-OC08007) of the Czech Republic. Further sup-

port included grants from the European Commission (LSHM-CT-2004-005272, EXGENESIS) and from EPAX AS (Norway), as well as the research project AV0Z50110509. No potential conflicts of interest relevant to this article were reported.

T.J. and M.R. performed experiments and wrote manuscript. O.K., Z.M.J., D.M., V.K., M.H., and P.J. performed experiments. I.M. quantified tissue nucleotides. M.B. performed analysis of hepatic lipids and contributed to discussion. J.G. performed analysis of hepatic lipids. S.H. contributed to experiments on hepatocytes. T.E.J. contributed to analysis of muscle metabolism. P.F. introduced AMPK$\alpha 2^{-/-}$ mouse model to the Prague laboratory and contributed to discussion. S.H. performed experiments on kidney cells. B.V. developed AMPK$\alpha 2^{-/-}$ mice and contributed to discussion. J.K. wrote manuscript.

The authors thank D. Grahame Hardie for the sheep AMPKα1 and AMPKα2 antibodies, Z. Szulc for the gift of *N*-palmitoyl-D-*erythro*-sphingosine (C17 base), and J. Jones (NMR Research Unit, Department of Biochemistry and Center for Neurosciences and Cell Biology, University of Coimbra, Coimbra, Portugal) for critical reading of the manuscript.

REFERENCES

1. Flachs P, Rossmeisl M, Bryhn M, Kopecky J. Cellular and molecular effects of n-3 polyunsaturated fatty acids on adipose tissue biology and metabolism. Clin Sci 2009;116:1–16
2. Nettleton JA, Katz R. n-3 long-chain polyunsaturated fatty acids in type 2 diabetes: a review. J Am Diet Assoc 2005;105:428–440
3. Mori TA, Bao DQ, Burke V, Puddey IB, Watts GF, Beilin LJ. Dietary fish as a major component of a weight-loss diet: effect on serum lipids, glucose, and insulin metabolism in overweight hypertensive subjects. Am J Clin Nutr 1999;70:817–825
4. Couet C, Delarue J, Ritz P, Antoine JM, Lamisse F. Effect of dietary fish oil on body fat mass and basal fat oxidation in healthy adults. Int J Obes 1997;21:637–643
5. Ruzickova J, Rossmeisl M, Prazak T, Flachs P, Sponarova J, Veck M, Tvrzicka E, Bryhn M, Kopecky J. Omega-3 PUFA of marine origin limit diet-induced obesity in mice by reducing cellularity of adipose tissue. Lipids 2004;39:1177–1185
6. Flachs P, Horakova O, Brauner P, Rossmeisl M, Pecina P, Franssen-van Hal N, Ruzickova J, Sponarova J, Drahota Z, Vlcek C, Keijer J, Houstek J, Kopecky J. Polyunsaturated fatty acids of marine origin upregulate mitochondrial biogenesis and induce beta-oxidation in white fat. Diabetologia 2005;48:2365–2375
7. Ikemoto S, Takahashi M, Tsunoda N, Maruyama K, Itakura H, Ezaki O. High-fat diet-induced hyperglycemia and obesity in mice: differential effects of dietary oils. Metabolism 1996;45:1539–1546
8. Kuda O, Jelenik T, Jilkova Z, Flachs P, Rossmeisl M, Hensler M, Kazdova L, Ogston N, Baranowski M, Gorski J, Janovska P, Kus V, Polak J, Mohamed-Ali V, Burcelin R, Cinti S, Bryhn M, Kopecky J. n-3 fatty acids and rosiglitazone improve insulin sensitivity through additive stimulatory effects on muscle glycogen synthesis in mice fed a high-fat diet. Diabetologia 2009;52:941–951
9. Storlien LH, Kraegen EW, Chisholm DJ, Ford GL, Bruce DG, Pascoe WS. Fish oil prevents insulin resistance induced by high-fat feeding in rats. Science 1987;237:885–888
10. Jucker BM, Cline GW, Barucci N, Shulman GI. Differential effects of safflower oil versus fish oil feeding on insulin-stimulated glycogen synthesis, glycolysis, and pyruvate dehydrogenase flux in skeletal muscle: a ^{13}C nuclear magnetic resonance study. Diabetes 1999;48:134–140
11. Fasching P, Ratheiser K, Waldhäusl W, Rohac M, Osterrode W, Nowotny P, Vierhapper H. Metabolic effects of fish-oil supplementation in patients with impaired glucose tolerance. Diabetes 1991;40:583–589
12. Pelikánová T, Kohout M, Válek J, Kazdová L, Base J. Metabolic effects of omega-3 fatty acids in type 2 (non-insulin-dependent) diabetic patients. Ann N Y Acad Sci 1993;683:272–278
13. Teran-Garcia M, Adamson AW, Yu G, Rufo C, Suchankova G, Dreesen TD, Tekle M, Clarke SD, Gettys TW. Polyunsaturated fatty acid suppression of fatty acid synthase (FASN): evidence for dietary modulation of NF-Y binding to the Fasn promoter by SREBP-1c. Biochem J 2007;402:591–600
14. Sanderson LM, de Groot PJ, Hooiveld GJ, Koppen A, Kalkhoven E, Müller M, Kersten S. Effect of synthetic dietary triglycerides: a novel research paradigm for nutrigenomics. PLoS One 2008;3:e1681
15. van Schothorst EM, Flachs P, Franssen-van Hal NL, Kuda O, Bunschoten A, Molthoff J, Vink C, Hooiveld GJ, Kopecky J, Keijer J. Induction of lipid oxidation by polyunsaturated fatty acids of marine origin in small intestine of mice fed a high-fat diet. BMC Genomics 2009;10:110
16. Neschen S, Morino K, Dong J, Wang-Fischer Y, Cline GW, Romanelli AJ, Rossbacher JC, Moore IK, Regittnig W, Munoz DS, Kim JH, Shulman GI. n-3 Fatty acids preserve insulin sensitivity in vivo in a peroxisome proliferator-activated receptor-alpha-dependent manner. Diabetes 2007;56:1034–1041
17. Serhan CN. Novel omega-3-derived local mediators in anti-inflammation and resolution. Pharmacol Ther 2005;105:7–21
18. González-Périz A, Horrillo R, Ferré N, Gronert K, Dong B, Morán-Salvador E, Titos E, Martínez-Clemente M, López-Parra M, Arroyo V, Clària J. Obesity-induced insulin resistance and hepatic steatosis are alleviated by omega-3 fatty acids: a role for resolvins and protectins. FASEB J 2009;23:1946–1957
19. Jump DB. Fatty acid regulation of gene transcription. Crit Rev Clin Lab Sci 2004;41:41–78
20. Neschen S, Morino K, Rossbacher JC, Pongratz RL, Cline GW, Sono S, Gillum M, Shulman GI. Fish oil regulates adiponectin secretion by a peroxisome proliferator-activated receptor-gamma-dependent mechanism in mice. Diabetes 2006;55:924–928
21. Dentin R, Benhamed F, Pégorier JP, Foufelle F, Viollet B, Vaulont S, Girard J, Postic C. Polyunsaturated fatty acids suppress glycolytic and lipogenic genes through the inhibition of ChREBP nuclear protein translocation. J Clin Invest 2005;115:2843–2854
22. Suchankova G, Tekle M, Saha AK, Ruderman NB, Clarke SD, Gettys TW. Dietary polyunsaturated fatty acids enhance hepatic AMP-activated protein kinase activity in rats. Biochem Biophys Res Commun 2005;326:851–858
23. Gabler NK, Radcliffe JS, Spencer JD, Webel DM, Spurlock ME. Feeding long-chain n-3 polyunsaturated fatty acids during gestation increases intestinal glucose absorption potentially via the acute activation of AMPK. J Nutr Biochem 2009;20:17–25
24. Kopecky J, Rossmeisl M, Flachs P, Kuda O, Brauner P, Jilkova Z, Stankova B, Tvrzicka E, Bryhn M. n-3 PUFA: bioavailability and modulation of adipose tissue function. Proc Nutr Soc 2009;68:361–369
25. Carling D. The AMP-activated protein kinase cascade–a unifying system for energy control. Trends Biochem Sci 2004;29:18–24
26. Viollet B, Andreelli F, Jørgensen SB, Perrin C, Geloen A, Flamez D, Mu J, Lenzner C, Baud O, Bennoun M, Gomas E, Nicolas G, Wojtaszewski JF, Kahn A, Carling D, Schuit FC, Birnbaum MJ, Richter EA, Burcelin R, Vaulont S. The AMP-activated protein kinase alpha2 catalytic subunit controls whole-body insulin sensitivity. J Clin Invest 2003;111:91–98
27. Andreelli F, Foretz M, Knauf C, Cani PD, Perrin C, Iglesias MA, Pillot B, Bado A, Tronche F, Mithieux G, Vaulont S, Burcelin R, Viollet B. Liver adenosine monophosphate-activated kinase-alpha2 catalytic subunit is a key target for the control of hepatic glucose production by adiponectin and leptin but not insulin. Endocrinology 2006;147:2432–2441
28. Foretz M, Ancellin N, Andreelli F, Saintillan Y, Grondin P, Kahn A, Thorens B, Vaulont S, Viollet B. Short-term overexpression of a constitutively active form of AMP-activated protein kinase in the liver leads to mild hypoglycemia and fatty liver. Diabetes 2005;54:1331–1339
29. Zhang BB, Zhou G, Li C. AMPK: an emerging drug target for diabetes and the metabolic syndrome. Cell Metab 2009;9:407–416
30. Kahn BB, Alquier T, Carling D, Hardie DG. AMP-activated protein kinase: ancient energy gauge provides clues to modern understanding of metabolism. Cell Metab 2005;1:15–25
31. Polak J, Kovacova Z, Jacek M, Klimcakova E, Kovacikova M, Vitkova M, Kuda O, Sebela M, Samcova E, Stich V. An increase in plasma adiponectin multimeric complexes follows hypocaloric diet-induced weight loss in obese and overweight pre-menopausal women. Clin Sci (Lond) 2007;112:557–565
32. Hardie DG, Salt IP, Davies SP. Analysis of the role of the AMP-activated protein kinase in the response to cellular stress. Methods Mol Biol 2000;99:63–74
33. Burcelin R, Crivelli V, Dacosta A, Roy-Tirelli A, Thorens B. Heterogeneous metabolic adaptation of C57BL/6J mice to high-fat diet. Am J Physiol Endocrinol Metab 2002;282:E834–E842
34. Foretz M, Guichard C, Ferré P, Foufelle F. Sterol regulatory element binding protein-1c is a major mediator of insulin action on the hepatic expression of glucokinase and lipogenesis-related genes. Proc Natl Acad Sci U S A 1999;96:12737–12742
35. Yamauchi T, Kamon J, Minokoshi Y, Ito Y, Waki H, Uchida S, Yamashita S, Noda M, Kita S, Ueki K, Eto K, Akanuma Y, Froguel P, Foufelle F, Ferre P,

Carling D, Kimura S, Nagai R, Kahn BB, Kadowaki T. Adiponectin stimulates glucose utilization and fatty-acid oxidation by activating AMP-activated protein kinase. Nat Med 2002;8:1288–1295

36. Kajikawa S, Harada T, Kawashima A, Imada K, Mizuguchi K. Highly purified eicosapentaenoic acid prevents the progression of hepatic steatosis by repressing monounsaturated fatty acid synthesis in high-fat/high-sucrose diet-fed mice. Prostaglandins Leukot Essent Fatty Acids 2009;80(4):229–238
37. Uyeda K, Repa JJ. Carbohydrate response element binding protein, ChREBP, a transcription factor coupling hepatic glucose utilization and lipid synthesis. Cell Metab 2006;4:107–110
38. Wakelam MJO. Diacylglycerol—when is it an intracellular messenger? BBA-Mol Cell Biol Lipids 1998;1436:117–126
39. Schmitz-Peiffer C, Biden TJ. Protein kinase C function in muscle, liver, and beta-cells and its therapeutic implications for type 2 diabetes. Diabetes 2008;57:1774–1783
40. Donnelly KL, Smith CI, Schwarzenberg SJ, Jessurun J, Boldt MD, Parks EJ. Sources of fatty acids stored in liver and secreted via lipoproteins in patients with nonalcoholic fatty liver disease. J Clin Invest 2005;115:1343–1351
41. Ohira M, Miyashita Y, Murano T, Watanabe F, Shirai K. Metformin promotes induction of lipoprotein lipase in skeletal muscle through activation of adenosine monophosphate-activated protein kinase. Metabolism 2009;58:1408–1414
42. Daval M, Diot-Dupuy F, Bazin R, Hainault I, Viollet B, Vaulont S, Hajduch E, Ferré P, Foufelle F. Anti-lipolytic action of AMP-activated protein kinase in rodent adipocytes. J Biol Chem 2005;280:25250–25257
43. Dobrzyn A, Dobrzyn P, Miyazaki M, Ntambi JM. Polyunsaturated fatty acids do not activate AMP-activated protein kinase in mouse tissues. Biochem Biophys Res Commun 2005;332:892–896
44. Salati LM, Clarke SD. Fatty acid inhibition of hormonal induction of acetyl-coenzyme A carboxylase in hepatocyte monolayers. Arch Biochem Biophys 1986;246:82–89
45. Woods A, Johnstone SR, Dickerson K, Leiper FC, Fryer LG, Neumann D, Schlattner U, Wallimann T, Carlson M, Carling D. LKB1 is the upstream kinase in the AMP-activated protein kinase cascade. Curr Biol 2003;13:2004–2008
46. Flachs P, Mohamed-Ali V, Horakova O, Rossmeisl M, Hosseinzadeh-Attar MJ, Hensler M, Ruzickova J, Kopecky J. Polyunsaturated fatty acids of marine origin induce adiponectin in mice fed a high-fat diet. Diabetologia 2006;49:394–397
47. Itoh M, Suganami T, Satoh N, Tanimoto-Koyama K, Yuan X, Tanaka M, Kawano H, Yano T, Aoe S, Takeya M, Shimatsu A, Kuzuya H, Kamei Y, Ogawa Y. Increased adiponectin secretion by highly purified eicosapentaenoic acid in rodent models of obesity and human obese subjects. Arterioscler Thromb Vasc Biol 2007;27:1918–1925
48. Nawrocki AR, Rajala MW, Tomas E, Pajvani UB, Saha AK, Trumbauer ME, Pang Z, Chen AS, Ruderman NB, Chen H, Rossetti L, Scherer PE. Mice lacking adiponectin show decreased hepatic insulin sensitivity and reduced responsiveness to peroxisome proliferator-activated receptor gamma agonists. J Biol Chem 2006;281:2654–2660
49. Villena JA, Viollet B, Andreelli F, Kahn A, Vaulont S, Sul HS. Induced adiposity and adipocyte hypertrophy in mice lacking the AMP-activated protein kinase-alpha2 subunit. Diabetes 2004;53:2242–2249
50. Cheung PC, Salt IP, Davies SP, Hardie DG, Carling D. Characterization of AMP-activated protein kinase gamma-subunit isoforms and their role in AMP binding. Biochem J 2000;346:659–669

JOURNAL OF PHYSIOLOGY AND PHARMACOLOGY 2009, 60, 4, 135-140
www.jpp.krakow.pl

O. KUDA[1], B. STANKOVA[2], E. TVRZICKA[2], M. HENSLER[1], T. JELENIK[1], M. ROSSMEISL[1], P. FLACHS[1], J. KOPECKY[1]

PROMINENT ROLE OF LIVER IN ELEVATED PLASMA PALMITOLEATE LEVELS IN RESPONSE TO ROSIGLITAZONE IN MICE FED HIGH-FAT DIET

[1]Department of Adipose Tissue Biology, Institute of Physiology of the Academy of Sciences of the Czech Republic, Prague, Czech Republic; [2]Charles University in Prague, First Faculty of Medicine, Fourth Department of Medicine, Prague, Czech Republic

In humans, antidiabetics thiazolidinediones (TZDs) upregulate stearoyl-CoA desaturase 1 (SCD1) gene in adipose tissue and increase plasma levels of SCD1 product palmitoleate, known to enhance muscle insulin sensitivity. Involvement of other tissues in the beneficial effects of TZDs on plasma lipid profile is unclear. In our previous study in mice, in which lipogenesis was suppressed by corn oil-based high-fat (cHF) diet, TZD rosiglitazone induced hepatic *Scd1* expression, while liver triacylglycerol content increased, VLDL-triacylglycerol production decreased and plasma lipid profile and whole-body glycemic control improved. Aim of this study was to characterise contribution of liver to changes of plasma lipid profile in response to a 8-week-treatment by rosiglitazone in the cHF diet-fed mice. Rosiglitazone (10 mg/kg diet) upregulated expression of *Scd1* in various tissues, with a stronger effect in liver as compared with adipose tissue or skeletal muscle. Rosiglitazone increased content of monounsaturated fatty acids in liver, adipose tissue and plasma, with palmitoleate being the most up-regulated fatty acid. In the liver, enhancement of SCD1 activity and specific enrichment of cholesteryl esters and phosphatidyl cholines with palmitoleate and vaccenate was found, while strong correlations between changes of various liver lipid fractions and total plasma lipids were observed (r=0.74-0.88). Insulin-stimulated glycogen synthesis was increased by rosiglitazone, with a stronger effect in muscle than in liver. Conclusions: changes in plasma lipid profile favouring monounsaturated fatty acids, mainly palmitoleate, due to the upregulation of *Scd1* and enhancement of SCD1 activity in the liver, could be involved in the insulin-sensitizing effects of TZDs.

Key words: *palmitoleic acid, hepatic lipogenesis, insulin resistance, stearoyl-CoA desaturase, thiazolidinediones*

Abbreviations: SCD: stearoyl-CoA desaturase; PPAR: peroxisome proliferator-activated receptors; TZD: thiazolidinedione; cHF: corn oil-based high-fat diet; TG: triacylglycerol; VLDL-TG: very low density lipoprotein triacylglycerol; CE: cholesteryl ester; PC: phosphatidylcholine; PE: phosphatidylethanolamine; AU: arbitrary unit

INTRODUCTION

It has been recognized that insulin sensitivity is inversely related to the degree of saturation of body lipids (1). In particular, palmitoleate (16:1 *n*-7) released from adipose tissue of transgenic mice has been recently shown to enhance muscle insulin action and to suppress its own synthesis in the liver (2). On the other hand, liver-derived lipoproteins represent a major source of plasma lipids, and liver could play a key role in the control of plasma palmitoleate levels and contribute to whole-body lipid profile. However, the consequences of changes in hepatic lipid metabolism with respect to whole-body insulin sensitivity, and especially the mechanisms underlying antidiabetic pharmacotherapy in human patients, remains largely unexplored (1).

Formation of palmitoleate marks lipogenesis and depends on the activity of stearoyl-CoA desaturase (SCD), which converts palmitoyl- and stearoyl-CoA into monounsaturated palmitoleoyl- and oleoyl-CoA, respectively. Hence, the ratio of monounsaturated to saturated fatty acids, especially the palmitoleic/palmitic (16:1/16:0) ratio in plasma or tissues, can be used to estimate SCD activity (3, 4). In mouse, four isoforms of the enzyme (*Scd1-4*) were identified, while two isoforms (*SCD1* and *SCD5*) exist in humans. In both organisms, high expression of SCD1 gene was detected in lipogenic tissues, *i.e.* the liver and adipose tissue. Transcription of SCD1 gene could be regulated by several factors, including peroxisome proliferator-activated receptors (PPAR), as reviewed by Paton and Ntambi (3).

Induction of SCD1 by antidiabetic drugs thiazolidinediones (TZDs), specific PPAR-γ agonists, was found in adipose tissue (4, 5) of both type 2 diabetic patients treated by rosiglitazone (4, 5) and in healthy human subjects treated by pioglitazone (6). Moreover, an increase in plasma 16:1/16:0 ratio correlated with improved insulin sensitivity, suggesting a role for the TZD-induced changes in plasma lipid profile in insulin sensitization (4). However, most experiments in rodents and 3T3-L1 adipocytes showed no change, or even a decrease in *Scd1* expression/activity due to TZDs, as reviewed by Toyama *et al*. (7). This discrepancy in the above studies could be explained, at least in part, by a different drive for de novo lipogenesis, which was probably higher in the animals fed standard chow or high carbohydrate diets than in humans consuming a habitual diet (8).

This relatively high lipogenesis in the treated animals, and also in the cultured adipocytes, could mask the stimulatory effect of TZDs. Indeed, up-regulation of *Scd1* in liver and muscle by a very low dose of rosiglitazone was observed in our recent study in mice, in which lipogenesis was suppressed by corn oil-based high-fat diet (cHF) (9). In the rosiglitazone-treated mice, liver triacylglycerol (TG) content increased, while hepatic VLDL-TG production, plasma non-esterified fatty acid and triacylglycerol levels decreased, and whole-body insulin sensitivity improved.

To characterise complex changes in lipid composition induced by rosiglitazone in the lipogenic tissues of the cHF diet-fed mice, and namely the role of liver in the effect of rosiglitazone on plasma lipid profile, lipidomic analysis of liver, adipose tissue and plasma was performed. Expression of *Scd1* in various tissues as well as insulin sensitivity in the liver and skeletal muscle were also assessed. Our results indicate a previously uncharacterized role of the liver in the induction of plasma lipid profile, which could contribute to the antidiabetic action of TZDs.

MATERIAL AND METHODS

Animals, plasma, and tissues

As described before (9), 3-month-old male C57BL/6N mice (Charles River Laboratories, Sulzfeld, Germany) were randomly assigned to cHF diet (lipid content ~35.2% wt/wt, mainly corn oil), or cHF diet supplemented with rosiglitazone (10 mg/kg diet; n=7) with free access to food and water. After 8 weeks of the differential dietary treatment (initial average body weight 27.8±0.7 g and 27.8±0.3 g; final average body weight 44.2±1.1 g and 41.8±1.3 g in the group fed cHF diet and cHF diet supplemented with rosiglitazone, respectively), mice were killed under anaesthesia (75 mg sodium pentobarbital/kg body weight) in ad libitum fed state and EDTA-plasma, liver and epididymal fat were collected. The rate of glycogen synthesis in the liver and skeletal muscle was assessed in a separate group of mice subjected to hyperinsulinaemic-euglycaemic clamp (9). Experiments were conducted under the guidelines for the use and care of laboratory animals of the Institute of Physiology and followed the 'Principles of laboratory animal care' (NIH publication no. 85-23, revised 1985).

Fatty acid composition

Lipids from plasma, liver, and adipose tissue were extracted with dichloromethane-methanol (2:1, v/v). In the case of liver, cholesteryl ester (CE), TG, phosphatidylcholine (PC), and phosphatidylethanolamine (PE) fractions were separated by preparative thin-layer chromatography and transmethylated as previously described (10). Fatty acid composition was measured using Shimadzu GC-17A gas chromatograph (Tokyo, Japan) equipped with capillary column DB-WAXETR 30 m x 0.32 mm I.D., d_f 0.25 μm (J&W Scientific, USA). The oven temperature was programmed from 80 to 130°C at 10°/min, to 240°C at 2 /min, then isothermal 25 min. The injector and detector temperatures were 250 and 270°C, respectively. Hydrogen carrier gas was maintained at a head pressure of 70 kPa and total flow 25 ml/min.

Quantitative RT-PCR

Levels of *Scd1* transcript were evaluated in total RNA isolated from the liver, adipose tissue and skeletal muscle, and normalized using elongation factor-1α as before (9).

Statistics

All statistics were performed using NCSS software (NCSS, Kaysville, Utah). All values are presented as means±SE. Comparisons were judged to be significant at p≤0.05. For principal component analysis, only fatty acids with p≤0.05 from a one-way ANOVA were included (2).

RESULTS

Differential stimulation of Scd1 expression by rosiglitazone in various tissues

In accordance with our previous study (9), a low dose of rosiglitazone stimulated *Scd1* expression in the cHF diet-fed mice in all the tissues analysed, with a much stronger induction observed in the liver than in skeletal muscle and adipose (*Fig. 1*).

Complex changes of liver lipid composition induced by rosiglitazone

Based on the strong *Scd1* upregulation in the liver, we decided to perform a detailed analysis of rosiglitazone-induced changes in liver lipid composition. Fatty acid composition of TG, PE, PC, and CE fractions separated from total liver lipids was analysed (*Fig. 2*). Palmitoleate was by far the most significantly upregulated fatty acid, showing a striking enrichment in all lipid fractions of rosiglitazone-treated mice, with ~3.0-fold induction in both TG and CE fractions and a smaller increase in phospholipids (fold increase: 3.06±0.33, 3.00±0.43, 2.40±0.18, and 1.84±0.13 in TG, CE, PE, and PC fraction, respectively; see *Fig. 2*). In addition, vaccenic acid (18:1 *n*-7), a product of palmitoleate elongation, showed a similar but less pronounced response to the rosiglitazone treatment (resulting in a ~1.2-fold increase in plasma levels of this acid). Total contents of saturated, monounsaturated, and polyunsaturated fatty acids in various fractions of hepatic lipids, as well as in total lipids in adipose tissue and plasma are shown in *Table 1*. Importantly, the amount of monounsaturated fatty acids was increased in all lipid

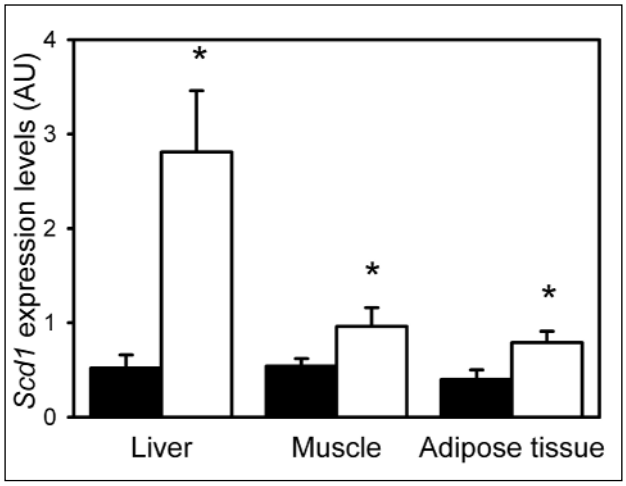

Fig. 1. Effect of rosiglitazone on *Scd1* gene expression. At 3 months of age, mice were randomly assigned to control cHF diet, or cHF diet supplemented with rosiglitazone. After 8 weeks of treatment, expression of *Scd1* was measured in the liver, skeletal muscle and adipose tissue. Black bar, cHF diet; white bar, cHF diet with rosiglitazone (10 mg/kg diet). Data are means ±SE (n=7). *Significantly different from cHF (p<0.05, *t*-test).

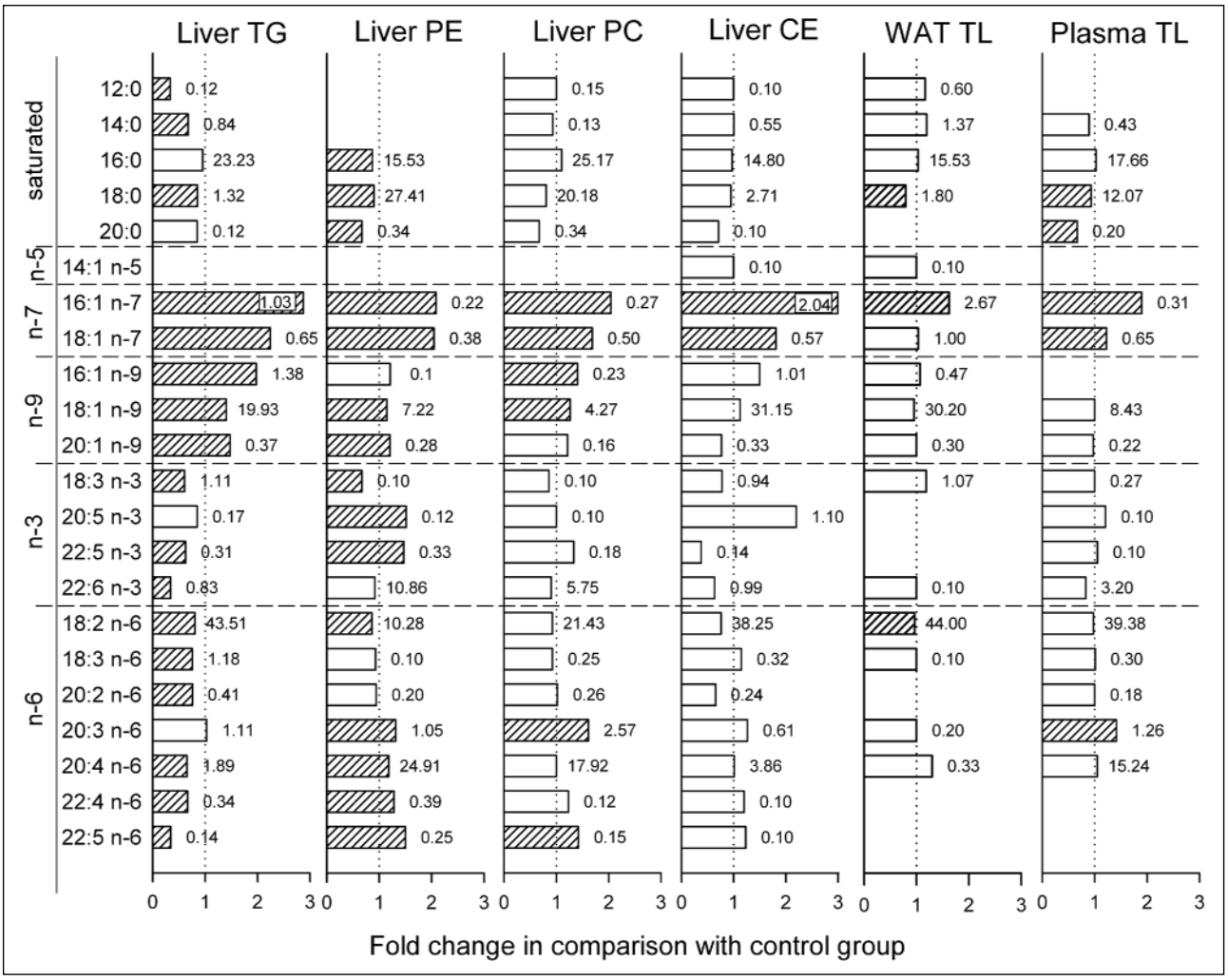

Fig. 2. Effect of rosiglitazone on individual fatty acids in the liver, adipose tissue and plasma lipids. At 3 months of age, mice were randomly assigned to control cHF diet, or cHF diet supplemented with rosiglitazone. After 8 weeks of treatment, fatty acid composition of various liver lipid fractions (Liver TG, PE, PC, and CE; *n*=7), total lipid in adipose tissue (WAT TL; *n*=3) and plasma (Plasma TL; *n*=3, individual samples pooled from 2-3 mice) was analysed in mice killed in ad libitum fed state. Bars represent fold changes of the means in rosiglitazone-treated over control mice. Numbers to the right of each bar indicate mean fatty acid concentrations (mol %) in control mice. Hatched bars, statistically significant effect of rosiglitazone ($p<0.05$, one-way ANOVA). Absence of a bar, any value below the detection limit (0.1 mol %) of the method.

Table 1. Fatty acid composition

Fatty acid (mol %)	Group	Liver TG	Liver PE	Liver PC	Liver CE	WAT TL	Plasma TL
Sum SFA	cHF	25.6 ± 0.4	43.3 ± 0.9	45.8 ± 1.2	18.2 ± 0.6	19.3 ± 0.5	30.4 ± 0.3
	cHF+Rosi	24.0 ± 0.5*	38.5 ± 0.6*	44.3 ± 0.6	17.7 ± 0.7	19.9 ± 0.4	30.0 ± 0.1
Sum MUFA	cHF	23.4 ± 0.8	8.2 ± 0.3	5.4 ± 0.2	35.1 ± 1.1	34.7 ± 0.5	9.6 ± 0.0
	cHF+Rosi	35.7 ± 1.8*	9.9 ± 0.1*	7.3 ± 0.2*	44.0 ± 1.2*	35.1 ± 0.1	10.1 ± 0.1*
Sum n-3 PUFA	cHF	2.4 ± 0.1	11.4 ± 0.7	6.1 ± 0.4	3.2 ± 0.4	1.2 ± 0.2	3.4 ± 0.3
	cHF+Rosi	1.3 ± 0.1*	10.7 ± 0.5	5.6 ± 0.9	3.8 ± 0.5	1.5 ± 0.1	2.8 ± 0.2
Sum n-6 PUFA	cHF	48.6 ± 1.1	37.2 ± 0.5	42.7 ± 1.0	43.5 ± 0.7	44.8 ± 0.2	56.4 ± 0.3
	cHF+Rosi	39.0 ± 1.7*	40.9 ± 0.3*	42.8 ± 0.5	34.5 ± 1.4*	43.5 ± 0.2*	56.8 ± 0.7

After 8 weeks of treatment, fatty acid composition of various liver lipid fractions (Liver TG, PE, PC, and CE; *n*=7), total lipid in adipose tissue (WAT TL; *n*=3) and plasma (Plasma TL; *n*=3, individual samples pooled from 2-3 mice) was analysed in mice killed in *ad libitum* fed state - for details see *Fig. 2*. Fatty acid concentrations (mol %); MUFA, monounsaturated fatty acid; PUFA, polyunsaturated fatty acid; SFA, saturated fatty acid. *Significantly different from cHF ($p<0.05$, *t*-test).

fractions from the liver and in total plasma lipids in response to the rosiglitazone treatment.

Next, principal component analysis was performed to reveal the main factor determining the structure of lipid profiles (*Fig. 3A-C*). The first principal component (y axis) separated mice into two distinct groups, reflecting the rosiglitazone administration and indicating that rosiglitazone induced identifiable changes in global lipid profile (*Fig. 3A*). If only

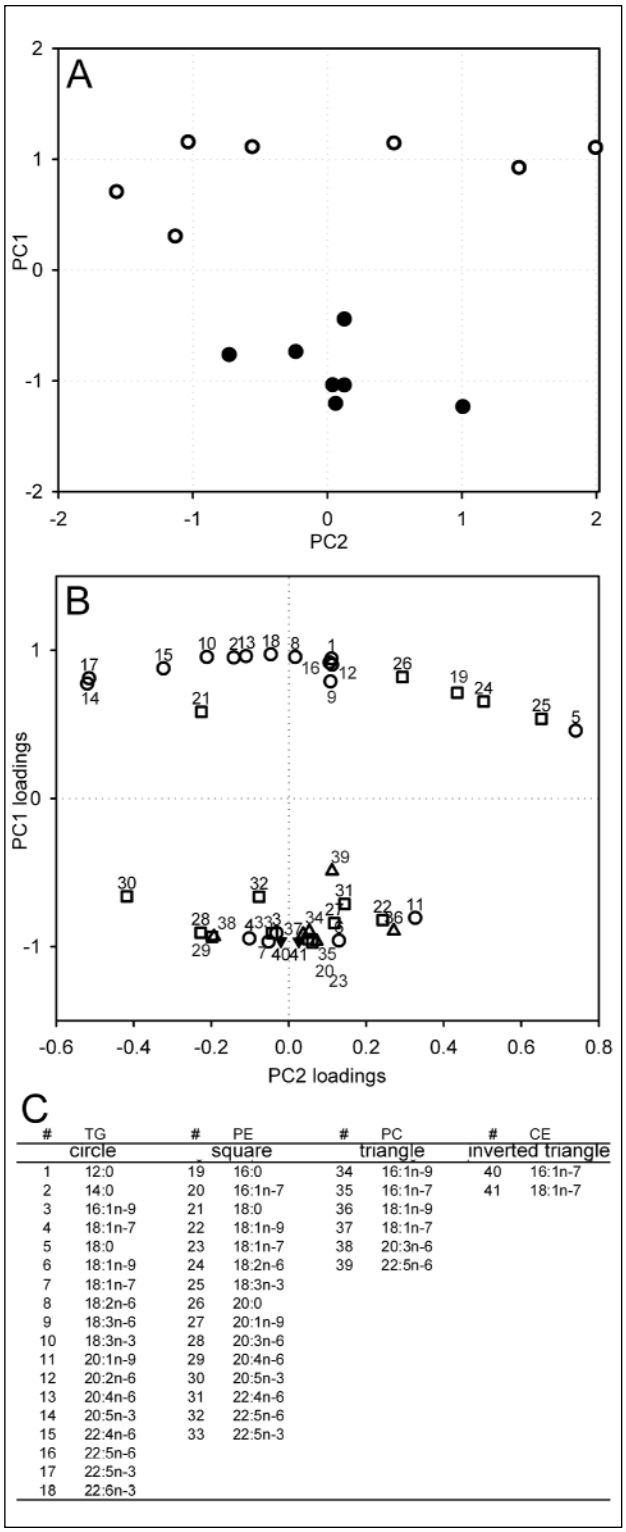

#	TG	#	PE	#	PC	#	CE
	circle		square		triangle		inverted triangle
1	12:0	19	16:0	34	16:1n-9	40	16:1n-7
2	14:0	20	16:1n-7	35	16:1n-7	41	18:1n-7
3	16:1n-9	21	18:0	36	18:1n-9		
4	18:1n-7	22	18:1n-9	37	18:1n-7		
5	18:0	23	18:1n-7	38	20:3n-6		
6	18:1n-9	24	18:2n-6	39	22:5n-6		
7	18:1n-7	25	18:3n-3				
8	18:2n-6	26	20:0				
9	18:3n-6	27	20:1n-9				
10	18:3n-3	28	20:3n-6				
11	20:1n-9	29	20:4n-6				
12	20:2n-6	30	20:5n-3				
13	20:4n-6	31	22:4n-6				
14	20:5n-3	32	22:5n-6				
15	22:4n-6	33	22:5n-3				
16	22:5n-6						
17	22:5n-3						
18	22:6n-3						

Fig. 3. Principle component analysis of liver lipid profile. Fatty acid composition of various lipid fractions from the liver (TG, PE, PC, and CE, see *Fig. 1*) was analysed using principal component analysis. Only fatty acids with p≤0.05 from a one-way ANOVA were included (animals n=7). (**A**) Scatter plot of the first (PC1) and the second (PC2) principal components in mice with (black circles) or without (empty circles) rosiglitazone admixed to cHF diet. (**B**) PC1 and PC2 loading values demonstrating the correlation of individual fatty acids in various fractions (variables symbols numbered from 1-41, see **C** for a detailed description) with the principle component. (**C**) Detailed description of numbered variables shown in **B**.

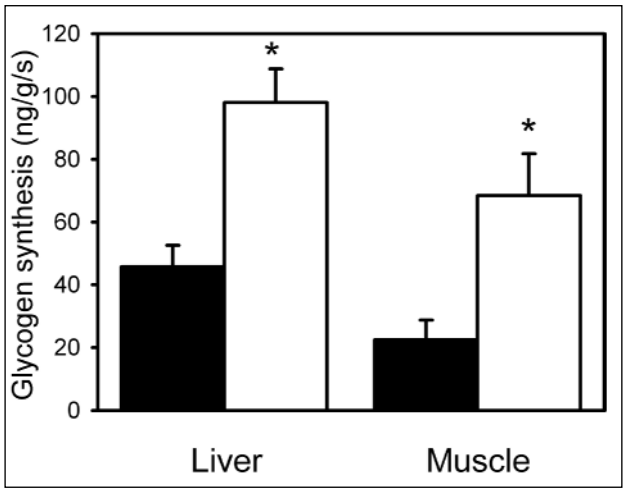

Fig. 4. Glycogen synthesis in the liver and skeletal muscle. At 3 months of age, mice were randomly assigned to various diets, and hyperinsulinaemic-euglycaemic clamps were performed following 8 weeks of dietary treatment (9). Glycogen synthesis in the liver and skeletal muscle (musculus quadriceps femoris) was determined. Black bar, cHF diet; white bar, cHF diet with rosiglitazone (10 mg/kg diet). Data are means±SE (n=5-8). *Significantly different from cHF (t-test).

variables with loading value >0.95 are considered, the first component could be unequivocally interpreted as a shift from polyunsaturated and saturated TG (18:2 *n*-6; 18:3 *n*-3; 20:4 *n*-6; 22:6 *n*-3; 14:0) to monounsaturated TG (18:1 n-7; 18:1 n-9), CE (16:1 n-7; 18:1 n-7), PE (16:1 *n*-7; 18:1 *n*-7) and PC (16:1 *n*-7) due to rosiglitazone (*Fig. 3B*). In addition, PC and CE influence on the first component was specific for the rosiglitazone group. These results are consistent with a strong activation of hepatic SCD1 by rosiglitazone and suggest possible importance of fatty acid composition of various lipid fractions for the effects of rosiglitazone. The second principle component (x axis) showed only a weak separation and its underlying mechanism was not apparent.

Enhancement of palmitoleate content in adipose tissue and plasma due to rosiglitazone

Effect of rosiglitazone on lipid composition in adipose tissue was also evaluated. Except for a ~1.8-fold increase in palmitoleate content in total tissue lipids by rosiglitazone, only negligible changes in the abundance of other fatty acids were observed (*Fig. 2*). Palmitoleate content exhibited also a prominent, ~2.0-fold increase due to rosiglitazone in plasma (*Fig. 2*). However, levels of several other fatty acids have also changed, and the change of fatty acid profile in plasma lipids highly correlated with that in the liver PC and CE fractions (Pearson's r=0.88, and r=0.83, respectively; p<0.001). Weaker correlations were also found for changes of fatty acid profile in plasma lipids and the liver TG and PE fraction (r=0.74 for both, p<0.001). In contrast, no such correlation between fatty acid profiles in plasma and adipose tissue was found (not shown).

Stimulation of hepatic and muscle glycogen synthesis

Under hyperinsulinaemic conditions, glycogen synthesis in the liver and skeletal muscle was significantly enhanced in mice treated with rosiglitazone (*Fig. 4*), in accordance with improved insulin sensitivity in these animals (9). The stimulatory effect of rosiglitazone on tissue insulin sensitivity was more pronounced

in the skeletal muscle compared to the liver (~3.0- and ~2.1-fold increase, respectively).

DISCUSSION

Our results demonstrate that in tissues of mice fed Western-type diet rich in corn oil rosiglitazone stimulates SCD1 activity, in conjunction with improved glycemic control, similar to the effects of TZDs found in humans (4-6). We show for the first time that increased palmitoleate synthesis and complex changes of lipid composition in the liver in response to the rosiglitazone treatment could represent the main mechanism underlying the changes in plasma lipid profile, which could be beneficial for the insulin-sensitizing effect of the treatment.

Thiazolidinediones are likely to improve glycemic control mostly by repartitioning fat away from skeletal muscle, as reviewed by Kuda *et al*. (9). Elevation of hepatic SCD1 by TZDs appears paradoxical given the abundant evidence linking increased lipogenesis in the liver to obesity and insulin resistance. However, in the cHF diet-fed mice treated by a low dose of rosiglitazone, which was sufficient to improve insulin sensitivity, both *Scd1* expression and TG content in the liver increased, while liver VLDL-TG production, plasma non-esterified fatty acids and TG decreased (9). That only *Scd1* but not fatty acid synthase gene was up-regulated (9) suggests a specific role of increased desaturation activity of hepatic SCD1 in the enhancement of insulin sensitivity by rosiglitazone, independent of de novo lipogenesis. Accordingly, SCD1 determines fatty acid composition of VLDL-TG secreted by the liver (3), while liver-derived lipoproteins represent a major source of plasma lipids. Importantly, also experiments in mice deficient for the long-chain fatty acid elongase Elovl6 documented that hepatic fatty composition, and palmitoleate content in particular, are determinants for insulin sensitivity (11). That our observations in mice could be relevant also to humans is supported by the results of a recent study showing a positive correlation between hepatic SCD1 activity and glycemic control in healthy human subjects; interestingly, this correlation was only found in obese but not in lean subjects (12).

Results of our lipidomic analysis in the liver suggest that specific enrichment of CE and phospholipid fractions by monounsaturated fatty acids, as well as a change of lipid profile from polyunsaturated and saturated TG to monounsaturated TG, CE and phospholipids, may be important for the antidiabetic effect of rosiglitazone. Consequently, rosiglitazone-induced changes in plasma lipid composition might affect lipid profiles in the skeletal muscle and contribute to its increased sensitivity to insulin, which was demonstrated by hyperinsulinaemic-euglycaemic clamps before (9). As shown in this study, complex changes of lipid composition in the liver and increased plasma palmitoleate levels in the rosiglitazone-treated mice were associated with enhanced glycogen synthesis under hyperinsulinaemic-euglycaemic conditions *in vivo*, with a stronger effect in the skeletal muscle than in the liver, thus supporting the functional relationship between increased plasma palmitoleate levels and improved muscle insulin sensitivity. This conclusion is further supported by the recent finding, demonstrating an enhancement of muscle insulin action by TG-palmitoleate infusion in mice (2). Furthermore, intramuscular fatty acid composition has been previously shown to shift towards a higher proportion of monounsaturates in obese rosiglitazone-treated rats (13). Besides rosiglitazone, another TZD pioglitazone, which is increasingly used for the treatment of type 2 diabetic patients (14), also upregulated liver *Scd1* and increased plasma palmitoleate levels, while improving glycemic control in our experiments in the cHF diet-fed mice in our experiments similar to the effects of rosiglitazone (not shown). Interestingly, in liver of chow diet-fed mice, pioglitazone treatment resulted in the decrease of total TG content, while the ratio of saturated to unsaturated fatty acids decreased only in the free fatty acid fraction, and it was not changed in other lipid fractions (15). Perhaps, the differences between the results of the above study and our experiments could be explained by different composition of the diets used (see the Introduction). Pioglitazone also decreased ceramide concentration in rat skeletal muscle by reducing its *de novo* synthesis that is dependent on the availability of palmitoyl-CoA, a substrate for SCD1 (16). These results support the notion that the beneficial effect of rosiglitazone on plasma lipid profile could be elicited also by other TZDs, and that this effect contributes to rather than reflects metabolic improvements resulting from the TZD treatment, namely in the muscle. The importance of changes in muscle lipid profile in the insulin-sensitizing effect of TZDs deserves further studies.

We identified the liver as previously uncharacterised tissue with major involvement in the TZD-induced changes of plasma lipid profile in mice fed obesogenic high-fat diet. Provided that hepatic lipid metabolism is similarly affected by TZDs in mice and humans, it is to be inferred that liver has a key role in the modulation of plasma lipid profile in response to TZDs in type 2 diabetic patients and that resulting changes in plasma lipid composition could contribute to improvement of muscle insulin sensitivity. Our results stress the importance of liver as a target in the TZD therapy of human diabetic patients.

Financial support: This work was supported by research project of the Ministry of Education, Youth and Sports (MSM 0021620820) and the grants from the Czech Science Foundation (303/08/0664 and 305/08/H037). Further support included a research project AV0Z50110509 and a grant from EPAX AS (Norway).

Conflict of interests: None declared.

REFERENCES

1. Vessby B, Gustafsson IB, Tengblad S, Boberg M, Andersson A. Desaturation and elongation of fatty acids and insulin action. *Ann N Y Acad Sci* 2002; 967: 183-195.
2. Cao H, Gerhold K, Mayers JR, Wiest MM, Watkins SM, Hotamisligil GS. Identification of a lipokine, a lipid hormone linking adipose tissue to systemic metabolism. *Cell* 2008; 134: 933-944.
3. Paton CM, Ntambi JM. Biochemical and physiological function of stearoyl-CoA desaturase. *Am J Physiol Endocrinol Metab* 2009; 297(1): E28-E37.
4. Riserus U, Tan GD, Fielding BA, Neville, *et al*. Rosiglitazone increases indexes of stearoyl-CoA desaturase activity in humans: link to insulin sensitization and the role of dominant-negative mutation in peroxisome proliferator-activated receptor-gamma. *Diabetes* 2005; 54: 1379-1384.
5. Kolak M, Yki-Jarvinen H, Kannisto K, *et al*. Effects of chronic rosiglitazone therapy on gene expression in human adipose tissue in vivo in patients with type 2 diabetes. *J Clin Endocrinol Metab* 2007; 92: 720-424.
6. Yao-Borengasser A, Rassouli N, Varma V, *et al*. Stearoyl-CoA desaturase 1 (SCD1) gene expression increases following pioglitazone treatment and is associated with PPAR-gamma responsiveness. *J Clin Endocrinol Metab* 2008; 93: 4431-4439.
7. Toyama T, Kudo N, Hibino Y, Mitsumoto A, Nishikawa M, Kawashima Y. Effects of pioglitazone on stearoyl-CoA desaturase in obese Zucker fa/fa rats. *J Pharmacol Sci* 2007; 104: 137-145.

8. Wang Y, Jones VB, Urs S, *et al*. The human fatty acid synthase gene and de novo lipogenesis are coordinately regulated in human adipose tissue. *J Nutr* 2004; 134: 1032-1038.
9. Kuda O, Jelenik T, Jilkova Z, *et al*. n-3 fatty acids and rosiglitazone improve insulin sensitivity through additive stimulatory effects on muscle glycogen synthesis in mice fed high-fat diet. *Diabetologia* 2009; 52: 941-951.
10. Tvrzicka E, Vecka M, Stankova B, Zak A. Analysis of fatty acids in plasma lipoproteins by gas chromatography-flame ionization detection. Quantitative aspects. *Anal Chim Acta* 2002; 465: 337-350.
11. Matsuzaka T, Shimano H, Yahagi N, *et al*. Crucial role of a long-chain fatty acid elongase, Elovl 6, in obesity-induced insulin resistance. *Nat Med* 2007; 13:1193-1202.
12. Stefan N, Peter A, Cegan A, *et al*. Low hepatic stearoyl-CoA desaturase 1 activity is associated with fatty liver and insulin resistance in obese humans. *Diabetologia* 2008; 51: 648-656.
13. Lessard SJ, Lo Giudice SL, Lau W, *et al*. Rosiglitazone enhances glucose tolerance by mechanisms other than reduction of fatty acid accumulation within skeletal muscle. *Endocrinology* 2004; 145: 5665-5670.
14. Miyazaki Y, DeFronzo RA. Rosiglitazone and pioglitazone similarly improve insulin sensitivity and secretion, glucose tolerance and adipocytokines in type 2 diabetic patients. *Diabetes Obes Metab* 2008; 10: 1204-1211.
15. Wierzbicki M, Chabowski A, Zendzian-Piotrowska M, Gorski J. Differential effects of in vivo PPARγ and α activation on fatty acid transport proteins expression and lipid content in rat liver. *J Physiol Pharmacol* 2009; 60: 99-106.
16. Zendzian-Piotrowska M, Baranowski M, Zabielski P, Gorski J. Effects of pioglitazone and high-fat diet on ceramide metabolism in rat skeletal muscles. *J Physiol Pharmacol* 2006; 57: 101-114.

Received: June 2, 2009
Accepted: November 6, 2009

Author's address: Prof. Jan Kopecky, Department of Adipose Tissue Biology, Institute of Physiology of the Academy of Sciences of the Czech Republic, Videnska 1083, 14220 Prague, Czech Republic; Phone: +420 241062554; Fax: +420 241062599; E-mail: kopecky@biomed.cas.cz

Diabetologia (2009) 52:941–951
DOI 10.1007/s00125-009-1305-z

ARTICLE

n-3 Fatty acids and rosiglitazone improve insulin sensitivity through additive stimulatory effects on muscle glycogen synthesis in mice fed a high-fat diet

O. Kuda · T. Jelenik · Z. Jilkova · P. Flachs · M. Rossmeisl · M. Hensler · L. Kazdova · N. Ogston · M. Baranowski · J. Gorski · P. Janovska · V. Kus · J. Polak · V. Mohamed-Ali · R. Burcelin · S. Cinti · M. Bryhn · J. Kopecky

Received: 12 December 2008 / Accepted: 2 February 2009 / Published online: 11 March 2009

Abstract
Aims/hypothesis Fatty acids of marine origin, i.e. docosahexaenoic acid (DHA) and eicosapentaenoic acid (EPA) act as hypolipidaemics, but they do not improve glycaemic control in obese and diabetic patients. Thiazolidinediones like rosiglitazone are specific activators of peroxisome proliferator-activated receptor γ, which improve whole-body insulin sensitivity. We hypothesised that a combined treatment with a DHA and EPA concentrate (DHA/EPA) and rosiglitazone would correct, by complementary additive mechanisms, impairments of lipid and glucose homeostasis in obesity.

Methods Male C57BL/6 mice were fed a corn oil-based high-fat diet. The effects of DHA/EPA (replacing 15% dietary lipids), rosiglitazone (10 mg/kg diet) or a combination of both on body weight, adiposity, metabolic markers and adiponectin in plasma, as well as on liver and muscle gene expression and metabolism were analysed. Euglycaemic–hyperinsulinaemic clamps were used to characterise the changes in insulin sensitivity. The effects of the treatments were also analysed in dietary obese mice with impaired glucose tolerance (IGT).
Results DHA/EPA and rosiglitazone exerted additive effects in prevention of obesity, adipocyte hypertrophy,

O. Kuda and T. Jelenik contributed equally to this work.

Electronic supplementary material The online version of this article (doi:10.1007/s00125-009-1305-z) contains supplementary material, which is available to authorised users.

O. Kuda · T. Jelenik · Z. Jilkova · P. Flachs · M. Rossmeisl · M. Hensler · P. Janovska · V. Kus · J. Kopecky (✉)
Department of Adipose Tissue Biology,
Institute of Physiology of the Academy
of Sciences of the Czech Republic, v.v.i.,
Videnska 1083,
142 20 Prague, Czech Republic
e-mail: kopecky@biomed.cas.cz

L. Kazdova
Institute of Clinical and Experimental Medicine,
Prague, Czech Republic

N. Ogston · V. Mohamed-Ali
Adipokines and Metabolism Research Group,
Centre for Clinical Pharmacology, Department of Medicine,
University College London,
London, UK

M. Baranowski · J. Gorski
Department of Physiology, Medical University of Bialystok,
Bialystok, Poland

J. Polak
Department of Sport Medicine, 3rd Faculty of Medicine,
Charles University,
Prague, Czech Republic

R. Burcelin
INSERM U858 Institute of Molecular Medicine,
IFR31, Rangueil Hospital,
Toulouse, France

S. Cinti
Institute of Normal Human Morphology, University of Ancona,
Ancona, Italy

M. Bryhn
Silentia AS,
Svelvik, Norway

low-grade adipose tissue inflammation, dyslipidaemia and insulin resistance, while inducing adiponectin, suppressing hepatic lipogenesis and decreasing muscle ceramide concentration. The improvement in glucose tolerance reflected a synergistic stimulatory effect of the combined treatment on muscle glycogen synthesis and its sensitivity to insulin. The combination treatment also reversed dietary obesity, dyslipidaemia and IGT.

Conclusions/interpretation DHA/EPA and rosiglitazone can be used as complementary therapies to counteract dyslipidaemia and insulin resistance. The combination treatment may reduce dose requirements and hence the incidence of adverse side effects of thiazolidinedione therapy.

Keywords Adiponectin · Diabetes · Docosahexaenoic acid · Eicosapentaenoic acid · Fish oil · Obesity · PPAR · Rosiglitazone · Thiazolidinedione

Abbreviations

Akt/PKB	Protein kinase B
cHF	Corn oil-based high-fat diet
cHF+F	cHF diet supplemented with eicosapentaenoic and docosahexaenoic acids
cHF+F+TZD	cHF diet supplemented with eicosapentaenoic and docosahexaenoic acids and rosiglitazone
cHF+TZD	cHF diet supplemented with rosiglitazone
DHA	Docosahexaenoic acid
EPA	Eicosapentaenoic acid
HMW	High molecular weight
IGT	Impaired glucose tolerance
n-3 LC-PUFA	*n*-3 Long-chain polyunsaturated fatty acids
PPAR	Peroxisome proliferator-activated receptor
TZD	Thiazolidinedione

Introduction

Both dietary and pharmacological interventions are required for therapy of type 2 diabetic patients. Naturally occurring *n*-3 long-chain polyunsaturated fatty acids (LC-PUFA), namely eicosapentaenoic acid (EPA; 20:5 *n*-3) and docosahexaenoic acid (DHA; 22:6 *n*-3), which are abundant in sea fish, act as hypolipidaemics, reduce cardiac events and decrease progression of atherosclerosis, as reviewed by Ruxton et al. [1]. Therefore, *n*-3 LC-PUFA are now regarded as healthy constituents of diets for diabetic patients [2, 3]. Several studies in obese humans even demonstrated reductions of adiposity after *n*-3 LC-PUFA supplementation [4, 5]. However, *n*-3 LC-PUFA appear to have little effect on glycaemic control in diabetic patients [4, 6, 7]. In rodents fed a high-fat diet, *n*-3 LC-PUFA efficiently prevented development of obesity [8–10] and of impaired glucose tolerance (IGT) [11, 12].

The effects of *n*-3 LC-PUFA are largely mediated by peroxisome proliferator-activated receptors (PPAR), with PPAR-α and PPAR-δ (-β) representing the main targets [13]. However, PPAR-γ, liver X receptor-α, hepatic nuclear factor-4 and sterol regulatory element binding protein-1 are also involved [12, 14, 15]. Besides acting directly as regulatory ligands, *n*-3 LC-PUFA also act through their active metabolites, eicosanoids and other lipid molecules [16]. The hypolipidaemic and anti-obesity effects of *n*-3 LC-PUFA probably depend on the in situ suppression of lipogenesis and increase of fatty acid oxidation in several tissues [10, 14, 17]. This metabolic switch might reduce accumulation of toxic fatty acid-derivatives, while protecting insulin signalling in liver and muscle [11, 12, 18].

On the other hand, PPAR-γ ligands [19] such as thiazolidinediones (TZDs) are the preferred therapeutic agents for insulin resistance in type 2 diabetic patients. However, TZDs like rosiglitazone and pioglitazone are also associated with unwanted side effects, such as oedema and weight gain [20], possible risk of heart failure [21] and bone loss [22]. These compounds are likely to improve glycaemic control mostly by repartitioning fat away from skeletal muscle [23], while augmenting insulin action in various tissues [24–29].

In spite of the differences in the ability of TZDs and *n*-3 LC-PUFA to reverse IGT, both types of compounds reduce adipose tissue inflammation [24, 30], one of the key factors contributing to the development of insulin resistance in obesity, while also increasing adiponectin [12, 15, 24, 25, 31, 32].

We hypothesised that partially overlapping mechanisms of action of *n*-3 LC-PUFA and TZDs, namely the activation of metabolic switch by *n*-3 LC-PUFA and the induction of lipid repartitioning by TZDs, could have synergistic effects in a combination treatment, leading to an improvement of glycaemic profile so far not described for these strategies when considered separately. We therefore evaluated the effects of: (1) partial replacement of dietary lipids by *n*-3 LC-PUFA; (2) a low non obesogenic dose of rosiglitazone; and (3) a combination of both on whole-body parameters of glucose and lipid metabolism in mice fed high-fat diet. To further elucidate the effects of the treatments, a detailed analysis of liver and muscle metabolism was also performed.

Methods

Animals and treatments Male mice were maintained (two animals per cage) at 22°C on a 12 h light–dark cycle (light on from 06:00 hours) and allowed free access to standard laboratory chow (lipid content ~3.4% wt/wt; extruded R/M-H diet; Ssniff Spezialdiäten, Soest, Germany). Two types of studies were used.

First, a 'prevention study' was performed to characterise the effects of *n*-3 LC-PUFA, rosiglitazone and their combination, on developing obesity and IGT in mice fed high-fat diet. At 3 months of age, male C57BL/6N mice (Charles River Laboratories, Sulzfeld, Germany) were randomly assigned to a corn oil-based high-fat diet (cHF; lipid content ~35.2% wt/wt, mainly corn oil) or to the following treatments: (1) cHF diet supplemented with EPA and DHA (cHF+F) as concentrate of *n*-3 LC-PUFA (46% DHA, 14% EPA; 1050TG; EPAX, Lysaker, Norway) replacing 15% of dietary lipids; (2) cHF diet supplemented with rosiglitazone (cHF+TZD) (10 mg/kg diet); and (3) cHF diet supplemented with EPA, DHA and rosiglitazone (cHF+F+TZD) (see Electronic supplementary material [ESM] Tables 1 and 2). Some mice were maintained on the standard chow diet. Various analyses (described below) were performed at 5 to 20 weeks after initiation of treatment. Mice were killed under anaesthesia (09:00–11:00 hours) by cervical dislocation in ad libitum fed state, unless stated otherwise.

Second, in a 'reversal study', obesity and IGT were induced by feeding male C57BL/6J mice (The Jackson Laboratory, Bar Harbor, ME, USA) the cHF diet between 3 and 7 months of age, prior to the subsequent 8-week-long treatment as above; i.e. with cHF, cHF+F, cHF+TZD and cHF+F+TZD, respectively.

During treatments, fresh rations of food were distributed daily. Food consumption and body weights were recorded once a week. Experiments were conducted under the guidelines for the use and care of laboratory animals of the Institute of Physiology and followed the 'Principles of laboratory animal care' (NIH publication no. 85-23, revised 1985).

Metabolites, hormones and enzymes Non-esterified fatty acids, triacylglycerols, total cholesterol and insulin were determined in EDTA-plasma [9]. Blood glucose was measured by calibrated glucometers (LifeScan, Milpitas, CA, USA). Total adiponectin was measured by ELISA [31] (R&D Systems, Abingdon, UK). Distribution of adiponectin multimeric complexes was determined using western blotting [33].

Body composition See ESM for details.

Tissue lipid content Liver and muscle triacylglycerol content was estimated in ethanolic KOH tissue solubilisates [32]. Ceramide content was estimated in lipid extracts from soleus muscle homogenates using HPLC [34].

Quantitative RT-PCR-based gene expression analysis Levels of various transcripts were evaluated in total RNA isolated from liver or gastrocnemius muscle [10]. For primers, see ESM Table 3.

Glycogen synthesis in diaphragm Left and right hemidiaphragms were dissected and separately incubated ex vivo to measure incorporation of glucose into glycogen, as previously described [35] (see ESM).

In vivo hepatic VLDL-triacylglycerol production The rate of liver triacylglycerol synthesis was evaluated using Triton WR1339 [36] and calculated from the slope of the curve of plasma triacylglycerol levels [37] (see ESM).

Light microscopy and immunohistochemical analysis Epididymal fat samples were processed to detect MAC-2/galectin and perilipin, using specific antibodies [32, 38] (see ESM).

Glucose tolerance test Intraperitoneal glucose tolerance test was performed in fasted mice as described [32].

Euglycaemic–hyperinsulinaemic clamp This was performed as described (ESM) [39–41].

Activation of protein kinase B Phosphorylation of protein kinase B (Akt/PKB) was measured in soleus muscles using western blots (ESM Fig. 1).

Statistics Data were analysed by ANOVA and *t* test, as described in ESM. All values are presented as means±SE. Comparisons were judged to be significant at $p \leq 0.05$.

Results

Prevention of body weight gain and lipid accumulation Body weight was increased by cHF diet with significant differences between chow and cHF becoming apparent at 4 weeks (Fig. 1a). Treatment by cHF+F or by cHF+TZD diets tended to prevent body weight gain (Fig. 1a). The combination treatment, cHF+F+TZD, reduced body weight gain significantly (Fig. 1a). The same pattern of body weight gain continued throughout the duration of the study, which lasted for 20 weeks. None of the diets affected mean food consumption over the course of the study (Fig. 1b). Body composition was analysed at 15 weeks (Fig. 1c), i.e. when the effect of cHF+F+TZD diet on

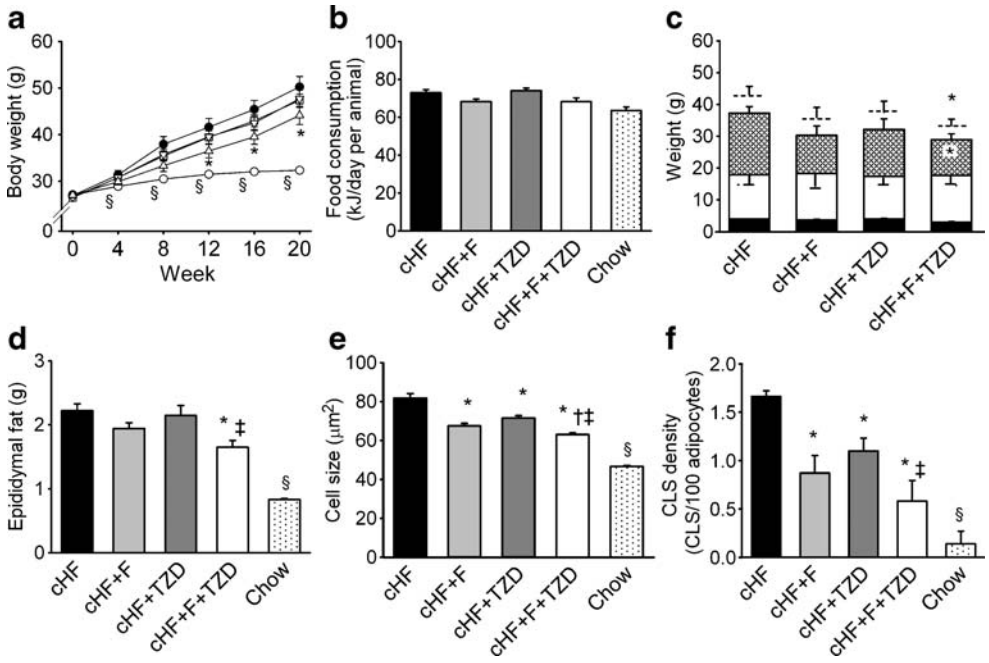

Fig. 1 Body weight (**a**), food consumption (**b**), body composition and size of adipocytes (**c–e**), and macrophage infiltration of adipose tissue (**f**). Three-month-old mice were placed on cHF diet or various cHF-based diets (cHF+F, cHF+TZD and cHF+F+TZD), or maintained on a chow diet; this treatment lasted for up to 20 weeks. **a** Body weights during 20-week treatment by cHF (black circles), cHF+F (white squares), cHF+TZD (white inverted triangles), cHF+F+TZD (white triangles) or chow (white circles) diet (n=16). **b** Mean food consumption during 20 week treatment (n=8). **c** Body composition at 15 weeks. Bar height, weight of eviscerated carcass; black section, protein; white + black sections, lean body mass; cross-hatched section, fat; dashed horizontal lines above bars, body weight of mice before killing. Error bars, SE (n=5–6). **d** Epididymal fat at 8 weeks, weight of fat depot. **e** Size of adipocytes. **f** Relative count of crown-like structures (CLS), formed by MAC-2-positive macrophages surrounding adipocytes. The morphometry data are based on measurements of more than 1,000 cells taken randomly from six different areas per animal. **d–f** Data are means±SE (n=7–8). *$p\leq0.05$ for difference from cHF (ANOVA); $^{\dagger}p\leq0.05$ for difference from cHF+F (ANOVA); $^{\ddagger}p\leq0.05$ for difference from cHF+TZD (ANOVA); $^{\S}p\leq0.05$ for difference from cHF (t test)

body weight became significant (Fig. 1a). Protein and lean body mass were similar in mice fed various cHF diets. On the other hand, total weight of eviscerated carcass and total lipid content reflected changes in body weight. Changes in body weight correlated with the changes in adipose tissue mass, with a significant reduction of the content of subcutaneous (not shown) and epididymal (Fig. 1d) fat in the animals treated for 8 weeks by cHF+F+TZD. Histological analysis combined with immunodetection of macrophages revealed cHF diet-induced hypertrophy of adipocytes in epididymal fat at 8 weeks (Fig. 1e), accompanied by increased content of macrophages aggregated in crown-like structures surrounding individual adipocytes (Fig. 1f), indicating induction of low-grade inflammation of adipose tissue in cHF-mice [38]. The induction of adipocyte hypertrophy and macrophage infiltration was significantly counteracted by cHF+F and cHF+TZD diets, with cHF+F+TZD diet exerting the strongest effect.

Indirect calorimetry at 8 weeks did not reveal any effect of the treatments on whole-body oxygen consumption or respiratory exchange ratio in mice with free access to their respective diets. No differences in physical activity between the groups were detected (not shown).

Given the induction of weight gain by rosiglitazone in previous studies on rodents, the induction of a lean phenotype by the cHF+TZD, and especially by the cHF+F+TZD diets was surprising and is, perhaps, related to higher doses of rosiglitazone used in other studies [24, 27]. Indeed, when rosiglitazone content in the diet was increased tenfold (i.e. from 10 to 100 mg rosiglitazone per kg diet), this increase was associated with higher body weight gain as early as 4 weeks after initiation of the feeding (26.3± 0.8 g vs 28.5±0.5 g; n=8; p=0.04).

Compared with standard chow, the cHF diet induced accumulation of triacylglycerols in liver and gastrocnemius, a mixed-fibre muscle, with a stronger effect observed at 20 than at 8 weeks (Table 1). Compared with cHF, none of the treatments significantly affected the triacylglycerol accumulation, except for cHF+TZD, which increased liver triacylglycerols at 8 weeks. The cHF+F+TZD diet also increased liver triacylglycerol content at 8 weeks, albeit to a smaller extent (Table 1). No differences in the triacylglycerol content between subgroups were observed in soleus,

Table 1 Lipid accumulation in liver and skeletal muscle

Tissue	cHF	cHF+F	cHF+TZD	cHF+F+TZD	Chow
Liver triacylglycerol (mg/g)					
8 weeks	80±15	70±8	197±23[ab]	123±15[b]	34±3[d]
20 weeks	159±16	153±11	171±10	153±15	36±2[d]
Gastrocnemius muscle triacylglycerol (mg/g)					
8 weeks	39±4	41±5	41±6	37±5	18±2[d]
20 weeks	56±3	61±3	50±4	60±4	25±3[d]
Soleus muscle triacylglycerol (mg/g)					
20 weeks	47±5	51±3	48±7	50±2	34±3
Soleus muscle ceramide (pmol/g)					
20 weeks	17.9±0.8	16.0±0.6	17.2±0.5	14.2±0.3[ac]	16.6±0.5

Data are means±SE (n=7–8)

Mice (3 months old) were placed on various diets and killed in ad libitum fed state, after 8 or 20 weeks on the diets.

[a]$p \leq 0.05$ for difference from cHF (ANOVA); [b]$p \leq 0.05$ for difference from cHF+F (ANOVA); [c]$p \leq 0.05$ for difference from cHF+TZD (ANOVA); [d]$p \leq 0.05$ for difference from cHF (t test)

an oxidative muscle, after the prolonged treatment. However, the cHF+F+TZD diet significantly lowered ceramide content in the soleus muscle as compared with cHF-fed mice (Table 1).

Prevention of dyslipidaemia and reduction of hepatic VLDL-triacylglycerol synthesis In ad libitum fed mice, triacylglycerol levels increased while NEFA and cholesterol levels remained unchanged between 8 and 20 weeks of cHF feeding (Table 2). Triacylglycerol and NEFA levels were significantly suppressed by cHF+F+TZD, even below the levels observed in chow diet-fed mice. Cholesterol levels were reduced at 8 but not at 20 weeks. The other treatments (cHF+F and cHF+TZD) induced smaller or no reduction of plasma lipid levels (Table 2).

We also investigated the effect of 8 weeks of treatment on liver VLDL-triacylglycerol synthesis (Fig. 2). Plasma triacylglycerol levels were measured in fasted mice just prior to and for 3 h after injection of Triton WR-1339. Under these conditions, the nonionic detergent blocks lipolytic degradation of triacylglycerol-rich lipoproteins in the peripheral tissues, with the rise in plasma triacylglycerols proportionate to production of VLDL in the liver. All the treatments significantly decreased the rate of VLDL-triacylglycerol synthesis, with the strongest reduction (approximately twofold) by cHF+F+TZD.

Prevention of IGT and insulin resistance Insulinaemia increased between 8 and 20 weeks of high-fat feeding, suggesting development of insulin resistance (Table 2). The rise in insulin levels was prevented to a similar extent by cHF+TZD and cHF+F+TZD diets, while the cHF+F diet exhibited a significant but smaller effect.

Both at 8 and 20 weeks, the cHF+F and cHF+TZD diets increased total immunoreactive adiponectin in plasma. An even stronger induction was observed with a combination of the two treatments (Table 2). Multimeric adiponectin complexes in plasma were also analysed. Although the ratio between high molecular weight (HMW) and total adiponectin was similar in the cHF- and chow-fed mice, it was increased by all the other treatments, with the highest additive effect observed in cHF+F+TZD-fed animals, irrespective of treatment duration (Table 2).

To characterise insulin sensitivity and glycaemic control, a glucose tolerance test was performed at 8 weeks (Fig. 3a). Fasted glycaemia was ~1.4-fold higher in the cHF- as compared with the chow-fed mice and was not significantly affected by any of the treatments (Fig. 3a, b). In contrast, feeding cHF resulted in IGT, as revealed by ~1.4-fold higher AUC values (glucose tolerance test) in the cHF- compared with the chow-fed mice (Fig. 3c). Both cHF+TZD and cHF+F+TZD diets prevented development of IGT, while cHF+F+TZD displayed the largest improvements in glucose tolerance.

At 8 weeks, a euglycaemic–hyperinsulinaemic clamp was also performed to evaluate precisely the changes in whole-body insulin sensitivity brought about by various treatments (Fig. 3d–i). In the hyperinsulinaemic conditions, the amount of exogenous glucose required to maintain euglycaemia, i.e. the glucose infusion rate, was significantly (~1.7-fold) higher in mice treated by cHF+F or cHF+TZD than in cHF-fed mice (Fig. 3e), suggesting improvements in insulin sensitivity. Importantly, cHF+F+TZD resulted in a ~2.4-fold higher glucose infusion rate than that in cHF-fed mice, representing the strongest effect among all the treatments. Hepatic glucose production in the hyperinsulinaemic conditions was decreased in the cHF+F mice to a significantly lower level than in the other subgroups (Fig. 3f), suggesting that DHA/EPA improves hepatic insulin sensitivity. The cHF+F+TZD and cHF+TZD (but not cHF+F) treatments significantly improved whole-body glucose turnover, with cHF+F+TZD showing the most dramatic effect (Fig. 3g). The rate of whole-body glycolysis was not significantly affected by the treatments (Fig. 3h). Whole-body glycogen synthesis was strongly stimulated by cHF+F+TZD, while cHF+F and cHF+TZD diets had no effect (Fig. 3i). No

Table 2 Prevention of dyslipidaemia and hyperinsulinaemia, and induction of adiponectin

Variable	cHF	cHF+F	cHF+TZD	cHF+F+TZD	Chow
8 weeks					
Triacylglycerol (mmol/l)	1.3±0.1	1.1±0.1	1.0±0.1	0.8±0.1[ab]	
NEFA (mmol/l)	0.49±0.05	0.43±0.04	0.38±0.03[a]	0.27±0.02[abc]	
Cholesterol (mmol/l)	3.7±0.2	3.2±0.2[a]	3.8±0.1[b]	3.1±0.1[ab]	
Insulin (pmol/l)	330±60	210±30	270±30	165±45[a]	
Adiponectin (μg/ml)	8.6±0.4	11.0±0.5	10.3±0.2	12.3±0.7[a]	
HMW:total	0.27±0.02	0.30±0.03	0.35±0.02[a]	0.41±0.01[abc]	
20 weeks					
Triacylglycerol (mmol/l)	2.1±0.1	1.8±0.2	1.5±0.1[a]	1.1±0.1[ab]	1.3±0.1[d]
NEFA (mmol/l)	0.50±0.03	0.35±0.07[a]	0.41±0.03	0.29±0.02[ac]	0.49±0.03
Cholesterol (mmol/l)	4.4±0.2	3.7±0.1[a]	3.8±0.2	3.7±0.2	2.1±0.1[d]
Insulin (pmol/l)	1125±165	630±120[a]	360±45[ab]	270±30[ab]	90±15[d]
Adiponectin (μg/ml)	5.3±0.3	8.2±0.6[a]	8.6±0.4[a]	10.1±0.4[abc]	4.4±0.3
HMW:total	0.33±0.03	0.46±0.01[a]	0.49±0.02[a]	0.55±0.02[ab]	0.34±0.02

Mice (3 months old) were placed on various diets, and after 8 or 20 weeks of treatment lipid metabolites and hormones were measured in plasma of mice killed in ad libitum fed state. Data are means±SE (n=8)
[a]$p\leq0.05$ for difference from cHF (ANOVA); [b]$p\leq0.05$ for difference from cHF+F (ANOVA); [c]$p\leq0.05$ for difference from cHF+TZD (ANOVA); [d]$p\leq0.05$ for difference from cHF (t test)
HMW:total; ratio of HMW:total adiponectin

differences in muscle glycogen content between groups were observed (not shown).

Muscle- and liver-specific effects of the treatments To confirm the results on whole-body glycogen synthesis, measurements were also performed ex vivo, in dissected diaphragms from mice subjected to various treatments (Fig. 4). Diaphragm contains glycolytic and oxidative muscle fibres and is suitable for this type of analysis due to its small diffusion barrier for oxygen [42]. Compared with chow, cHF reduced the rate of basal (~2.5-fold) and insulin-stimulated (~2.8-fold) glycogen synthesis. This deleterious effect of cHF feeding was completely prevented by cHF+F+TZD (Fig. 4). Neither cHF+F nor cHF+TZD had any significant effect on basal or insulin-stimulated glycogen synthesis. Improvements in insulin-stimulated glycogen synthesis also correlated with the induction of Akt/PKB phosphorylation at Ser473 in soleus muscle of mice fed cHF+F+TZD (ESM Fig. 1).

Analysis of gene expression from gastrocnemius, a mixed-fibre muscle, revealed a trend (Fig. 5a) for induction by the combination treatment of *Pdk4*, *Cpt1a* and *Cpt1b*, supporting the notion that the combination treatment induced a switch augmenting lipid over glucose catabolism. Interestingly, the cHF+TZD diet strongly induced expression of *Scd1*, while cHF+F and cHF+F+TZD treatments had an opposite effect.

Analysis of hepatic gene expression (Fig. 5b) revealed a downregulation of gluconeogenic genes *Pck2* and *G6pc* by cHF+F+TZD, while cHF+F and cHF+TZD diets exerted less pronounced effects. The cHF+F+TZD diet strongly induced expression of *Acot2*, in correlation with upregulation of *Cpt1b*, suggesting increased turnover of acyl-CoA and fatty acid oxidation in mitochondria. A similar pattern of induction of *Acox1*, a marker of peroxisomal fatty acid oxidation, was observed. Both cHF+TZD and cHF+F+TZD strongly induced expression of *Scd1*, while cHF+F had no effect. In contrast, *Fas* was downregulated by cHF+F and cHF+F+TZD, while cHF+TZD had no effect.

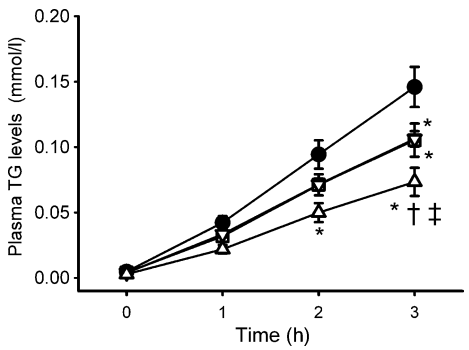

Fig. 2 Hepatic VLDL-triacylglycerol production. At 3 months of age, mice were randomly assigned to various diets. After 8 weeks of treatment, mice were fasted for 6 h, anaesthetised, injected with Triton WR1339 and plasma triacylglycerol (TG) levels were measured before (time 0) and at 1, 2 and 3 h after injection in mice fed cHF (black circles), cHF+F (white squares), cHF+TZD (white inverted triangles) and cHF+F+TZD (white triangles). Data are means±SE (n=5–8). *$p\leq0.05$ for difference from cHF; †$p\leq0.05$ for difference from cHF+F; ‡$p\leq0.05$ for difference from cHF+TZD (repeated measures ANOVA)

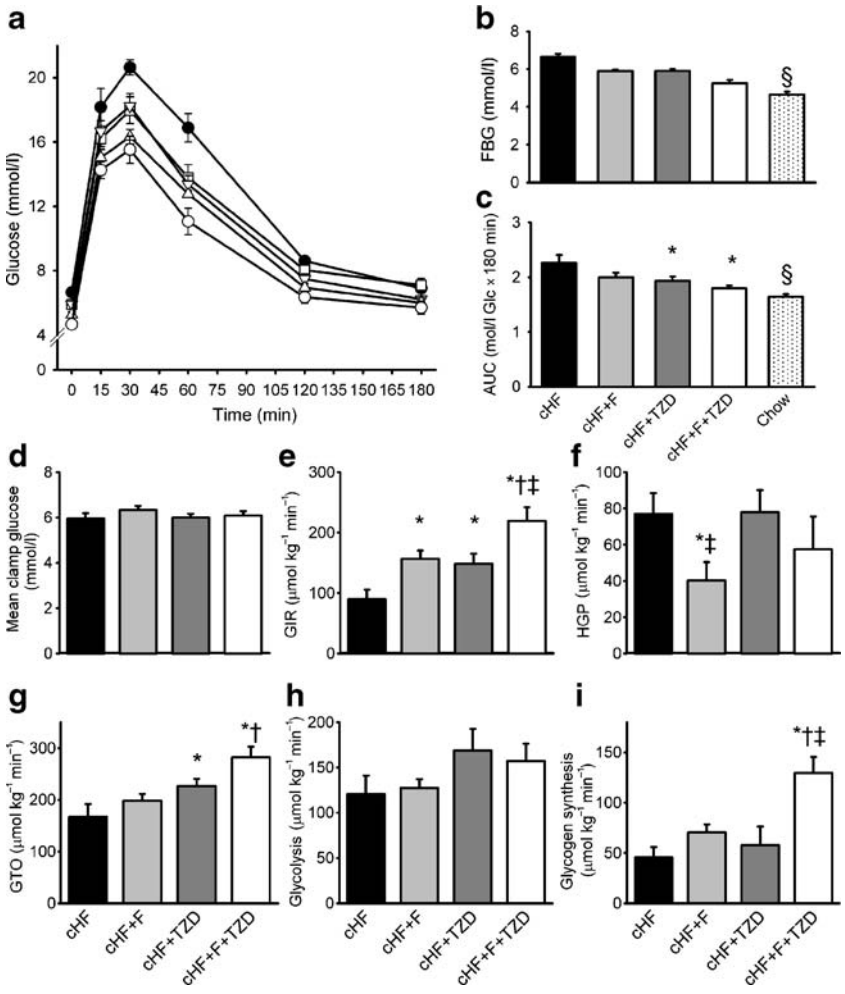

Fig. 3 Glucose homeostasis. At 8 weeks after treatment as described, glucose tolerance test (**a–c**) or euglycaemic–hyperinsulinaemic clamp (**d–i**) were performed in two separate experiments. **a** Plasma glucose levels following intraperitoneal glucose injection (time 0) to fasted mice treated by cHF (black circles), cHF+F (white squares), cHF+TZD (white inverted triangles), cHF+F+TZD (white triangles) or chow (white circles). **b** Fasted blood glucose (FBG) levels at time 0 as above (**a**). **c** Area under the glycaemic curve values as above (**a**). **d** Mean plasma glucose levels during euglycaemic–hyperinsulinaemic clamp. **e–h** Variables, as indicated, that were evaluated during stimulation by insulin. Data are means±SE (n=6–9). *$p\leq0.05$ for difference from cHF; $^{\dagger}p\leq0.05$ for difference from cHF+F; $^{\ddagger}p\leq0.05$ for difference from cHF+TZD (ANOVA); $^{\S}p\leq0.05$ for difference from cHF (t test). GIR, glucose infusion rate; GTO, glucose turnover: HGP, hepatic glucose production

Interestingly, no adverse effects of the combination treatment on enzymatic markers of muscle and liver damage were observed (ESM Table 4).

Reversal of obese phenotype Given both the high efficacy of the cHF+F+TZD treatment in prevention of the high-fat diet-induced disorders in mice and the failure of n-3 LC-PUFA to reverse insulin resistance in humans (see Introduction), the effects of cHF+F and cHF+TZD and their combination were also studied in obese mice with IGT (Table 3). Compared with cHF-fed animals, body weight gain, triacylglycerols and NEFA levels were suppressed by cHF+F, while cHF+TZD decreased plasma triacylglycerols and insulin levels. Only cHF+F+TZD affected all the variables studied, showing additive effects of DHA/EPA and rosiglitazone in the reversal of obesity, while decreasing plasma NEFA and cholesterol levels. The cHF+F+ TZD diet also lowered plasma triacylglycerol and insulin concentrations, to a similar extent to that achieved by cHF+TZD (Table 3).

To evaluate the capacity of treatments to reverse IGT in dietary obese mice, a glucose tolerance test was performed 1 week before the end of the study. Fasting glycaemia was decreased to a similar extent by all treatments (Table 3). However, glucose tolerance measured as AUC was markedly improved by cHF+F+TZD, indicating additive effects of DHA/EPA and rosiglitazone in the reversal of IGT. Both cHF+F and cHF+TZD improved glucose tolerance, but to a smaller extent than cHF+F+TZD (Table 3).

Discussion

Combination of life style changes with pharmacological interventions is required for treatment of diabetes and other metabolic diseases associated with obesity. However, safer, more efficacious and less expensive strategies are still needed. We show here that long-term treatment combining partial replacement of dietary lipids by DHA/EPA and a low dose of rosiglitazone markedly and in an additive manner prevented development of dyslipidaemia and insulin resistance, reduced accumulation of body fat and adipocyte hypertrophy, and also induced adiponectin in mice fed a high-fat diet. Importantly, this treatment also reversed IGT in obese mice.

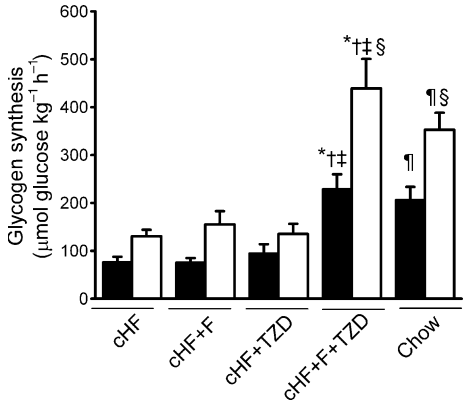

Fig. 4 Glycogen synthesis in diaphragm muscle. At 5 weeks after initiation of treatment as described, left and right hemidiaphragms of mice were dissected and incubated with [U ^{14}C]glucose in the absence (black bars) or presence (white bars) of 250 μU/ml insulin to measure the rate of glycogen synthesis. Data are means±SE (n=7–8). *p≤0.05 for difference from cHF; †p≤0.05 for difference from cHF+F; ‡p≤0.05 for difference from cHF+TZD (ANOVA); §p≤0.05 for difference from non-insulin-stimulated value within the diet (ANOVA); ¶p≤0.05 for difference from cHF (t test)

As described before [9, 10], DHA/EPA reduced fat accumulation, without affecting food consumption. Unexpectedly, a relatively low dose of rosiglitazone (10 mg rosiglitazone per kg diet) was sufficient to augment the induction of lean phenotype by DHA/EPA. In contrast, at a tenfold higher dose, rosiglitazone promoted obesity, as observed in most other studies in mice [24, 27]. In humans, rosiglitazone therapy reduced abdominal and increased subcutaneous fat weight [20]. However, weight of both fat depots in mice was decreased by the combination treatment of DHA/EPA with rosiglitazone, suggesting that treatment by a low dose of rosiglitazone combined with dietary n-3 LC-PUFA intake may also reduce adiposity in humans.

Indirect calorimetry in mice did not reveal any differences in fuel partitioning or energy expenditure between groups. In addition, no difference in physical activity was detected. Therefore, the mechanism for reduced body weight gain in the cHF+F+TZD-treated mice remains unclear. However, even small undetectable changes in the above variables (or in food intake) or their combination, lasting for several weeks, could result in a substantial difference in body weight.

It has been observed previously that treatment by DHA/EPA or rosiglitazone ameliorated adipocyte hypertrophy [9, 43]. In line with these observations, the greatest reduction of adipocyte hypertrophy was observed with the combination of DHA/EPA and rosiglitazone. Compared with large adipocytes, small cells are more insulin-sensitive and less lipolytic, while releasing fewer inflammatory cytokines, as reviewed [20], and more adiponectin [44]. While treatment with DHA/EPA [15, 31] or TZD [15, 25] has previously been shown to induce adiponectin in mice, the current study showed for the first time that the combination of the two increased plasma adiponectin more potently. Importantly, the stimulatory effect of the combination treatment was specific for HMW adiponectin, the form of adiponectin associated with insulin sensitivity [33, 45]. Importantly, the combination treatment also reduced most potently the low-grade adipose tissue inflammation associated with obesity

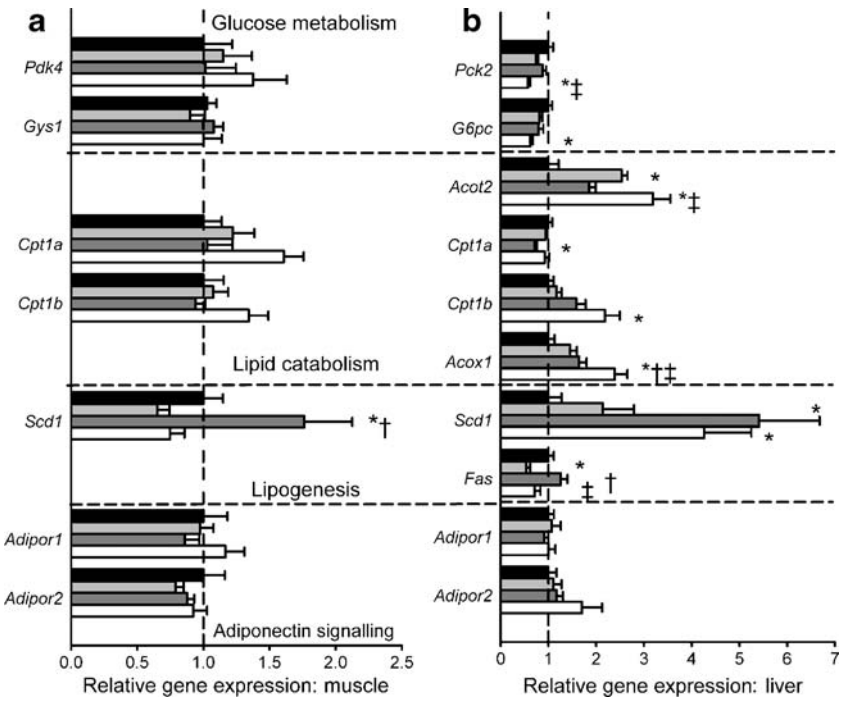

Fig. 5 Quantitative RT-PCR data showing gene expression in mouse gastrocnemius muscle (**a**) and liver (**b**) after 8 weeks of dietary treatments. Black bars, cHF; light grey bars, cHF+F; dark grey bars, cHF+TZD; white bars, cHF+F+TZD. Data are means±SE (n=6–7). *p≤0.05 for difference from cHF (ANOVA); †p≤0.05 for difference from cHF+F (ANOVA); ‡p≤0.05 for difference from cHF+TZD (ANOVA)

Table 3 Reversal of obesity, dyslipidaemia and impaired glucose homeostasis

Variables	cHF	cHF+F	cHF+TZD	cHF+F+TZD
Body weight				
Initial (g)	43.2±2.4	43.3±2.2	45.0±2.0	44.9±1.7
Final (g)	47.3±2.4	43.0±2.2	47.5±1.7	41.8±1.3
Gain (g)	4.1±1.0	−0.3±1.0[a]	2.5±1.1	−3.1±1.8[abc]
Plasma lipids and insulin				
Triacylglycerols (mmol/l)	1.34±0.16	0.90±0.10[a]	0.94±0.03[a]	0.84±0.08[a]
NEFA (mmol/l)	0.46±0.04	0.36±0.03[a]	0.40±0.02	0.27±0.03[abc]
Cholesterol (mmol/l)	5.10±0.36	3.94±0.15	4.02±0.48	3.24±0.34[a]
Insulin (pmol/l)	510±54	356±80	285±74[a]	215±33[a]
Glucose tolerance test				
FBG (mmol/l)	7.49±0.55	5.94±0.22[a]	5.88±0.55[a]	5.22±0.22[a]
AUC (mmol l^{-1} × 180 min)	3,404±201	2,739±136[a]	2,592±161[a]	2,109±124[abc]

Data are means±SE (n=8)

To induce obesity and IGT, mice were fed cHF diet between 3 and 7 months of age, and then treated by different diets for 8 more weeks. Body weight was recorded just before and at the end of the 8-week-treatment. After the treatment, plasma lipids and insulin were measured in ad libitum fed mice. Glucose tolerance test was performed in fasted mice 7 weeks after initiation of treatment

[a]$p \leq 0.05$ for difference from cHF; [b]$p \leq 0.05$ for difference from cHF+F; [c]$p \leq 0.05$ for difference from cHF+TZD (ANOVA)

FBG, fasting blood glucose

[24, 38]. Thus, the additive effects of DHA/EPA and rosiglitazone in the reduction of fat cell hypertrophy, induction of HMW adiponectin and decrease of adipose tissue inflammation might contribute to the beneficial effects on glucose homeostasis.

In a previous study [24], dual pharmacological activation of PPAR-α (by Wy-14,643) and PPAR-γ (by rosiglitazone) in mice improved insulin sensitivity with increased efficacy compared with treatment by either PPAR agonist alone, while increasing both adiponectin and adiponectin receptors in adipose tissue [24]. In our experiments, the treatments did not significantly affect expression of adiponectin receptor genes *Adipor1* and *Adipor2*, either in muscle or in liver, while DHA/EPA and rosiglitazone still improved insulin sensitivity in an additive manner. Importantly, in our experiments, naturally occurring *n*-3 LC-PUFA rather than synthetic PPAR-α agonists were used in the combination with a relatively low dose of rosiglitazone.

Euglycaemic–hyperinsulinaemic clamps in mice and ex vivo measurements in diaphragm muscle showed synergistic induction of glycogen synthesis at the basal and insulin-stimulated conditions by the combination treatment, indicating that skeletal muscle was the major organ responsible for the additive effects of DHA/EPA and rosiglitazone on whole-body glycaemic control. Interestingly, and in accordance with previous studies, neither treatment by DHA/EPA [11, 12, 18], nor rosiglitazone alone (at the relatively low dose used) [23], significantly affected the rate of glycogen synthesis [34]. Increased insulin sensitivity of skeletal muscle is further supported by changes in Akt/PKB phosphorylation. A putative mechanism behind the synergistic effect of the combination treatment is reduction of muscle ceramide concentration. Interestingly, improvements in glucose homeostasis by the treatments became more pronounced with a longer duration of cHF feeding, despite the absence of any effect on triacylglycerol accumulation in the liver and muscle. This observation is not without precedent [12].

In accordance with previous studies, DHA/EPA [11, 12, 18], but not the low dose of rosiglitazone [23], were able to depress hepatic glucose production under hyperinsulinaemic conditions, suggesting improvement of hepatic insulin sensitivity by the former treatment. Given the ability of *n*-3 LC-PUFA to prevent development of IGT, the above data also suggest that the effect on hepatic glucose production mentioned above may be required for this protection to occur. On the other hand, the reversal of IGT and insulin resistance by TZDs may be more dependent on the enhancing of insulin action in skeletal muscle. The latter mechanism could be mediated either by TZDs, or even more potently, according to our results, by the combination of DHA/EPA and TZDs.

The additive improvement of glycaemic control correlated with the hypolipidaemic effect of the treatments. Plasma levels of NEFA and triacylglycerols were even lower in mice treated by cHF+F+TZD than in mice fed chow diet, in spite of the higher dietary supply of lipids and the adipose tissue content of the former mice. These results are in accordance with the known hypolipidaemic effects of *n*-3 LC-PUFA [1] and rosiglitazone [25] in mice. Interest-

ingly, in humans, only pioglitazone but not rosiglitazone exerted a hypolipidaemic effect [19], documenting that the hypolipidaemic effect of TZDs may be dissociated from their effect on insulin sensitivity [25].

The lowering of NEFA levels in mice subjected to various treatments could reflect several mechanisms, including adipose tissue lipolysis, re-esterification of NEFA in liver and adipose tissue, and stimulation of lipid oxidation in liver [14] and other organs [10] by *n*-3 LC-PUFA, as well as by TZDs [26, 27]. The fact that *n*-3 LC-PUFAs are able to counteract the inhibition of hepatic fatty acid oxidation by insulin [46] may contribute to the additive effect of the DHA/EPA and rosiglitazone treatment on lipid catabolism. The suppression of plasma triacylglycerol levels possibly resulted from an increased triacylglycerol uptake by muscle and other tissues induced by TZDs [47] and by *n*-3 LC-PUFA [48], or from decreased hepatic VLDL-triacylglycerol production. The former mechanism was not studied in our experiments; however, we did demonstrate the inhibition of hepatic VLDL-triacylglycerol production by either DHA/EPA or rosiglitazone, with the strongest effect being observed in the combination treatment. The decrease of hepatic triacylglycerol production by DHA/EPA may represent a functional outcome of the coordinated suppression of lipogenic genes by *n*-3 LC-PUFA [17]. In addition, stimulation of AMP-activated protein kinase by *n*-3 LC-PUFA, resulting in a metabolic switch from lipogenesis to lipid catabolism, may also be involved [49].

In contrast, the mechanism of suppression of VLDL-triacylglycerol formation by rosiglitazone must be different, since rosiglitazone increased *Scd1* expression and triacylglycerol content in the liver. The mechanism may reflect an increased rate of fatty acid re-esterification induced by rosiglitazone [50], rather than suppression of de novo lipogenesis in hepatocytes. Our data, in accordance with the effects of the treatments on muscle *Scd1*, document differential modulation of the genes involved in de novo fatty acid synthesis (*Fas*) and desaturation (*Scd1*) by DHA/EPA and rosiglitazone. The induction of *SCD1* expression and activity in association with insulin sensitisation by rosiglitazone has been observed before [29], but the underlying mechanism remains unknown.

In conclusion, an original combined treatment using *n*-3 LC-PUFA with low-dose rosiglitazone generated additive effects in the prevention as well as reversal of adipose tissue hypertrophy, hyperlipidaemia and impaired glycaemic control in mice fed an obesogenic diet. Multiple mechanisms underlined the beneficial whole-body effects of the combination treatment with a prominent synergistic stimulation of insulin-sensitive muscle glycogen synthesis. The combined use of *n*-3 LC-PUFA and TZDs thus represents a potential strategy for treatment of type 2 diabetes and other obesity-associated metabolic disorders. The inclusion of *n*-3 PUFA in treatment with TZDs may reduce the dose requirement and the incidence of adverse side effects associated with the TZD-based therapy.

Acknowledgements This work was supported by the grants from the Czech Science Foundation (303/08/0664) and the Ministry of Education, Youth and Sports (1M6837805002, COST BMB0602-OC08007) of the Czech Republic. Further support included grants from the European Commission (LSHM-CT-2004-005272, EXGENESIS) to J. Kopecky and V. Mohamed-Ali, and from EPAX AS (Norway), as well as research project AV0Z50110509. The authors thank B. Stankova and E. Tvrzicka for the analysis of fatty acid composition of dietary lipids.

Duality of interest The authors declare that there is no duality of interest associated with this manuscript.

References

1. Ruxton CH, Reed SC, Simpson Double Dagger MJ, Millington KJ (2004) The health benefits of omega-3 polyunsaturated fatty acids: a review of the evidence. J Hum Nutr Diet 17:449–459
2. MacLean CH, Konica WA, Morton SC et al (2004) Effects of omega-3 fatty acids on lipids and glycemic control in type II diabetes and the metabolic syndrome and on inflammatory bowel disease, rheumatoid arthritis, renal disease, systemic lupus erythematosus, and osteoporosis. Evid Rep Technol Assess (Summ) 89:1–4
3. Nettleton JA, Katz R (2005) *n*-3 long-chain polyunsaturated fatty acids in type 2 diabetes: a review. J Am Diet Assoc 105:428–440
4. Mori TA, Bao DQ, Burke V, Puddey IB, Watts GF, Beilin LJ (1999) Dietary fish as a major component of a weight-loss diet: effect on serum lipids, glucose, and insulin metabolism in overweight hypertensive subjects. Am J Clin Nutr 70:817–825
5. Couet C, Delarue J, Ritz P, Antoine J-M, Lamisse F (1997) Effect of dietary fish oil on body fat mass and basal fat oxidation in healthy adults. Int J Obes 21:637–643
6. Fasching P, Ratheiser K, Waldhausl W et al (1991) Metabolic effects of fish-oil supplementation in patients with impaired glucose tolerance. Diabetes 40:583–589
7. Pelikanova T, Kohout M, Valek J, Kazdova L, Base J (1993) Metabolic effects of omega-3 fatty acids in type 2 (non-insulin-dependent) diabetic patients. Ann NY Acad Sci 683:272–278
8. Ikemoto S, Takahashi M, Tsunoda N, Maruyama K, Itakura H, Ezaki O (1996) High-fat diet-induced hyperglycemia and obesity in mice: differential effects of dietary oils. Metabolism 45:1539–1546
9. Ruzickova J, Rossmeisl M, Prazak T et al (2004) Omega-3 PUFA of marine origin limit diet-induced obesity in mice by reducing cellularity of adipose tissue. Lipids 39:1177–1185
10. Flachs P, Horakova O, Brauner P et al (2005) Polyunsaturated fatty acids of marine origin upregulate mitochondrial biogenesis and induce beta-oxidation in white fat. Diabetologia 48: 2365–2375
11. Storlien LH, Kraegen EW, Chisholm DJ, Ford GL, Bruce DG, Pascoe WS (1987) Fish oil prevents insulin resistance induced by high-fat feeding in rats. Science 237:885–888
12. Neschen S, Morino K, Dong J et al (2007) *n*-3 fatty acids preserve insulin sensitivity in vivo in a PPAR-alpha-dependent manner. Diabetes 56:1034–1041
13. Sanderson LM, de Groot PJ, Hooiveld GJ et al (2008) Effect of synthetic dietary triglycerides: a novel research paradigm for nutrigenomics. PLoS ONE 3:e1681

14. Jump DB (2004) Fatty acid regulation of gene transcription. Crit Rev Clin Lab Sci 41:41−78
15. Neschen S, Morino K, Rossbacher JC et al (2006) Fish oil regulates adiponectin secretion by a peroxisome proliferator-activated receptor-dependent mechanism in mice. Diabetes 55:924−928
16. Serhan CN (2005) Novel omega-3-derived local mediators in anti-inflammation and resolution. Pharmacol Ther 105:7−21
17. Teran-Garcia M, Adamson AW, Yu G et al (2007) Polyunsaturated fatty acid suppression of fatty acid synthase (FASN): evidence for dietary modulation of NF-Y binding to the Fasn promoter by SREBP-1c. Biochem J 402:591−600
18. Jucker BM, Cline GW, Barucci N, Shulman GI (1999) Differential effects of safflower oil versus fish oil feeding on insulin-stimulated glycogen synthesis, glycolysis, and pyruvate dehydrogenase flux in skeletal muscle: a ^{13}C nuclear magnetic resonance study. Diabetes 48:134−140
19. Goldberg RB, Kendall DM, Deeg MA et al (2005) A comparison of lipid and glycemic effects of pioglitazone and rosiglitazone in patients with type 2 diabetes and dyslipidemia. Diabetes Care 28:1547−1554
20. Yang X, Smith U (2007) Adipose tissue distribution and risk of metabolic disease: does thiazolidinedione-induced adipose tissue redistribution provide a clue to the answer? Diabetologia 50: 1127−1139
21. Nissen SE, Wolski K (2007) Effect of rosiglitazone on the risk of myocardial infarction and death from cardiovascular causes. N Engl J Med 356:2457−2471
22. Lazarenko OP, Rzonca SO, Hogue WR, Swain FL, Suva LJ, Lecka-Czernik B (2007) Rosiglitazone induces decreases in bone mass and strength that are reminiscent of aged bone. Endocrinology 148:2669−2680
23. Kim JK, Fillmore JJ, Gavrilova O et al (2003) Differential effects of rosiglitazone on skeletal muscle and liver insulin resistance in A-ZIP/F-1 fatless mice. Diabetes 52:1311−1318
24. Tsuchida A, Yamauchi T, Takekawa S et al (2005) Peroxisome proliferator-activated receptor (PPAR)alpha activation increases adiponectin receptors and reduces obesity-related inflammation in adipose tissue: comparison of activation of PPARalpha, PPAR-gamma, and their combination. Diabetes 54:3358−3370
25. Kim H, Haluzik M, Gavrilova O et al (2004) Thiazolidinediones improve insulin sensitivity in adipose tissue and reduce the hyperlipidaemia without affecting the hyperglycaemia in a transgenic model of type 2 diabetes. Diabetologia 47:2215−2225
26. Lebrasseur NK, Kelly M, Tsao TS et al (2006) Thiazolidinediones can rapidly activate AMP-activated protein kinase (AMPK) in mammalian tissues. Am J Physiol Endocrinol Metab 291(1):E175−E181
27. Wilson-Fritch L, Nicoloro S, Chouinard M et al (2004) Mitochondrial remodeling in adipose tissue associated with obesity and treatment with rosiglitazone. J Clin Invest 114:1281−1289
28. Hevener AL, Olefsky JM, Reichart D et al (2007) Macrophage PPAR gamma is required for normal skeletal muscle and hepatic insulin sensitivity and full antidiabetic effects of thiazolidinediones. J Clin Invest 117:1658−1669
29. Riserus U, Tan GD, Fielding BA et al (2005) Rosiglitazone increases indexes of stearoyl-CoA desaturase activity in humans: link to insulin sensitization and the role of dominant-negative mutation in peroxisome proliferator-activated receptor-gamma. Diabetes 54:1379−1384
30. Todoric J, Loffler M, Huber J et al (2006) Adipose tissue inflammation induced by high-fat diet in obese diabetic mice is prevented by *n*-3 polyunsaturated fatty acids. Diabetologia 49:2109−2119
31. Flachs P, Mohamed-Ali V, Horakova O et al (2006) Polyunsaturated fatty acids of marine origin induce adiponectin in mice fed high-fat diet. Diabetologia 49:394−397
32. Rossmeisl M, Jelenik T, Jilkova Z et al (2009) Prevention and reversal of obesity and glucose intolerance in mice by DHA-derivatives. Obesity doi:10.1038/oby.2008.602
33. Polak J, Kovacova Z, Jacek M et al (2007) An increase in plasma adiponectin multimeric complexes follows hypocaloric diet-induced weight loss in obese and overweight pre-menopausal women. Clin Sci (Lond) 112:557−565
34. Baranowski M, Zabielski P, Blachnio A, Gorski J (2008) Effect of exercise duration on ceramide metabolism in the rat heart. Acta Physiol (Oxf) 192:519−529
35. Pravenec M, Kazdova L, Landa V et al (2003) Transgenic and recombinant resistin impair skeletal muscle glucose metabolism in the spontaneously hypertensive rat. J Biol Chem 278:45209−45215
36. Rossmeisl M, Kovar J, Syrovy I et al (2005) Triglyceride-lowering effect of respiratory uncoupling in white adipose tissue. Obes Res 13:835−844
37. Haemmerle G, Zimmermann R, Hayn M et al (2002) Hormone-sensitive lipase deficiency in mice causes diglyceride accumulation in adipose tissue, muscle, and testis. J Biol Chem 277:4806−4815
38. Cinti S, Mitchell G, Barbatelli G et al (2005) Adipocyte death defines macrophage localization and function in adipose tissue of obese mice and humans. J Lipid Res 46:2347−2355
39. Burcelin R, Crivelli V, Dacosta A, Roy-Tirelli A, Thorens B (2002) Heterogeneous metabolic adaptation of C57BL/6J mice to high-fat diet. Am J Physiol Endocrinol Metab 282:E834−E842
40. Park SY, Kim HJ, Wang S et al (2005) Hormone-sensitive lipase knockout mice have increased hepatic insulin sensitivity and are protected from short-term diet-induced insulin resistance in skeletal muscle and heart. Am J Physiol Endocrinol Metab 289: E30−E39
41. Rossetti L, Giaccari A (1990) Relative contribution of glycogen synthesis and glycolysis to insulin-mediated glucose uptake. A dose−response euglycemic clamp study in normal and diabetic rats. J Clin Invest 85:1785−1792
42. Bonen A, Clark MG, Henriksen EJ (1994) Experimental approaches in muscle metabolism: hindlimb perfusion and isolated muscle incubations. Am J Physiol 266:E1−E16
43. Okuno A, Tamemoto H, Tobe K et al (1998) Troglitazone increases the number of small adipocytes without the change of white adipose tissue mass in obese Zucker rats. J Clin Invest 101:1354−1361
44. Gahceci M, Gokalp D, Bahceci S, Tuzcu A, Atmaca S, Arikan S (2007) The correlation between adiposity and adiponectin, tumor necrosis factor alpha, interleukin-6 and high sensitivity C-reactive protein levels. Is adipocyte size associated with inflammation in adults? J Endocrinol Invest 30:210−214
45. Pajvani UB, Hawkins M, Combs TP et al (2004) Complex distribution, not absolute amount of adiponectin, correlates with thiazolidinedione-mediated improvement in insulin sensitivity. J Biol Chem 279:12152−12162
46. Baker PW, Gibbons GF (2000) Effect of dietary fish oil on the sensitivity of hepatic lipid metabolism to regulation by insulin. J Lipid Res 41:719−726
47. Laplante M, Festuccia WT, Soucy G et al (2009) Tissue-specific postprandial clearance is the major determinant of PPAR-gamma-induced triglyceride lowering in the rat. Am J Physiol Regul Integr Comp Physiol 296:R57−R66
48. Ton MN, Chang C, Carpentier YA, Deckelbaum RJ (2005) In vivo and in vitro properties of an intravenous lipid emulsion containing only medium chain and fish oil triglycerides. Clin Nutr 24:492−501
49. Suchankova G, Tekle M, Saha AK, Ruderman NB, Clarke SD, Gettys TW (2005) Dietary polyunsaturated fatty acids enhance hepatic AMP-activated protein kinase activity in rats. Biochem Biophys Res Commun 326:851−858
50. Gibbons GF, Wiggins D, Brown AM, Hebbachi AM (2004) Synthesis and function of hepatic very-low-density lipoprotein. Biochem Soc Trans 32:59−64

Prevention and Reversal of Obesity and Glucose Intolerance in Mice by DHA Derivatives

Martin Rossmeisl[1], Tomas Jelenik[1], Zuzana Jilkova[1], Kristyna Slamova[1], Vladimir Kus[1], Michal Hensler[1], Dasa Medrikova[1], Ctibor Povysil[2], Pavel Flachs[1], Vidya Mohamed-Ali[3], Morten Bryhn[4], Kjetil Berge[4], Anne K. Holmeide[4] and Jan Kopecky[1]

The n-3 polyunsaturated fatty acids, especially eicosapentaenoic acid (EPA) and docosahexaenoic acid (DHA), exert hypolipidemic effects and prevent development of obesity and insulin resistance in animals fed high-fat diets. We sought to determine the efficacy of α-substituted DHA derivatives as lipid-lowering, antiobesity, and antidiabetic agents. C57BL/6 mice were given a corn oil–based high-fat (35% weight/weight) diet (cHF), or cHF with 1.5% of lipids replaced with α-methyl DHA ethyl ester (Substance 1), α-ethyl DHA ethyl ester (Substance 2), α,α-di-methyl DHA ethyl ester (Substance 3), or α-thioethyl DHA ethyl ester (Substance 4) for 4 months. Plasma markers of glucose and lipid metabolism, glucose tolerance, morphology, tissue lipid content, and gene regulation were characterized. The cHF induced obesity, hyperlipidemia, impairment of glucose homeostasis, and adipose tissue inflammation. Except for Substance 3, all other substances prevented weight gain and Substance 2 exerted the strongest effect (63% of cHF-controls). Glucose intolerance was significantly prevented (~67% of cHF) by both Substance 1 and Substance 2. Moreover, Substance 2 lowered fasting glycemia, plasma insulin, triacylglycerols, and nonesterified fatty acids (73, 9, 47, and 81% of cHF-controls, respectively). Substance 2 reduced accumulation of lipids in liver and skeletal muscle, as well as adipose tissue inflammation associated with obesity. Substance 2 also induced weight loss in dietary obese mice. In contrast to DHA administered either alone or as a component of the EPA/DHA concentrate (replacing 15% of dietary lipids), Substance 2 also reversed established glucose intolerance in obese mice. Thus, Substance 2 represents a novel compound with a promising potential in the treatment of obesity and associated metabolic disturbances.

Obesity (2009) **17,** 1023–1031. doi:10.1038/oby.2008.602

INTRODUCTION

Obesity, and especially abdominal obesity, is a risk factor for insulin resistance (IR), type 2 diabetes, and cardiovascular disease. "Dysfunctional" adipose tissue, which cannot properly handle the energy surplus resulting from a sedentary lifestyle combined with excessive calorie consumption, plays a central role in obesity-associated IR and type 2 diabetes (1). In general, IR develops as a consequence of exposure of insulin-responsive tissues to elevated dietary nutrients, resulting in the accumulation of lipid-derived metabolites and impairment of inter-organ communication networks that are mediated by peptide hormones and inflammatory molecules (2). Lifestyle modification therapies, such as reduced caloric intake and increased physical activity, for the obesity-associated IR and metabolic abnormalities have proved to be difficult for the general population. However, current pharmacological interventions often require the use of multiple agents and are also associated with adverse side effects, as documented in the case of the thiazolidinediones (3). Therefore, new treatment strategies are sought.

At the same time, the quality of dietary lipids is important. The n-3 long-chain polyunsaturated fatty acids (n-3 LC-PUFA), namely, eicosapentaenoic acid (EPA; 20:5n-3) and docosahexaenoic acid (DHA; 22:6n-3), which are abundant in marine fish oils, act as potent hypolipidemics in both rodents (4–6) and humans (7). The n-3 LC-PUFA also prevented development of obesity and IR in rodents fed high-fat diets (8). However, their beneficial effect on body weight and IR in overweight patients was only apparent when n-3 LC-PUFA were combined with

[1]Department of Adipose Tissue Biology and Center for Applied Genomics, Institute of Physiology, Academy of Sciences of the Czech Republic, Prague, Czech Republic; [2]Institute of Pathology, 1st Medical Faculty, Charles University, Prague, Czech Republic; [3]Adipokines and Metabolism Research Group, Centre for Clinical Pharmacology, Department of Medicine, University College London, London, UK; [4]Pronova BioPharma AS, Lysaker, Norway. Correspondence: Jan Kopecky (kopecky@biomed.cas.cz)

Received 6 June 2008; accepted 3 October 2008; published online 15 January 2009. doi:10.1038/oby.2008.602

a weight-loss regimen (9). In general, the insulin-sensitizing effects of n-3 LC-PUFA in subjects with impaired glucose tolerance (IGT) are minimal (10).

The hypolipidemic and antiobesity actions of n-3 LC-PUFA depend on a suppression of lipogenesis combined with increased fatty acid oxidation in the liver (4,11). However, enhanced mitochondrial biogenesis and β-oxidation in white adipose tissue (WAT) may also contribute (12). Moreover, n-3 LC-PUFA reduce WAT inflammation associated with obesity (13), while stimulating secretion of the insulin-sensitizing hormone adiponectin (6,14). The effects of n-3 LC-PUFA are largely mediated by peroxisome proliferator–activated receptors (PPARs), with PPAR-α and PPAR-δ (-β) representing the main targets for n-3 LC-PUFA (15,16); however, other factors, such as liver X receptor, hepatocyte nuclear factor-4α, and sterol-regulatory element binding protein, are also involved (for review see refs. 17,18). Decreased binding of both sterol-regulatory element binding protein–1c and nuclear factor-Y to promoters of lipogenic genes (19), as well as activation of AMP-activated protein kinase (20), may be of great importance for the liver effects. In addition to being ligands themselves, n-3 LC-PUFA might also act indirectly through their metabolites, eicosanoids, and other lipid molecules (21).

Concerning new pharmacotherapies for obesity-associated IR and type 2 diabetes, mixed agonists of various PPARs (22) or higher-affinity analogues of currently available agonists are being developed. Based on a relatively low efficiency of EPA/DHA in the treatment of IR in humans, the aim of this study was to explore several chemical DHA derivatives, substituted at the C(2)-position, as potential antiobesity and antidiabetic agents. In a mouse model of high-fat feeding, the efficiency of DHA derivatives in the prevention and reversal of obesity, IGT, dyslipidemia, WAT inflammation, and lipid accumulation in nonadipose tissues was analyzed.

METHODS AND PROCEDURES

Animals and experimental design

Male mice of either C57BL/6N genetic background (Charles River, Sulzfeld, Germany) or C57BL/6J background were maintained on a 12:12-h light–dark cycle at 22 °C (2–4 animals/cage). Mice were allowed an unrestricted access to water and a standard chow (STD; extruded Ssniff R/M-H diet; Ssniff Spezialdieten GmbH, Soest, Germany). At 3 months of age, mice were randomly assigned to a composite high-fat diet (cHF; lipids ~35% wt/wt, mostly corn oil), while some mice were maintained on STD diet. Energy content of STD and cHF diet was 13.0 and 22.8 kJ/g, respectively (see http://www.ssniff.com, and (5)). STD diet served as a control for the obesogenic effect of the HF diet. Two experimental approaches were used (see also **Figure 1**):

1. In the "prevention study," various DHA derivatives (Substance 1–4; see below) were admixed to the cHF diet (1.5% of dietary lipids replaced by a DHA derivative) and administered to the 3-month-old C57BL/6N mice for a period of 4 months. The DHA derivatives were tested in three separate experiments A, B, and C (Experiment A: Substance 1; Experiment B: Substance 2 and 3; Experiment C: Substance 4).
2. In the "reversal study," obesity and IGT were induced in C57BL/6J mice by feeding cHF diet for a period of 4 months prior to the subsequent 2-month-long administration of Substance 2 admixed to the cHF diet (1.5% of dietary lipids). To analyze potential contribution of a lower food intake in the beneficial effect of Substance 2 on glucose homeostasis (as observed in the "prevention study"), food intake in a subgroup of cHF-fed mice was reduced by 12% compared with mice fed cHF diet *ad libitum* during the final 2 months of the "reversal study." A separate experiment was also performed to evaluate the effect of EPAX1050 TG (Pronova BioPharma AS, Lysaker, Norway), a triglyceride concentrate of EPA (~15%) and DHA (~45%; EPA/DHA), as well as of pure DHA (~99%; ethyl ester; Pronova BioPharma AS) in *ad libitum*–fed mice; compared with all the experiments with DHA derivatives, a tenfold higher fraction of dietary lipids (i.e., 15% of lipids) was replaced by either EPA/DHA or DHA alone (see also our previous studies (5,6) and **Figure 1**).

The cHF-fed mice always served as controls. Body weight and food intake were monitored weekly, while a fresh ration was offered daily. Mice were killed by cervical dislocation under diethylether anesthesia between 9–11 AM, subcutaneous dorsolumbar and epididymal WAT, interscapular brown adipose tissue, liver, and skeletal muscle (*musculus quadriceps femoris*) were dissected and snap-freezed in liquid nitrogen. Truncal blood was collected into the EDTA-containing tubes and plasma was isolated by centrifugation at 5,000*g* for 10 min at 4 °C. Tissues and plasma were stored at −70 °C for future analyses. The experiments were conducted under the guidelines for the use and care of laboratory animals of the Institute of Physiology.

Chemical α-substituted DHA derivatives

DHA derivatives (for chemical structures, see **Supplementary Figure S1** online) were provided by Pronova BioPharma AS, including α-methyl DHA ethyl ester (Substance 1), α-ethyl DHA ethyl ester (Substance 2), α,α-di-methyl DHA ethyl ester (Substance 3), and α-thioethyl DHA ethyl ester (Substance 4).

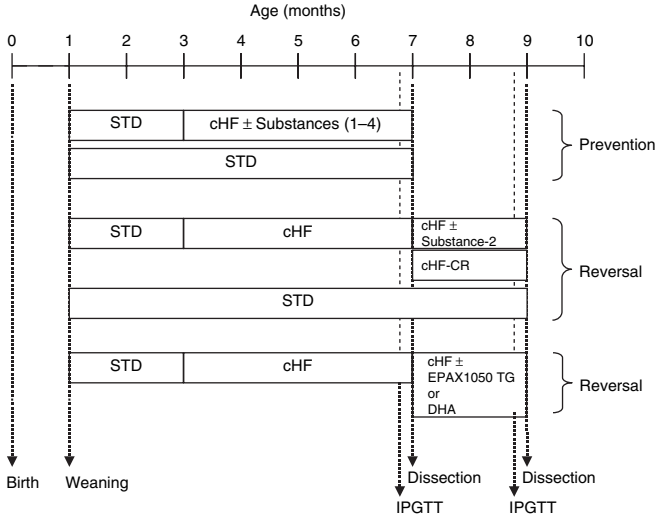

Figure 1 Timeline of experiments. In the "prevention study," 3-month-old mice were switched from a low-fat chow (STD) diet to either composite high-fat (cHF) diet, or cHF diets containing 1.5% of their lipids as DHA derivatives (Substance 1–4). In the "reversal study," 3-month-old mice were fed a cHF diet for a period of 4 months, followed by the treatment with Substance 2 for additional 2 months. A group of mice were also subjected to a 12% caloric restriction diet (cHF-CR; relative to food intake in the cHF group). In the "reversal study," an intraperitoneal glucose tolerance test (IPGTT) was performed 1 week before the end as well as 1 week before the initiation of dietary treatments. In a separate "reversal study" experiment, the effect of EPA/DHA concentrate (EPAX1050 TG) and DHA on *ad libitum*–fed mice was also studied using cHF diets containing 15% of their lipids as the tested compounds (using cHF-fed mice as controls).

Preparation of DHA derivatives

The NMR spectra were recorded in $CDCl_3$, with a Bruker Avance DPX 200 instrument. Mass spectra were recorded with a LC/MS Agilent 1100 series, with a G 1956 A mass spectrometer (electrospray, 3000 V). (University of Oslo, Norway). All reactions were performed under nitrogen or argon atmosphere.

Ethyl (all-Z)-2-methyl-4,7,10,13,16,19-docosahexaenoate (Substance 1)

In this phase, *n*-Butyllithium (1.6 mol/l in hexane, 228 ml, 370 mmol) was added dropwise to a stirred solution of diisopropylamine (60 ml, 420 mmol) in dry tetrahydrofuran (THF; 800 ml) at 0 °C under N_2. The resulting solution was stirred at 0 °C for 30 min, cooled to −78 °C and stirred an additional 30 min before dropwise addition of ethyl (all-Z)-4,7,10,13,16,19-docosahexaenoate (100 g, 280 mmol) in dry THF (500 ml) during 2 h. The resulting solution was stirred at −78 °C for 30 min before methyl iodide (28 ml, 450 mmol) was added. The solution was allowed to reach −20 °C during 1.5 h and then poured into water (1.5 l). The resulting mixture was extracted with heptane (2 × 800 ml). The combined organic extracts were washed with 1 mol/l HCl (1 l), dried (Na_2SO_4) and evaporated *in vacuo*. The residue was purified by flash chromatography (SiO_2, heptane/ethyl acetate 99:1). Yield: 50 g (48%) as a slightly yellow oil. ^{1}H-NMR (200 MHz, $CDCl_3$): δ 1.02 (t, J = 7.5 Hz, 3H), 1.20 (d, J = 6.8 Hz, 3H), 1.29 (t, J = 7.1 Hz, 3H), 2.0–2.6 (m, 5H), 2.8–3.0 (m, 10H), 4.17 (t, J = 7.1 Hz, 2H), 5.3–5.5 (m, 12H), MS (ESI): 393 $[M+Na^+]^+$.

Ethyl (all-Z)-2-ethyl-4,7,10,13,16,19-docosahexaenoat (Substance 2)

n-Butyllithium (1.6 mol/l in hexane, 440 ml, 670 mmol) was added dropwise to a stirred solution of diisopropylamine (111 ml, 780 mmol) in dry THF (750 ml) at 0 °C under N_2. The resulting solution was cooled to −78 °C and stirred an additional 45 min before dropwise addition of ethyl (all-Z)-4,7,10,13,16,19-docosahexaenoate (200 g, 560 mmol) in dry THF (1.6 l) during 4 h. The resulting solution was stirred at −78 °C for 30 min before ethyl iodode (65 ml, 810 mmol) was added. The solution was allowed to reach −40 °C before an additional amount of ethyl iodide (5 ml, 60 mmol) was added, and finally reach −15 °C (during 3 h from −78 °C) before the mixture was poured into water. The resulting mixture was extracted with hexane (2×). The combined organic extracts were washed with 1 mol/l HCl and water, dried (Na_2SO_4) and evaporated *in vacuo*. The residue was purified by flash chromatography (SiO_2, heptane/ethyl acetate 99:1–50:1). Yield: 42 g (20%) as a yellow oil. ^{1}H-NMR (200 MHz; $CDCl_3$): δ 0.8–1.0 (m, 6H), 1.2–1.4 (m, 4H), 1.5–1.7 (m, 2H), 2.12 (m, 2H), 2.3–2.5 (m, 2H), 2.8–3.0 (m, 10H), 4.18 (t, J = 7.1 Hz, 2H), 5.3–5.6 (m, 12H), MS (ESI): 407 $[M+Na^+]^+$.

Ethyl (all-Z)-2,2-dimethyl-4,7,10,13,16,19-docosahexaenoate (Substance 3)

n-Butyllithium (1.6 mol/l in hexane, 100 ml, 170 mmol) was added dropwise to a stirred solution of diisopropylamine (28 ml, 200 mmol) in dry THF (100 ml) at 0 °C under N_2. The resulting solution was stirred at 0 °C for 30 min, cooled to −78 °C before dropwise addition of (50 g, 140 mmol) in dry THF (200 ml). The resulting solution was stirred at −78 °C for 30 min before methyl iodide (17 ml, 280 mmol) was added. The solution was allowed to reach −10 °C and then poured into water. The resulting mixture was extracted with hexane (2×). The combined organic extracts were washed with 1 mol/l HCl, dried (Na_2SO_4) and evaporated *in vacuo*. This procedure was repeated, but the crude product was used instead of ethyl (all-Z)-4,7,10,13,16,19-docosahexaenoate. The residue was purified by flash chromatography (SiO_2, heptane/ethyl acetate 99:1–98:2). Yield: 32 g (59%) as a slightly yellow oil.^{1}H-NMR (200 MHz; $CDCl_3$): δ 1.01 (t, J = 7.5 Hz, 3H), 1.21 (s, 6H), 1.28 (t, J = 7.1 Hz, 3H), 2.08 (m, 2H), 2.34 (d, J = 6.8 Hz, 2H), 2.8–3.0 (m, 10H), 4.15 (q, J = 7.5 Hz, 2H), 5.3–5.6 (m, 12H) ^{13}C-NMR (50 MHz; $CDCl_3$): δ 14.7, 21.0, 25.3, 26.0, 26.1, 38.3, 42.8, 60.7, 125.8, 127.4, 128.3, 128.5, 128.6, 128.7, 129.0, 130.7, 132.4, 177.9, MS (ESI): 385 $[M+H^+]^+$.

Ethyl (all-Z)-2-thioethyl-4,7,10,13,16,19-docosahexaenoate (Substance 4)

Step 1: Synthesis of ethyl (all-Z)-2-iodo-4,7,10,13,16,19-docosahexaenoate. *n*-Butyllithium (1.6 mol/l in hexane, 158 ml, 253 mmol,) was added dropwise to a stirred solution of diisopropylamine (42 ml, 298 mmol) in dry THF (150 ml) at 0 °C under N_2. The resulting solution was cooled to −78 °C and stirred for 35 min before dropwise addition of ethyl (all-Z)-4,7,10,13,16,19-docosahexaenoate (75 g, 210 mmol) in dry THF (300 ml). The resulting solution was stirred at −78 °C for 30 min before iodine (91 g, 359 mmol) in THF (200 ml) was added dropwise. The solution was stirred at −78 °C for 20 min, then poured into water (200 ml). The resulting mixture was extracted with heptane (300 ml). The organic extract was washed with 1 mol/l HCl (150 ml) and water (200 ml), dried (Na_2SO_4) and evaporated *in vacuo*. The residue was purified by flash chromatography (SiO_2, heptane/ethyl acetate 100:1). Yield: 26 g (26%) as a yellow oil. ^{1}H-NMR (200 MHz, $CDCl_3$): δ 0.94 (t, J = 7.5 Hz, 3H), 1.24 (t, J = 7.1 Hz, 3H), 2.04 (quint, J = 7.1 Hz, 2H), 2.69–2.84 (m, 12 H), 4.17 (q, J = 7.1 Hz, 2H), 4.22 (t, J = 7.9 Hz, 1H), 5.24–5.49 (m, 12 H), ^{13}C NMR (50 MHz, $CDCl_3$): δ 13.7, 14.2, 25.5, 26.0 (2 signals), 25.8, 34.0, 61.7, 126.1, 127.0, 127.4, 127.8, 127.9, 128.0, 128.2, 128.5, 128.5, 131.6, 131.9, 170.9 (4 signals hidden), MS (ESI): 505 $[M+Na^+]^+$.

Step 2: Synthesis of ethyl (all-Z)-2-thioethyl-4,7,10,13,16,19-docosahexaenoate. Sodium ethyl thiolate (2.1 g, 25 mmol) was added to a solution of ethyl (all-Z)-2-iodo-4,7,10,13,16,19-docosahexaenoate (11.0 g, 23 mmol) in THF (100 ml) at 0 °C under N_2. The resulting mixture was stirred at 0 °C for 1 h. 1 mol/l HCl was added followed by heptane. The phases were separated and the organic phase was washed with water (2×), dried (Na_2SO_4) and evaporated *in vacuo*. The residue was purified by flash chromatography (SiO_2, heptane/ethyl acetate 30:1. Yield: 7.3 g (76 %) as a pale yellow oil. ^{1}H-NMR (200 MHz, $CDCl_3$): δ 1.1–1.3 (m, 9H), 2.05 (m, 2H), 2.3–2.7 (m, 4H), 2.7–2.9 (m, 10H), 3.25 (m, 1H), 4.17 (q, J = 7.1 Hz, 2H), 5.3–5.5 (m, 12H), MS (ESI): 439 $[M+Na^+]^+$.

Plasma metabolites, hormones, and enzymes

Blood glucose was measured using calibrated glucometers OneTouch Ultra (Life Scan, Milpitas, CA). Plasma triglycerides, cholesterol, aspartate aminotransferase, alanine aminotransferase, and creatine kinase were measured using a clinical analyzer and enzymatic kits from Roche Diagnostics (Mannheim, Germany). Nonesterified fatty acids (NEFA) were measured by a kit from Waco Chemicals (Neuss, Germany). Plasma insulin levels were determined by the Sensitive Rat Insulin RIA Kit (LINCO Research, St Charles, MO), and total immunoreactive adiponectin and leptin were measured by a 2-site ELISA (R&D Systems, Minneapolis, MN; (6)).

Glucose tolerance test

An intraperitoneal glucose tolerance test was performed after an overnight fasting (15–16 h). Blood glucose was assessed by tail bleeds at the baseline (fasting blood glucose; FBG) and after the injection of D-glucose (1 g/kg body weight). In the "reversal study," intraperitoneal glucose tolerance test was performed 1 week before the start (baseline) and 1 week before the end (final) of the 2-month-long treatment period. Results were expressed either as area under the curve (AUC) for glucose or as a change in blood glucose levels (ΔBlood glucose; final–baseline), derived from the glycemic curves of intraperitoneal glucose tolerance test measured before and after the treatment. In the latter case, the greater was the beneficial effect on glucose tolerance after the treatment, the greater was the negative deviation of a glycemic curve from the baseline.

RNA extraction and real-time quantitative PCR analysis

Total RNA was isolated from samples of WAT, liver, and skeletal muscle stored in RNA*later* Solution (Ambion, Austin, TX) by using TRIzol Reagent (Invitrogen, Carlsbad, CA). Muscle samples were grinded

under liquid nitrogen prior to homogenization. A quantity of 0.5 µg of total RNA was reverse transcribed to cDNA, and gene expression was analyzed by real-time PCR, using the LightCycler Instrument (Roche Diagnostics, Mannheim, Germany) as before (6). Oligonucleotide primers, described in **Supplementary Table S1** online, were designed using Lasergene software (DNAStar, Madison, WI). Gene expression data were expressed as a percentage of the cHF-fed controls.

Tissue triglycerides

Tissue fragments (~50 mg) were digested in 0.15 ml of 3 mol/l alcoholic KOH and the resulting homogenates were diluted tenfold with H_2O. After neutralization by 2.5 N $HClO_4$, deliberated glycerol was assayed in supernatants (4 µl) by Free Glycerol Reagent (Sigma-Aldrich, Prague, Czech Republic). Tissue triglyceride concentration was calculated relative to a glycerol standard (1 mg/ml; Sigma-Aldrich, Prague, Czech Republic) using a ratio of 1:10 for molecular weights of glycerol:triglyceride.

Light microscopy and immunohistochemical analysis

Samples of epididymal WAT and liver were fixed in 4% formaldehyde, embedded in paraffin and cut into 5 µm-sections. The liver sections were stained by hematoxylin-eosine, while the sections of epididymal fat were processed to detect a macrophage marker, MAC-2/galectin-3, by the use of specific antibodies (23). Digital images were captured using Olympus AX70 light microscope and a DP 70 camera (Olympus, Tokyo, Japan). Adipocyte morphometry was performed using a Lucia IMAGE version 4.81 (Laboratory Imaging, Prague, Czech Republic).

Statistical analysis

Data are presented as means ± s.e. Data were analyzed by a one-way ANOVA or two-way Repeated Measures ANOVA (only the analysis of glucose tolerance in the "reversal study") using SigmaStat statistical software. Logarithmic transformation was used to stabilize variance in cells when necessary. The Holm–Sidak test for multiple comparisons was used. Threshold of significance was defined at $P < 0.05$.

RESULTS

Reduction of body weight and adiposity by DHA derivatives

The effect of four different DHA derivatives (Substance 1–4) on body weight, food intake, and adiposity in the "prevention study" is summarized in **Table 1**. Compared to the cHF-fed mice, all DHA derivatives except Substance 3 reduced weight gain and Substance 2 exerted the strongest effects. Mice fed Substance 2 had a reduced food intake, and the feeding efficiency was decreased by ~70% in these animals. Substance 2 reduced the weight of subcutaneous and epididymal WAT by 73 and 42%, respectively, while the remaining DHA derivatives had less effect on adiposity. The dramatic effect of Substance 2 could be partly explained by a reduction of cellularity of WAT, as reflected by a 66% decrease in the DNA content of epididymal WAT. Furthermore, Substance 2 and 3 also decreased the weight of interscapular brown adipose tissue.

The effect of the most potent DHA derivative, Substance 2, was also examined in dietary obese mice in the "reversal study" (**Table 2**). Administration of Substance 2 for a period of 2 months resulted in a net weight loss in obese mice. This effect could be explained, at least in part, by a decreased weight of fat depots, which was accompanied by a reduction of cellularity (DNA data in **Table 2**). In line with the "prevention study," the average food intake in Substance 2-fed mice was decreased

Table 1 The effect of DHA derivatives on energy balance and tissue parameters in the "prevention study"

	STD	cHF	Substance 1	Substance 2	Substance 3	Substance 4
Whole-body parameters						
Body weight (g)	32.4 ± 0.7*	49.6 ± 0.6	44.0 ± 1.5*	30.1 ± 1.1*	46.3 ± 1.6	45.9 ± 1.1*
Weight gain (g)[a]	7.8 ± 0.4*	25.2 ± 0.5	20.2 ± 1.3*	6.4 ± 0.8*	22.4 ± 1.4	21.7 ± 0.9*
Food intake[b]	3.64 ± 0.04*	2.70 ± 0.02	2.64 ± 0.03	2.38 ± 0.05*	2.62 ± 0.02	100 ± 1
Feeding efficiency[c]	0.13 ± 0.02*	0.62 ± 0.08	0.48 ± 0.07	0.17 ± 0.03*	0.57 ± 0.06	0.55 ± 0.06
Tissue weight (mg)						
Subcutaneous WAT	345 ± 31*	1,361 ± 55	916 ± 57*	357 ± 39*	1,189 ± 71	1,417 ± 131
Epididymal WAT	980 ± 102*	1,551 ± 99	2,029 ± 176	877 ± 112*	2,427 ± 186*	2,449 ± 194*
BAT	130 ± 9*	263 ± 7	251 ± 24	91 ± 9*	194 ± 14*	260 ± 29
Liver	1,612 ± 30*	2,122 ± 71	2,055 ± 220	2,404 ± 95	2,405 ± 175	2,109 ± 161
Epididymal WAT DNA						
µg DNA/depot	300 ± 37*	1043 ± 86	ND	355 ± 56*	ND	ND
µg DNA/mg tissue	0.31 ± 0.02*	0.74 ± 0.08	ND	0.42 ± 0.05*	ND	ND
Triglycerides (mg/g tissue)						
Liver	36 ± 2*	122 ± 8	ND	74 ± 10*	ND	ND
Skeletal muscle	25 ± 3*	56 ± 6	ND	22 ± 2*	ND	ND

The data represent the mean ± s.e. (STD, $n = 13$; cHF, $n = 27$; Substance 1–4, $n = 8$); the data for cHF-fed mice were pooled from three experiments (see also METHODS AND PROCEDURES and **Supplementary Table S2** online).
BAT, brown adipose tissue; cHF, composite high-fat diet; ND, not determined; STD, low-fat chow diet; WAT, white adipose tissue.
[a]Calculated for a period of 16 weeks, from the start of feeding until the time point, when glucose tolerance test was performed one week before the killing of animals. [b]Measured weekly and expressed as grams of diet consumed by a mouse per day. [c]Calculated as body weight gained for each week divided by the amount of food consumed for that week (grams/grams). *$P < 0.05$ vs. cHF. 1.5% of dietary lipids was replaced by a DHA derivative.

Table 2 The effect of Substance 2 in the "*reversal study*"

	STD	cHF	Substance 2
Whole-body parameters			
Body weight (g)	34.8 ± 1.1*	52.8 ± 1.9	41.2 ± 1.5*
Weight gain (g)[a]	1.38 ± 0.30*	5.88 ± 1.19	−7.61 ± 1.11*
Food intake[b]	ND	3.19 ± 0.05	2.89 ± 0.07*
Tissue weight (mg)			
Subcutaneous WAT	622 ± 66*	1,872 ± 191	986 ± 122*
Epididymal WAT	1,146 ± 147*	2,021 ± 90	1,364 ± 134*
BAT	158 ± 5*	330 ± 32	158 ± 11*
Liver	1,596 ± 28*	2,556 ± 161	3,017 ± 60*
Epididymal WAT DNA			
µg DNA/depot	335 ± 11*	750 ± 72	515 ± 47*
µg DNA/mg tissue	0.31 ± 0.04	0.37 ± 0.03	0.40 ± 0.04
Tissue triglycerides (mg/g tissue)			
Liver	66 ± 14*	268 ± 22	83 ± 7*
Skeletal muscle	49 ± 6*	190 ± 31	77 ± 10*
Blood/plasma			
Triglycerides (mmol/l)	1.56 ± 0.09	1.60 ± 0.09	0.72 ± 0.06*
NEFA (mmol/l)	0.89 ± 0.08	0.97 ± 0.05	0.73 ± 0.04*
Cholesterol (mmol/l)	1.76 ± 0.14*	5.24 ± 0.27	3.90 ± 0.13*
FBG (mg/dl)	86 ± 5*	118 ± 4	99 ± 4*
Insulin (ng/ml)	1.12 ± 0.54*	4.34 ± 0.33	1.40 ± 0.33*

The data are means ± s.e. (STD, $n = 4$; cHF, $n = 9$; Substance 2, $n = 9$).
BAT, brown adipose tissue; cHF, composite high-fat diet; FBG, fasting blood glucose; ND, not determined; NEFA, nonesterified fatty acids; STD, low-fat chow diet; WAT, white adipose tissue. [a]Calculated for a period of 7 weeks, from the start of feeding until the time point, when glucose tolerance test was performed one week before the killing of animals. [b]Measured weekly and expressed as grams of diet consumed by a mouse per day. *$P < 0.05$ vs. cHF. 1.5% of dietary lipids was replaced by Substance 2.

by 9%. A separate experiment revealed that the reduction in body weight gain induced by either DHA alone or EPA/DHA concentrate (admixed at a tenfold higher dose to cHF diet as compared to Substance 2; that is, replacing 15% vs. 1.5% of dietary lipids) was relatively mild, while no effect on food intake was observed (**Supplementary Table S2** online).

Prevention of adipocyte hypertrophy and macrophage infiltration of WAT by Substance 2

In the "prevention study," histological analysis of epididymal WAT (**Figure 2a,b,c**) revealed adipocyte hypertrophy in the cHF-fed mice, resulting in a approximately twofold increase in the mean cell size. This effect was completely prevented by Substance 2 (**Figure 2d**). Moreover, Substance 2 also completely prevented obesity-associated macrophage infiltration of WAT, as revealed by immunohistochemical detection of Mac-2 (**Figure 2**; white arrows). Macrophages aggregate in crown-like structures surrounding individual adipocytes (23). While the density of crown-like structures was ~77-fold higher in cHF-fed compared with STD-fed mice, Substance 2 completely prevented this effect (**Figure 2e**). Moreover, in

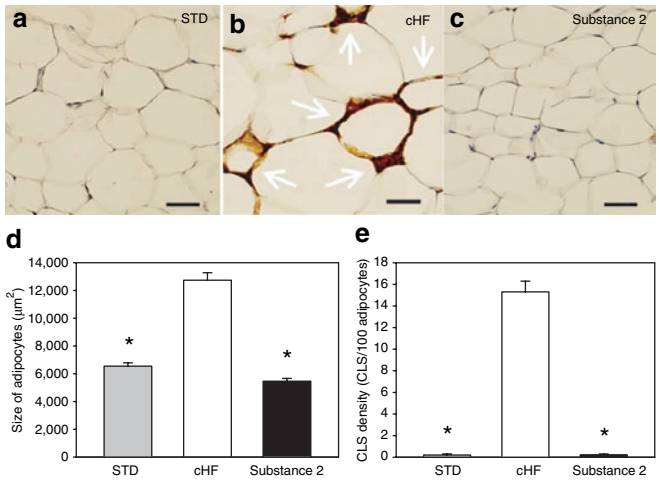

Figure 2 The effect of Substance 2 on adipose tissue morphology and macrophage infiltration in the "prevention study." The amount of MAC-2 immunoreactive macrophages (brownish color) was analyzed in epididymal fat. Sections were counterstained with hematoxylin-eosin. (**a**) Mice fed a low-fat chow (STD) diet. (**b**) Composite high-fat (cHF) diet. (**c**) Substance 2. Arrows indicate crown-like structures (CLS) surrounding individual adipocytes, where the majority of macrophages are lozalized. Bar = 50 µm. (**d**) Size of adipocytes. (**e**) CLS density. The morphometry data are based on >1,000 cells taken randomly from 5 different areas per animal ($n = 3$). *$P < 0.05$ vs. cHF diet (ANOVA).

epididymal WAT Substance 2 reduced mRNA levels of *CD68* and monocyte chemoattractant protein-1 (*MCP-1*), two factors that are closely linked to macrophage function, by 91 and 56%, respectively (**Supplementary Table S4** online). In the "reversal study," Substance 2 reduced the accumulation of macrophages in epididymal WAT by 65% (not shown) and expression of *CD68* and *MCP-1* by 32 and 50%, respectively (**Supplementary Table S4** online). Thus, Substance 2 completely prevents and even partially reverses adipocyte hypertrophy and macrophage infiltration of WAT, induced by the obesogenic cHF diet.

Given the strong effect of Substance 2 on adiposity and obesity-associated inflammation of WAT, two major adipokines, leptin and adiponectin, were evaluated after 2 months of treatment in the "prevention study." Compared with cHF-fed mice, plasma leptin levels were strongly reduced by Substance 2 (4.4 ± 0.3 vs. 86.0 ± 6.2 ng/ml; $P < 0.00001$) and reached the levels observed in the STD-fed mice (6.9 ± 0.9 ng/ml). Plasma adiponectin levels were also slightly reduced (Substance 2, 7.1 ± 0.6 vs. cHF, 9.3 ± 0.5; $P < 0.05$) and were similar to those observed in STD-fed mice (6.9 ± 0.4 ng/ml).

The effects on liver and muscle

In both "prevention" (**Table 1**) and "reversal" (**Table 2**) study, cHF diet significantly increased liver weight. Compared to cHF-fed mice, Substance 2 increased the liver weight in the "reversal study." Importantly, in both studies, Substance 2 reduced the accumulation of triglycerides in liver and skeletal muscle, normally induced after cHF feeding. The induction of liver steatosis by cHF diet and a decrease of triglyceride accumulation by Substance 2 in the "reversal

study" were also confirmed by light microscopy (**Figure 3**). Importantly, livers from mice treated with Substance 2 contained small parenchymal cells of normal morphology, a picture compatible with active regeneration and extensive remodelling of the tissue.

While aspartate aminotransferase levels in plasma of Substance-2-treated mice were unchanged (not shown), alanine aminotransferase levels were increased (Substance 2, 11.33 ± 2.61 vs. cHF, 1.04 ± 0.11 μkat/l; $P < 0.01$) in the "prevention study." Plasma levels of creatine kinase, a marker of muscle cell integrity, were unchanged (not shown). In the "reversal study," Substance 2 increased both aspartate aminotransferase (Substance 2, 12.07 ± 2.30 vs. cHF, 4.98 ± 0.55 μkat/l; $P < 0.05$) and alanine aminotransferase (Substance 2, 11.19 ± 2.45 vs. cHF, 0.97 ± 0.17 μkat/l; $P < 0.05$). The elevated plasma levels of hepatic markers in Substance-2-treated mice, especially in the "reversal study," can be explained by intense regeneration of liver parenchyma accompanying removal of lipid-engorged hepatocytes.

The expression of genes involved in fatty acid oxidation in the liver, such as acyl-CoA oxidase-1 (*Aox-1*) and carnitine palmitoyltransferase-1α (*Cpt-1α*), was higher in animals fed cHF compared with STD diet. This was evident in both the "prevention" and the "reversal" study. These genes were even more upregulated by Substance 2. There was a stronger induction of the peroxisomal (*Aox-1*) than the mitochondrial (*Cpt-1α*) pathway. In both cases, the induction was stronger in the "reversal" than in the "prevention" study (**Supplementary Table S4** online and **Figure 3f**). In a separate "reversal study" experiment, EPA/DHA concentrate and to a lesser extent also DHA alone upregulated *Cpt-1α* (but not *Aox-1*) mRNA levels. However, these changes were relatively small compared to the effects of Substance 2 admixed at a tenfold lower dose to cHF diet. Strong induction of *Aox-1* and *Cpt-1α* expression by Substance 2 correlated well with a marked increase in the expression of their regulatory transcription factor PPAR-α (**Supplementary Table S4** online).

n-3 LC-PUFA are known to decrease expression of lipogenic genes like stearoyl-coenzyme A desaturase-1 (*Scd-1*), as well as other genes (*Spot 14* and farnesyl diphosphate synthase (*Fdps*); (19)). Expression of *Scd-1, Spot 14*, and *Fdps* was downregulated by cHF when compared with STD diet. In the "reversal study," expression of *Scd-1* and *Spot 14* was decreased by both EPA/DHA and by DHA alone. In contrast, expression of *Scd-1* and *Fdps* was markedly induced by Substance 2, namely in the "reversal study" (**Supplementary Table S4** online).

In the skeletal muscle, Substance 2 exerted negligible effects on gene expression except for a downregulation of *Scd-1* (**Supplementary Table S4** online).

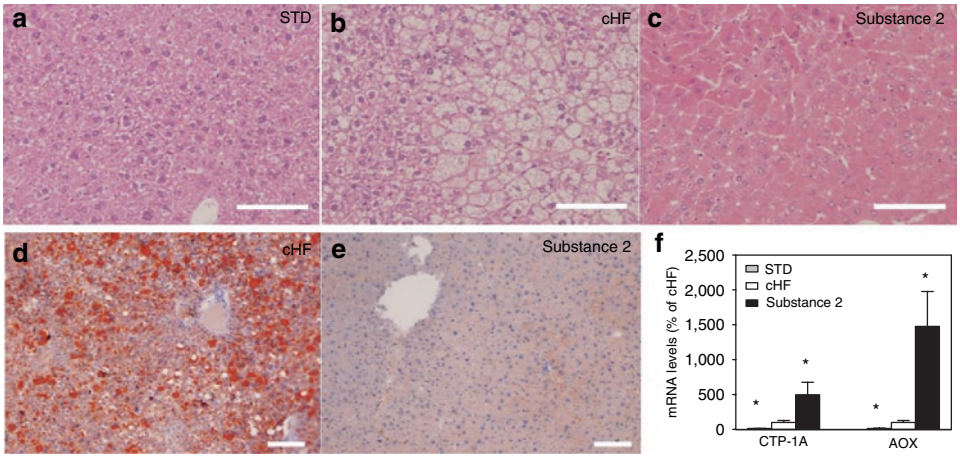

Figure 3 The effect of Substance 2 on liver histology and gene expression in the "reversal study." Liver morphology assessed by hematoxyline-eosin staining of liver sections from mice fed (**a**) low-fat chow (STD) diet, (**b**) composite high-fat (cHF) diet, and (**c**) Substance 2. Visualization of neutral lipids (in red) by Sudan III staining in the liver of mice fed (**d**) cHF diet and (**e**) Substance 2. Nuclei (in blue) were counterstained by hematoxyline. Bar = 50 μm. (**f**) The expression of genes involved in fatty acid oxidation in the liver. Values represent means ± s.e. (n = 4–8). AOX, acyl-CoA oxidase; CPT-1α, carnitine palmitoyltransferase-1α. *$P < 0.05$ vs. cHF diet (ANOVA).

Table 3 The effect of DHA derivatives on plasma markers of lipid metabolism in the *"prevention study"*

	STD	cHF	Substance 1	Substance 2	Substance 3	Substance 4
Triglycerides	89 ± 6	100 ± 6	99 ± 5	47 ± 7*	79 ± 4*	101 ± 7
NEFA	122 ± 11	100 ± 9	134 ± 7*	81 ± 5*	110 ± 8	100 ± 7
Cholesterol	53 ± 1*	100 ± 4	97 ± 4	80 ± 2*	85 ± 2*	83 ± 13

The data are expressed as percentages of the control cHF diet (~ 100%). 1.5% of dietary lipids was replaced by a DHA derivative. Means ± s.e. (STD, n = 13; cHF, n = 7–13; Substance 1–4, n = 8); the data for cHF-fed mice were pooled from three experiments (see METHODS AND PROCEDURES and **Supplementary Table S2** online).
STD, low-fat chow diet; cHF, composite high-fat diet; NEFA, nonesterified fatty acids.
*$P < 0.05$ vs. cHF.

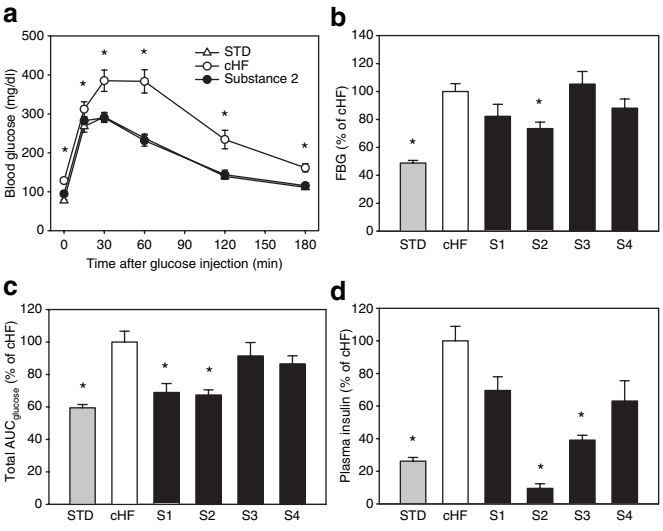

Figure 4 The effect of DHA derivatives on glucose homeostasis in the "prevention study." Mice were fed either a low-fat chow (STD), composite high-fat (cHF) diet, or cHF diet in which 1.5% of lipids was replaced by various DHA derivatives (S1, Substance 1; S2, Substance 2; S3, Substance 3; S4, Substance 4). (**a**) Intraperitoneal glucose tolerance test (IPGTT; glycemic curves for mice fed the STD, cHF, and Substance 2 diets are shown). *$P < 0.05$ vs. other groups (ANOVA). (**b**) Fasting blood glucose (FBG) corresponding to baseline blood glucose levels from IPGTT. (**c**) Total area under the curve for glucose ($AUC_{glucose}$) derived from IPGTT data. (**d**) Plasma insulin in *ad libitum*–fed mice at the time of killing, that is, 1 week after IPGTT. Data are expressed as percentages of the control cHF diet and represent means ± s.e. (STD, $n = 11$; cHF, $n = 7$–13; Substances, $n = 8$). *$P < 0.05$ vs. cHF diet (ANOVA).

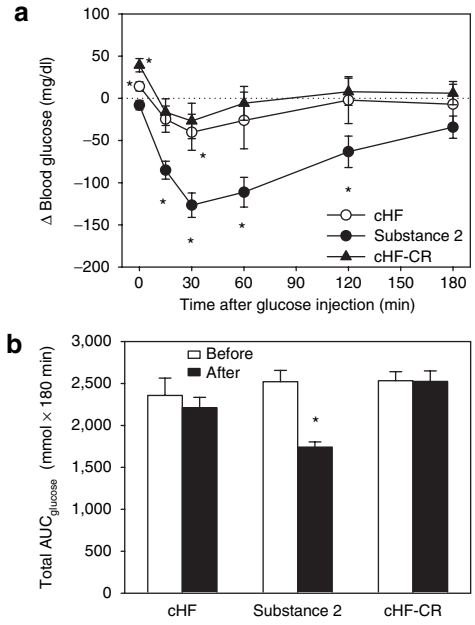

Figure 5 Reversal of impaired glucose tolerance in dietary obese mice by Substance 2 in the "reversal study." Glucose tolerance was assessed by intraperitoneal glucose tolerance test (IPGTT) performed 1 week before the start and 1 week before the end of 2-month-long treatment in mice fed *ad libitum* either a composite high-fat (cHF) diet or cHF diet, containig DHA derivative (Substance 2). Calorie-restricted cHF-fed mice (cHF-CR; 12% restriction) were also analyzed. (**a**) Glycemic curves, representing a change in blood glucose levels during IPGTT measured before and after the treatment. (**b**) Total area under the curve for glucose ($AUC_{glucose}$) derived from IPGTT data obtained before and after the treatment. Values represent means ± s.e. (cHF, $n = 20$; Substance 2, $n = 21$; cHF-CR, $n = 12$). *$P < 0.05$ before vs. after the treatment (two-way repeated measures ANOVA).

Beneficial effects of DHA derivatives on systemic markers of lipid metabolism

In the "prevention study" study, Substance 2 reduced plasma levels of total triglycerides, NEFA, and total cholesterol by 53, 19, and 20%, respectively (**Table 3**). The other substances exerted less pronounced lipid-lowering effects, while Substance 1 even increased plasma NEFA by 34%. In the "reversal study," Substance 2 lowered plasma triglycerides, NEFA, and cholesterol levels by 55, 24, and 25%, respectively (**Table 2**). A separate experiment revealed that DHA alone admixed at a tenfold higher dose to cHF diet compared to Substance 2 had no effect on plasma triglycerides, while EPA/DHA concentrate reduced plasma triglycerides by 40% (**Supplementary Table S2** online), that is, similarly to Substance 2 admixed at a tenfold lower dose (see above).

Beneficial effects of DHA derivatives on glucose homeostasis

In the "prevention study," FBG and glucose tolerance were markedly impaired by cHF feeding, while Substance 2 improved FBG and both Substance 1 and Substance 2 improved glucose tolerance (**Figure 4**). cHF-fed mice also demonstrated hyperinsulinemia, while Substance 2 and Substance 3 exerted protective effects (**Figure 4d**).

Substance 2 also lowered FBG and plasma insulin in dietary obese mice in the "reversal study" (**Table 2**). Importantly, glucose tolerance was also improved by Substance 2 (**Figure 5**). In contrast, neither EPA/DHA nor DHA alone (both admixed at a tenfold higher dose to cHF diet as compared to Substance 2) exerted significant effects on FBG and glucose tolerance (total AUC glucose) in dietary obese mice in the "reversal study," although there was a trend for EPA/DHA to improve glucose tolerance (**Supplementary Table S2** online).

Because Substance 2 reduced food intake by 12% during the "prevention" study, the effect of a 12% calorie restriction on glucose tolerance was analyzed in the "reversal study." Except for increasing FBG, calorie restriction did not have any significant effect on glycemia during intraperitoneal glucose tolerance test (**Figure 5a**) or on total AUC (**Figure 5b**) in obese cHF diet-fed mice. In contrast, calorie restriction decreased body weight by 1.25 ± 0.62 g as compared to a weight loss of 6.89 ± 1.23 g induced by Substance 2 ($P < 0.001$).

DISCUSSION

We report for the first time the metabolic effects of DHA derivatives substituted at the C(2)-position of the molecule. We show that replacement of 1.5% of dietary lipids by various DHA derivatives affected the development of diet-induced obesity and associated metabolic traits in C57BL/6 mice fed a high-fat diet. Substance 2 (α-ethyl DHA ethyl ester) completely prevented and even partially reversed the development

of obesity, fat accumulation, IGT, dyslipidemia, and WAT inflammation. Therefore, besides the general characterization of various DHA derivatives, our study was largely focused on a detailed description of the action of Substance 2.

In agreement with its effect on body weight and adiposity, Substance 2 profoundly affected WAT properties. Similar to the effect of EPA/DHA (5,13), Substance 2 reduced (i) tissue cellularity, (ii) the size of adipocytes, and (iii) macrophage infiltration of WAT. Small adipocytes are more insulin sensitive and less lipolytic, while releasing less inflammatory cytokines, including MCP-1 (24). The reduction of macrophage infiltration should have beneficial systemic effects, as macrophages represent an additional source of proinflammatory cytokines, which induce IR and contribute to a state of chronic low-level inflammation in obesity (25). Similar to the effects of n-3 LC-PUFA (5), Substance 2 also partially prevented downregulation of *Glut4* in WAT, otherwise induced by high-fat diet. WAT is also a source of antiinflammatory and insulin-sensitizing adipokines, leptin and adiponectin. Circulating leptin levels reflect adiposity and obesity is associated with leptin resistance (26,27). Substance 2 markedly decreased plasma leptin levels, reflecting the reduction of adiposity. However, downregulation of *Scd-1* in skeletal muscle of Substance-2-treated mice could also imply improved muscle leptin sensitivity and elevated fatty acid oxidation (28). In contrast to the induction of adiponectin by EPA/DHA (6), Substance 2 decreased plasma adiponectin by ~25% despite dramatically improving glucose tolerance. However, similar plasma adiponectin levels in Substance-2-treated mice and mice fed a low-fat STD diet suggest that plasma adiponectin might not be the best predictor of the metabolic state in this mouse model.

A relatively strong suppression of insulin levels by Substance 2 could hardly represent an indirect effect secondary to improvements in insulin sensitivity. It has been shown that n-3 LC-PUFA reversed glucose-stimulated insulin hypersecretion, normally induced by obesogenic diet, in rat islets (29,30). Therefore, in addition to its effects in other tissues, Substance 2 might act directly on pancreatic β-cells via reduction of insulin secretion. However, further studies are required to clarify this issue.

As published by others (31), DHA derivatives with a hydrophilic substituent at the C(4)-position could lower glucose levels in animal models of diabetes. However, they did not lower blood triglycerides. In contrast, Substance 2 not only prevented and even partially reversed IGT, but it also lowered plasma triglycerides, NEFA, and cholesterol levels. Substance 2 strongly reduced the accumulation of triglycerides in both liver as well as skeletal muscle, resembling the effects of n-3 LC-PUFA (30). The reduced lipid accumulation in the liver and muscle might be a major mechanism, by which Substance 2 counteracted development of IGT.

Substance 2, and to a lesser extent also EPA/DHA concentrate and DHA alone, upregulated *Ppar-α* and its target genes *Aox-1* and *Cpt-1α* in the liver, documenting induction of lipid catabolism and suggesting that Substance 2 acted as a potent PPAR-α agonist (18). In agreement with the known induction of lipogenic genes by pharmacological stimulation of PPAR-α in mouse liver (32), lipogenic *Scd-1* and *Fdps* were strongly induced by Substance 2. Importantly, hepatic *Scd-1* gene expression has been shown to be upregulated by PPARs directly, through a mechanism distinct from the regulation of this gene by polyunsaturated fatty acids (33). A set of sterol-regulatory element binding protein–1c target genes (*Scd-1, Spot 14, and Fdps*) was downregulated by EPA/DHA concentrate or DHA alone as expected (19).

The induction of *Scd-1* and other lipogenic genes by Substance 2 seems to be liver specific because it did not occur in skeletal muscle, where Substance 2 even downregulated *Scd-1* expression. The simultaneous stimulation of *in situ* lipogenesis and lipid oxidation by Substance 2 in the liver suggests induction of futile substrate cycling, which may be responsible for the reduced accumulation of triglycerides in the tissue and possibly also for decreased feeding efficiency of Substance-2-treated mice.

Besides increasing the expression of fatty acid oxidation genes, Substance 2 also lowered FBG in both "prevention" and "reversal" study, suggesting a reduction in hepatic glucose production and gluconeogenesis. This finding is in disagreement with previously published reports, linking increased oxidation of fatty acids to the activation of gluconeogenesis in the liver (34,35). However, the coordinated regulation of these metabolic pathways by physiological stimuli such as fasting (35) might be dramatically different from the situation, when hepatic fatty acid oxidation is stimulated by pharmacological activation of PPAR-α. In fact, improved liver insulin sensitivity in response to PPAR-α agonist treatment, as evidenced by lower endogenous glucose production, has been already observed before (36).

The efficacy of Substance 2 is striking because the dose used in our experiments (1.5% of dietary lipids replaced by the DHA derivative) was approximately six- to tenfold lower compared either with the dose of EPA/DHA concentrate (or DHA alone) also used in this study or with other animal studies in which significant effects of EPA and DHA on body weight, adiposity, and plasma lipids (5,6), or IR (8) were observed. Substance 2 reduced body weight gain in association with a reduced feeding efficiency; however, food intake was also slightly reduced. Calorie restriction itself exerts beneficial effects on lipid and glucose metabolism (6,37). However, the "reversal study," which also included the calorie-restricted cHF diet-fed mice, indicated that Substance 2 reversed glucose intolerance independently of the reduction in food intake. Nevertheless, the contribution of body weight change to improved glucose tolerance in Substance-2-treated mice could not be directly estimated. In contrast to Substance 2 and in agreement with human studies (10), EPA/DHA or DHA alone could not reverse established glucose intolerance.

In summary, among the four DHA derivatives tested, Substance 2 (α-ethyl DHA ethyl ester) appeared to exhibit a similar range of beneficial effects on obesity and associated metabolic traits as naturally occurring n-3 LC-PUFA, but with a higher efficacy. Therefore, this compound could qualify as a novel drug for the treatment of obesity, dyslipidemia, and insulin resistance.

SUPPLEMENTARY MATERIAL

Supplementary material is linked to the online version of the paper at http://www.nature.com/oby

ACKNOWLEDGMENTS

This study was supported by the grants from the Czech Science Foundation (303/08/0664 and 303/07/0708), Pronova BioPharma AS (Lysaker, Norway), and MITOFOOD (COST Action FA0602). We acknowledge Synthetica AS (Forskningsparken, Oslo) for the synthesis of the DHA derivatives. We also thank Saverio Cinti (University of Ancona, Italy) for advice concerning histological analysis.

DISCLOSURE

Dr Bryhn, Dr Berge, and Dr Holmeide were employees of Pronova BioPharma AS at the time of this study.

REFERENCES

1. Despres JP, Lemieux I. Abdominal obesity and metabolic syndrome. *Nature* 2006;444:881–887.
2. Muoio DM, Newgard CB. Mechanisms of disease: molecular and metabolic mechanisms of insulin resistance and beta-cell failure in type 2 diabetes. *Nat Rev Mol Cell Biol* 2008;9:193–205.
3. Nissen SE, Wolski K. Effect of rosiglitazone on the risk of myocardial infarction and death from cardiovascular causes. *N Engl J Med* 2007;356:2457–2471.
4. Rustan AC, Christiansen EN, Drevon CA. Serum lipids, hepatic glycerolipid metabolism and peroxisomal fatty acid oxidation in rats fed omega-3 and omega-6 fatty acids. *Biochem J* 1992;283:333–339.
5. Ruzickova J, Rossmeisl M, Prazak T *et al*. Omega-3 PUFA of marine origin limit diet-induced obesity in mice by reducing cellularity of adipose tissue. *Lipids* 2004;39:1177–1185.
6. Flachs P, Mohamed-Ali V, Horakova O *et al*. Polyunsaturated fatty acids of marine origin induce adiponectin in mice fed high-fat diet. *Diabetologia* 2006;49:394–397.
7. Woodman RJ, Mori TA, Burke V *et al*. Effects of purified eicosapentaenoic and docosahexaenoic acids on glycemic control, blood pressure, and serum lipids in type 2 diabetic patients with treated hypertension. *Am J Clin Nutr* 2002;76:1007–1015.
8. Storlien LH, Kraegen EW, Chisholm DJ *et al*. Fish oil prevents insulin resistance induced by high-fat feeding in rats. *Science* 1987;237:885–888.
9. Mori TA, Bao DQ, Burke V *et al*. Dietary fish as a major component of a weight-loss diet: effect on serum lipids, glucose, and insulin metabolism in overweight hypertensive subjects. *Am J Clin Nutr* 1999;70:817–825.
10. Fasching P, Ratheiser K, Waldhausl W *et al*. Metabolic effects of fish-oil supplementation in patients with impaired glucose tolerance. *Diabetes* 1991;40:583–589.
11. Berge RK, Madsen L, Vaagenes H, Tronstad KJ, Gottlicher M, Rustan AC. In contrast with docosahexaenoic acid, eicosapentaenoic acid and hypolipidaemic derivatives decrease hepatic synthesis and secretion of triacylglycerol by decreased diacylglycerol acyltransferase activity and stimulation of fatty acid oxidation. *Biochem J* 1999;343:191–197.
12. Flachs P, Horakova O, Brauner P *et al*. Polyunsaturated fatty acids of marine origin upregulate mitochondrial biogenesis and induce beta-oxidation in white fat. *Diabetologia* 2005;48:2365–2375.
13. Todoric J, Loffler M, Huber J *et al*. Adipose tissue inflammation induced by high-fat diet in obese diabetic mice is prevented by n-3 polyunsaturated fatty acids. *Diabetologia* 2006;49:2109–2119.
14. Neschen S, Morino K, Rossbacher JC *et al*. Fish oil regulates adiponectin secretion by a peroxisome proliferator-activated receptor-γ-dependent mechanism in mice. *Diabetes* 2006;55:924–928.
15. Forman BM, Chen J, Evans RM. Hypolipidemic drugs, polyunsaturated fatty acids, and eicosanoids are ligands for peroxisome proliferator-activated receptors α and δ. *Proc Natl Acad Sci USA* 1997;94:4312–4317.
16. Neschen S, Morino K, Dong J *et al*. N-3 fatty acids preserve insulin sensitivity *in vivo* in a PPARα-dependent manner. *Diabetes* 2007;56:1034–1041.
17. Sampath H, Ntambi JM. Polyunsaturated fatty acid regulation of genes of lipid metabolism. *Annu Rev Nutr* 2005;25:317–340.
18. Sanderson LM, de Groot PJ, Hooiveld GJ *et al*. Effect of synthetic dietary triglycerides: a novel research paradigm for nutrigenomics. *PLoS ONE* 2008;3:e1681.
19. Teran-Garcia M, Adamson AW, Yu G *et al*. Polyunsaturated fatty acid suppression of fatty acid synthase (FASN): evidence for dietary modulation of NF-Y binding to the Fasn promoter by SREBP-1c. *Biochem J* 2007;402:591–600.
20. Suchankova G, Tekle M, Saha AK *et al*. Dietary polyunsaturated fatty acids enhance hepatic AMP-activated protein kinase activity in rats. *Biochem Biophys Res Commun* 2005;326:851–858.
21. Serhan CN. Novel omega—3-derived local mediators in anti-inflammation and resolution. *Pharmacol Ther* 2005;105:7–21.
22. Fievet C, Fruchart JC, Staels B. PPARα and PPARγ dual agonists for the treatment of type 2 diabetes and the metabolic syndrome. *Curr Opin Pharmacol* 2006;6:606–614.
23. Cinti S, Mitchell G, Barbatelli G *et al*. Adipocyte death defines macrophage localization and function in adipose tissue of obese mice and humans. *J Lipid Res* 2005;46:2347–2355.
24. Yang X, Smith U. Adipose tissue distribution and risk of metabolic disease: does thiazolidinedione-induced adipose tissue redistribution provide a clue to the answer? *Diabetologia* 2007;50:1127–1139.
25. Wellen KE, Hotamisligil GS. Inflammation, stress, and diabetes. *J Clin Invest* 2005;115:1111–1119.
26. Frederich RC, Hamann A, Anderson S *et al*. Leptin levels reflect body lipid content in mice: evidence for diet-induced resistance to leptin action. *Nat Med* 1995;1:1311–1314.
27. Caro JF, Kolaczynski JW, Nyce MR *et al*. Decreased cerebrospinal-fluid/serum leptin ratio in obesity: a possible mechanism for leptin resistance. *Lancet* 1996;348:159–161.
28. Dobrzyn A, Dobrzyn P. Stearoyl-CoA desaturase—a new player in skeletal muscle metabolism regulation. *J Physiol Pharmacol* 2006;57:31–42.
29. Holness MJ, Greenwood GK, Smith ND, Sugden MC. Diabetogenic impact of long-chain omega-3 fatty acids on pancreatic β-cell function and the regulation of endogenous glucose production. *Endocrinology* 2003;144:3958–3968.
30. Lombardo YB, Chicco AG. Effects of dietary polyunsaturated n-3 fatty acids on dyslipidemia and insulin resistance in rodents and humans. A review. *J Nutr Biochem* 2006;17:1–13.
31. Yamamoto K, Itoh T, Abe D *et al*. Identification of putative metabolites of docosahexaenoic acid as potent PPARγ agonists and antidiabetic agents. *Bioorg Med Chem Lett* 2005;15:517–522.
32. Knight BL, Hebbachi A, Hauton D *et al*. A role for PPARα in the control of SREBP activity and lipid synthesis in the liver. *Biochem J* 2005;389:413–421.
33. Miller CW, Ntambi JM. Peroxisome proliferators induce mouse liver stearoyl-CoA desaturase 1 gene expression. *Proc Natl Acad Sci USA* 1996;93:9443–9448.
34. Williamson JR, Kreisberg RA, Felts PW. Mechanism for the stimulation of gluconeogenesis by fatty acids in perfused rat liver. *Proc Natl Acad Sci USA* 1966;56:247–254.
35. Koo SH, Satoh H, Herzig S *et al*. PGC-1 promotes insulin resistance in liver through PPAR-α-dependent induction of TRB-3. *Nat Med* 2004;10:530–534.
36. Haluzik MM, Lacinova Z, Dolinkova M *et al*. Improvement of insulin sensitivity after peroxisome proliferator-activated receptor-α agonist treatment is accompanied by paradoxical increase of circulating resistin levels. *Endocrinology* 2006;147:4517–4524.
37. Guarente L. Sirtuins as potential targets for metabolic syndrome. *Nature* 2006;444:868–874.

SUPPLEMENTARY MATERIAL

Figure 1

DHA ethyl ester

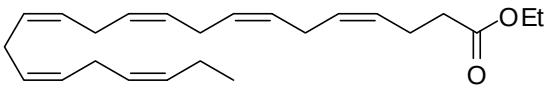

Substance-1, α-methyl DHA ethyl ester

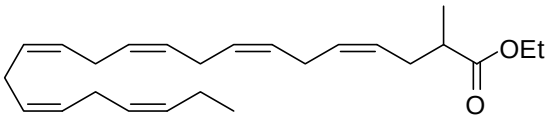

Substance-2, α-ethyl DHA ethyl ester

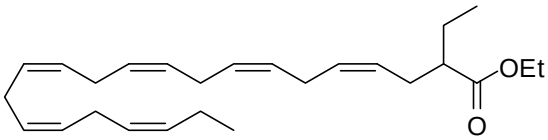

Substance-3, α,α – di-methyl DHA ethyl ester

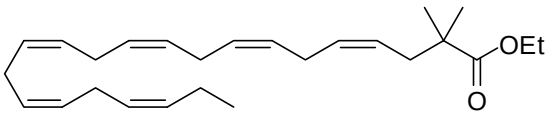

Substance-4, α–thioethyl DHA ethyl ester

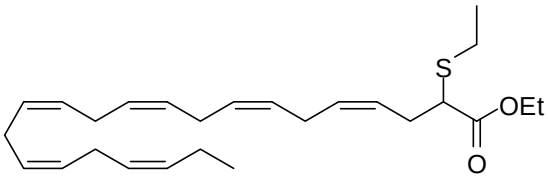

Table 1 Oligonucleotide primers for real-time quantitative PCR analysis

Gene	Primer (forward/reverse)
Aox-1	GCTGGGCTGAAGGCTTTTACTACC/CACCTGCTGCGGCTGGATAC
CD68	CACTTCGGGCCATGTTTCTCTTG/AGGGGCTGGTAGGTTGATTGTCGT
Cpt-1α (liver type)	GCAGCTCGCACATTACAAGGACAT/AGCCCCCGCCACAGGACACATAGT
Fdps	ATGCCATCAACGACGCTCTGCT/TGGCCCTGGGGTGCTGTCA
Glut-4	ACCGGCTGGGCTGATGTGTCT/GCCGACTCGAAGATGCTGGTTGAATAG
MCP-1	GTTAACGCCCCACTCAC/GGTTCCGATCCAGGTTT
Pdk-4	GGCTTGCCAATTTCTCGTCTCTA/TTCGCCAGGTTCTTCGGTTCC
Pgc-1α	CCCAAAGGATGCGCTCTCGTT/TGCGGTGTCTGTAGTGGCTTGATT
Ppar-α	TGCGCAGCTCGTACAGGTCATCAA/CCCCCATTTCGGTAGCAGGTAGTCTTA
Ppib (Cyclophilin β)	GGGAGATGGCACAGGAGGAAAGAG/ACCCAGCCAGGCCCGTAGTG
Scd-1	ACTGGGGCTGCTAATCTCTGGGTGTA/GGCTTTATCTCTGGGGTGGGTTTGTTA
SPOT 14	GCTGCTGCCAAGGGAGGAATG/CCGGGTCAGGTGGGTAAGGATG

AOX-1, acyl-CoA oxidase-1; CPT-1α, carnitine palmitoyltransferase-1α; FDPS, farnesyl diphosphate synthase; GLUT-4, glucose transporter-4; MCP-1, monocyte chemoattractant protein-1; PDK-4, pyruvate dehydrogenase

kinase-4; PGC-1α, peroxisome proliferator-activated receptor-γ coactivator-1α; PPAR-α, peroxisome proliferator-activated receptor-α; PPIB, peptidylpropyl isomerase β; SCD-1, stearoyl-coenzyme A desaturase-1; SPOT 14, thyroid hormone responsive SPOT 14

Table 2 The effects of EPA/DHA concentrate and pure DHA in dietary obese mice in the context of „*reversal study*“ setup

	cHF	EPA/DHA	DHA
Whole body parameters			
Weight gain (g)[a]	5.2 ± 0.3	2.4 ± 0.9*	3.4 ± 0.7*
Food intake[b]	2.82 ± 0.07	2.94 ± 0.10	2.71 ± 0.07
Plasma parameters			
Triglycerides (mmol/l)	2.00 ± 0.29	1.21 ± 0.17*	2.05 ± 0.25
NEFA (mmol/l)	0.70 ± 0.05	0.44 ± 0.03*	0.47 ± 0.02*
Cholesterol (mmol/l)	5.58 ± 0.26	4.24 ± 0.23*	4.44 ± 0.21*
FBG (mg/dl)	103 ± 6	89 ± 5	97 ± 5
Glucose tolerance (AUC; mmol x 180 min)[c]			
Before treatment	2161 ± 174	2459 ± 181	2231 ± 203
After treatment	2223 ± 143	1995 ± 188	2002 ± 144

The data represent the mean ± s.e. (n = 7-8). *P < 0.05 vs. cHF [one-way ANOVA except for the analysis of glucose tolerance (before vs. after), where two-way Repeated Measures ANOVA was used].

15% of dietary lipids was replaced by EPA/DHA concentrate or DHA.

AUC, area under the curve; cHF, composite high-fat diet; DHA, docosahexaenoic acid; EPA/DHA, the concentrate of eicosapentaenoic and docosahexaenoic acids; FBG, fasting blood glucose; NEFA, non-esterified fatty acids.

[a]Calculated for a period of 7 weeks, from the start of feeding until the time point, when glucose tolerance test was performed one week before the killing of animals.

[b]Measured weekly and expressed as grams of diet/mouse/day.

[c]Asessed 1 week before the start (before treatment) and one week before the end (after treatment) of the experiment (as also described in the legend to Fig. 5 in the main text).

Table 3 Comparison of the cHF diet-fed groups from the experiment A, B, and C in the „*prevention study*“

	Experiment A	Experiment B	Experiment C
Whole body parameters			
Body weight (g)	50.3 ± 1.1	48.0 ± 0.5	49.8 ± 0.4
Weight gain (g)	25.8 ± 1.0	24.1 ± 0.5	25.1 ± 0.4
Food intake[a]	2.73 ± 0.04	2.69 ± 0.03	2.68 ± 0.05
Feeding efficiency[b]	0.088 ± 0.012	0.085 ± 0.013	0.086 ± 0.015
Plasma parameters			
Triacylglycerols (mmol/l)	1.59 ± 0.10	1.51 ± 0.11	1.14 ± 0.11
NEFA (mmol/l)	0.47 ± 0.04	0.66 ± 0.02	0.82 ± 0.05
Cholesterol (mmol/l)	4.31 ± 0.16	4.44 ± 0.12	4.58 ± 0.12
FBG (mg/dl)	159 ± 11	129 ± 7	136 ± 13
Insulin (ng/ml)	3.93 ± 0.41	6.32 ± 0.56	6.66 ± 0.28
Glucose tolerance			
AUC (mmol x 180 min)[c]	1820 ± 277	1569 ± 143	1319 ± 219

The data represent the mean ± s.e. (*n* = 7-13).

AUC, area under the curve; cHF, composite high-fat diet; FBG, fasting blood glucose; NEFA, non-esterified fatty acids.

[a]Measured weekly and expressed as grams of diet/mouse/day.

[b]Calculated as body weight gained for each week divided by the amount of food consumed for that week (grams/grams).

[c]Asessed 1 week before the end of the experiment.

Table 4 The effect of Substance-2 on mRNA levels of selected genes

	Prevention study			*Reversal study*				
	STD	cHF	Substance-2	STD	cHF	Substance-2	EPA/DHA	DHA
Adipose tissue								
CD68	7 ± 1*	100 ± 24	9 ± 3*	17 ± 2*	100 ± 16	68 ± 16	NM	NM
MCP-1	20 ± 3*	100 ± 15	44 ± 19*	33 ± 3*	100 ± 13	50 ± 14*	NM	NM
Pgc-1α	109 ± 3*	100 ± 2	100 ± 2	99 ± 8	100 ± 3	101 ± 4	NM	NM
Glut-4	647 ± 61*	100 ± 24	193 ± 45	229 ± 72*	100 ± 16	68 ± 16	NM	NM
Liver								
Cpt-1α	52 ± 6*	100 ± 7	140 ± 13*	14 ± 2*	100 ± 24	563 ± 203*	196 ± 54*	145 ± 49
Aox-1	68 ± 10	100 ± 8	308 ± 23*	12 ± 5*	100 ± 27	1477 ± 500*	88 ± 35	114 ± 33
Ppar-α	73 ± 8*	100 ± 8	135 ± 10*	6 ± 2*	100 ± 19	296 ± 100*	113 ± 31	78 ± 15
Scd-1	243 ± 39*	100 ± 7	410 ± 34*	293 ± 71*	100 ± 15	1004 ± 98*	44 ± 19	23 ± 11*
Spot 14	155 ± 49	100 ± 17	65 ± 17	132 ± 22	100 ± 14	149 ± 31	49 ± 18	43 ± 10*
Fdps	211 ± 24*	100 ± 13	260 ± 28*	174 ± 43	100 ± 13	452 ± 46*	84 ± 21	81 ± 23
Skeletal muscle								

Glut4	139 ± 6*	100 ± 15	109 ± 13	83 ± 9	100 ± 6	79 ± 5	NM	NM
Pdk-4	31 ± 6*	100 ± 13	96 ± 12	23 ± 10*	100 ± 14	89 ± 10	NM	NM
Scd-1	319 ± 151	100 ± 25	49 ± 6*	79 ± 12	100 ± 8	87 ± 5	NM	NM

The data represent the mean ± s.e. (*n* = 7-9 except for STD-fed mice in the „*reversal study*"; *n* = 4).

**P* < 0.05 vs. cHF (ANOVA).

Gene expression data were expressed as a percentage of the cHF-fed controls.

1.5% of dietary lipids was replaced by Substance-2, while 15% of dietary lipids was replaced by EPA/DHA concentrate or DHA.

AOX-1, acyl-CoA oxidase-1; CPT-1α, carnitine palmitoyltransferase-1α; FDPS, farnesyl diphosphate synthetase; GLUT-4, glucose transporter-4; MCP-1, monocyte chemoattractant protein-1; PDK-4, pyruvate dehydrogenase kinase-4; PGC-1α, peroxisome proliferator-activated receptor-γ coactivator-1α; PPAR-α, peroxisome proliferator-activated receptor-α; SCD-1, stearoyl-coenzyme A desaturase-1; SPOT 14, thyroid hormone responsive SPOT 14; NM, not measured.